Identification of genetic regulators of longevity in dark-held detached Arabidopsis inflorescences

A thesis presented in partial fulfilment of the requirements for the degree

of

Doctor of Philosophy

in

Plant Biology

Massey University, Palmerston North, New Zealand
Rubina Jibran
2014

Abstract

Harvested green plant tissues experience a number of stresses including energy deprivation, water disruption, and changes in hormone levels. These stresses accelerate the senescence of the tissues, which causes their deterioration. A comprehensive understanding of how these stresses cause senescence is essential if this unwanted deterioration is to be minimised. In this thesis, I used detached dark-held immature inflorescences of *Arabidopsis thaliana* (Arabidopsis) to investigate the regulatory programme responsible for the senescence of harvested energy-deprived tissue. Detached dark-held Arabidopsis inflorescences completely degreened at day 5 when held in the dark at 21°C. The degreening was accelerated by exogenously applying ACC, ethrel, MeJA, and ABA that have previously been shown to accelerate senescence in detached dark-held leaves. Higher MeJA concentrations unexpectedly delayed rather than accelerated degreening of the detached dark-held inflorescences and this was associated with reductions in transcripts for the senescence-associated genes *SEN4*, *ANAC029*, *NAC3,* and *SAG12*. To identify key genetic regulators of inflorescence senescence an untargeted forward genetics approach was utilized. This involved detaching the immature inflorescences grown from ~20,000 ethyl methane-sulfonate-treated (EMS-treated) Arabidopsis (Landsberg *erecta*) seeds, holding them in the dark at 21°C and visually identifying those that showed a different timing of degreening to wild type. This approach successfully identified inflorescences that were completely degreened at day 3 of dark incubation (two days earlier than wild type) that were designated *accelerated inflorescence senescence* (*ais*) and inflorescences that were more green than wild type at day 5 that were designated *delayed inflorescences senescence* (*dis*). A total of 10 *ais* and 20 *dis* mutants were identified. Interestingly, most of the *dis* mutants were specific for inflorescence senescence as they did not show delayed senescence in detached dark-held leaves. By utilizing a traditional map-based cloning approach, five *dis* mutants were mapped to particular chromosomal regions. *dis9* was mapped to the top arm of chromosome 3, *dis15* was to the bottom of chromosome 2, and *dis1*, *dis34*, and *dis58* were mapped to chromosome 4. Whole genome sequencing of *dis15* and *58* identified the EMS-induced lesions as G to A transitions in the eukaryotic *ASPARTYL PROTEASE* (AT2G28030) and *NON-CODING RNA* (AT4G13495), respectively. Transformation of the AT4G13495 DNA fragment into *dis58* reverted the *dis58* phenotype to wild-type confirming that the non-coding RNA is involved in

regulating inflorescence senescence. In addition to these fertile mutants, a sterile *agamous-like* mutant that had a sepal-petal-petal phenotype was identified. The mutant showed delayed degreening of detached dark-held inflorescences. This prompted me to investigate the mechanism behind the delayed senescence of the sterile homeotic *ag-1* mutant. The sepals of the *ag-1* inflorescences were found to have both delayed *in planta* and detached dark-induced senescence. They were also found to be devoid of JA and like wild-type senesced when treated with MeJA. The delayed *in planta* sepal senescence appeared to be due to the lack of produced JA as the *dde2* mutant (defective in JA biosynthesis and devoid of JA) also showed delayed *in planta* sepal senescence. However, the *dde2* mutant did not show delayed dark-induced senescence suggesting that the delayed dark-induced senescence of *ag-1* may be through a mechanism that is unrelated to the JA hormone. Taken together, in addition to identifying common regulators of inflorescence and leaf senescence, this screen has also identified novel regulators specific to inflorescence senescence that traditional screens based on leaf senescence would have missed. This suggests that there are both similarities and differences in the genetic pathways regulating leaf and inflorescence senescence. The identification of a range of mutants, some of which appear to be novel, also indicates that the immature detached Arabidopsis inflorescences are a useful system for studying energy-deprivation driven senescence. Understanding the role of the *dis58* non coding RNA and the other regulators in the mutant collection offers a new and exciting opportunity for ascertaining the regulatory genetic network initiated in energy-deprived tissues that control the deterioration of harvested produce.

Blank page

Blank page

Acknowledgements

I am grateful to both of my supervisors Dr. Donald Hunter and Dr. Paul Dijkwel who have been supportive throughout the years of my PhD. I remember the day when I met Paul, and since then he has always challenged me to excel. Thanks for the critical analysis, which drove me to do the good science. I am also very grateful for Paul helping me understand how to analyse EMS mutants for gene mapping and incredibly appreciative of him obtaining funding for me from IMBS during my thesis writing.

Especially I want to thank Don, who provided me immense support in understanding, writing, and performing the science. I am also very grateful for your insightful and detailed scientific discussions that led me to think, analyse, and perform my experiments. Most of all you taught me how to celebrate the science and I will never forget the day when you showed me how to hold the pipettes. I really appreciate your support in my academic, social, and personal affairs. You are a really amazing person and competent supervisor. Thanks for everything.

I thank Professor Michael McManus for teaching me how to understand, analyze, and deduce the scientific research. I also thank David Chagne for teaching me HRM-PCR and how to analyze the differences between homozygotes and heterozygotes through colours. Thanks to Darren Allerby for computer support and Ian Brooking for Endnote help. Thanks to Janine Cooney for performing LC-MS analysis on tissue samples and Sue Nicholson for helping me in measuring ethylene. I am also thankful to Ian King and Julie Ryan who helped me in taking care of Arabidopsis. Thanks to V. Vaughan Symonds who taught me about evolution. I also want to thank Marian McKenzie, David Brummell, Erin O'Donoghue and David Lewis for their welcoming attitudes. Special thanks to NZSPB and NZSBMB for financial support to attend the national and international conferences.

I thank my brothers Zafar, Asim, Qasim, and sister Maryium who made my every day a fun day. I am highly thankful to my colleagues and friends (Steve Arathoon, Annet Deveries, Jay Jarayaman, Alvina Grace Lai, Afsana Islam, Muhammad Faisal, Mathew Giles, Susana Leung, Srishti Joshi, Nick Albert, Lyn Watson, Jun Zhou, Diantha Smith, Sam, Ihsan, and Daniel) for their support, help, and good times in New Zealand. Thanks to Massey University

for financially supporting my PhD and Plant and Food Research for hosting me during my research.

It was hard for me being a mother to manage this journey alone but you, Jibran, did beyond the appreciation. I don't have words to say thanks to you, but I really appreciate your support that you provided me as a husband, colleague, competitor, and most importantly as a father of my lovely girls. I extend my appreciation to my mother in law Badar Tahir and father in law Tahir Hussain who provided moral and financial support through this journey. Special thanks to my lovely daughters Elizay and Adivay who have given me the endless happiness of life and I enjoyed the every single moment with both of them. Deeply, I acknowledge my father Muhammad Zubair and mother Razia Begum, who trusted on me and encouraged me during the hard periods of my life. Thanks to God who blessed me with patience, health, and happiness. I dedicate this thesis to my parents.

Table of contents

List of Figures

List of Tables

Abbreviations

AAF	ARABIDOPSIS A FIFTEEN
ABA	abscisic acid
ABI3	ABSCISIC ACID INSENSITIVE 3
ACC	1 aminocyclopropane 1 carboxylic acid
ACO	1 AMINOCYCLOPROPANE 1 CARBOXYLATE OXIDASE
ACS	1 AMINO CYCLOPROPANE 1 CARBOXYLATE SYNTHASE
AHK1	ARABIDOPSIS HISTIDINE KINASE 1
ag-1	*agamous-1*
agl	*agamous-like*
agl15	*agamous like 15*
ais	*accelerated inflorescence senescence*
AMP	adenosine monophosphate
AMPK	ADENOSINE MONOPHOSPHATE ACTIVATED PROTEIN KINASE
ANAC	ABSCISIC-ACID-RESPONSIVE NO APICAL MERISTEM *ARABIDOPSIS THALIANA* ACTIVATING FACTOR1/2 CUP-SHAPED COTYLEDONS 2
AP	APETALA
APG	autophagy
ARR2	ARABIDOPSIS RESPONSE REGULATOR 2
AS	ANTHRANILATE SYNTHASE
NAP	NAC-LIKE ACTIVATED BY AP3/PI
ant5	*arabidopsis nac domain containing protein 5*
aos	*allene oxide synthase*
AOS	ALLENE OXIDE SYNTHASE
ARCs	age-related changes
ASK1	ARABIDOPSIS SERINE/THREONINE KINASE 1
Asn	asparagine
ATP	adenosine triphosphate
AZF2	A Cys2/His2 TYPE ZINC FINGER 2
6-BAP	6-benzylaminopurine

BoCLH	*Brassica oleracea* CHLOROPHYLLASE
BoPaO	*Brassica oleracea* PHEOPHORBIDE A OXYGENASE
BOT1	BOTERO1
BoCP1	*Brassica oleracea* CYSTEINE PROTEASE
BR	Brassinosteroids
bri1	*brassinosteroids insensitive 1*
bp	base pair
BZIP1	BASIC LEUCINE-ZIPPER 1
CAB	CHLOROPHYLL A/B BINDING PROTEIN
CBF2	C-REPEAT/DRE BINDING FACTOR 2
CKs	cytokinins
CKX6	CYTOKININ OXIDASE/DEHYDROGENASE 6
cM	centimorgan
CND41	CHLOROPLAST NUCLEOID DNA-BINDING 41
Col-0	Columbia-0
coi1	*coronatine insensitive 1*
COS1	CORONATINE INSENSITIVE 1 SUPPRESSOR 1
CPR5	CONSTITUTIVE EXPRESSION OF PR GENES 5
cuc1	*cup shaped cotyledon 1*
cuc2	*cup shaped cotyledon 2*
DAD1	DEFECTIVE IN ANTHER DEHISCENCE 1
DDE2	DELAYED DEHISCENCE 2
DET	detached dark-held leaves
dis	*delayed inflorescence senescence*
DIS	attached shaded leaves
D-2HG	d-2-hydroxyglutarate
d-2HGDH	d-2-HYDROXYGLUTARATE DEHYDROGENASE
dls1	*delayed senescence 1*
DNA	deoxyribonucleic acid
AtαDOX1	ARABIDOPSIS ALPHA-DIOXYGENASE 1
EBF1	ETHYLENE-INSENSITIVE 3-BINDING F BOX PROTEIN 1
EBF2	ETHYLENE-INSENSITIVE 3-BINDING F BOX PROTEIN 2
EEP	EARLY EXTRA PETALS
EIN2	ETHYLENE INSENSITIVE 2

EIN3	ETHYLENE INSENSITIVE 3
EIL3	ETHYLENE-INSENSITIVE 3 LIKE
EMS	ethyl methane-sulphonate
ER	ethylene receptor
EREBP	ETHYLENE RESPONSE ELEMENT BINDING PROTEIN
ERF	ETHYLENE RESPONSE FACTOR
ESTs	expressed sequence tags
ESR	EPITHIOSPECIFYING SENESCENCE REGULATOR
ETD	ethylene detector
ETP1	ETHYLENE INSENSITIVE 2 TARGETING PROTEIN 1
ETR1	ETHYLENE RESPONSE 1
ETR2	ETHYLENE RESPONSE 2
F1	*filial 1*
F2	*filial 2*
FTS	FILAMENTING TEMPERATURE-SENSITIVE
FTSH5	FILAMENTOUS TEMPERATURE SENSITIVE H PROTEIN 5
g	gravity or g-force
GA	gibberellic acid
GABA	gamma-aminobutyric acid
GDH	GLUTAMATE DEHYDROGENASE
GIN2	GLUCOSE INSENSITIVE 2
GFP	green fluorescent protein
Gln	glutamine
GMO	genetically modified organism
GmSARK	GLYCINE MAX SENESCENCE-ASSOCIATED RECEPTOR-LIKE KINASE
GS	GLUTAMINE SYNTHETASE
GUS	β-glucuronidase
HIF	heterogeneous inbred family
HRM	high-resolution melting
HXK	HEXOKINASE
IDT	integrated DNA technologies
IPT	ISOPENTENYL TRANSFERASE
JA	jasmonic acid

JAZ10	JASMONATE-ZIM-DOMAIN PROTEIN 10
KIN10	KINASE 10
LP	left primer
LBP	left border primer
L*er*-0	Landsberg *erecta*-0
LC-MS	liquid chromatography-mass spectrometry
lfy-4	*leafy-4*
lfy-5	*leafy-5*
LOX	LIPOXYGENASE
LRR	leucine-rich repeat
LHCII	LIGHT HARVESTING COMPLEX II
M	molar
MAPK	MITOGEN-ACTIVATED PROTEIN KINASES
MAP65	MICROTUBULES ASSOCIATED PROTEIN 65
MAP70-1	MICROTUBULES ASSOCIATED PROTEINS 70-1
MeJA	methyl jasmonate
Mg^{2+}	magnesium
µg	microgram
µL	microlitre
µM	micromolar
min	minutes
mg	milligram
mL	milliliter
mM	millimolar
MKK	MITOGEN-ACTIVATED PROTEIN KINASE KINASE
MMP	MATRIX METALLOPROTEINASE
MT	microtubules
ms5	*male sterile 5*
MYB	myeloblastosis
MYBL	MYELOBLASTOSIS-LIKE PROTEIN
MYC2	MYELOCYTOMATOSIS VIRAL ONCOGENE 2
NAC	NAM (NO APICAL MERISTEM), ATAF1,2 (Arabidopsis thaliana NAC transcription factor1,2) and CUC2 (CUP SHAPED COTYLEDON 2)

NCCs	non-fluorescent chlorophyll catabolites
ncRNA	non coding RNA
NIKS	needle in *K*-stack
NGS	next generation sequencing
NO	nitric oxide
NOL	NYC-ONE LIKE
NR	NITRATE REDUCTASE
NS	natural leaf senescence
NOS1	NITRIC OXIDE SYNTHASE 1
NTAG1	CHINESE NARCISSUS AGAMOUS HOMOLOGUE 1
NYC1	NON-YELLOW COLORING 1
$^1O_2$	singlet oxygen
O_2	oxygen
2OG	2-oxoglutarate
ORA59	OCTADECANOID-RESPONSIVE ARABIDOPSIS AP2/ERF 59
OLD5	ONSET OF LEAF DEATH 5
OPR3	OXOPHYTODIENOATE REDUCTASE 3
ore	*oresara*
ORF	open reading frame
PAO	PHEOPHORBIDE A OXYGENASE
PCD	programmed cell death
PCR	polymerase chain reaction
PDF1.2	PLANT DEFENSE 1.2
pH	potential of Hydrogen
PI	PISTILLATA
Pi	inorganic phosphate
PHEIDE A	PHEOPHORBIDE A
PLD-α	PHOSPHOLIPASE D-A
PPH	PHEOPHYTIN PHEOPHORBIDE HYDROLASE
PPDK	PYRUVATE ORTHOPHOSPHATE DIKINASE
PT2	PHOSPHOROUS TRANSPORT 2
qRT-PCR	quantitative real-time polymerase chain reaction
RAP2.4	RELATED TO AP 2.4
RAV1	RELATED TO ABI3/VP1

RCBs	rubisco-containing bodies
RCC	red chlorophyll catabolite
RCCR	RED CHLOROPHYLL CATABOLITE REDUCTASE
reb1-1	*rabbit ears 1-1*
DsRed	red fluorescent proteins
RLK	receptor like kinases
ROS	reactive oxygen species
RNA	ribonucleic acid
RNAi	RNA interference
RNS2	RIBONUCLEASE 2
RP	right primer
RPK1	RECEPTOR-LIKE PROTEIN KINASE 1
RTPCR	reverse transcriptase PCR
AtS40-3	ARABIDOPSIS SENESCENCE 40-3
SA	salicylic acid
SAGs	senescence associated genes
SAVs	senescence-associated vacuoles
SAUL1	SENESCENCE-ASSOCIATED E3 UBIQUITIN LIGASE 1
SEN1	SENESCENCE 1
SEN4	SENESCENCE 4
sep1/sep2/sep3	*sepallata 1/ sepallata 2 /sepallata 3*
SGR	STAY-GREEN
sid2	*salicylic acid induction deficient 2*
SIRK	SENESCENCE-INDUCED RECEPTOR LIKE KINASE
SnRK	SUCROSE NON-FERMENTING RELATED PROTEIN KINASE
Snf1	SUCROSE NON-FERMENTING
SNP	single nucleotide polymorphism
TAIR	The Arabidopsis Information Resource
TCA	tricarboxylic acid
T6P	trehalose-6-phosphate
VIN2	VACUOLAR INVERTASE ENZYME 2
VP1	VIVIPAROUS-1
VSP1	VEGETATIVE STORAGE PROTEIN 1
VTC1	VITAMIN C DEFECTIVE 1

WGS	whole genome sequencing
wt	wild-type
XDH	XANTHINE DEHYDROGENASE

Blank page

Blank page

Chapter 1

Blank page

Chapter 1 Senescence overview

Senescence is the final stage in the development of a leaf that may lead to the death of the whole plant. During leaf senescence, macromolecules are sequentially degraded and nutrients remobilized from dying parts of the plant to growing parts including newly emerging leaves (Noodén, 1988; Noodén et al., 1997). Although at first glance senescence may appear to be a deleterious process, it is in fact an evolutionarily selected developmental programme. The programme contributes to the fitness of whole plants by ensuring their optimal production of offspring and better survival in their given temporal and spatial niches (Noodén, 1988; Lim et al., 2007; Gregersen et al., 2008; Thomas et al., 2009).

Plant senescence can be categorized as monocarpic or polycarpic. Monocarpic plants die after they reproduce, which can be after several years. Senescence of monocarpic plants is associated with three coordinated processes, senescence of somatic cells and tissues (e.g., in the leaf), arrest of the shoot apical meristem and suppression of axillary buds to inhibit formation of new shoots (Davies and Gan, 2012; Guo and Gan, 2012; Thomas, 2013). Polycarpic plants, by contrast, can grow and reproduce for up to thousands of years. For example, giant sequoia trees can live for 3200 years before they die (Thomas, 2013).

Whole plant senescence of monocarpic plants occurs in annuals (e.g., Arabidopsis), biennials (e.g., wheat) and perennials (e.g., bamboo) and is associated with grain filling and maturation (Lim et al., 2007). Thus, whole plant senescence of monocarpic plants is under correlative control of reproduction and as such critically dependent on the plant developmental programme (Davies and Gan, 2012). In some monocarpic plants, e.g., Arabidopsis, although whole plant senescence is under correlative control, senescence of the individual leaves is not (Henkel et al., 1993; Nooden and Penney, 2001). Interestingly, correlative control is not unique to plants, but is also seen in some animals such as mayfly and octopus (Skulachev and Longo, 2005).

Leaf senescence occurring during favourable growth conditions has been defined as age- or developmentally-induced senescence. It is regulated by the interaction of various developmental (e.g., age), hormonal (e.g., ethylene) and environmental factors (e.g., dark)

(Lim et al., 2003). Age-dependent leaf senescence is typically a slow but active process that initiates in mesophyll cells at the leaf tip and progresses towards the leaf base (Noodén et al., 1997). Leaf senescence can also be induced rapidly by various stresses such as darkness and detachment and this is known as artificially induced leaf senescence (Lim et al., 2007). Various transcriptomic studies have revealed both differences and commonalities between the developmentally- and artificially-induced senescence programmes (Buchanan-Wollaston et al., 2005; van der Graaff et al., 2006; Trivellini et al., 2012).

Leaf senescence is accompanied by distinctive structural and biochemical changes (Thompson et al., 1987; Noodén, 1988), which proceed in an ordered manner and reflect the transition from anabolic to catabolic metabolism in the cells (Bate et al., 1991; Bleecker and Patterson, 1997). Chloroplast disassembly occurs early and is associated with chlorophyll loss and degradation of proteins, such as ribulose 1-5 biphosphate carboxylase (Rubisco) and chlorophyll a/b binding protein (CAB) (Thomas and Stoddart, 1980; Matile et al., 1996; Gan and Amasino, 1997). The nucleus and mitochondria remain intact until the last stages of senescence in order to provide instructions and essential energy for progression of senescence (Taylor et al., 1993). Macromolecules, such as proteins and lipids are hydrolysed and remobilized. Proteins are hydrolyzed by senescence-associated cysteine proteases present in the vacuole (Brouquisse et al., 2001; Hortensteiner and Feller, 2002). Membrane lipids are hydrolyzed by phospholipase D, phosphatidic acid phosphatase, lytic acyl hydrolase and lipoxygenase (Ueda and Kato, 1980; Thomson and Platt-Aloia, 1987). At the end of their life, plant cells show typical symptoms of animal programmed cell-death (PCD), such as controlled vacuolar collapse, chromatin condensation and DNA laddering (van der Graaff et al., 2006; Cao et al., 2007). Cell death finally occurs when the plasma membrane loses its integrity and cellular homeostasis is disrupted (Lim et al., 2007).

Proper timing of senescence confers various plant fitness benefits by influencing multiple characteristics of plants. Senescence maximises the active leaf area available for photosynthesis by controlling leaf turnover in the canopy. The programme supports growth in the following season by redirecting nutrients to storage organs (Lewandowski and Heinz, 2003; Robson et al., 2012). Senescence influences the yield in cereal crops, such as wheat and barley by remobilising nutrients from old leaves to grains. Improper timing of senescence conversely can negatively affect the yield of crop-grown plants and on the quality of produce following harvest.

Thus, the study of the mechanisms underlying leaf senescence not only provides insight into a fundamental developmental process, but may also lead to crops that have significant economic benefit.

1.1 Age-related leaf senescence

Leaf senescence is a succession of physiological and molecular events, which can be categorized into three stages initiation, degeneration and termination (Yoshida, 2003). In Arabidopsis, leaf senescence initiates when a particular developmental time point is reached. It is when photosynthetic activity declines as the leaf transforms from a sink to source. The degeneration stage is characterized by the disassembly of cellular components and degradation of their macromolecule components. The termination stage is characterized by the initiation of apoptosis-like processes, such as chromatin condensation and DNA laddering, leading to the death of the whole leaf.

Leaf transcriptome studies have offered new insight into the complex web of senescence control, providing snapshots in time of multiple pathways working in concert to orderly dismantle the tissue. The collections of senescence associated genes have been identified through sequencing of expressed sequence tags (ESTs) of libraries derived from senescent leaf tissues (Guo et al., 2004) and microarray profiling (Lin and Wu, 2004; Buchanan-Wollaston et al., 2005; van der Graaff et al., 2006; Breeze et al., 2011). These studies have highlighted the importance of transcript abundance changes during progression of the senescence programme. For example, large numbers of catabolic-genes (involved in degradation of proteins, lipids and nucleotide) and signalling genes (involved in controlling the signalling of the senescence process) are up-regulated during leaf senescence and genes involved in the photosynthetic and anabolic processes, such as, chlorophyll a/b binding (CAB) and Rubisco protein are down regulated. Meta-analysis of transcript profiles of genes altered during age- and artificially-induced leaf senescence has revealed that transcriptome changes can be very different during senescence initiation, but very similar when the programme is executing irrespective of how it is initiated (Guo and Gan, 2012).

1.1.1 Metabolites affecting age-related leaf senescence

The onset and progression of leaf senescence is mediated by the interplay between age and various molecular entities such as hormones, enzymes and metabolites. Senescence can also be regulated by source-sink relationships particularly during the reproductive phases of growth (van Doorn, 2008a). These internal factors are controlled by a complex network of regulatory genes and can be modulated by external environmental factors, such as darkness, detachment, drought and oxidative stress (Li et al., 2012b). This section describes the effect of various substances such as carbohydrates, hormones, ROS and NO on the initiation of leaf senescence in intact plants.

1.1.1.2 Sugars

Sugars are produced by photosynthesis in mature (source) leaves and transported in the form of sucrose to young (sink) growing leaves. Both leaf sugar status and light-mediated signalling control growth activities in mature and young leaves. Low sugar concentrations enhance photosynthetic activities, sucrose export and nutrient re-mobilization to young leaves. Conversely, high sugar concentrations decrease photosynthetic activity in order to maintain sugar homeostasis (Rolland et al., 2006).

In addition to serving as nutrients, sugars regulate diverse plant growth and development processes including cell division, embryo establishment, seed germination, flowering, leaf development and senescence (Eveland and Jackson, 2012). Sugars regulate these processes by crosstalk with other factors such as light, stress, carbon to nitrogen ratios and hormone signalling components (Rolland et al., 2002). Hence, the role of sugars in leaf senescence has been complicated because of its dual function as a metabolite and signalling molecule in a wide variety of processes.

Researchers have long debated whether sugars act to promote or inhibit leaf senescence, because yellowing occurs in both dark-held tissues that are carbon-starved and in naturally senescing leaves that accumulate high concentrations of hexoses (Van Doorn, 2008b; Wingler et al., 2009). Evidence for higher sugar concentrations inducing leaf

senescence has come from studies investigating carbohydrate mobilization between source and sink. Carbon is mobilised from fully mature photosynthetically active leaves to young growing leaves until the young leaves begin producing their own photosynthates (Ono et al., 2001). At this stage, sugar import into the young leaves is inhibited and the older leaves accumulate higher concentrations of sugars. This increased sugar accumulation correlates strongly with the occurrence of senescence in the leaf tissue suggesting that the change in carbon partitioning between sink and source is the actual trigger of onset of the programme. Similarly, disruption in nutrient export of wheat leaves by stem-girdling results in early leaf senescence, which was attributed to the increased accumulation of carbohydrates (Fröhlich and Feller, 1991). The source-sink senescence hypothesis is further supported by the delayed senescence phenotype of old leaves of darkened plants. This was attributed to the older leaves reinitiating export of carbon to the young leaves because of the inability of the darkened new leaves to photosynthesize (Ono et al., 2001).

The view that age-related leaf senescence is driven by increased accumulation of sugars is further supported by meta-analysis of microarray data on developmental leaf senescence; dark-induced leaf senescence; intact seedlings fed glucose in presence of low or high N_2 and carbon-starved cell cultures (Wingler et al., 2009). The transcript abundance changes during developmental leaf senescence clustered most closely with seedlings fed glucose in the presence of low N_2 suggesting that developmental leaf senescence is triggered more by high sugar and low nitrogen conditions than by starvation and/or dark stresses. Consistent with the above is the finding that exogenously applying glucose to Arabidopsis seedlings causes precocious leaf senescence (Craftsbrandner et al., 1984; Wingler et al., 1998; Quirino et al., 1999; Stessman et al., 2002). This is also supported by the observation that transcripts of *SAG12*, a widely used marker of age-associated leaf senescence, increased 900-fold in the leaves of nitrogen starved Arabidopsis seedlings fed glucose (Pourtau et al., 2004).

Increasing amounts of data suggest that the elevated sugar concentration in old leaves causes senescence through hexokinase (HXK) activity. HXK is involved both in phosphorylation (catalytic) and sensing of glucose (Harrington and Bush, 2003; Moore et al., 2003). Leaf senescence is accelerated in HXK over-expressing plants and inhibited in HXK antisense Arabidopsis transgenic plants (Jang et al., 1997; Dai et al., 1999; Xiao et al., 2000).

When phosphorylation by HXK is inhibited, e.g., in the Arabidopsis *glucose insensitive2* (*gin2*) mutant, glucose sensitivity is reduced and senescence delayed (Quirino et al., 2000).

Data suggesting that senescence is initiated by declining sugar concentration is limited. It comes mostly from studies where individual detached leaves were induced to senesce by darkness (section 1.3.2.1). However, senescence also happens rapidly in individually shaded attached leaves in an age-dependent manner (Weaver and Amasino, 2001). This led Weaver and Amasino to propose that source-sink status, light and nitrogen concentrations integrate to regulate leaf senescence during sugar-starved conditions. Interestingly the authors also found that leaves of whole plants incubated for an extended period in the dark showed decreased senescence upon subsequent reexposure to light compared with leaves of plants that did not experience the dark period. Thus, the imbalance in carbohydrate homeostasis appears to an important determinant of onset and progression of leaf senescence.

1.1.1.2 Hormones

Hormones play a crucial role in developmental processes as well as in the integration of environmental signals to plant development. Indeed, all classical hormones have been described to play a role in the regulation of leaf senescence (Schippers et al., 2007). For example, senescence is accelerated by ethylene, jasmonic acid (JA), abscisic acid (ABA) and salicylic acid (SA) and delayed by auxin, gibberellic acid (GA) and cytokinins (CKs). Defense-related hormones, such as ethylene, JA and SA increase during the later stages of leaf senescence (Breeze et al., 2011; Guo and Gan, 2012) and were proposed to protect the plant from biotic infections because older leaves become more susceptible to biotic hazards (von Saint Paul et al., 2011). Hormones can potentially affect leaf senescence during all three leaf developmental stages: (1) by affecting leaf development and as such altering the time by which the leaf acquires competence to senesce (2) by integrating environmental signals and (3) by affecting the speed at which the senescence process occurs, once the leaf has committed to senesce. For a review on the role of hormones in controlling developmental senescence, see Jibran et al., (2013) and Schippers et al., (2007).

1.1.1.3 Reactive oxygen species (ROS)

Age-related or stress-induced leaf senescence results in increased production of superoxides, hydrogen peroxide, hydroxyl radicals and singlet oxygen (O^-) collectively known as reactive oxygen species (ROS) (Bhattacharjee, 2005). Functional studies of genes involved in ROS production and antioxidant enzymes have demonstrated the significance of redox factors and antioxidant enzymes in the regulation of leaf senescence. For example, OLD5/CPR5 causes accelerated leaf senescence in Arabidopsis due to deregulation of the cellular redox balance (Jing et al., 2008). Furthermore, the Arabidopsis delayed leaf senescence *ore1*, *ore3* and *ore9* mutants have increased tolerance to oxidative stress indicating close association between leaf senescence and ROS (Woo et al., 2004). Increased amounts of ROS cause lipid peroxidation, cellular damage and cell death (Kukavica and Jovanovic, 2004). ROS can also cause senescence by acting as signalling molecules to activate genetic components of the programme (Khanna-Chopra, 2012). For example, ozone induced cell death was inhibited in the *ein2* mutant (Overmyer et al., 2000). ROS are also produced because of hormone activity. For example, ABA induces ROS production in senescing leaves of rice (Hung and Kao, 2004) and JA causes leaf senescence both in barley and rice through ROS production (Zhang and Xing, 2008).

1.1.1.4 Nitric oxide (NO)

Nitric oxide (NO) is an unstable free radical gas and its lipophilic nature allows it to pass through cell membranes without a requirement for any specific membrane transporters (Feldman et al., 1993; Leshem, 1996). Plants produce NO during nitrogen assimilation i.e. during conversion of nitrate into nitrite by NITRATE REDUCTASE (NR) (Rockel et al., 2002). NO generation and leaf senescence are closely associated. Decreased emission of NO in loss of function mutants *nos1* (*nitric oxide synthase 1*) or transgenic Arabidopsis plants expressing NO degrading enzymes leads to accelerated leaf senescence (Guo and Crawford, 2005; Mishina et al., 2007).

The senescence inhibiting effect of NO is attributed to its ability to disrupt lipid peroxidation, preserve photosynthetic pigments and prevent the formation of hydroxyl

radicals (ROS) (Wink et al., 1995). Guo and Crawford (2005) proposed that NO acts as an antioxidant during dark-induced leaf senescence in Arabidopsis. NO may also regulate senescence by affecting ethylene production and signalling. For example, NO reduces ATP-METHIONINE S-ADENOSYLTRANSFERASE activity, which decreases ethylene production (Leshem, 1996) and recently it was found that the early leaf senescence caused by NO deficiency is regulated by EIN2 (Niu and Guo, 2012).

In the cell, the above-mentioned factors influence the timing of leaf senescence through affecting signalling pathways, which are discussed in the following section.

1.1.2 Age-related senescence signal transduction

Metabolites influence senescence progression through signal transduction pathways. Senescence signalling starts with receptor(s) perceiving the metabolites. The signal(s) is then relayed through protein phosphorylation/dephosphorylation events to eventually modulate activity of transcription factors in the nucleus to drive expression of the target genes. Proteins that modify chromatin architecture also regulate senescence-associated transcription (Balazadeh et al., 2008). In addition, post-transcriptional processing mediated by the 26S-proteosomal degradation pathway also intricately controlled senescence-associated signalling (Section 1.2.3.6).

More than 150 genes encoding putative enzymes of signal perception and signal transduction pathways are up-regulated during senescence (Buchanan-Wollaston et al., 2005; van der Graaff et al., 2006).

1.1.2.1 Senescence-associated hormone receptors

The role of ETHYLENE RESPONSE 1 (ETR1), a component of the ethylene transduction pathway, in perception of senescence signal was suggested by the delayed leaf senescence phenotype of *etr1-1* in Arabidopsis and overexpression of a mutant form of the ETR1-1 in transgenic tobacco (Grbic and Bleecker, 1995; Oh et al., 1997; Yang et al., 2008; Shi et al., 2012). There are three cytokinin receptors in Arabidopsis. One of them, AHK3, was shown to mediate the cytokinin-induced delay in leaf senescence. AHK3 does this by phosphorylating ARR2, a type B Arabidopsis response regulator (Kim et al., 2006). BRI1 (BRASSINOSTEROID INSENSITIVE 1) is a cell surface plasma-membrane localized protein that perceives brassinosteroid signals (Clouse et al., 1996; Wang et al., 2001). The BRI1 receptor was found to regulate leaf senescence. For instance, *bri1* null mutants displayed prolonged life span concomitant with reduced transcript abundance of several SAGs (He et al., 2007) and the *bri1-EMS-suppressor 1* exhibited accelerated senescence due to a constitutively active BR response pathway (Yin et al., 2002).

1.1.2.2 Senescence-associated receptor-like protein kinases (RLKs)

Plant receptor-like kinases (RLK) also known as cell surface receptors, are transmembrane proteins that have amino-terminal extracellular domains to perceive signals and carboxyl-terminal intracellular kinase domains to phosphorylate specific substrates for transducing the signal downstream (Stone and Walker, 1995; Shiu and Bleecker, 2001). Several motifs are present in the putative extra-cellular domain of RLKs. These motifs bind to various proteins and carbohydrates. In Arabidopsis, the majority of RLKs have a LRR (leucine-rich repeat) motif in their extra-cellular domain that participates in protein-protein interactions (Kobe and Kajava, 2001; Kinoshita et al., 2005). RLKs regulate plant growth and development, plant-microbe interactions, stress responses and senescence (Shiu and Bleecker, 2001).

RLKs associated with senescence include the receptor like kinase (SARK) and the LRR-senescence-induced receptor like kinase (SIRK) which show increased transcript abundance in bean and Arabidopsis leaves, respectively (Hajouj et al., 2000; Robatzek and Somssich, 2001). GmSARK (GLYCINE MAX SENESCENCE-ASSOCIATED RECEPTOR-LIKE KINASE), which is up-regulated in senescing soybean leaves, is proposed to regulate soybean leaf senescence by controlling chloroplast development and chlorophyll accumulation (Xu et al., 2011b). For example, GmSARK-RNAi soybean transgenic lines showed delayed leaf senescence (Li et al., 2006). Similarly, increased expression of Arabidopsis AtSARK, an ortholog of GmSARK, resulted in precocious leaf senescence (Xu et al., 2011b), whereas T-DNA mutant of AtSARK showed delayed leaf senescence (Xu et al., 2011b). GmSARK and AtSARK promote autophosphorylation of both serine/threonine and tyrosine residues of target proteins.

1.1.2.3 Senescence-associated sucrose Non-fermenting Related Protein kinases

The SnRK (SUCROSE NON-FERMENTING RELATED PROTEIN KINASE) family of plants is closely related to Snf1 (SUCROSE NON-FERMENTING) of yeast and AMPK (ADENOSINE MONOPHOSPHATE ACTIVATED PROTEIN KINASE) of mammals (Rolland et al., 2006). Snf1 of yeast controls the transition from a fermentative to oxidative (respiratory) metabolism when glucose becomes limiting. This results in the ethanol formed during fermentation being used to produce ATP (Polge and Thomas, 2007). Similarly, AMPK in mammalian cells senses the ratio of AMP to ATP, e.g., during exercise and turns off ATP consuming pathways (e.g., fatty acid synthesis) and on ATP producing pathways (e.g., fatty acid oxidation and glycolysis).

In plants, SnRK1 appears to have a similar role in the control of energy or carbon depletion. Arabidopsis plants with increased expression of KIN10, a catalytic subunit of SnRK1, show increased survival under a low light intensity that limits photosynthesis (Baena-González et al., 2007). This is consistent with KIN10 being activated by low glucose or darkness to induce catabolic genes (e.g., ALPHA AMYLASE for starch degradation; SUCROSE SYNTHASE for sucrose breakdown) leading to ATP generation (Baena-González et al., 2007; Polge and Thomas, 2007). The plants also showed delayed flowering and whole plant senescence when grown under long days (16 h photoperiod). The authors suggested that this is reminiscent of life span extension by caloric restriction seen in some animals.

1.1.2.4 Senescence-associated mitogen-activated protein kinases (MAPK)

A number of mitogen-activated protein kinases (MAP), also known as mitogen protein kinases (MPKs), are up-regulated during senescence. MAP kinase cascades relay the signals derived from extracellular stimuli to a wide range of cellular responses in animals and yeast (Zhou et al., 2009). Recent data suggests that certain MPKs also control senescence timing. For example, in Arabidopsis, phosphorylation of MPK6 by MKK9 (MAP KINASE KINASE 9) causes leaf senescence and when either *MKK9* or *MPK6* is silenced, leaf senescence is delayed (Zhou et al., 2009).

1.1.2.5 Senescence-associated transcription factors

Perception and transduction of senescence inducing signal(s) up-regulates transcription factors that in turn execute senescence-related gene expression by binding to specific *cis* elements in the promoters of the targeted genes (Gepstein et al., 2003).

Transcription factors up-regulated during age-induced leaf senescence include NAC, WRKY, C2H2-type zinc finger, AP2/EREBP and MYB (Buchanan-Wollaston et al., 2005; Breeze et al., 2011). The strong association of certain transcription factor families with senescence was recently highlighted by Li et al., (2012a) who used information from the Leaf Senescence Database (Liu et al., 2011). The two largest groups of senescence-associated transcription factors are WRKY and NAC transcription factors.

The WRKY gene family comprises 72 to 100 members (Eulgem et al., 2000; Riechmann et al., 2000). WRKY transcription factors bind the W box *cis* element sequence (TGACC/T) in target promoters (Eulgem et al., 2000; Yu et al., 2001). WRKY transcript abundance increases in tissues as part of the defense response and during age-related leaf senescence (Robatzek and Somssich, 2002; Liu and Howell, 2010; Breeze et al., 2011). In Arabidopsis, WRKY6 has an early role in leaf senescence where it targets and up-regulates SAGs including the receptor like protein kinase *SIRK* (Robatzek and Somssich, 2002). WRKY54 and WRKY70 both interact with WRKY30 and by doing this they negatively regulate leaf senescence in a partially redundant manner. However, WRKY53 positively regulates leaf senescence by interacting with WRKY30. Furthermore, the interaction of both positive and negative regulators of leaf senescence with WRKY30 is independent of each other (Besseau et al., 2012).

NAC family proteins are plant specific transcription factors that have a highly conserved N-terminal DNA binding domains known as the NAC domain. NAC proteins bind to the sequences TTNCGTA and TTGCGTGT in target promoters (Olsen et al., 2005). There are more than one hundred NAC genes in Arabidopsis (Riechmann et al., 2000). The NAC transcription factor group appears to be a key element in the regulation of senescence. Approximately one fifth of the genes encoding NAC proteins (20 genes out of 109 genes number) show increased expression during developmental- and dark-induced senescence

(Guo et al., 2004). Their senescence association is more likely due to promoter activation (Guo and Gan, 2006), but they can also be regulated post-transcriptionally. For example, *ore1*/ *ANAC092* transcript abundance is decreased by miR164 that cleaves the transcript (Kim et al., 2009). The functional importance of NAC family members in controlling natural senescence has been confirmed through the use of T-DNA knock out mutants, RNAi-based and over-expression approaches. Depending on the type of NAC gene, over-expression or suppression can result in delayed senescence suggesting that they are both positive and negative regulators of the programme (Guo and Gan, 2006; Hu et al., 2006; Balazadeh et al., 2010; Balazadeh et al., 2011).

Transcription factors in other families can also alter senescence timing although the linkage of their family as a whole to the senescence programme is less than that for the NAC and WRKY transcription factors. For example, overexpressing the MADS-box transcription factor AGL15 delays leaf senescence (Li et al., 2012b), whereas overexpressing the ABI3/VP1 type transcription factor RAV1 accelerates the programme (Woo et al., 2010b).

Other proteins can alter transcription associated with senescence by modifying chromatin architecture or through their cleavage and translocation of their cleaved peptide to the nucleus. For example, ORE7, a protein with an AT hook DNA binding motif negatively affects transcription of senescence-related genes by modifying chromatin architecture (Balazadeh et al., 2008). EIN2 is similar to NRAMP metal ion transporter proteins and is localized to endoplasmic reticulum (Alonso et al., 1999). In the presence of ethylene, the carboxyl terminus of EIN2 is cleaved and moves to the nucleus where it participates in promoter activation (Ju et al., 2012). EIN2 controls senescence timing in part through regulating transcript abundance of the ethylene-inducible positive regulator of senescence *ANAC092*/*ORE1*/*AtNAC2* (Kim et al., 2009). Transcript accumulation of *ANAC092* increases during developmental senescence because its promoter is more active (Balazadeh et al., 2010) and EIN2 causes an age-related decline in miR164, which targets *ANAC092* transcripts for degradation (Kim et al., 2009).

1.1.2 Degradation pathways activated during age-related leaf senescence

One of the hallmarks of senescence is an ordered dismantling of the organelles and degradation of their macromolecular constituents, the proteins, nucleic acids, chlorophyll, lipids and carbohydrates (Noodén et al., 1997).

1.1.3.1 Chloroplast degradation

The dismantling of the chloroplast and its components is the most conspicuous and ordered event of senescence (Noodén et al., 1997). Controlled chloroplast disassembly is important for efficient reutilization of the large quantity of nitrogen tied up in the organelle. It also prevents the rapid death that can be caused by uncontrolled release of toxic intermediates of chlorophyll catabolism (Hörtensteiner, 2006). Up to 75% of the leaf nitrogen present in mesophyll cells, is tied up as protein in the chloroplasts and the majority of this, up to 50%, is in the form of Rubisco (Feller et al., 2008). Various mechanisms have been proposed to account for the degradation of chloroplast components, particularly the photosynthetic proteins, such as Rubisco and chlorophyll a/b binding proteins (Hortensteiner and Feller, 2002). Rubisco degradation and chlorophyll catabolism are often well correlated and are considered as major indicators of senescence symptoms, but under certain conditions these two processes may be partially or completely uncorrelated, such as in stay-green mutants (Hortensteiner and Feller, 2002; Hörtensteiner, 2006).

The initial degradation steps of chloroplast proteins appear to occur in the intact organelle, however later catabolic steps may be located outside of the plastid (Hortensteiner and Feller, 2002). Often no Rubisco fragments are detected in naturally senescing leaves, but they are observed in leaves induced to senesce under low light (Thoenen et al., 2007). It was proposed that when carbohydrates are in excess, Rubisco is preferentially degraded in plastids, whereas under low carbohydrates (energy deficiency conditions) Rubisco is broken down by vacuolar endo-peptidases (Feller et al., 2008). Evidence for plastid-derived proteolytic cleavage of Rubisco during senescence has come from the study of CND41, a DNA-binding aspartic protease that degrades Rubisco *in vitro* at physiological pH.

Suppression of CND41 in antisense *cnd41* tobacco plants delayed chlorophyll and protein loss (Kato et al., 2005).

A novel class of lytic vacuoles has been found in senescing leaves of soybean and Arabidopsis (Otegui et al., 2005). These senescence-associated vacuoles (SAVs) are small in diameter and more acidic than the central vacuole. SAVs usually occur in chloroplast-containing mesophyll cells and have high proteolytic activity *in vivo*, so it has been postulated that SAVs might be involved in degradation of chloroplast proteins during senescence. Moreover, isolation and biochemical analysis of SAVs indicate that chloroplast components are found in SAVs of senescing leaves and isolated SAVs possess ability to degrade Rubisco. Therefore, these observations suggest that SAVs are a specific class of vacuole involved in degradation of the photosynthetic machinery during senescence (Martinez et al., 2008).

1.1.3.2 Chlorophyll breakdown

Chlorophyll is composed of a heterocyclic aromatic ring (chlorin) with an Mg^{2+} ion in the centre surrounded by several side chain groups. The type of side groups attached to the chlorin ring determines the type of chlorophyll. In chlorophyll b the methyl ($-CH_3$) group of the ring is replaced by an aldehyde. Chlorophyll a and b are the two main types of chlorophyll in terrestrial plants and both have the same phytol side chain. Chlorophyll breakdown is critical for recycling of nitrogen. Its removal is a prerequisite for the degradation of chlorophyll-binding proteins (such as LHCII) which constitute 20% of cellular nitrogen (Hörtensteiner, 2006).

Chlorophyll is broken down in the plastid (Hörtensteiner, 2009). The final products of chlorophyll breakdown in plants are water soluble tetrapyrroles known as nonfluorescent chlorophyll catabolites (NCCs), which are stored in the vacuoles. In Arabidopsis, all of NCCs are derived from chlorophyll a. This suggests that the first step in chlorophyll breakdown is conversion of chlorophyll b into chlorophyll a, which is catalysed by the activity of chlorophyll b reductase encoded by *NYC1* (*NON-YELLOW COLORING1*) and *NOL* (*NYC-ONE LIKE*) (Sato et al., 2009). The degradation of chlorophyll a initiates when Mg^{2+} at the centre of the chlorin ring is removed by metal chelating substance. The

removal of Mg^{2+} converts chlorophyll a into phein a that in turn is dephytylated by PHEOPHYTIN PHEOPHORBIDE HYDROLASE (PPH)/NON-YELLOW COLORING3 to pheophorbide a (Pheide a) (Schelbert et al., 2009). Pheide a is then converted by PHEOPHORBIDE A OXYGENASE (PAO) into red chlorophyll catabolite (RCC). RED CHLOROPHYLL CATABOLITE REDUCTASE (RCCR) converts RCC into primary fluorescent chlorophyll catabolite (pFCC) that is modified in the plastid to FCC. FCC is finally transported to the cytosol, where it is non-enzymatically converted into NCC isomers (Hörtensteiner, 2009).

Controlled breakdown of chlorophyll in photosynthetic tissues is important, as the intermediates of the reaction are toxic to cells. Mutants defective in PAO or RCCR, which catalyse the last step of the catabolic pathway, develop a lesion mimic phenotype (necrotic lesions in the absence of pathogens), due to accumulation of breakdown intermediates (Hörtensteiner, 2006). Thus, controlled chlorophyll degradation is a prerequisite to detoxify the potentially phototoxic pigments within vacuoles in order to ensure that remobilization of nitrogen from chlorophyll-binding proteins can be proceeded during senescence (Hörtensteiner, 2009).

Mutants that are delayed in degreening are known as stay green mutants. They can be divided into two groups, functional and non-functional (cosmetic). Functional stay green mutants are defective in the onset and progression of senescence processes leading to maintenance of green colour (Thomas et al., 2002; Yoo et al., 2007; Hörtensteiner, 2009). Conversely, non-functional mutants are defective in chlorophyll breakdown but senescence keeps progressing in background. Functional stay green mutants include *ore1*, *ore4-1*, *ore7*, *ore9* and *ore12* (Hörtensteiner, 2009). Examples of cosmetic stay green mutants are *pao*, *nyc1* (*chlorophyl b reductase*), *sgr* (*stay-green*) and *sid2*. *sid2* is defective in the ring opening step of the chlorophyll catabolic pathway controlled by PAO activity. The mutant showed decreased transcript abundance of *PAO* and increased retention of chlorophyll binding proteins, such as LHCII but not of Rubisco. *sid2* mutant also retained higher levels of Chlides and Pheide a in older leaves compared to wild-type *Lolium temulentum* (Roca et al., 2004). SGR is not directly involved in chlorophyll breakdown, but is required for the dismantling of photosynthetic chlorophyll-protein complexes, thus allowing chlorophyll-breakdown enzymes access to their substrate (Hörtensteiner, 2009).

1.1.3.3 Nucleic acid breakdown

In addition to their role as a carrier of genetic information, the nucleic acids, in particular the rRNA also serves as a source of nitrogen, carbon and phosphorus during senescence-induced nutrient recycling. The amount of DNA in a senescing cell remains relatively constant as senescence progresses, but RNA quantity rapidly diminishes concomitant with a rise in RNAse activity (Makrides and Goldthwaite, 1981). In Arabidopsis, the RNase encoding gene *RNS2* shows increased transcript abundance in senescing tissues and under phosphate-limited conditions. Therefore, it is likely to be important for the degradation of RNA and remobilization of Pi (inorganic phosphate) in senescing leaves (Taylor et al., 1993; Bariola et al., 1994).

Purine (building blocks of DNA and RNA) recycling is highly significant during age- and stress-induced leaf senescence, because its catabolic products (ureides) are essential for plant survival during nutrient re-mobilization (Brychkova et al., 2008). Arabidopsis plants with decreased transcript abundance of *XANTHINE DEHYDROGENASE* (*XDH*) showed enhanced leaf senescence, because of the accumulated xanthine. XDH converts xanthine (product of purine catabolism) into urate (Stasolla et al., 2003; Zrenner et al., 2006).

1.1.3.4 Lipid breakdown

Senescence is characterized in part by metabolism of lipids, particularly membrane lipids. Membrane perturbations, such as increased membrane permeability, loss of ionic gradients and decreased function of key membrane proteins occur early in the senescence process (Thompson et al., 1998). In Arabidopsis, a senescence-enhanced *ACYL HYDROLASE* (*SAG101*) has been identified that may be a key regulator of senescence-associated membrane perturbations (He and Gan, 2002). ACYL HYDROLASES catalyze the release of oleic acid from the triglyceride triolein. Over-expression of *SAG101* causes precocious leaf senescence, whereas its antisense suppression delays the normal progression of senescence (He and Gan, 2002). SAG101 may act by either releasing α-linoleic acid for jasmonic acid production or by attacking the phospholipid bilayers of membranes that allows access to other lipid-degrading enzymes to the perturbed membranes (He and Gan, 2002).

Another lipid metabolizing gene, *PHOSPHOLIPASE D-A* (*PLD-α*), mediates hormone-induced leaf senescence in Arabidopsis. Interestingly, the *PLD α* is not senescence-enhanced with it being more highly expressed in actively metabolizing tissue. Despite this, antisense suppression of *PLD-α* expression retards ABA- and ethylene-promoted senescence in detached Arabidopsis leaves. *PLD-α* expression does however have no effect on natural leaf senescence (Fan et al., 1997).

More recently, d-2HG dehydrogenase (d-2HGDH) has been shown to be involved in lipid catabolism during age- and stress-induced leaf senescence (Engqvist et al., 2011). D-2HG dehydrogenase (D-2HGDH) converts 2-Hydroxyglutarate (D-2HG) to 2-oxoglutarate (2OG) that enters the TCA cycle (tricarboxylic acid cycle) to generate energy. *D2hgdh1* loss-of-function and overexpression Arabidopsis plants showed increased and decreased accumulation of D-2HG, respectively, in naturally senescing leaf. However, transgenic plants showed normal age- and dark-induced leaf senescence.

1.1.3.5 Autophagy

Autophagy is an intra-cellular process involved in the removal and degradation of cellular components by the vacuole and increases plant survival in hostile environments. Microarray studies have shown that a number of autophagy-encoding genes are up-regulated during age-related leaf senescence (Buchanan-Wollaston et al., 2005; Lim et al., 2007). Disruption of some of these genes such as *AtAPG7*, *AtAPG9* and *AtAPG18a* results in accelerated senescence suggesting they have a pro-survival type function (Doelling et al., 2002; Hanaoka et al., 2002; Liu and Howell, 2010). This may be particularly important for maintaining the cellular viability needed during the controlled massive degradation of cellular constituents that occurs during senescence (Buchanan-Wollaston et al., 2005; Love et al., 2008).

Functional studies have provided genetic evidence for the direct involvement of autophagy in degradation of cellular components, such as, the chloroplast (Izumi et al., 2010). Rubisco is degraded faster during the early phases of senescence than the latter (Friedrich and Huffaker, 1980; Mae et al., 1984). In senescing wheat leaves, Rubisco is exported from the chloroplast to the cytoplasmic vacuole for subsequent degradation in chloroplast derived-

small spherical bodies called Rubisco-containing bodies (RCBs) (Chiba et al., 2003). In Arabidopsis leaves, stroma-targeted green fluorescent protein (GFP) and Red Fluorescent Proteins (DsRed) and GFP-labelled Rubisco were mobilized to the vacuole by autophagy via RCBs (Ishida et al., 2008). Recently, autophagy was demonstrated during degradation of chloroplast and Rubisco in living cells (Ono et al., 2013). Similarly, a recent study suggested that autophagy contributed to the proteolysis of stromal proteins, including Rubisco large subunit, chloroplast glutamine synthetase and Rubisco activase (Lee et al., 2013). Although autophagy is involved in degradation of stroma proteins, it is not the only mechanism for degrading chloroplast proteins (Levine and Klionsky, 2004; Bassham et al., 2006).

1.3.1.6 Ubiquitin-proteosome system

Genetic, biochemical and cellular biological studies carried out on mammalian and yeast cells have demonstrated the importance of the ubiquitin-proteosome system for the degradation of proteins in living cells. Ubiquitination is required for cell viability and plays a major role in DNA repair, protein synthesis, transcriptional regulation and stress responses (Varshavsky, 2005). Specific proteins are targeted for degradation through the ubiquitin-26S proteosome pathway, by the attachment of ubiquitin to them, through the action of the conjugating enzymes E1, E2 and E3. The ubiquitinated proteins are then recognized and degraded by the ATP-dependent 26S proteosome. In plants, the ubiquitin-26S proteosome pathway appears to have a significant role in the control of transcription protein turnover and reallocation of nutrients that occur during senescence. The transcript abundance of genes encoding polyubiquitin and ubiquitin pathway enzymes increases during senescence (Yoshida, 2003; Lin and Wu, 2004). These genes encode F-box proteins, C3HC4-type RING finger proteins, ASK1 proteins and E2 conjugation enzymes (Smalle and Vierstra, 2004). F-box proteins are components of the multi-protein ubiquitin E3 ligase complexes, which target proteins for degradation by transferring ubiquitin from the E2 enzyme to the substrate protein (Smalle and Vierstra, 2004).

The importance of the ubiquitin-26S proteosome degradation pathway during senescence has been confirmed by functional analysis of three mutants, defective in components of the programme. The *oresara9* mutant of Arabidopsis is defective in the F-box protein ORE9, which causes a delay in the initiation of age-dependent, dark/detached-

induced and hormone-mediated leaf senescence (Oh et al., 1997; Woo et al., 2001). Although it is still unclear how ORE9 functions to delay senescence it was speculated that it might do so by degrading a putative repressor of the senescence pathway (Woo et al., 2001). Interestingly, ORE9 gene has been identified in other genetic screens where it was shown to affect leaf shape and light-dependent germination illustrating how seemingly unrelated processes as senescence, leaf shape and light signalling can be linked through the same regulatory proteins (Somers and Fujiwara, 2009). The second mutant *delayed senescence 1* (*dls1*) is defective in the R-TRANSFERASE AtATE1 that is a component of the N-end rule pathway. The N-end rule relates the *in vivo* half-life of a protein to the nature of N-terminal amino acids of a protein. R-TRANSFERASES transfer arginine, a primary destabilizing residue, to the target protein, which is then directly recognized by the E3 ligase and ubiquitinated. The *dls1* mutant was found to show a delay in both natural and dark-induced whole plant senescence (Yoshida et al., 2002). The third mutant *senescence-associated E3 ubiquitin ligase 1* (*saul1*), as its name suggests is defective in a particular E3 ligase activity. These plants show accelerated leaf yellowing, increased expression of known senescence-associated genes and an early decline in photochemical efficiency (Raab et al., 2009).

The proteosomal pathway controls ethylene mediated senescence signalling. In the absence of ethylene, the proteosomal pathway degrades EIN2. EIN2 degradation is mediated by two F-box proteins ETP1 (EIN2 TARGETING PROTEIN 1) and -2 (Qiao et al., 2009). These proteins interact with highly conserved EIN2 C-terminal domain responsible for most of the ethylene responses. By contrast, ethylene down regulates the activities of ETP1 and ETP2 and stabilizes EIN2 concentration. Interestingly, ethylene does not regulate the transcription of EIN3 but instead it stabilizes the protein concentration (Yanagisawa et al., 2003; Trobacher, 2009). Similar to EIN2, in absence of ethylene, EIN3 is continuously degraded through 26-proteasomal degradation pathway mediated by EIN3-binding F box protein 1 and 2 (EBF1 and EBF2) (Trobacher, 2009). EIN3 stabilization is carried out by EIN2 that destabilizes EBF1 and allows EIN3 to accumulate (Shi et al., 2012).

1.1.3 Transport pathways activated during leaf senescence

An important component of the senescence programme is remobilization of degraded molecules to the new sinks in the plant. A transcriptome study that examined the response of 963 putative transporter genes during leaf senescence found that 60 were down-regulated and 153 were induced (3-fold or more) during natural leaf senescence (van der Graaff et al., 2006). The prominent down-regulated families of transporter genes include those encoding the major intrinsic proteins, divalent anion and auxin efflux carriers. The increased abundance of up-regulated transporter proteins corresponds well with the substrates reported to be transported from senescent leaves to sink organs, such as amino acids, inorganic phosphorus, sugars, purines, pyrimidines and metal ions (Himelblau and Amasino, 2001; Soudry et al., 2005). The up-regulation of genes encoding amino acid and oligopeptide transporter proteins is consistent with the high amount of protein degradation occurring during senescence and the subsequent need to export the breakdown products to the sink organs (Hortensteiner and Feller, 2002). A considerable amount of nitrogen is transported in the form of glutamine in naturally senescing leaves (Finnemann and Schjoerring, 2000). Several genes encoding enzymes which are involved in glutamate metabolism, are up-regulated during senescence. These include *GLUTAMATE DECARBOXYLASE* genes, genes encoding GLUTAMATE RECEPTOR and *CYSTOLIC GLUTAMINE SYNTHASES* (Buchanan-Wollaston et al., 2005). Transcriptome studies have revealed that a number of ABC transporter and several other transporter genes, involved in transport of amino acid, sugars and cations exhibit increased transcript abundance during senescence (Buchanan-Wollaston et al., 2005; Breeze et al., 2011).

In tobacco and rice the GLUTAMINE SYNTHETASE (GS1) activity increases during leaf senescence (Kamachi et al., 1992; Masclaux et al., 2000). The chloroplastic and cytosolic PYRUVATE ORTHOPHOSPHATE DIKINASE (PPDK) isoforms control nitrogen remobilization during natural leaf senescence. Transgenic Arabidopsis and tobacco plants expressing *AtPPDK* under the control of *SAG12* promoter showed enhanced accumulation of cytosolic *PPDK* and faster nitrogen export from senescing leaves (Taylor et al., 2010).

1.1.5 Ontogeny of leaf senescence

The dramatic biochemical shift from anabolic to catabolic metabolism in senescing leaves is mediated by an array of endogenous and exogenous factors, such as age, hormones and environmental cues. Many genes whose products accelerate or delay leaf senescence have been confirmed by mutational and functional studies (Li et al., 2012b). Table 1.1 and 1.2 show how transcript abundance of these genes changes during development and senescence of attached leaves. Regulation of their transcript abundance during leaf development is complex. One might hypothesise that genes that accelerate leaf senescence would increase in transcript abundance as the leaf ages and vice versa. However, some genes shown to promote senescence actually decrease in transcript abundance during senescence and conversely others that delay senescence increase in abundance. Clearly, leaf senescence is regulated by a complex interaction of both positive and negative regulators of the programme.

The majority of genes that promote leaf senescence (Table 1.1) showed increased mRNA abundance by ~23 days after leaf emergence, which is well before the visible sign of leaf yellowing occurred (at ~31 days after leaf emergence). These include *RPK1*, *EIL3*, *NAP*, *EIN3*, *PPH*, *ORE9* and *ORE1*. The early increase in their transcript abundance suggested that these genes might be involved in the initiation of leaf senescence, whereas genes whose transcript abundance increased late in leaf development might be involved in progression of the process e.g. *RAV1*, *ACS2*, *WRKY6* and *SEN1*. Interestingly, the mRNA abundance of some senescence inducing genes e.g. *BOT1, FTSH5, ORE4, AtMYBL* and *COS1* decreased with progression of leaf senescence. These will be discussed in more detail in the following paragraphs.

BOT1 (BOTERO1) is required for development of cortical microtubules (MT) that are involved in cell elongation, cell division and organelle positioning (Dixit and Cyr, 2004). MTs are composed of heterodimeric polymers of the globular proteins α- and β-tubulin and their functions are closely linked to their organizational states (Keech et al., 2010). The *bot1* mutant that shows delayed whole plant senescence has more juvenile stems (stem continue to elongate and produce flowers), slower maturation of the tissue and reduced fertility (Bichet et al., 2001). Interestingly, these characteristics are similar to sterile mutants

that also show delayed whole plant senescence. MT changes appear to also be part of the leaf senescence programme, as it has been shown that during natural- and dark-induced leaf senescence cortical MT are disassembled (Keech et al., 2010). The MT-associated proteins MAP65 and MAP70-1 decrease in transcript abundance during dark- and age-induced leaf senescence, whereas transcript abundance of the MT-destabilizing protein MAP18 strongly increases. These MAPs control reorganization of the MT array through their stabilizing, bundling, or severing activities (Lloyd and Hussey, 2001; Hashimoto and Kato, 2006; Hamada, 2007). From this study, it was suggested that suppression of genes involve in MAP assembly together with induction of genes involve in MAP degradation play key roles in MT disassembly during senescence (Keech et al., 2010).

ORE4 encodes a plastid ribosomal small subunit prote/in 17 (PRPS17) and regulates chloroplast function, leaf growth and activity of photosystem I. The *ore4-1* mutant showed reduced leaf growth, defects in chloroplast functions, reduced accumulation of chlorophyll and reduced activity of photosystem1 (Woo et al., 2002). This suggested that delayed leaf senescence was due to reduced metabolic activity of the chloroplast in the *ore4-1* mutant (Woo et al., 2002). Therefore, ORE4 may not actively promote senescence and is the part of maintaining the normal growth activity.

AtMYBL (MYB-like protein) overexpression in Arabidopsis accelerates leaf senescence (Li et al., 2012b), yet its transcript abundance decreases in ageing leaves (Table 1). Interestingly, analysis of AtMYBL promoter-β-glucuronidase (GUS) transgenic plants suggest that this gene is highly expressed in old leaves and in response to ABA and salt stress treatments (Zhang et al., 2011b). Presumably, the lower transcript abundance in ageing leaves is due to some form of posttranscriptional degradation of the transcripts.

COS1 encodes LUMAZINE SYNTHASE that catalyzes the synthesis of riboflavin (Zhang and Xing, 2008). *cos1* (*coi1 suppressor1*) showed restoration in JA-mediated leaf senescence (Xiao et al., 2004). The role of JA in regulating developmental leaf senescence is still questionable (Jibran et al., 2013). Therefore, taken together it may be that *AtMYBL* and *COS1* are not directly involved in the promotion of developmental leaf senescence.

Table 1.1. Transcript abundance of genes that are positive regulators of developmental leaf senescence.

Green bars indicate down-regulation of the genes indicated by minus 1, whereas red bars indicate up-regulation of the genes indicated by plus 1. Open bars indicate no change. The numbers 19, 21, 23, 25, 27, 29, 31, 33, 35, 37, 39 represent days after leaf emergence. Gene set was obtained from Li et al., (2012) and the transcript abundance change in ageing leaves determined by using the data set of Breeze et al., (2011).

Promote	**AGI #**	**Function**	19	21	23	25	27	29	31	33	35	37	39
BOT1	AT1G80350	cortical microtubule organization	-1	-1	-1	-1	-1	-1	-1	-1	-1	0	0
ORE4/PRPS17	AT1G79850	Protein biosynthesis	0	-1	-1	-1	0	0	-1	-1	-1	-1	0
AtMYBL	AT1G49010	Transcription factor	0	0	-1	-1	-1	-1	-1	-1	-1	0	0
COS1	AT2G44050	Hormone transduction	0	0	-1	0	0	0	-1	-1	-1	-1	0
EIL1	AT2G27050	transcription factor	0	0	0	0	0	0	0	-1	-1	0	0
RPK1	AT1G69270	Environmental stress	1	1	1	1	1	1	1	1	1	0	0
EIL3	AT1G73730	Transcription factor	1	1	1	1	1	1	1	1	1	0	0
NPR1	AT1G64280	Hormone transduction	1	1	1	1	0	0	-1	-1	-1	-1	0
NYC1	AT4G13250	Chlorophyll degradation	0	1	0	0	0	0	1	1	1	0	0
NAP	AT1G69490	Transcription factor	0	1	1	1	1	1	1	1	1	0	0
EIN3	AT3G20770	Transcription factor	0	1	1	1	1	1	1	1	0	0	0
PPH	AT5G13800	Chlorophyll degradation	0	1	1	1	1	1	0	1	1	0	0
AtNAC3	AT5G39610	Transcription factor	0	1	1	1	1	1	1	1	1	0	0
ORE1/NAC2	AT5G39610	Transcription factor	0	1	1	1	1	1	1	1	1	0	0
ARF2	AT5G62000	Hormone response pathway	0	1	1	1	0	0	0	0	-1	0	0
ORE9/MAX2	AT2G42620	Protein degradation	0	1	1	1	1	1	0	0	-1	0	0
Rap2	AT4G28140	Transcription factor	0	0	1	0	0	0	0	0	0	0	0
LOX4	AT1G72520	Hormone transduction	0	0	1	0	-1	0	0	0	0	0	0
LOX3	AT1G72520	Hormone transduction	0	0	1	0	-1	0	0	0	0	0	0
Pht1;5	AT2G32830	Nutrient recycling	0	0	1	1	0	0	1	1	1	0	0
SAG113	AT5G59220	Hormone response pathway	0	0	1	1	0	0	1	1	1	0	0
MKK9	AT1G73500	Signal transduction	0	0	1	1	1	1	1	1	1	0	0
AtMYB2	AT2G47190	Transcription factor	0	0	1	1	1	1	1	1	1	1	1
NAC053/NTL4	AT5G04410	Transcription factor	0	0	1	1	1	1	1	1	1	1	1
TCP2	AT4G18390	Transcription factor	0	0	0	1	0	0	-1	-1	-1	-1	0
RAV1/EDF4	AT1G13260	Transcription factor	0	0	0	0	1	1	0	0	-1	0	0
ACS2	AT1G01480	Hormone response pathway	0	0	0	0	1	1	1	1	1	1	1
KAT2	AT2G33150	Hormone response pathway	0	0	0	0	1	1	1	1	1	0	0
WRKY53	AT5G24110	Transcription regulation	0	0	0	0	0	1	1	1	1	0	0
WRKY6	AT1G62300	Transcription regulation	0	0	0	0	0	0	1	1	1	0	0
SEN1	AT3G45590	Environment response	0	0	0	0	0	0	0	1	1	1	0

Genes whose products delay leaf senescence also showed variable expression profiles during leaf senescence (Table 1.2). *AtNOS1*, *ARR4*, *GIN1*, *AHK1*, *ARR6, ARR8*, *ETDQO*, *ESR*, *ARR9* and *CAO* transcript abundance decreased in ageing leaves consistent with their role in delaying leaf senescence. However, many genes particularly those that are involved in nutrient cycling showed enhanced transcript abundance during leaf senescence e.g. *AtAPG7*, *AtAPG9* and *AtAPG18a*. TDNA insertion mutants of these genes exhibited early leaf senescence possibly due to decreased availability and utilization of nutrients (Lim et al., 2007). However, these early senescence phenotypes were exhibited during nutrient starved conditions. APG7 was found to be not involved in normal leaf growth and development but its loss of activity resulted in early leaf senescence during nutrient starved conditions. In contrast to Breeze et al., (2011), Doelling et al., (2002) found that *APG7* and *APG8* mRNAs accumulated in ageing leaves suggesting the involvement of these autophagy pathways ATG8/12 in autophagic recycling, particularly when substantial nitrogen and carbon mobilization is required.

Thus, up regulation of autophagy genes as senescence progresses ensures efficient nutrient utilization and availability of components required for execution and progression of leaf senescence. However, in addition to autophagy genes, some other genes e.g. *VIN2*, *CBF2*, *ETR2*, *AtXDH1*, *BAP1*, *At2-MMP* and *ETR1* showed increased transcript abundance particularly at the last stages of leaf senescence suggesting that these genes are involved in cellular protecting mechanisms necessary to avoid sudden cellular collapse.

Taken together, it can be concluded that transcripts of positive regulators of leaf senescence tend to increase in ageing leaves and where it was found that they did not it was explained by the regulators being positive regulators of whole plant senescence or stress induced senescence rather than leaf senescence. Similarly, the transcripts of inhibitors of leaf senescence, except for those that are involved in nutrient recycling, were found to be decreased in senescing leaves. Thus, the information obtained from transcript profiling of genes during different stages of leaf development can be informative in determining the function of genes as positive or negative regulators of senescence.

Table 1.2. Transcript abundance of genes that are negative regulators of developmental leaf senescence.

Green bars indicate down-regulation of the genes indicated by minus 1, whereas red bars indicate up-regulation of the genes indicated by plus 1. Open bars indicate no change. The numbers 19, 21, 23, 25, 27, 29, 31, 33, 35, 37, 39 represent days after leaf emergence. Gene set was obtained from Li et al., (2012) and the transcript abundance change in ageing leaves determined by using the data set of Breeze et al., (2011).

Delay	AGI #	Function	19	21	23	25	27	29	31	33	35	37	39
AtNOS1	AT3G47450	Hormone response pathway	0	-1	-1	-1	-1	-1	-1	-1	-1	-1	-1
ARR4	AT1G10470	Cytokinin mediated signalling	0	0	-1	-1	-1	-1	-1	-1	-1	-1	0
GIN1	AT1G52340	Hormone response pathway	0	0	-1	-1	-1	-1	-1	-1	-1	0	0
CRE1/AHK4	AT2G01830	Cytokinin receptor	0	0	-1	-1	-1	-1	-1	-1	-1	0	0
ARR6	AT5G62920	Cytokinin mediated signalling	0	0	-1	-1	-1	-1	-1	-1	0	0	0
ARR8	AT2G41310	Cytokinin mediated signalling	0	0	0	-1	-1	-1	-1	-1	-1	0	0
ETFQO	AT2G43400	Protein degradation	0	0	0	-1	-1	-1	-1	-1	-1	-1	0
ESR	AT1G54040	Hormone response pathway	0	0	0	-1	-1	-1	-1	-1	-1	0	0
ARR9	AT3G57040	Cytokinin mediated signalling	0	0	0	0	-1	-1	-1	-1	-1	0	0
CAO	AT1G44446	chlorophyll biosynthesis	0	0	0	0	0	0	-1	-1	-1	0	0
BAH1/NLA	AT1G02860	nitrogen limitation adaptation	1	1	1	1	1	1	1	1	0	0	0
VTI12	AT1G26670	Nutrient recycling	1	1	1	1	1	1	0	0	0	0	0
ATG12A	AT1G54210	Nutrient recycling	1	1	1	1	1	1	1	0	0	0	0
ATG8C	AT1G62040	Nutrient recycling	1	1	1	1	1	1	1	1	1	0	0
RCD1	AT2G35510	Cell death	1	1	1	1	1	1	1	1	0	0	0
ATG8I	AT3G15580	Nutrient recycling	1	1	1	1	1	1	1	1	0	0	0
ATG8G	AT3G60640	Nutrient recycling	1	1	1	1	1	1	1	1	0	0	0
ATG6	AT3G61710	Nutrient recycling	1	1	1	1	1	1	1	1	1	1	0
ATG8B	AT4G04620	Nutrient recycling	1	1	1	1	1	1	1	1	1	1	0
OLD1/CPR5	AT5G64930	age and ethylene responses	1	1	1	1	1	1	1	0	0	0	0
AHK3/ORE12	AT1G27320	Hormone response pathway	0	1	1	0	0	0	0	0	1	0	0
ATG2	AT3G19190	Nutrient recycling	0	1	1	1	0	0	0	1	1	0	0
ATG8E	AT2G31260	Nutrient recycling	0	1	0	0	0	0	0	1	1	1	0
COR15B	AT2G42540	Environment response	0	1	1	1	0	0	0	0	0	0	0
UPL5	AT4G12570	Protein degradation	0	1	1	1	1	0	0	0	0	0	0
ATG8A	AT4G21980	Nutrient recycling	0	1	1	1	1	1	1	1	1	1	0
VNI2	AT5G13180	Transcription factor	0	1	1	1	1	1	1	1	1	0	0
ATG4B	AT3G59950	Nutrient recycling	0	0	1	1	0	0	0	0	0	0	0
CBF2	AT4G25470	Environment response	0	0	1	0	0	0	0	0	-1	0	0
ETR2	AT3G23150	Hormone response pathway	0	0	1	1	1	1	1	1	0	0	0
ATG8H	AT3G06420	Nutrient recycling	0	0	1	1	1	1	1	1	1	1	1
AtXDH1	AT4G34890	Nucleic acid degradation	0	0	1	1	1	1	1	1	1	1	1
ATG18A	AT3G62770	Nutrient recycling	0	0	0	1	1	1	1	1	1	1	0
APG7	AT5G45900	Nutrient recycling	0	0	0	0	1	1	1	1	1	1	1
BAP1	AT3G61190	Cell death	0	0	0	0	1	1	1	1	1	0	0
At2-MMP	AT1G70170	Signal transduction	0	0	0	0	0	1	1	1	1	1	0
ETR1	AT1G66340	Signal transduction (ET)	0	0	0	0	0	0	1	1	1	0	0

1.2 Postharvest senescence

1.2.1 Importance of postharvest senescence

Over the next fifty years, the food sector will face significant challenges, because of rapidly expanding human populations, water scarcity, limited cultivated area and huge food losses during handling and storage (Beddington, 2011). The increasing demand for food in coming years will exert enormous pressure on the food sector. Hence, development of new strategies to maintain a balance between food supply and demands will be a major task for plant biologists.

Food losses occur at various stages from production to consumption, due to postharvest handling and trade, storage, processing and packaging (Lundqvist et al., 2008; Kummu et al., 2012). Food losses can be divided into agricultural losses, postharvest losses, processing losses, distribution losses and consumption losses. Approximately, 50% or 614 kcal/cap/day of food is lost within various steps of the food supply chain including harvesting, transport, storage and packaging (Lundqvist et al., 2008; Parfitt et al., 2010; Kummu et al., 2012).

Postharvest losses of horticulture commodities, such as fruits and vegetables are a significant component of all food losses that varies from 10 to 50% depending on the storage facilities, growing conditions and genetic potential of varieties (Parfitt et al., 2010). Postharvest food losses occur during storage, distribution and degradation during handling. The introduction of measures to reduce food losses is considered the most crucial step for improving food security in the future. For example, a recent survey, held to investigate postharvest losses in Switzerland, reported that 48% of the total produced calories are lost across the whole food chain (Lundqvist et al., 2008).

Postharvest losses can be reduced by improving on-farm facilities and more reliable transportation networks, energy and market systems and enhanced infrastructure during transportation and storage (Rolle, 2006; Stuart, 2009). It has been estimated that the adoption of proper strategies to reduce food losses over the globe can help to feed almost one

billion more people by the year 2025 (Kummu et al., 2012). Besides feeding the rapidly expanding population, saving of food wastage will help to protect other resources, such as fertilizer inputs, farming efforts and importantly fresh water, the scarcity of which is another big threat in the next future (Lundqvist et al., 2008).

1.2.2 Regulation of postharvest leaf and inflorescence senescence

Harvested commodities are typically transported in the dark and if sea freighted this can be for long periods. Therefore, a full understanding of the molecular and genetic mechanisms of dark- and detachment-induced leaf, flower and inflorescence senescence may open up novel opportunities to extend postharvest life.

1.2.2.1 Postharvest leaf senescence

Senescence can be prematurely induced in leaves by detachment and further accelerated by dark incubation and certain hormones (Noodén, 1988; Azumi and Watanabe, 1991; Chen et al., 1991; Quirino et al., 2000).

1.2.1.1.1 Transcript profiling comparison of detached dark-held leaves with natural leaf senescence

Since the early 1990s it became evident that despite commonalities the genetic programme induced in dark-held detached leaves is not identical to that which occurs during natural senescence (Becker and Apel, 1993; Weaver et al., 1998; Buchanan-Wollaston et al., 2005; van der Graaff et al., 2006). Recent microarray-based profiling studies comparing natural leaf senescence (NS) with that initiated in sucrose-starved cell cultures (PCD), in leaves of dark-held plants (PDIS), in attached shaded leaves (DIS) and detached dark-held leaves (DET) have indicated that there are both significant similarities and differences in the senescence transcriptome, depending upon how it is initiated (Lin and Wu, 2004; Buchanan-Wollaston et al., 2005; van der Graaff et al., 2006; Guo and Gan, 2012). For example, comparison of NS with DIS and DET senescence indicated that ~22% of up-regulated genes were common to all three senescence programmes (van der Graaff et al., 2006).

Approximately 28% of up-regulated genes showed similarities between NS, PCD and PDIS (Buchanan-Wollaston et al., 2005). Interestingly, more transcripts were altered in abundance during NS (3513) than during DIS (1833) or DET (2158) indicating that the slower occurring developmental senescence induces more physiological processes compared to fast occurring dark-induced senescence. Furthermore, the proportion of up-regulated genes was higher than down-regulated during NS, whereas in DIS and DET senescence down-regulated genes outnumbered up-regulated genes. The precocious senescence induced by a wide variety of treatments is similar to developmental leaf senescence at the execution (latter) phase of senescence, but very different at the initiation phase (Guo and Gan, 2012).

1.2.1.1.2 Hormonal control of dark-induced senescence is different to that of age-related senescence

Hormone regulated pathways play greater or lesser roles in the initiation and progression of leaf senescence depending upon how it is induced. JA appears to have an important role in age-related senescence, but not in DIS or DET. Exogenously applied JA induces premature leaf senescence and its levels increase in naturally senescing leaves (He et al., 2002). Eight of the 19 JA-biosynthesis genes are specifically and transiently expressed during natural senescence but not during DIS or DET (van der Graaff et al., 2006). Two other JA biosynthetic genes encoding AtαDOX1 and AtLOX1 are up-regulated only in dark-detached tissue and not during NS or DIS suggesting that these genes are regulated by wounding.

SA signalling like JA mediates plant responses to stress and appears to be important only for the progression of age-related and not dark-induced senescence. The majority of the senescence associated SA-responsive genes is up regulated during developmental senescence and not or only weakly expressed during DIS and DET senescence (van der Graaff et al., 2006). Arabidopsis plants with reduced SA content due to over-expression of the bacterial *SALICYLIC HYDROXYLASE* (*NahG*) show delayed yellowing during developmental-, but not dark-induced senescence (Morris et al., 2000; Buchanan-Wollaston et al., 2005).

1.2.1.1.3 Starch is produced by tissues in light to allow them to cope with expected dark period

The transcript changes that occur during dark-induced leaf senescence have been associated with rapid and dramatic changes in leaf metabolite composition, particularly the loss of carbohydrates resulting from lack of light. To cope with dark-induced carbon deprivation, Arabidopsis leaves produce starch during the day that can be remobilized during the night. The production of the starch is finely tuned to the expected length of night, so that by the end of the night period, the starch content of the leaf is typically only 10% of what it was at the beginning and reducing sugars are at about 50% (Usadel et al., 2008). If the night is extended further, then content of starch, sucrose reducing sugars and soluble protein decrease dramatically while the amounts of free amino acids such as asparagine and phenylalanine increase. These metabolite changes are reflective of the more than 90% of biochemical pathways affected in the dark-held tissue as it becomes nutrient deprived (Lin and Wu, 2004).

1.2.1.1.4 Nitrogen mobilization is different in dark-held tissues compared with light-held

Different nitrogen remobilization pathways are activated during dark-detachment and age- induced leaf senescence (Lin and Wu, 2004; Buchanan-Wollaston et al., 2005; van der Graaff et al., 2006). Nitrogen is exported in the form of glutamine (Gln) during age-related senescence and asparagine (Asn) during dark-induced leaf senescence. Asn contains less carbon than Gln, which presumably is why it is used in carbon-deficient dark-held tissues to store and transport nitrogen (Lam et al., 1994). In response to dark treatment genes involved in Asn biosynthesis, such as *GLUTAMATE DEHYDROGENASE* and *ASPARAGINE SYNTHASE*, are substantially up-regulated (Buchanan-Wollaston et al., 2005; van der Graaff et al., 2006). In contrast, during age-related senescence transcript abundance of *GLUTAMINE SYNTHETASE* involved in ammonia assimilation and *GLUTAMATE DECARBOXYLASES* controlling conversion of glutamate to GABA (4-aminobutyrate) increase substantially. This suggests that GABA might be involved in signalling to coordinate the C:N balance during natural senescence.

1.2.1.1.5 Energy deprivation leads to production of alternative carbohydrate sources

Various biochemical pathways become activated in dark incubated sugar-starved leaves to provide alternative carbohydrate sources. These include induction of β-oxidation genes responsible for breaking down straight chain fatty acids in plants (Graham and Eastmond, 2002). By contrast, sugar levels do not get depleted during developmental senescence and β-oxidation genes are not induced (Lin and Wu, 2004). Genes encoding enzymes involved in catabolism of branched-chain amino acids, e.g., BCKDH subunits E1 and E2, are up-regulated to provide an alternative carbohydrate source to dark-held sugar-starved cell culture tissue of Arabidopsis (Fujiki et al., 2000).

1.2.1.1.6 Trehalose-6-phosphate is a sugar metabolite that regulates age-related senescence and coping response in dark-held tissues

Trehalose-6-phosphate (T6P) is required for the timely onset of leaf senescence. When its increase in concentration is suppressed in Arabidopsis plants by over-expression of the bacterial gene encoding TREHALOSE-6-PHOSPHATE PHOSPHATASE (TPP), leaf senescence is delayed (Wingler et al., 2012). This delay is found despite the tissue having increased glucose, fructose and sucrose contents, which have been linked to causing leaf senescence (Pourtau et al., 2006). The effects of altering T6P concentration on delaying glucose mediated senescence were only seen when glucose was added to young (3-week-old) plants leading (Wingler et al., 2012) to suggest that the effect of T6P on controlling senescence timing is established early in the life of the plant.

T6P serves as a signalling molecule during high carbon availability (Wingler et al., 2012). Its concentration increases during developmental leaf senescence in Arabidopsis in parallel with a rise in sugar concentration of the tissues (Wingler, et al., 2012). T6P concentration also increases in leaf tissues treated with sucrose (Schluepmann et al., 2004; Lunn et al., 2006). The exact mechanism by which T6P controls signalling is not clear although it has been shown to suppress catalytic activity of SnRK1 (Eastmond and Graham, 2003; Paul et al., 2008; Schluepmann and Paul, 2009; Zhang et al., 2009; Schluepmann et al., 2012). Wingler et al. (2012) also noted that the effects of decreasing T6P content (reduced

leaf anthocyanin content and delayed senescence) were consistent with it leading to increased SnRK1 activity. This is because plants over-expressing the SnRK1 catalytic subunit KIN10 also have reduced anthocyanin content and delayed whole plant senescence (Baena-González, 2010).

T6P may reduce the carbohydrate imbalance caused by carbon limiting conditions, such as darkness, hypoxia and flooding. T6P levels decline under these conditions allowing de-repression of SnRK1 activity as mentioned above. The increased SnRK1 activity causes repression of energy (ATP) consuming processes and activation of catabolic processes, which results in carbon availability (Baena-González et al., 2007; Baena-González and Sheen, 2008). Thus, T6P serve as central signalling molecules to regulate plant responses in response to energy-starved conditions (O'Hara et al., 2013).

Taken together it can be concluded that high carbon availability, in young leaves, causes increased T6P activity, which suppresses SnRK1 activity and increases utilization of available carbon for rapid growth. This increased activity at early stages results in senescence during late developmental stage of leaf. Conversely, carbon depletion causes decreased T6P activity resulting in increased SnRK1 activity, which suppresses growth and energy consuming processes and activation of catabolic activities resulting in carbon availability. Therefore, under carbon available and limited conditions T6P activities keep a balance between available pool of starch and sugars (Fig. 1.1).

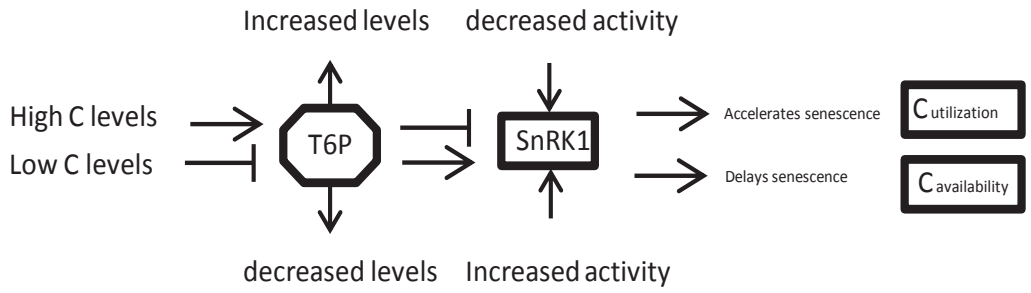

Figure 1.1. Possible role of T6P on senescence during low and high carbon availability.

T6P regulates leaf senescence according to tissue sugar status. In response to high carbon availability the levels of T6P increase, causing suppression of SnRK1 activity resulting in rapid growth and development of young leaves and later in senescence of older leaves. Under low carbon availability T6P levels decrease and suppression of SnRK1 activity is released. The increased SnRK1 activity causes increased activity of catabolic processes, availability of carbon and ATP production. Up and down arrows indicate increased and decreased activity or concentration, respectively.

1.2.1.1.7 Transcription factors associated with senescence of dark-held tissues

Transcription factors AtWRKY22 and OsWRKY23 affect timing of dark-induced senescence of detached Arabidopsis and rice leaves, respectively (Jing et al., 2009; Zhou et al., 2011). Darkness, H_2O_2, SA and pathogens induce *WRKY22* expression, whereas light suppresses its expression. This suggests that *WRKY22* is involved in regulating plant defense responses against abiotic stresses. Over-expression and silencing of *WRKY22* accelerated and delayed dark-induced senescence of detached Arabidopsis leaves, respectively. The altered senescence in these transgenic plants is concomitant with altered expression of *SAG12*, *SAG18*, *SAG20* and *SIRK*. WRKY22 regulates the expression of these genes indirectly or by mutually working with other WRKY transcription factors such as WRKY53, WRKY6 and WRKY70. WRKY22 activates WRKY53 and WRKY6 and suppresses WRKY70. WRKY53 participates in early events of leaf senescence, WRKY6 controls leaf senescence by binding to SIRK and WRKY70 is a suppressor of leaf senescence. Therefore, it was concluded that WRKY22 regulates dark-induced leaf senescence by interacting with WRKY mediated signal pathways (Zhou et al., 2011).

Similarly, AtS40-3, predicted DNA binding protein, showed a role in dark-induced senescence of detached Arabidopsis leaves. A T-DNA- insertion mutant *ats40*-3, with constitutive expression of AtS40-3 displayed stay-green phenotype (enhanced leaf longevity). It was suggested that AtS40 controls leaf senescence by regulating expression of *WRKY53*, *SAG12* and *SEN1*. The AtS40-mediated *SAG12* and *SEN1* regulation is independent of WRKY53 (Fischer-Kilbienski et al., 2010).

Despite the regulatory differences between age- and dark-detachment induced leaf senescence, some transcription factors are involved in controlling both programmes. The Arabidopsis NAC (NAM, ATAF1, -2 and CUC2) transcription factor ANAC092 (ANAC092/AtNAC2/ORE1) has been demonstrated as a positive regulator of age- and dark-detachment induced Arabidopsis leaf senescence (Kim et al., 2009; Balazadeh et al., 2010). RAV1, a RAV family transcription factor, is a positive regulator of age- and dark-detachment induced leaf senescence in Arabidopsis (Woo et al., 2010a). Similarly EIN3, a key transcription factor involve in ethylene signalling, also positively regulates dark-induced

senescence of detached leaves (Chao et al., 1997). Furthermore, AZF2, a Cys2/His2 type zinc finger protein, was demonstrated as a positive regulator of developmental- and dark-detachment induced leaf senescence in Arabidopsis (Li et al., 2012b). *BZIP1* and *BZIP53* TFs were found to be involved in the regulation of low energy stress response of Arabidopsis. An extended night treatment resulted in substantial increase in *BZIP1* (~30 fold) and *BZIP53* (~3 fold) transcript abundance in old senescing leaves. Conversely, during natural growth activities of BZIP1 and BZIP53 were observed only in young leaves.

1.2.1.1.8 Senescence of dark-held tissues is initially reversible

The dark-induced senescence of attached leaves in certain plant species including Arabidopsis can be recovered upon re-illumination depending upon the length of time for which tissue was subjected to shading (Weaver and Amasino, 2001). To investigate the molecular mechanisms regulating the reversible nature of dark-induced leaf senescence, expression profiles of transcription factors were quantified in attached leaves that were re-illuminated after two days of shading. Two days shading induces the expression of 150 transcription factors. Out of those, 39 were up regulated in response to two days of leaf shading but regained the pre-senesced expression levels upon re-illumination. Transcription factors that regulate the dark-induced reversibility of Arabidopsis senescence are MYB2, WRKY45, NAC47, AP2-related and BZIP54 (Parlitz et al., 2011). Furthermore, (Fukao et al., 2012) found that SUBMERGENCE1A (submergence tolerance regulator) was involved in the recovery of rice leaves from dark stress by inhibiting ethylene production and decreasing jasmonate and salicylic acid tissue responsiveness.

1.2.1.1.9 Autophagy

Autophagy is induced by sugar starvation, senescence, dark treatment and treatment with glucose in the presence of low nitrogen (Usadel et al., 2008). The significance of autophagy during starvation-induced senescence has been illustrated by finding that it is required for the senescence-dependent degradation of Rubisco (Ishida et al., 2008; Wada et al., 2009). *autophagy* mutants were found to be hypersensitive to nitrogen deficiency and carbon starvation (Thompson et al., 2005). Expression of autophagy genes is induced by treatment with sugars in the presence of low but not high nitrogen. Autophagy genes are also

induced by KIN10, which regulates signalling response to carbon depletion (Baena-González et al., 2007). Recently a close link was demonstrated between autophagic degradation of chloroplasts via RCB and leaf carbon but not N status (Izumi and Ishida, 2011). Their study suggested that during nitrogen-limited senescence, increased carbohydrate levels suppress accumulation of RCBs both during induced and developmental leaf senescence. Taken together these studies indicate that C:N balance may play a significant role in the induction of autophagy genes.

1.2.2.2 Postharvest inflorescence senescence

The genus Brassica (family Brassicaceae or Cruciferae) contains many commercially important vegetables e.g., the edible inflorescences of broccoli and cauliflower or edible leaves of cabbage. Broccoli (*Brassica oleracea* L. *italica*) has enormous health benefits, because it contains nutrients such as vitamins A and C, nutraceuticals such as ascorbic acid, phenolics and glucosinolates, high fiber content and low caloric values (King and Morris, 1994a; Gómez-Lobato et al., 2012).

At harvest, the head of broccoli is a compressed inflorescence composed of multiple branchlets each containing hundreds of immature green florets, arranged in whorls on top of a fleshy stem. Each floret comprises an immature flower enclosed within chlorophyll-containing sepals. Harvested broccoli is highly perishable deteriorating rapidly within 3 to 5 days when stored at room temperature (Rushing, 1990; King and Morris, 1994b; Page et al., 2001). This is associated with the broccoli pedicels ceasing their elongation, florets failing to open and their sepals becoming yellow (Wang, 1977). This rapid deterioration of broccoli following harvest is potentially related to the large number of physiological stresses the head experiences; for example, the sudden loss of xylem-supplied water from the roots and decreased phloem import. This reduces availability of sugars to support signalling, metabolism and growth and changes in hormone levels, as cytokinin import is reduced and ethylene and ABA levels are increased. Harvested broccoli heads lose ~50% of their sucrose by 6 h and by 12 h their respiration has declined coincident with the decline in sugars (Downs et al., 1997). Transport of amino acids (glutamine and asparagines) transiently has been found to rise from ~24 to 72 h after detachment and ammonia levels rise substantially from 72 h onwards (Downs et al., 1997).

1.2.2.1.1 Hormonal control of broccoli senescence

Following harvest, broccoli florets produce a burst of ethylene that peaks at 3 h. The ethylene produced after harvest has a role in regulating harvest-associated sepal yellowing (Chen et al., 2008). However, no clear association between patterns of ethylene production and de-greening rate has been shown for a range of cultivars (King and Morris,

1994a; Tian et al., 1994). The burst in ethylene arises predominantly from the reproductive organs, particularly the stamens, whereas the sepals, by contrast, produce comparatively low amounts of ethylene and only after that produced by the reproductive organs. A change in sensitivity of broccoli florets to ethylene appears to be more important than ethylene production by the sepal (Tian et al., 1994). Ethylene produced by the reproductive organs may be what increases the sensitivity of the sepals to ethylene and causes yellowing as removing them from the florets reduced the rate of sepal de-greening (Tian et al., 1994).

Inhibiting ethylene production in broccoli by driving an antisense ACC oxidase (BoACO2) delays chlorophyll loss, lowers protease activity and maintains total soluble protein in the broccoli florets (Gapper et al., 2005). The broccoli transgenic lines with decreased expression of *ACO1, ACO2* or *ACS1* showed increased shelf life (Higgins et al., 2006). Furthermore, it was also reported that transgenic lines carrying the mutant broccoli ethylene response sensor (boers) gene showed delayed yellowing of harvested florets (Chen et al., 2004).

Exogenously applied cytokinins inhibit floret yellowing (Tian et al., 1995) and broccoli over-expressing the bacterial cytokinin-biosynthesis gene *IPT* showed retarded senescence (Chen et al., 2001). Cytokinin-mediated delay of postharvest senescence of transgenic broccoli harboring *IPT* was suggested due to the accumulation of stress-responsive proteins and antioxidant enzyme activity (Liu et al., 2011). 6-benzylaminopurine (6-BAP) application delayed the senescence of broccoli florets by regulating the activities of CHLOROPHYLLASE and Mg-DECHELATASE (Xu et al., 2011a). 6-BAP application was also found to delay the expression of BoPaO, involved in chlorophyll degradation and degreening of detached broccoli heads (Gomez-Lobato et al., 2012).

1.2.2.1.2 Chlorophyll catabolism in harvested broccoli

Loss of chlorophyll is the major change that affects the quality index of broccoli (Amir-Shapira et al., 1987). One of the key steps in the breakdown of chlorophyll is the opening of the chlorin ring by pheophorbide a oxygenase (PaO). Increasing amounts of data have suggested that PaO activity is positively correlated with chlorophyll loss (Pružinská et al., 2003; Chung et al., 2006). Recently, Gómez-Lobato et al. (2012) found that *BoPaO*

expression was four fold higher in senesced heads of dark-held broccoli at 20°C compared to pre-senesced heads. These researchers also showed that the *PaO* transcripts were high in ethylene treated dark-held broccoli heads and lower in heads treated with cytokinins and variety of physical treatments (UV and visible light, hot air and modified atmosphere) that delay broccoli senescence. This indicates that *PaO* transcript abundance is a good marker of broccoli head chlorophyll loss and deterioration.

1.2.2.1.3 Proteolysis during postharvest senescence of broccoli

The association of proteases with postharvest senescence of broccoli florets is well documented (Page et al., 2001; Coupe et al., 2003; Eason et al., 2005). For example, four hydration responsive cysteine protease cDNAs (*BoCP1*, *BoCP2*, *BoCP3* and *BoCP4*) have been identified in broccoli floret tissues and their mRNAs shown to increase in transcript abundance within 24 h of harvest (Coupe et al., 2003). These workers also found using protease activity assays that 44% of the harvest-induced protease activity in the broccoli florets was due to cysteine and serine proteases (Coupe et al., 2003).

1.3 Identifying novel key genetic regulators of postharvest inflorescence senescence

As mentioned in the previous chapter, the postharvest metabolism of broccoli has been well studied over the past two decades and our knowledge of its postharvest biology has increased substantially (Chen et al., 2008; Aiamla-or et al., 2012; Gómez-Lobato et al., 2012; Gomez-Lobato et al., 2012). However, there is still much to be learnt of the biological mechanisms of its postharvest senescence. Broccoli has been particularly useful for studying physiological and biochemical aspects of inflorescence senescence. However, transforming broccoli with potential key regulatory genes necessary for understanding the harvest syndrome is a long process requiring six or more months and considerable space which is limiting in containment facilities. Therefore, it would be useful if there were more convenient systems that could be used to help understand the harvest programme initiated in broccoli inflorescences.

1.3.1 Modeling postharvest metabolism of broccoli with Arabidopsis

Arabidopsis has long been used to study fundamental processes associated with a wide variety of developmental and stress conditions. This is because, from an experimental standpoint, it has huge advantages over most species, i.e., it is physically small, has a small genome, is easy to transform, a rapid life cycle, a large number of mutant collections and a huge array of web-based genomic resources. An extensive amount of research work with Arabidopsis also enables comparative transcriptome analysis with previously published senescence studies on leaves (Lin and Wu, 2004; Buchanan-Wollaston et al., 2005; van der Graaff et al., 2006; Breeze et al., 2011), siliques (Wagstaff et al., 2009) and cell cultures (Swidzinski et al., 2002).

Previous work at Plant and Food Research established that detached dark-held Arabidopsis inflorescences were useful for uncovering the regulatory control underlying energy-deprivation-mediated senescence. When immature inflorescences of *Arabidopsis thaliana* Landsberg *erecta* were detached and held in the dark at 21°C they were found to reproducibly degreen to be completely yellow at day 5. The degreening of the detached dark-

held inflorescences was also affected by natural and synthetic hormonal regulators of leaf senescence suggesting that the system could be used to conveniently understand and model the mechanisms underlying postharvest deterioration of harvested immature tissues.

In this thesis I further characterize senescence of detached dark-held Arabidopsis inflorescences and use it to uncover novel genetic regulators that control energy-deprivation-driven deterioration.

1.4 Thesis Aims

1. To describe the senescence of detached dark-held Arabidopsis immature inflorescences (Chapter 3.1)

2. To determine the effect of stress hormones on timing of dark-induced inflorescence senescence (Chapter 3.2)

3. To use an ethyl methane-sulfonate (EMS) mutagenesis approach to identify Arabidopsis mutant(s) with inflorescences that show altered timing of degreening (Chapter 3.3)

4. To identify and characterize at least one genetic lesion behind the delayed senescence mutants (Chapter 3.4 to 3.7)

Blank page

Chapter 2

Blank page

Chapter 2 Materials and Methods

2.1 Plant material and growth conditions

2.1.1 EMS and T-DNA plant material

A population of 20,000 EMS mutagenized M2 seeds of *Arabidopsis thaliana* (Arabidopsis), ecotype Landsberg *erecta* (L*er*-0) was obtained from LEHLE seed company (Round Rock Tx, USA). T-DNA insertion mutants were obtained from The Arabidopsis Information Resource (http://www.arabidopsis.org). Two different ecotypes of Arabidopsis were used because most T-DNA mutants were only available in Col-0. To decrease the effects of different ecotypes on the results EMS and T-DNA mutants were compared with their respective wild-types. Seeds were germinated and grown in a temperature-regulated growth chamber (20°C–22°C, 16 h light and 8 h dark cycle, white light 180 µE and 60% relative humidity unless otherwise stated). Inflorescences of growth stages 6.00–6.10 (as described by Boyes et al., 2001) from the primary bolts of 6 to 8-week-old EMS mutated Arabidopsis plants were typically used for the experiments. Inflorescences were harvested by excising at the junction between the peduncle and the pedicel of the lowest unopened floret at the base of the inflorescence. The detached inflorescences were then placed with their cut ends in ~200 µL water in wells of a 96-well micro-titre plate. The plate was housed on moistened blotting paper in a closed plastic container at 21°C. At day 3 of dark incubation inflorescences were sampled in low light to minimize the effects of brief light exposure. Degreening observations were typically stopped at D7 because after this time fungal growth was increasingly observed as no preservatives were included in the holding solution.

2.1.2 General plant growth conditions

Seeds were vernalized at 4°C in the dark for at least 3-4 days. Seeds of mutants and wild-type plants (L*er*-0 and Col-0) were grown in wet seed Raising Mix™ from Oderings in a temperature-regulated growth chamber (20°C–22°C, 16 h light and 8 h dark cycle, white light 180 μE and 60% relative humidity unless otherwise stated). Harvested seeds of transformed plants (T0 and T1) were sieved and dried for 15-20 days at 25°C and stored at 4°C for at least 7 days before sowing. BASTA selection for transformants was performed by spraying 50 mgL^{-1} of BASTA, a total of four times, starting from the day 4 after germination (DAG), with an interval of four days.

2.2 Chemicals and general methods

Chemicals and reagents were sourced from BDH, Sigma, Merck and Roche unless otherwise stated. Solvents were supplied by Merck. Buffers and solutions were made up to volume with Milli-Q purified water unless otherwise stated. Solutions were sterilised by autoclaving for 20 min at 120°C and 100 kPa or by passing through 0.2 µm Puradisc™ polyethersulfone filters (Whatman).

2.3 Biochemical and physiological methods

2.3.1 Chlorophyll quantitation

Chlorophyll was extracted from inflorescences and leaves by incubating the detached uncrushed tissue in 96% (v/v) ethanol (10 mg of tissue per 30 µL of ethanol) for 4 d in the dark at 4°C. The chlorophyll content was then determined from 2 µL of the supernatant by measuring the absorbance at wavelengths 649 and 665 nm with a Nanodrop ND-1000 spectrophotometer and performing calculations as described by Wintermans and De Mots, (1965).

Chlorophyll *a* = 13.70 A_{665nm} -5.76 A_{649nm} µg mL^{-1}
Chlorophyll *b* = 25.80 A_{649nm} -5.76 A_{665nm} µg mL^{-1}
Total Chlorophyll = 6.1 A_{665nm} +20.04 A_{649nm} µg mL^{-1}

The change in chlorophyll content from day 0 to the other days for each line or treatment was compared with that of wild-type L*er*-0. One way ANOVA and Student's *t* test were applied for statistical analysis of the regression parameter estimates.

2.3.2 Protein quantitation

Reagents:

Extraction buffer: (100 mM Tris- HCl, pH 7.6, 10 mM MgSO4 and 10 mM dithiothreitol)

Soluble proteins were extracted according to the method of Coupe et al. (2003). In brief, 50 mg of tissue was grounded in 500 µL of extraction buffer incubated on ice for 1 h with intermittent vortexing and the cellular debris was pelleted by centrifugation at 10,000 x *g* for 10 min at 4 °C. Soluble protein was then determined from the supernatant using the Coomassie dye-binding assay (Bio-Rad Laboratories) with bovine serum albumin as the standard.

2.3.3 Ion leakage

Relative electrolyte leakage was determined according to the method of Jing et al. (2002). Ten inflorescences (~90 mg of total weight) were harvested at each time point, placed in a 50 mL tube containing 10 ml of de-ionized water and incubated at 25°C for 30 min on an orbital shaker (200 rpm). The initial conductivity of the fluid was measured with Konduktometer model E527 (Metrohm Herisau). The total conductivity was determined after boiling the sample for 10 min. The relative electrolyte leakage was expressed as the percentage of the initial conductivity versus total conductivity.

2.3.4 Ethylene measurement

Ethylene was measured using a laser-based ETD-300 ethylene detector (Sensor Sense BV, Nijmegen, The Netherlands). Ethylene measurement was performed by using stop and flow method. In the stop and flow method selected cuvettes were flushed with air for 30 min to measure ethylene. Arabidopsis inflorescences (~100 mg) were removed and placed in a closed screw-capped 2 mL microfuge tube. The microfuge tube with inflorescences were connected to the instrument by first inserting two needles into the microfuge tube (to serve as inlet and outlet). Tubing was then fitted to the needles. The inlet tubing served to allow air from the catalyzer (that removes hydrocarbons) to enter the microfuge tube and the outlet

tubing enabled the ethylene emanating from the tissue to move through a scrubber (to remove water and CO2) and then to the ETD for ethylene measurement. Ethylene production was measured in nL/h by using ethylene flow and accumulation.

2.3.5 JA and ACC measurement

JA and ACC concentrations were measured by using Liquid Chromatography-Mass Spectrometery (LC-MS) by Dr. Janine Cooney from Plant & Food Research Ruakura, Hamilton.

Preparation of Standards and Samples

A stock solution containing jasmonic acid (JA), salicylic acid (SA), abscisic acid (ABA) and 1-aminocyclopropane-1-carboxylic acid (ACC) each at 1000 µg mL^{-1} was prepared in methanol. A labelled internal standard stock solution containing the isotopically labelled analogues, [$^2H_5$]JA, [$^2H_4$]SA and [$^2H_6$]ABA each at 10 µg mL^{-1}, was also prepared in methanol. Calibration standards containing 0.1, 1, 10, 100 and 1000 ng mL^{-1} each of JA, SA, ABA and ACC were prepared by diluting the stock solution with 1:1 methanol:water. 25 ng of the labelled internal standard solution mix was added to 400 µL of each calibration standard. To 110 mg FW of freeze dried tissue on ice was added 25 ng of the labelled internal standard solution mix and 400 µL of the extraction solvent (20:79:1 methanol:isopropanol:acetic acid). The samples were shaken for 30 min at 4ºC and stored overnight at -20ºC. Following centrifugation at 4ºC and 13,000 x *g* for 10 min, a 100 µL aliquot of the supernatant was taken and diluted 10-fold with water before analysis by LCMS.

LC-MS Method

LC-MS experiments were carried out on a 5500 QTrap triple quadrupole/linear ion trap (QqLIT) mass spectrometer equipped with a TurboIon-SprayTM interface (AB Sciex, Concord, ON, Canada) coupled to an Ultimate 3000 UHPLC (Dionex, Sunnyvale, CA, USA). Chromatographic separation was achieved on a Kinetex column (Phenomenex, Torrance, CA, USA) maintained at 60 ºC. Solvents were (A) water + 1% formic acid and (B) acetonitrile + 0.1% formic acid and the flow rate was 600 µL min^{-1}. For analysis of JA, SA and ABA, the initial mobile phase 15% B was ramped linearly to 50% B at 8 min, then ramped to 100% B at 8.1 min and held for 2 min before resetting to the original conditions. Injection volume was 50 µL. MS data was acquired in the negative mode using a multiple reaction monitoring (MRM) method. For analysis of ACC the initial mobile phase 10% B was ramped linearly to 50% B at 10 min and held for 2 min before resetting to the original conditions. MS data was acquired in the positive mode using a multiple reaction monitoring (MRM) method. The transitions monitored, (Q1 and Q3), along with their optimised parameters (declustering potential (DP), entrance potential (EP), collision energy (CE) and collision cell exit potential (CXP) are listed in Table 2.1.

Table 2.1. MRM transitions used for plant hormones and their isotopically labelled internal standard analogues

Q1	Q3	Compounds	DP	EP	CE	CXP
37.1	2.8	salicylic acid	140	10	22	9
09.0	9.0	jasmonic acid	25	10	25	15
63.0	53.0	abscisic acid	25	10	17	15
41.1	7.0	salicylic acid	35	10	30	15
14.0	2.0	jasmonic acid	25	10	25	15
69.0	59.0	abscisic acid	25	10	17	15
02.1	6.2	1-aminocyclopropane-1-carboxylic acid	0	0	5	5

Other operating parameters were as follows: dwell time, 60 ms; ionspray voltage, -4500 V for negative mode and 4500 V for positive mode; temperature, 600 ºC; curtain gas, 45 psi; ion source gas 1, 60 psi; ion source gas 2, 60 psi. Quantification was performed by the internal standard ratio method for JA, SA and ABA and by external calibration for ACC.

2.4 Bacterial methods

2.4.1 Media, stock solutions and antibiotics

Reagents:

LB (Luria–Bertani) pH 7.5: (1% [w/v] bacto-tryptone; 0.5% [w/v] bacto-yeast extract; 1% [w/v] NaCl)

LB liquid media was autoclaved and stored at room temperature until needed. LB solid media used for plates was prepared with 1.5% (w/v) Bacto-agar (Difco). Following autoclaving the LB media was allowed to solidify in the Schott bottle and stored at room temperature until needed. When plates were to be made, the LB solidified media was melted in a microwave, cooled to ~ 50°C and then supplemented with appropriate antibiotics before pouring into the plates.

Antibiotic salts were dissolved in water to make 100 mg mL^{-1} stocks. Each stock was filter sterilised and stored in an aluminium foil wrapped tube. Spectinomycin (spectinomycin dihydrochloride), kanamycin (kanamycin sulphate) and, gentamicin (gentamicin sulphate) were stored at 4°C and ampicillin (sodium salt of ampicillin) was stored at -20°C. Rifampicin was prepared by dissolving rifampicin crystals in DMSO to get final concentration of 50 mg mL^{-1}. It was then stored in a foil-covered tube at -20°C. Tetracycline was prepared by dissolving tetracycline hydrochloride in 50% (v/v) ethanol to a final concentration of 10 mg mL^{-1}. The solution was then filter sterilized and stored at -20°C in foil wrapped tubes.

2.4.2 Bacterial strains and growth conditions

Escherichia coli strain NovaBlue (NB, Novagen) was used for general lab manipulations and *Agrobacterium tumefaciens* strain GV3101::pMP90 was used for plant transformation. NB and GV3101 were grown at 37°C and 28°C, respectively, on LB-agar plates or in LB broths containing appropriate antibiotics. The broths were shaken at 250 rpm.

NB contains resistance to tetracycline and GV3101 contains chromosomal resistance to rifampicin and resistance to gentamicin due to presence of the disarmed pMP90 T_i plasmid (Hellens et al., 2000).

2.4.3 Preparation of chemically competent NB cells

Lab stocks of chemically competent NB cells were used for general cloning of ligated plasmids. The lab stocks had been prepared according to the method of Inoue et al. (1990) using tetracycline (10 mg L^{-1}) as the antibiotic.

2.4.4 Preparation of electro-competent GV3101::pMP90 cells

Binary plasmids were electroporated into lab stocks of electro-competent GV3101::pMP90 cells in preparation for plant transformation. The electro-competent GV3101::pMP90 cells had been prepared according to the method of McCormac et al. (1998). In brief, GV3101::pMP90 cells were grown at 28°C in LB media containing 20 mg L^{-1} rifampicin (to select for Agrobacterium) and 20 mg L^{-1} gentamicin (to select for the disarmed T_i plasmid MP90). The cells were harvested at mid log-phase (A_{600} = 1.0) by centrifugation at 700 x *g*, washed three times in ice-cold 10% (v/v) glycerol and re-suspended in 0.01 volume of 10% glycerol. The cells were aliquotted into 50 µL volumes, snap frozen in liquid nitrogen and stored at -80°C.

2.5 RNA methods

2.5.1 RNA isolation

Total RNA was extracted from approximately 0.5-1.0 µg FW of frozen, ground, plant tissue by acidic phenol extraction using a modified method of Chomczynski and Sacchi (1987). Frozen tissue was added to guanidine extraction buffer and 0.3 volumes of chloroform:isoamyl alcohol (49:1) were sequentially added, vortexing well after each addition. The phases were separated by centrifugation 10000 x *g*; the aqueous phase was collected and RNA was precipitated with 1 volume of isopropanol. The RNA was collected by centrifugation and the RNA pellet was desalted with 70% (v/v) ethanol, centrifuged, ethanol removed and air-dried. RNA was dissolved in an appropriate volume of sterile water and stored at-20 °C.

2.5.2 RNA quantitation

RNA concentration and purity in samples was measured with a Nanodrop Spectrophotometer ND-1000 (Thermo Fisher Scientific, Wilmington, USA). The instrument measures RNA concentration using Beer's law, which states that absorbance, is directly proportional to the concentration of a solution. This more specifically can be written as:

$(A * e)/b = c.$

Where c is nucleic concentration in ng μL^{-1}, A is absorbance in absorbance units, e is extinction coefficient in ng-cm μL^{-1} and b is the path length in cm.

A_{260} x 40* x dilution factor = ng μL^{-1}

* assumes 40 µg mL^{-1} RNA has an A_{260} = 1.0.

RNA purity was determined by measuring absorbance ratios at 260/280 and 260/230 nm. An $A_{260/280}$ >1.8 indicates a sample free of protein since proteins; particularly aromatic amino acids absorb light at 280 nm. An $A_{260/230}$ > 2 indicates a sample free of carbohydrates and/or solvent.

2.5.3 RNA gel analysis

Reagents:

37% (v/v) formaldehyde (stored at RT)
10 X MOPS buffer: (0.2 M MOPS, 50 mM NaOAC, 10 mM EDTA) made to pH 7.0, autoclaved, stored at RT.
Formamide/BB/XC: (0.01% [w/v] bromophenol blue (BB), 0.01% [w/v] xylene cyanol (XC) dissolved in formamide.
Loading buffer (1mL): 625 µL formamide/BB/XC, 212.5 µL of formaldehyde, 125 µL MOPS and 5 µL (of 10 mg mL^{-1} stock) ethidium bromide. Used at minimum ratio of 2:1 (Loading buffer:RNA).
0.24-9.5 Kb RNA Ladder (Life Technologies)

The RNA gel apparatus and combs were sterilised in 0.1 M NaOH for ~20 min and then rinsed with autoclaved water prior to use to remove potential contaminating ribonucleases. Total RNA was resolved in 1% agarose gel containing 1 X MOPS buffer and 0.22 M formaldehyde (i.e., 1.82 mL formaldehyde in 100 mL gel). The agarose was melted in the 1 X MOPS buffer in a microwave and any water lost to evaporation was replaced. The formaldehyde was added to the melted agarose after it had cooled to ~55°C. After the gel had set, running buffer (1 X MOPS) was added to just cover the gel and RNA samples loaded. The RNA samples were denatured for 10 min at 65°C and cooled on ice for ~2 min to break their secondary structures before loading. Electrophoresis was conducted at 80 V.

2.6 DNA isolation methods

2.6.1 Plasmid DNA isolation

Reagents:

Solution I: (50 mM Glucose, 10 mM EDTA, 25 mM Tris pH 8.0)
Solution II: (0.2 M NaOH, 1% (w/v) SDS)

Solution III: (3 M potassium acetate, 11.5% (v/v) glacial acetic acid)

Plasmid DNA was isolated from NB and GV3101 cells by a modification of the alkaline lysis method of Sambrook et al. (1989). Cells from ~1.5 mL (for NB) or 3 mL (for GV3101) overnight cultures were pelleted by centrifugation at 10000 x *g* for 30 s at room temperature. The supernatant was decanted and the cells re-suspended in 200 µL of solution I by running the base of the microfuge tube over the holes of a microfuge rack. The re-suspended cells were then lysed by gently inverting in 200 µL of solution II for ~10 s and neutralized with 200 µL of solution III. The protein, carbohydrates and genomic DNA were pelleted by centrifugation at 10000 x *g* for 10 min at 4°C and ~500 µL of the cleared lysate removed to a fresh microfuge tube where it was precipitated with 1 volume of isopropanol. The precipitated plasmid DNA was pelleted by centrifugation at 10000 x *g* for 10 min at 4 °C, washed with 700 µL of 70% (v/v) ethanol and air-dried for ~10 min. The DNA was then dissolved in 20 µL sterile water and stored at -20°C until needed.

2.6.2 Genomic DNA isolation

Fresh leaves from two different ecotypes (L*er*-0 and Columbia) and their heterozygous plants were frozen in liquid nitrogen. Genomic DNA for HRM analysis and cloning was isolated by Slipstream automation (Plant & Food Research, Tennent Drive, Palmerston North, New Zealand) or by utilizing the previously described DNA extraction protocol of Dellaporta et al., (1983). The purity and quantity of isolated DNA was tested with Nanodrop ND-1000 Spectrophotometer. Pure DNA samples with A 260/280 values of ~1.8 and A 260/230 values of ~2.0-2.2 were selected for downstream analysis.

2.6.3 Nuclear enriched genomic DNA isolation

Reagents:

Extraction Buffer 1: (0.4M sucrose, 10 mM Tris-HCl pH 8.0, 10 mM $MgCl_2$, 5 mM β-mercaptoethanol [β –ME]) To make 100 mL: 20mL of 2M sucrose, 1 mL of 1M Tris-HCl pH 8.0, 1 mL of 1M $MgCl_2$, 35 µL of 14.3M β –ME, made to volume with water and stored at 4 °C. β -ME was added before use.

Extraction Buffer 2: (0.25 M sucrose, 10 mM Tris-HCl pH 8.0, 10 mM $MgCl_2$, 1% Triton X-100, 5 mM β –ME) To make 10 mL: 1.25 mL 2M Sucrose, 100 µl of 1M Tris-HCl pH 8.0, 100 µL of 1M $MgCl_2$, 0.1 mL of 100% Triton X-100 and 3.5 µL of 14.3M β –ME made to volume with water. β –ME was added before use.

Extraction Buffer 3: (1.7 M sucrose, 10 mM Tris-HCl pH 8.0, 2 mM $MgCl_2$, 0.15% Triton X-100, 5 mM β –ME) To make 10 mL: 8.5 mL of 2M Sucrose, 100 µL of 1M Tris-HCl pH 8.0, 20 µL of 1M $MgCl_2$, 15 µL of 100% Triton X-100 and 3.5 µL of 14.3M β –ME, made to volume with water. β –ME was added before use.

TE buffer (10 mM Tris-HCl pH 8.0, 1 mM EDTA pH 8.0)

Tris-buffered phenol: 250 g phenol crystals dissolved in 100 mL water containing 0.25g (0.1% w/v to phenol) of hydroxy quinoline. 100 mL 0.5 M Tris-HCl (pH 8.0) was mixed for ~15 min with the phenol. After phase separation, the upper layer was discarded the procedure repeated with 0.1 M Tris-HCl and ~1 cm layer of the Tris left over the phenol and the phenol stored at 4°C in the dark. The pH of buffer saturated phenol should be ≤ 7.5 for DNA extraction. PCI, Phenol:chloroform:isoamyl alcohol (25:24:1)

Nuclear enriched genomic DNA was isolated according to the procedure of Lutz et al. (2010). Leaf tissue (~200 mg FW) was harvested into 2 mL microfuge tubes then snap frozen in liquid nitrogen and stored at -80°C until needed. On the day of DNA isolation, the tissue was removed to a mortar filled with liquid nitrogen and crushed with a pestle. The tissue was then transferred to a 50 mL Falcon tube containing 25 mL of ice-cold Extraction Buffer 1 and vortexed. The solution (green coloured) was then filtered through two layers of Miracloth (Calbiochem-Novabiochem, La Jolla, CA, USA) into a fresh sterile 50 mL falcon tube on ice. If cellular debris was present in the filtrate the solution was filtered again. The filtrate was then centrifuged at 1940 x *g* for 20 min at 4ºC to pellet the organelles including chloroplasts, which made the pellet green in colour. The supernatant was then discarded and the organelle-containing pellet re-suspended in 1 mL of ice-chilled Extraction Buffer 2, which contained Triton X-100 for preferential elimination of chloroplasts. The re-suspended enriched intact nuclei were pelleted by centrifugation at 12 000 x *g* for 10 min at 4ºC. Then re-suspended in 300 µL of ice-chilled Extraction Buffer 3 (by gently pipetting up and down to remove all signs of clumps) and gently overlaid on 300 µL of chilled Extraction Buffer 3 present in a clean 1.5 mL microfuge tube. The nuclei were then pelleted by centrifugation at 14 000 x *g* for 1 h at 4 °C and re-suspended in 720 µl TE buffer.

Contaminating RNA was removed from the DNA by digesting with RNase (10 µL 5 mg ml^{-1} RNase, 16 µL 5M NaCl and 64 µL water) at 65ºC for 30 min. The RNase and other contaminating proteins were removed from the DNA by digesting with Proteinase K (12 µL 10 mg mL^{-1} Proteinase K, 80 µL 10% SDS) at 45ºC for 1 h. The DNA was further cleaned by adding 800 µL PCI to the DNA in a 2 mL microfuge tube, shaking the mixture for 2 min by hand and centrifuging for 2 min at 980 x *g*. The supernatant was transferred to a clean tube and the PCI step repeated. The supernatant was then transferred to a clean tube containing one volume of chloroform (to remove traces of phenol), the tube shaken for 2 min and centrifuged and the supernatant containing the DNA collected. The procedure was repeated and the DNA then removed and precipitated with ~1 volume of isopropanol and 1/10 volume 3M NaOAc. The DNA was pelleted by centrifugation at 980 x *g* for 30 min at 4ºC and the pellet washed twice with 70% ethanol. The DNA was air-dried at room temperature for 10 min and re-suspended in 50 µL TE. An aliquot (1 µL) of DNA was run on a 1% (w/v) agarose gel against lambda DNA of known concentrations to help quantify and look for degradation. DNA concentration was confirmed with a Nanodrop ND-1000 Spectrophotometer.

2.7 Polymerase chain reaction (PCR)-based methods

2.7.1 Genomic PCR

Genomic PCR was used for amplifying plant DNA sequences for use in complementation experiments (Section 2.12.1). PCR was performed with KAPA™ LongRange DNA Polymerase (www.kapabiosystems.com) according to instructions provided by the manufacturer. PCR thermal cycling conditions were adjusted according to the length of amplicon expected and the annealing temperature of primers used.

2.7.2 Reverse transcriptase PCR

For quantitative real-time reverse-transcription PCR, RNA was extracted from cauline leaves and immature inflorescences of Arabidopsis tissues. Total RNA (~1µg) was

treated with RNAse-free DNAse 1 (Invitrogen) and this was used as a template for first strand cDNA synthesis. cDNA was synthesized from the RNA using SuperScript III (Invitrogen) and the reverse-strand primer KS-DT (Appendix 3.5.1).

2.7.3 High resolution melt (HRM)-PCR

Single nucleotide polymorphism (SNP) markers for genotyping of F2 plants were either selected from the SNPs identified by (Warthmann et al., 2007) or by aligning Col-0 genome (ftp://ftp.arabidopsis.org/home/tair/Sequences/whole_chromosomes/) and L*er*-0 genome (kindly provided by Richard Mott) in Geneious. Selection of informative SNPs was performed by using high resolution melt (HRM)-PCR. ~70-150 bp encompassing the SNP was amplified by using primers designed in Prime 3 (http://frodo.wi.mit.edu/primer3/). The following criteria were used for selection of primer pairs. Max self complementarity and max 3' self complementarity was changed from 8 to 4 and from 3 to 1 respectively. GC contents were changed from min to 40% and max to 55%. The detailed list of primers used for HRM-analysis is presented in appendix 3.4.1. SNP analysis by the high-resolution melting (HRM) technique (Liew et al., 2004) was performed on a LightCycler 480 instrument (Roche Diagnostics). The SNPs screening was performed on DNA samples of homozygous L*er*-0, homozygous Col-0, heterozygous F1 progeny of outcross of L*er*-0 and Col-0. PCR amplification was performed in 10 µL reaction mixture. The amplification mixture contained 3.5 µL master mix (Light cycler 480 HRM master mix by Roche applied sciences), 0.7 µL Mg^{+2}, 10µM forward primer, 10µM reverse primer, 2ng/uL genomic DNA. The amplification was achieved by using the following thermal cycling conditions, pre-incubation at 95°C for 5 min, 40 cycles of 95 °C 10 sec, 60 °C 30 sec, 72 °C 15 sec. HRM data was analyzed by using LightCycler 480 SW1.5 software. The melting data were normalised by adjusting start and end fluorescence signals, respectively, of all samples to the same levels. The HRM curve for each individual was visually scored. Heterozygous DNA was identified by the low melting temperature of heteroduplexes. Fluorescence intensity values were normalized between 0 and 100%.

2.8 DNA analysis

2.8.1 Agarose gel electrophoresis

Reagents:

10 × TBE buffer stock: (0.89 M tris-base, 0.89 M boric acid and 20 mM EDTA) stored at RT.
10 × loading dye: (20% (w/v), Ficoll 400, 0.1 M EDTA (pH 8.0), 1% (w/v) SDS, 0.25 (w/v) bromophenol blue and 0.25% (w/v) xylene cyanol) stored at RT.

DNA fragments produced by PCR (Section 2.7.1 and 2) and restriction digestion (Section 2.9.1) were resolved in 1% (w/v) agarose gels. Typically, 100 mL gels were made by melting 1 g of agarose in 1 X TBE buffer in a microwave. The melted agarose was then cooled to ~50°C and ethidium bromide (2 µl of 10 mg mL^{-1}) added and the gel poured. Once set, the gels were covered with 1 X TBE buffer and the DNA samples in 1 X Loading dye added. The DNA fragments were resolved at 6 V cm^{-1}. Following electrophoresis, the fragments were visualized using a Molecular Imager Gel Doc TM XR System (BioRad) and photographs taken using the attached video printer vd-1500 (Sony). Size of DNA was estimated by comparing the mobility of the DNA to that of the fragments in the 1 kb plus DNA Ladder (Life Technologies). Quantity of DNA was estimated by comparison to masses of fragments of either the Low DNA Mass™ Ladder or High DNA Mass™ Ladder (Life Technologies).

2.8.2 DNA sequencing

Sequencing was performed upon plasmids containing gene of interest. 300ng of plasmid DNA was used for sequencing reaction with 3.2 pmol of sequencing primers. Sequencing reactions were prepared separately for both reverse and forward primers. The plasmid DNA with primers were sent to Allan Wilson Centre Genome Service (Massey university). The sequencing was performed by using BigDye Terminator V3.1 chemistry. The obtained sequence data was cleaned of vector and poor sequences and errors edited. The editing, alignments and contigs of sequencing data were performed with Geneious.

2.9 DNA cloning

2.9.1 DNA endonuclease digestion

DNA was digested with Roche restriction endonucleases at their recommended temperatures and in their recommended buffers. The total concentration of glycerol in the reactions was kept at 5% (v/v) or below to reduce the incidence of 'star' activity, whereby the endonucleases cleave additional sequences similar to their normal targets.

Typically, plasmid DNA was digested with 10 U of restriction enzyme (1 μL) in their appropriate SuRE/Cut buffer in a volume of 20 μL. Where two restriction enzymes, e.g., NotI and PstI required the same buffer, the DNA was simultaneously digested with both enzymes together. Endonuclease reactions were typically carried out at 37°C for 1-16 h depending upon whether it was for diagnostic purposes (short incubation) or for gel purification (long incubation). The DNA fragments were resolved after digestion by agarose gel electrophoresis (Section x).

2.9.2 DNA purification for cloning

PCR products and plasmids were purified for sequencing reactions and cloning either by using the High Pure PCR Product Purification Kit (www.roche-applied-science.com) or by gel purification. Gel purification was carried out with the Zymoclean™ Gel DNA Recovery kit (Zymo Research Corporation, Irvine, CA, USA). Purification was performed to remove unused dNTPS and primers.

2.9.3 DNA quantification

DNA was quantified by gel and spectrophotometric methods. For in-gel quantification, the DNA was separated in an ethidium-bromide-containing agarose gel (section) alongside the Low DNA Mass™ Ladder or High DNA Mass™ Ladder (Life

Technologies). The fluorescence intensity of the DNA under UV was then visually compared to fragments of known mass in the ladders. DNA was also quantified and its purity measured with a Nanodrop Spectrophotometer ND-1000 (Thermo Fisher Scientific) as described in section 2.5.2 for RNA quantitation. In this case

A_{260} x 50[1] x dilution factor = ng μL^{-1}

[1]assumes 50 µg mL^{-1} double stranded DNA has an A_{260} = 1.0.

2.9.4 DNA ligation

PCR products were initially TA cloned into pGEM®-T Easy Vector (Promega BioSciences, San Luis Obispo, CA, USA). Ligation reactions to generate plasmid constructs were performed by using the Rapid ligation kit (Roche) according to the manufacturers' instructions. For directional cloning vector PgREEN0229 was digested with two different restriction endonucleases. PCR products amplified by primer induced restriction enzymatic sites were digested with the corresponding enzymes. The digested PCR products were gel purified either by using Zymoclean Gel DNA Recovery Kit (Zymo Research) or High pure PCR product purification kit (Roche). For non-directional cloning vectors were dephosphorylated with Shrimp Alkaline PHOSPHATASE (Roche), following the manufacturer's instructions to prevent intra-molecular ligation. For ligation the insert and vector were quantified by using spectorophotometer and the amount of insert was determined by the following formula.

ng of insert = (ng of vector × kb size of insert/ kb size of vector) × insert to vector ratio

2.9.5 Transformation of NB cells

Chemically competent NB cells were transformed with plasmids using the heat shock method. Competent cells (50 µL) were removed from the minus 80°C freezer and immediately placed on ice. When the cells thawed 10-20 µL of the ligation reaction was gently added to them and the mixture placed on ice for ~5 min. The cells were then heat-shocked at 42°C for 30 sec in a water bath and transferred back to ice for ~5 min. Depending upon the antibiotic used cells were either immediately plated (when ampicillin was used) or

allowed to recover in LB-broth for 1 h at 37°C (when streptomycin and kanamycin were used). NB cells transformed with pGEM®-T Easy Vector (Promega) were selected in cultures or on plates containing 100 mg mL^{-1} ampicillin. NB cells transformed with pGreen0229were selected in media containing 50 mg mL^{-1} kanamycin.

2.9.6 Transformation of GV3101::pMP90 cells

Electro-competent GV3101::pMP90 cells were transformed with approximately 0.5 µg of plasmid DNA by electroporation. Aliquots (20 µL) of freshly thawed GV3101 competent cells were gently added to 1 µL of pGreen0229 and 1µL of pSOUP (to enable efficient replication of pGreen0229in GV3101::pMP90, Hellens et al. 2000). The mixture was then carefully placed between the electrodes of a pre-chilled electroporation cuvette (BioRad Laboratories Ltd, Auckland New Zealand). Cells were electroporated at 300 V in a Cell-Porator Electroporation System (Life Technologies) following the instructions of the manufacturer and then transferred to a 14 mL bacterial culture tube containing 1 mL of LB-media for recovery at 28°C with shaking (250 rpm) for 3 h. The recovered transformed cells were then spread on LB agar plates containing 50 mg L^{-1} kanamycin (to select for pGreen0229), 50 mg L^{-1} rifampicin (to select for GV3101) and 20 mg L^{-1} gentamicin (to select for pMP90 of GV3101).

2.9.7 Construction of plasmid constructs to complement *dis58*

Genomic DNA of AT4G13495 was amplified from DNA of *Arabidopsis thaliana* (L*er*-0) using the following primers, ggcCTGCAGGTTGTGGAATAATCTCTTGTCAGG (forward primer) and cgcGCGGCCGCCCAGATAAGGCAAGTGTAGGATTC (reverse primer). To facilitate the cloning in to pGrenn 0229, a PST1 site was added to 5′ of forward primer, a NOT1 restriction site was added to the 5′ of reverse primer. The length of amplified product was 5642 bp including 1832bp DNA sequence upstream of 5′ region of the AT4G13495 gene (native promoter of the gene). The amplified gene fragment was first cloned into pGEM T Easy vector by TA cloning (58TA) (Appendix 3.5.2). The plasmid was digested with *ECO*R1 to identify successfully transformed plasmids. The plasmid DNA was sequenced by using M13 and M14 reverse primer from ABI Sequencing and Genotyping Services at Massey. The cloned DNA fragment was excised as NOT1-PST1 fragment and

was cloned into corresponding site of binary vector to make 58comp construct (Hellens et al., 2000). 58comp (Appendix 3.5.3) was digested with *ECOR*1 restriction enzymes to confirm the presence of wild-type AT4G13495 in to the vector.

2.10 Linkage analysis

For linkage analysis, the *dis* mutants were out-crossed to Col-0 and F1 population was raised to get F2 mapping population. Initial mapping of mutations to the chromosome was performed by isolating DNA from at least 10 to 30 F2 recombinants, homozygous for the *dis* mutations. Linkage of the *dis* mutations to single nucleotide polymorphism (SNP) markers was analysed by HRM-PCR technique. The map distance between *dis* mutations and SNP markers was estimated by the number of recombinant offspring divided by the total number of offspring, multiplied by hundred. The map distance between genetic markers was expressed as centimorgan (cM). One cM is equal to a 1% frequency of recombination.

2.10.1 Segregation and mapping population of mutants

To create the F2 segregation and mapping population, the *dis* mutants were backcrossed with wild-type (L*er*-0) and opposite ecotype Col-0, respectively. At least six reciprocal crosses were made between mutants and wild-types. The seeds of crosses were sown to raise F1 segregation and mapping population. F1 plants were selfed and F2 seeds were collected. F2 seeds were sown to get F2 segregation and mapping populations.

2.10.2 Determination of inheritance of mutations

To determine whether the altered inflorescence senescence mutations are recessive, co-dominant or dominant inflorescences of at least 30 F2 plants of segregation population (mutant x L*er*-0) were incubated in the dark for five days. Chi-squared (χ^2) test was used to determine different segregation ratios such as 3:1, 2:1 and 1:1. On the basis of calculated χ^2 values null hypothesis about segregation ratios was accepted at $p>0.05$. χ^2 values were calculated by using $(O-E)^2/E$, where O is observed frequency of F2 plants and E

is expected of F2 plants. The P values were determined at 1degree of freedom by using calculated χ^2 in P value calculator available on line http://graphpad.com/quickcalcs/PValue1.cfm.

Tabulated χ^2 values were calculated from the table of χ^2 at 0.05 probabilities. For 0.05 probabilities the tabulated χ^2 value was 3.84. If calculated χ^2 values were greater than the tabulated χ^2 values then null hypothesis was rejected (http://www.biology.ed.ac.uk/archive/jdeacon/statistics/table2.html#Chi squared test).

2.10.3 Primer design

Primers for genomic and HRM-PCR (used for linkage analysis) were designed by using Prime 3 software (http://frodo.wi.mit.edu/). To design HRM-PCR primers the following criteria was used. The max self complementarity was changed from 8 to 4, max 3'self complementarity from 3 to 1, GC min to 40 and GC max to 55 and product size ranging between 70-150 bp. Primers for genetic analysis of AT4G13495 SALK line were designed by using T-DNA primer Design (http://signal.salk.edu/tdnaprimers.2.html).

2.11 Whole genome sequencing (WGS)

Whole genome sequencing (WGS) was performed by utilizing Axeq technology http://www.axeq.com/axeq.html. The quality of raw reads was tested by using FastQC software and reads with poor sequence quality were trimmed to get good quality reads (http://www.bioinformatics.babraham.ac.uk/projects/fastqc/) by Dr. Ross Crowhurst (PFR, Auckland). Reverse and forward raw reads of WGS were pair-end aligned in Geneious. SNPs were detected after assembly to L*er*-0 (kindly provided by Richard Mott) mapped region and then confirmed with each mutant sequenced as a second background reference for the other.

2.12 Plant transformation

Plant transformation was performed by using the protocol developed by Clough

and Bent, (1998). Arabidopsis L*er*-0 plants were grown under normal plant growth conditions and when they started to flower, the first bolt was clipped to encourage the proliferation of secondary bolts. When plants had enough flowers open then plant transformation was performed. A 500 ml agrobacterium culture carrying the gene of interest was grown at 28°C in LB with appropriate antibiotic to an optical density O.D. 600 of 0.8. Agrobacterium culture was pelleted by centrifugation at 14000 × *g* for 10 mins. The supernatant was discarded and the pellet was dissolved in 500 mL of 5% sucrose solution and 0.5% SilweL-77. Aerial parts of plants were dipped in the solution containing agro-bacterium for 5-10 min. The dipped plants were laid on their side in autoclaved bags for 16-24 hrs to maintain high humidity. After 16-24 h, plants were grown under standard growth conditions and seeds were harvested upon maturity. To identify transformants, seeds from plants dipped with the agrobacterium, were sown under normal plant growth conditions (explained in section 2.1.2). Upon germination, seedlings were sprayed with 100 mg/L of BASTA after every two days. The transformants carrying BASTA resistant gene were survived and were used for downstream analysis.

Chapter 3

Blank page

Chapter 3 Results

3.1 Dark-mediated carbon starvation induces degreening in Arabidopsis inflorescences

Abstract

Physiological and biochemical responses occurring in dark-held detached immature inflorescences of Arabidopsis were investigated. When the detached immature Arabidopsis inflorescences were held in the dark at 21°C with their cut ends in water, their growth rapidly ceased and they de-greened to be completely yellow by day 5. There was no flower opening, pedicel extension, self-pollination or silique development. By contrast, immature detached inflorescences held in a 16 h photoperiod continued to develop like their attached counterparts to produce siliques. The visible degreening of dark-held detached inflorescences was quantified by measuring three hallmarks of senescence, chlorophyll and protein loss and electrolyte leakage. Chlorophyll and protein contents declined to ~5% and 22% of their initial values by day 5 respectively. Membrane permeability increased to be two fold higher than its initial value. Although the whole immature inflorescences showed complete degreening by day 5, the timing of degreening of the individual florets did occur in an age-dependent manner with the outermost florets degreening first. Inflorescence degreening was delayed when the inflorescences were held in 0.27% or 3.0% glucose. Together the data suggests that dark-induced inflorescence degreening is an age-dependent phenomenon driven by dark-mediated energy deprivation responses.

3.1.0 Introduction

Arabidopsis immature inflorescences of ecotype Landsberg *erecta* are composed of whorls of immature florets attached by their pedicels to a central peduncle (Fig. 3.1.1B). Each floret within the inflorescence has a structure characteristic of the Brassicaceae, comprising whorls of four sepals, four petals, six stamens and two carpels (Fig. 3.1.1A) (Passardi et al., 2007). Arabidopsis inflorescences have been classified into different types of inflorescences depending on the structural arrangement of their florets. For instance, Col-0 inflorescences are of the racemose type, i.e., they have an unbranched, indeterminate inflorescence with pedicellate flowers along their axis (Fig. 3.1.1C). L*er*-0 inflorescences are of the racemose corymb type structure, i.e., flat topped due to reduced internode length of the florets and the florets of the outermost (older) whorl having progressively longer pedicels (Fig. 3.1.1D) (Douglas et al., 2002).

Understanding the regulatory programme responsible for senescence of the complex Arabidopsis inflorescence is more problematic than that of leaves. The study of floret senescence is not just that of the outer green sepals but of all the organs enveloped within them. Although each floret organ presumably has its own characteristic transcriptome and response to various senescence inducing signals, increasing amount of data suggests that all the floret organs interact with each other to respond to various environmental signals (Tripathi and Tuteja, 2007). For instance, the importance of the inter-organ signalling between the different floret organs for influencing sepal senescence of immature broccoli inflorescence was demonstrated by (Tian et al., 1994) who showed that removing stamens from the florets delayed the rate of sepal de-greening.

Arabidopsis has been successfully used to study various plant developmental processes due to its annual growth habit and small genome size. Furthermore, the availability of huge genomic resource, e.g., the feasibility to identify the SNPs between different ecotypes of Arabidopsis and availability of T-DNA insertion lines makes it a popular model plant. Therefore, in this study immature Arabidopsis inflorescences were used as a model to understand dark-induced degreening of detached immature floret

tissues. The study suggests that dark-induced degreening of Arabidopsis inflorescences is influenced by the absence of light and concomitant sugar deprivation.

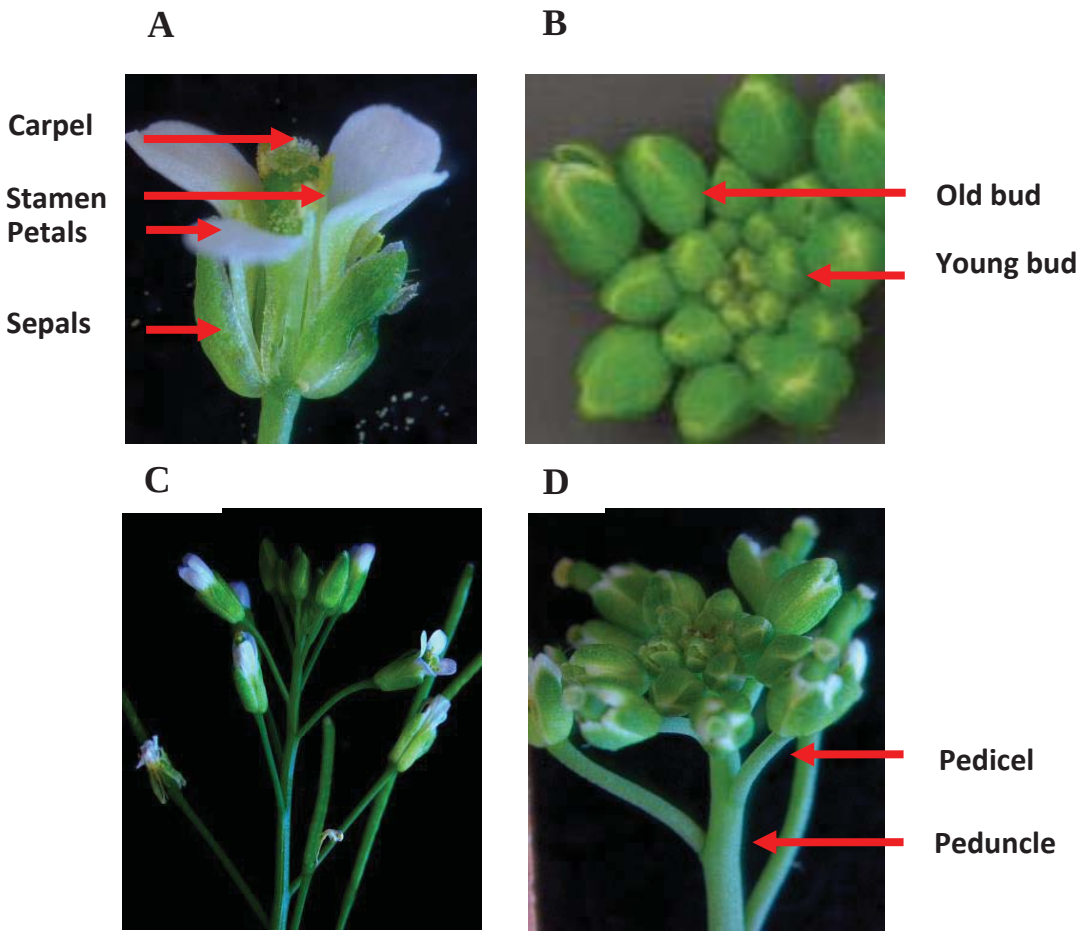

Figure 3.1.1. Structure of Arabidopsis flower and inflorescences.

A. The four whorls of Arabidopsis flower that are sepals, petals, stamens and central carpel region. The floral organs are indicated by arrows. B. L*er*-0 inflorescence with older buds in outer periphery and younger buds in centre of the inflorescence. The arrows indicate older and younger floret buds. C. Col-0 raceme inflorescence. D. L*er*-0 corymb-like inflorescence. The arrows indicate the pedicel of the floret and peduncle of the inflorescence.

3.1.1 Results

3.1.1.1. Darkness causes senescence of detached immature Arabidopsis inflorescences

To investigate the response of immature Arabidopsis inflorescences to detachment and dark stress, immature L*er*-0 inflorescences were detached at the junction between their peduncle (stem that supports inflorescence) and the pedicel (stem of individual flower) of their lowermost unopened floret (3.1.1D). For consistency the inflorescences were preferably detached from the primary bolts of plants. The detached inflorescences were placed with their cut peduncle end in sterile water at 21°C in the light (16 h light and 8 h dark cycles, 100 μmol m^{-2} s^{-1}) or dark for 5 days. At day 3 of dark incubation, the florets of the older outermost whorls were more degreened than the younger central florets at day 3 (Fig. 3.1.2B). At day 5 all florets of the inflorescences had become yellow irrespective of their age.

The detached immature inflorescences held in a 16 h photoperiod showed continuous development like their attached counterparts. Light-held detached inflorescences showed pedicel extension, floret opening and self-pollination, as judged by siliques development (Fig. 3.1.2A). By contrast, the dark-held detached inflorescences were developmentally arrested (no pedicel elongation or flower opening) and their sepals degreened over the 5-day examined period (Fig. 3.1.2B).

The visible inflorescence degreening was quantified by three physiological hallmarks of senescence: chlorophyll content, protein content and ion leakage (Fig. 3.1.2C). The chlorophyll and protein contents of the dark-held detached inflorescences declined rapidly within 24 h and continued to decline steadily over the examined period of five days. At day 3, the dark-held detached inflorescences had lost ~75% of their chlorophyll content and 65% of their protein content. At day 5 the dark-held detached inflorescences had lost ~95% and 70% chlorophyll and protein contents, respectively. Over the same time period electrolyte leakage of the detached dark-held inflorescences increased two fold.

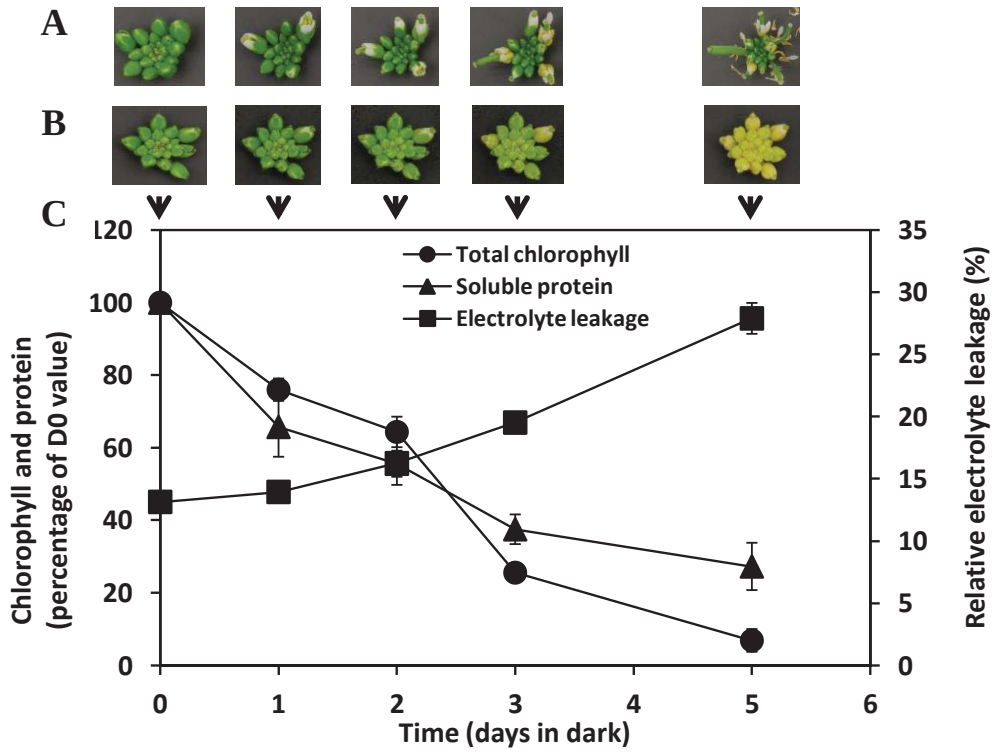

Figure 3.1.2. The effects of light and dark treatments on the growth and development of detached immature Arabidopsis inflorescences.

Inflorescences were harvested, placed with their cut ends in water at 21°C, and exposed to a 16 h photoperiod or held in the dark. A. Detached inflorescences held in 16 h photoperiod. B. Detached inflorescences held in darkness. C. Senescence parameters used to quantify inflorescence senescence. Plants were grown in a green house under long day conditions (16 h light and 8 h dark) for 8 weeks and inflorescences were detached. Chlorophyll and protein contents were expressed as percentage of their initial contents at DAY 0. Bars indicate the standard error of 6 biological replicates. The inflorescences were photographed at day 0, 1, 2, 3 and 5.

3.1.1.2. Dark-induced sugar starvation causes degreening of the detached inflorescences

To investigate whether energy deprivation due to absence of light was the cause of degreening of dark-held detached inflorescences, the inflorescences were treated with 0.27 and 3% glucose (Fig. 3.1.3). Glucose feeding to dark-held detached inflorescences resulted in a significant delay in loss of chlorophyll content. At day 5 of the dark incubation, the glucose treated inflorescences lost ~55% chlorophyll contents of their initial values, whereas control inflorescences lost ~90% (Fig. 3.1.3A). Furthermore, when the dark-held detached inflorescences were fed with glucose they showed pedicel elongation and silique development (Fig. 3.1.3B), that was similar to light-held detached inflorescences (Fig. 3.1.2A). The data suggested that dark-induced carbon deprivation in part causes the growth suppression and degreening of detached inflorescences.

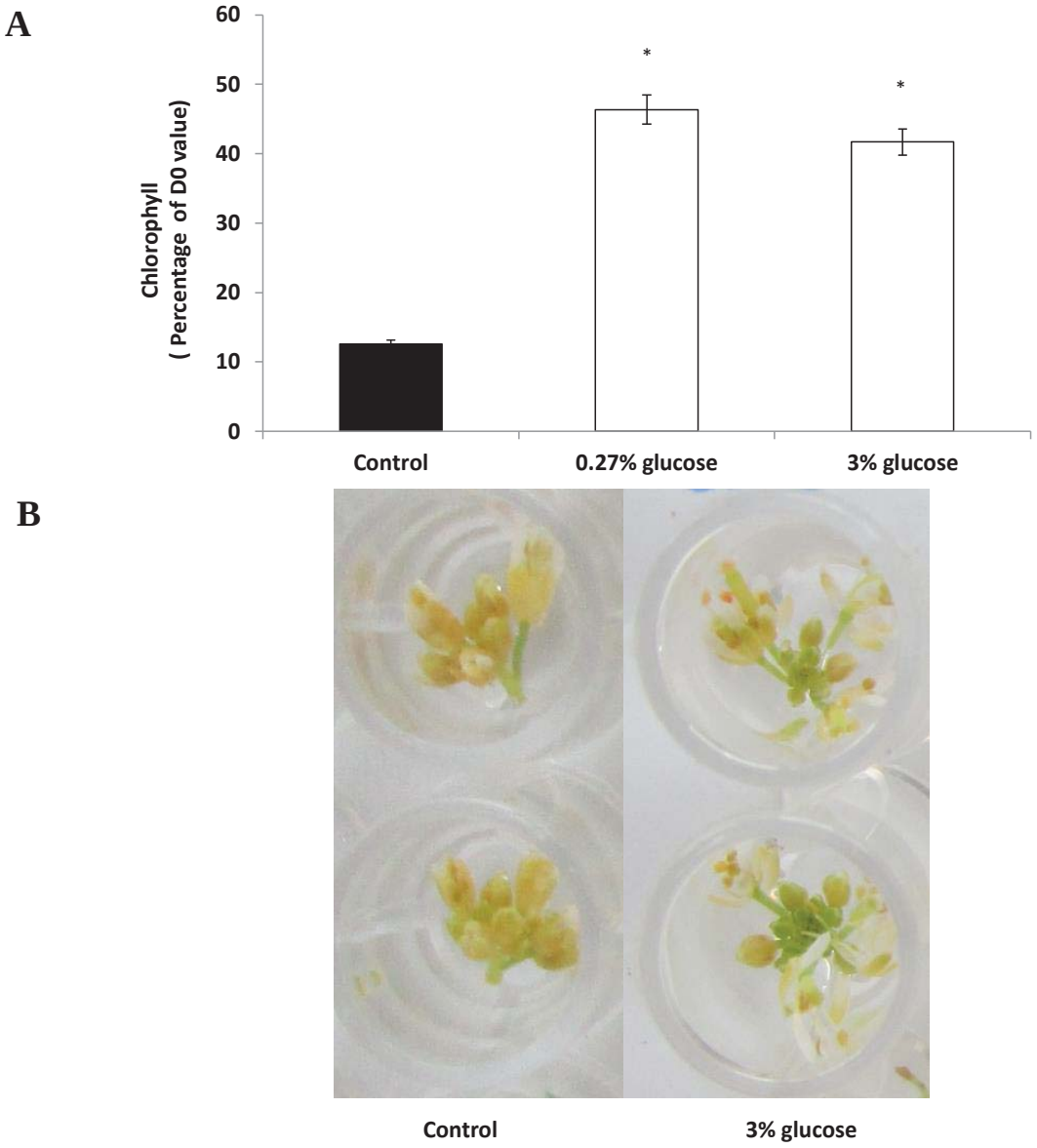

Figure 3.1.3. Exogenously applied glucose results in silique development and delayed senescence in dark-held detached inflorescences.

A. Percentage chlorophyll content of dark-held detached inflorescences when treated with glucose and non-glucose solutions for 5 days. B. Dark-held detached inflorescence treated with 3% glucose. Plants were grown in a green house under long day conditions (16 h light and 8 h dark) for 8 weeks. The inflorescences were detached from the primary bolt of the plants placed in water with and without glucose and held in the dark for 5 days at 21°C. Bars indicate standard errors of six biological replicates. Satistically significant differences in percentage chlorophyll content between treatment and control were determined using Student's *t-test* (* $P < 0.05$).

3.1.1.3 Dark-held florets of detached inflorescences degreen in an age-dependent manner

Figure 3.1.2B showed that older florets, present at the periphery of the inflorescence degreened earlier than the central younger florets indicating control of age on floret senescence. To further confirm the age-dependent control of floret senescence, I investigated the timing of degreening of younger floret in the dark by using detached inflorescences having different proportion of younger and older florets. For convenience, the inflorescences were divided into different groups depending on the number of florets present in the two outermost whorls of the inflorescence. The inflorescence groups included those with 6 florets (group 1), 9 florets (group 2), 12 florets (group 3) and 12 florets with 3 opened flowers at time of detachment (group 4) (Fig. 3.1.4). The florets of the two outermost whorls in group 1 were younger than the florets of the two outermost whorls of other three groups. The age of the florets was judged by its size, as with age the size of the floret increases. The detached inflorescences, except inflorescences of group 1, had both older (in the two outermost whorls) and younger florets (central). This means that florets of two outermost whorls of group 1 were similar in age to the central florets of all the other groups or younger than the florets present in the two outermost whorls of the inflorescences belonging to other three groups.

The inflorescences belonging to different groups were detached and placed in the dark for five days at 21°C (Fig. 3.1.5). Interestingly, at day 3 the outer florets of group 1 did not show any visible degreening, whereas the outer florets of all other groups became yellow. At day 5, all the florets of all the groups became completely yellow.

Taken together the data suggested that degreening of dark-held florets was under the control of age and younger florets required sometime in the dark before they responded to the senescence inducing signals.

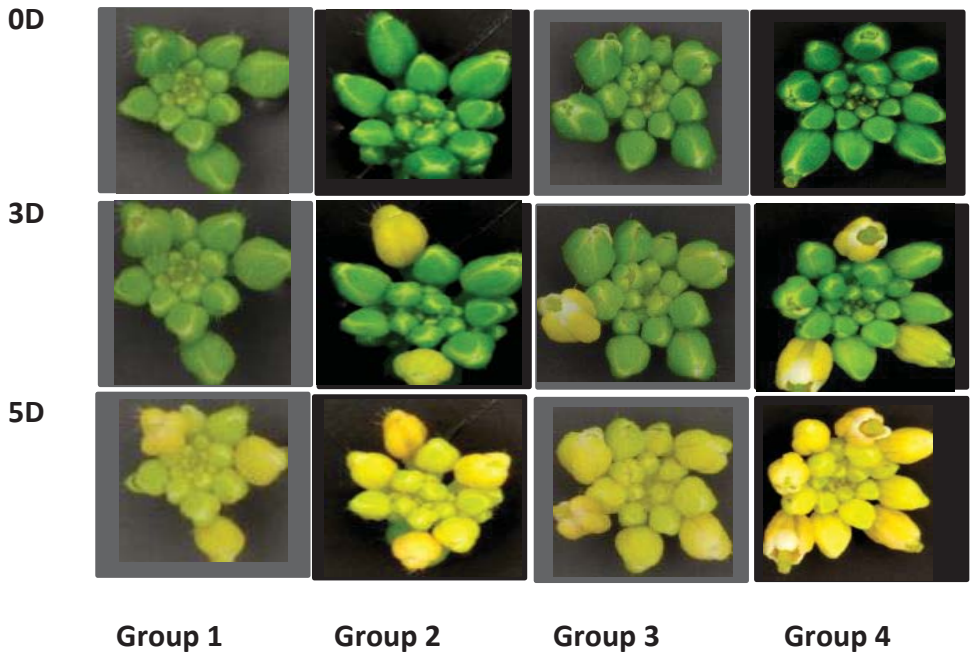

Figure 3.1.5. Dark-induced inflorescence degreening is an age-dependent phenomenon.

The inflorescences were detached from the primary bolt of the plants, placed in water and held in the dark for 5 days at 21°C. The inflorescences were divided into four groups including 6 florets (group 1), 9 florets (group 2), 12 florets (group 3) and 12 florets with 3 opened flowers at time of detachment (group 4). The inflorescences were photographed at day 0, 3 and 5.

3.1.2 Discussion

The results in this chapter suggest that degreening of detached dark-held Arabidopsis inflorescences is a senescence regulated event driven by energy-deprivation in an age-dependent manner. The detached dark-held immature inflorescences held at 21°C ceased floral growth and reproducibly degreened to be completely yellow at day 5 of dark incubation. Inflorescence degreening was quantified by measuring three physiological markers of senescence and the data indicated that inflorescence degreening was a reliable marker of inflorescence senescence. Finding that the detached light-held inflorescences continued their development in the light indicated that the developmental arrest was due to light deprivation and not from stresses such as wounding or restricted nutrient import. The degreening was inhibited by glucose addition suggesting that carbon starvation is one of the signals responsible for the dark-driven chlorophyll loss.

Darkness causes early onset of senescence in detached Arabidopsis inflorescences

The loss of chlorophyll, protein content and increased membrane leakage suggests that the degreening of the detached dark-held inflorescences was the result of senescence being induced in the tissues (Fig. 3.1.2C).

Chlorophyll is one of the primary pigments in the chloroplasts, which are the first organelles to be degraded during senescence. During senescence chloroplasts transform into gerontoplasts (senescing chloroplast) and carbon and nitrogen is released to developing seeds and other growing points (Wittenbach, 1978). Chloroplast disassembly initiates by degradation of the chlorophyll confined to the chloroplast thylakoid membranes and light harvesting complexes (LHCs) (Matile et al., 1996; Hörtensteiner, 2006). It is this chlorophyll loss that results in tissue yellowing (Park et al., 2007). In many studies chlorophyll content has been used as a physiological marker of senescence as its loss is often tightly linked with senescence initiation (Thomas and Stoddart, 1980; Matile et al., 1996; Gan and Amasino, 1997; Hortensteiner and Feller, 2002; Chen et al., 2012). Because of this linkage, loss of the pigment has been used as a convenient screen to successfully identify delayed leaf and whole plant senescence

mutants. For example, the Arabidopsis mutant *ore4-1*, which was identified in an EMS mutagenised population as having delayed chlorophyll loss, showed delayed senescence as judged by maintenance of photochemical efficiency and reduced ion leakage compared to wild-type (Woo et al., 2002). It should be noted that chlorophyll loss is not always an indicator of senescence because in some instances, e.g., in cosmetic stay-green mutants (which have defects in chlorophyll catabolism) chlorophyll loss can be unlinked from the senescence programme (Smart, 1994). However, in the majority of wild type plants chlorophyll loss is a reliable indicator of senescence and its loss in the inflorescences suggest the senescence programme was initiated.

Like chlorophyll loss, protein loss is a typical outcome of senescence progression and the substantial loss in total soluble content in the inflorescences is similar to what has been reported to occur in senescing flowers and leaves (Thomas, 1976; Noodén, 1988; Hashimoto et al., 1989). Coupe et al., (2003) found that during senescence of immature broccoli floret tissues protein content declined as protease activity increased. In rice seedlings decreased chloroplast size was positively linked with decreased photosynthesis and increased protein degradation (Hashimoto et al., 1989). The decline in total protein content of the degreened dark-held detached inflorescences is therefore suggestive of senescence occurring in the inflorescences.

The third physiological marker of senescence investigated in the dark-held detached inflorescences was ion leakage, which is considered to be a measure of membrane permeability (Rolny et al., 2011). Increased membrane permeability is damaging as it disrupts the electrochemical gradient of various cations (e.g., ammonium) and disintegrates cellular membranes (Rolny et al., 2011). Many studies have shown that ion leakage increases in tissues as they senesce (Fan et al., 1997; Woo et al., 2001; Tripathi and Tuteja, 2007; Shahri and Tahir, 2011). The increased ion leakage detected in the dark-held detached inflorescences indicated that the dark and/or detached stress had caused cellular damage. The ~112% (2-fold) increase in ion leakage was almost similar to the ~80% increase reported for dark induced senescence of detached leaves (Fan et al., 1997).

Together the data showing chlorophyll and protein loss and increased ion leakage suggest that detachment and placement of the inflorescences in the dark leads to initiation of the senescence programme.

Dark-induced inflorescence degreening is under the direct control of age

Older florets present at the edge of the Arabidopsis inflorescence senesced earlier than the central younger florets (Fig. 3.1.2B). This suggests that the timing of dark-induced senescence of the individual florets was under age-related control. This is similar to what has been reported for the florets of immature inflorescences of detached broccoli heads where the older florets at the edge of the heads degreened earlier than the central younger florets (Clarke et al., 1994; Tian et al., 1995). Tian et al., (1995) further demonstrated that broccoli florets of different developmental ages showed significant differences in ethylene production and sensitivity, respiratory activity and chlorophyll loss. Senescence induced by ethylene in Arabidopsis leaves is also dependent on leaf age (Grbic and Bleecker, 1995; Jing et al., 2002). Furthermore, detached carnation petals showed senescence in an age dependent manner (Mor and Reid, 1980). The detached petals of 5-day old flowers showed higher ethylene production and early onset of senescence than the petals of 1 day old flowers.

Further evidence in support of age-dependent control of floret senescence came from dark incubation of detached inflorescences of different ages (Fig. 3.1.4). The florets of outermost whorl of the young inflorescences did not show any visible degreening at day 3 of the dark incubation. However, the florets of outer-most whorls of the old inflorescences became completely yellow at day 3 of the incubation. However, at day 5, all younger florets became completely degreened. This may be because younger florets need time in the dark before they gain competence to respond to the dark-induced senescence signals.

Dark-induced sugar starvation causes inflorescence degreening

Light-held detached inflorescences continued to develop like their attached counterparts (Fig. 3.1.2A). The continuous growth of light-held detached inflorescences

indicated that the photosynthetic machinery of the green tissues (sepals and pedicels) was capable of assimilating enough carbon to maintain inflorescence growth. In contrast to light-held detached inflorescences, dark-held detached inflorescences ceased growth and showed accelerated degreening (Fig. 3.1.2B). This was presumably because the dark-held inflorescences rapidly became carbon-starved as the carbon assimilated into starch during the day was used up to maintain metabolism as has been documented for leaves of dark-held plants (Smith and Stitt, 2007; Usadel et al., 2008). Even as little as a 4 to 6 h night extension was shown to acutely deplete the starch content of leaves and lead to growth suppression of the plants reviewed by (Smith and Stitt, 2007; Usadel et al., 2008). The developmental arrest of the inflorescences is consistent with this and with the finding that resupplying a carbon source inhibited the degreening and led to re-initiation of macroscopic development to silique formation (Fig. 3.1.4). Thus, it appears that it was not the detached stress alone, but the dark stress leading to carbon deprivation that was the major driver of the developmental arrest and onset of senescence of the inflorescences.

Blank page

Blank page

3.2 Exogenously applied MeJA delays dark-induced inflorescence senescence in Arabidopsis

Abstract

Hormones significantly affect the timing and progression of age-related and stress-induced plant senescence. However, little is known about how the different concentrations of the hormones affect this type of response. To study this, detached dark-held immature inflorescences of Arabidopsis were treated with different concentrations of ACC, ABA, SA and MeJA (10 μM to 5 mM). The tissue response to the hormones was quantified by measuring chlorophyll concentration and gene transcript abundance changes. ACC and ABA accelerated inflorescence senescence, whereas SA did not. MeJA at lower concentrations (10 and 100 μM) had little effect on senescence timing, whereas surprisingly at higher concentrations (3 and 5 mM) significantly delayed the process. The underlying gene transcript abundance changes resulting from applying different concentrations of MeJA were determined by qRT-PCR. The lower MeJA dosages did not significantly increase transcript accumulation of the senescence-associated, *SEN4*, *ANAC029*, *NAC3* and *SAG12* and JA responsive genes, *ERF11, ORA59, RAP2.4, PDF1.2* and *JAZ10.* However, the higher MeJA treatments caused a decrease in the transcript abundance of senescence associated genes and an increase in the mRNA abundance of JA responsive genes. The decreased transcript abundance of senescence associated genes indicated that higher MeJA treatments not only inhibited chlorophyll breakdown but delayed the process of occurrence of senescence. Furthermore, the transcript abundance of *ACS2*, *ACO4* and *EIN2* was significantly reduced by higher MeJA concentrations. Here, it is proposed that increased jasmonate signalling delayed the timing of inflorescence senescence by blocking the ethylene response pathway.

3.2.0 Introduction

Plant senescence is the final stage in plant development. Under optimum growth conditions plant senescence is regulated by plant age. However, various environmental stresses such as pathogens, drought, salt, frost and detachment can also affect its timing of initiation (Noodén, 1988). To survive unfavourable growth conditions plants have developed several defense mechanisms including growth inhibition, hypersensitive response and accelerated organ (leaf and flower) senescence. Precocious leaf and flower senescence caused by environmental stresses is known as stress-induced, whereas senescence under favourable conditions is called natural/developmental/age-induced senescence (Noodén, 1988; Rogers, 2006).

Detached leaves, immature inflorescences and flowers experience various kinds of stresses including wounding, carbon deprivation and hormonal imbalance (Doi and Reid, 1995; Hoeberichts et al., 2007; Rogers, 2012; Trivellini et al., 2012). This stress-induced senescence can have a negative economic impact on the agricultural industry by causing grain, vegetable and fruit losses (Miller et al., 2008; Reguera et al., 2012). For example, precocious senescence of edible flowers (carnations and snapdragons) and inflorescence vegetables (broccoli and asparagus) caused by detachment and dark storage limit their economic value (Reviewed by Gepstein and Glick, (2013). Thus understanding mechanisms that confer plant tolerance to biotic and abiotic stresses and inhibit senescence may improve crop yield and nutritional quality (Gepstein and Glick, 2013).

Hormones serve to integrate environmental stresses of both biotic and abiotic origin into the plant senescence programme (Grbic and Bleecker, 1995; Morris et al., 2001; He et al., 2002; Cho et al., 2010; Xue-Xuan et al., 2010; Jibran et al., 2013). Ethylene, ABA, SA and JA are known as stress hormones because they enhance plant adaptation to biotic and abiotic stresses by regulating plant defense responses and senescence (Zeevaart and Creelman, 1988; Xue-Xuan et al., 2010; Li et al., 2012a). These hormones regulate both natural- and/or stress-induced senescence by altering signalling pathways that have been identified by examining expression patterns of senescence marker genes (Buchanan-Wollaston et al., 2005; van der Graaff et al., 2006; Guo and Gan, 2012; Trivellini et al., 2012). For example, 10-25% of those genes that were found to be upregulated during

Arabidopsis leaf senescence showed significantly reduced expression (at least two fold) in *ein2* (defective in ethylene signalling), *NahG* (defective in SA signalling) and *coi1* (defective in JA signalling) mutants (Buchanan-Wollaston et al., 2005).

Concentrations of hormones that alter plant response are considered physiological concentrations (Davies, 1995). Classical hormone theory suggests that hormones act at low concentrations and as their concentration increases the physiological response they cause becomes greater reviewed in Rohwer and Erwin, (2008). For example, ABA was found to suppress ethylene production in wheat leaves and the suppression was greater as the concentration of applied ABA was increased from 100 μM to 1 mM (Wright, 1980). Conversely, it has also been shown that hormones do not affect all plant developmental processes in a dosage dependent manner. For example, the expression of *GS1* (*CYTOSOLIC GLUTAMINE SYNTHETASE*) and *GDH* (*GLUTAMATE DEHYDROGENASE*), involved in plant defense responses, in tobacco leaves was not altered in a dosage dependent manner when plants were treated with different concentrations of SA and JA (50 μM, 100 μM and 1mM) (Pageau et al., 2006). However, as far as I am aware no dosage-dependent effects of hormones on plant senescence have been reported.

Here the study investigated the effect of different concentrations of hormones on the timing of senescence of detached dark-held Arabidopsis inflorescences. It was found that the exogenously applied hormones differentially affected inflorescence senescence during dark incubation. ABA and ethylene (based on ACC response) accelerated senescence, whereas SA had no effect on the process. Surprisingly, MeJA had insignificant effects at lower concentrations and delayed senescence at higher concentrations.

3.2.1 Results

3.2.1.1 Higher applied concentrations of MeJA delay degreening of detached dark-held immature inflorescences of Arabidopsis

The role of stress hormones ethylene, ABA, JA and SA during developmental- and stress-induced leaf senescence has been well documented (Jibran et al., 2013). To understand the role of these stress hormones in dark-induced inflorescence senescence, I detached the immature primary inflorescences of 45-day-old Arabidopsis plants (ecotype L*er*-0) and treated them for 3 days in the dark with different concentrations of ABA, ACC, MeJA and SA (10µM, 100 µM, 1mM, 3 mM and 5 mM) (Fig. 3.2.1).

To investigate the role of ethylene, detached inflorescences were treated with ACC (precursor of ethylene) (Fig. 3.2.2A). The detached dark-held inflorescences treated with 1 to 5 mM ACC had ~15% less chlorophyll content than the untreated control at day 3 of dark incubation. The rate of senescence at the lower concentrations of 10 & 100 µM ACC was not different to the untreated control.

ABA treatments, at all concentrations tested, promoted loss of chlorophyll in the inflorescences at day 3 of dark incubation (Fig. 3.2.2B). The percentage chlorophyll lost by the inflorescences did not simply increase in proportion to the applied concentration of ABA Rather, as the ABA concentration increased from 10 µM to 1 mM the detached inflorescences lost increasing amounts of chlorophyll compared to the untreated control. However, when the concentration of ABA was increased further to 3 and 5 mM, the percentage chlorophyll lost by the tissue was actually less than that observed for inflorescences treated with lower ABA concentrations. In contrast to ACC and ABA, different dosages of SA had no effect on the timing of the senescence of detached dark-held inflorescences (Fig. 3.2.2C).

Treatment of the detached inflorescences with 10 and 100 µM MeJA did not significantly increase chlorophyll loss over that measured in the untreated control (Fig 3.2.2D). In addition, 1 mM MeJA treatment had no effect on the inflorescence senescence.

Interestingly, treatment of the inflorescences with 3 and 5 mM MeJA inhibited chlorophyll loss. The inflorescences treated with 3 mM MeJA retained ~12% and those treated with 5 mM MeJA retained ~18%, more chlorophyll content than the untreated control.

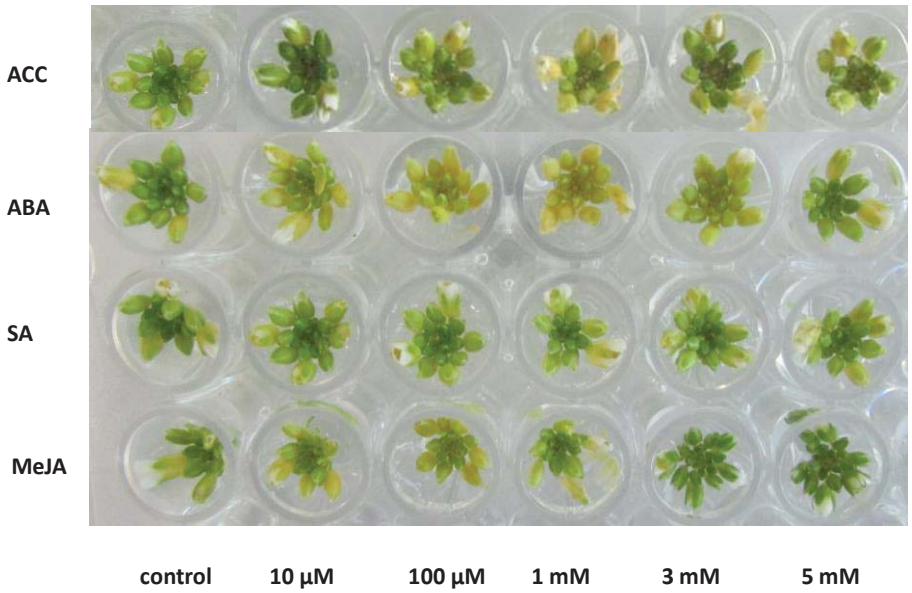

Figure 3.2.1. Exogenous application of ACC, ABA, SA and MeJA to detached dark-held inflorescences.

The detached dark-held Arabidopsis inflorescences were placed in holding solutions of 10 µM, 100 µM, 1 mM, 3 mM and 5 mM ACC, ABA, SA and MeJA for 3 days. Plants were grown in a green house under long day conditions (16 h light and 8 h dark) for 8 weeks and their inflorescences were detached and placed in the dark.

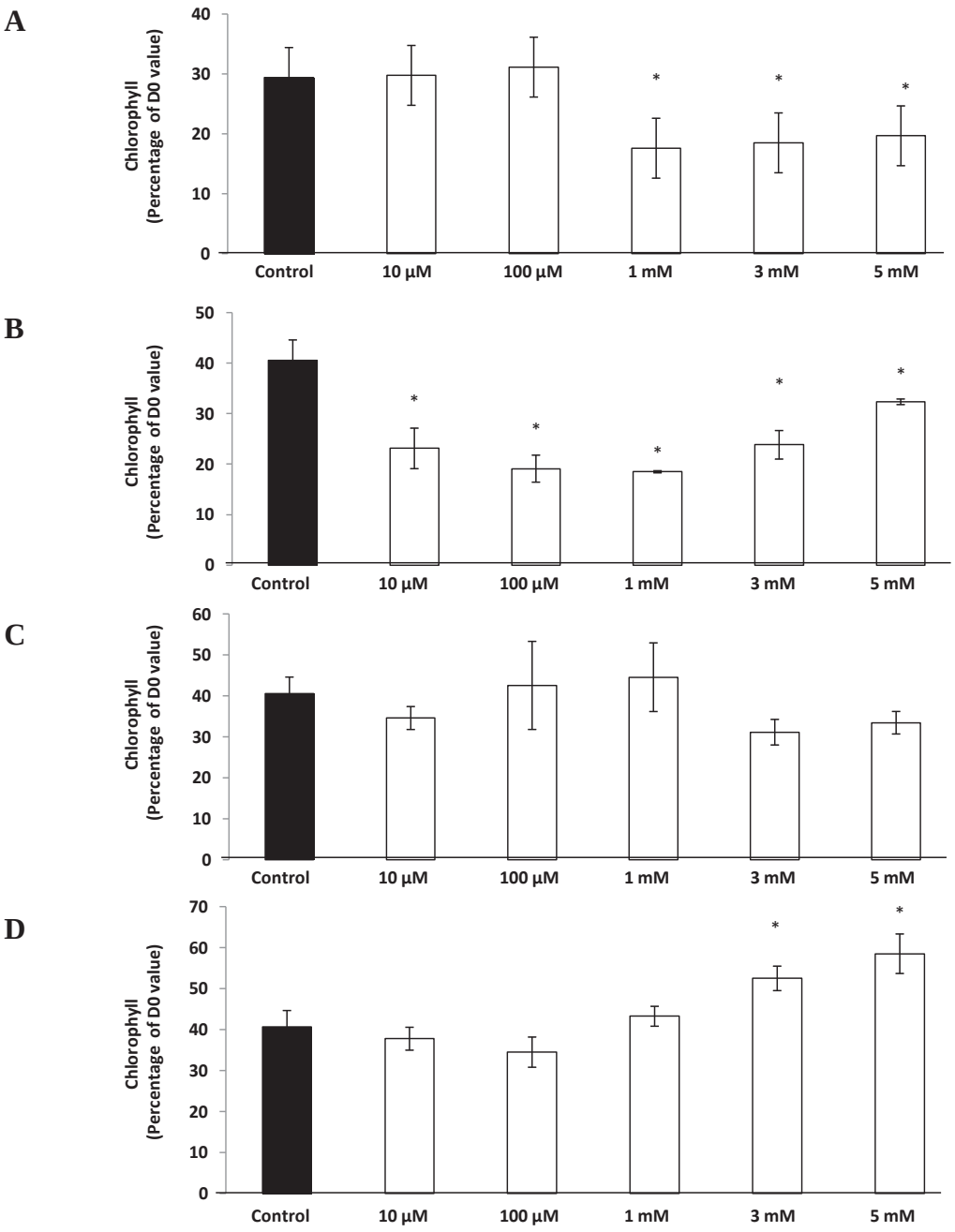

Figure 3.2.2. Effects of different concentrations of plant hormones on chlorophyll content of detached dark-held Arabidopsis inflorescences.

Plants were grown in a green house under long day conditions (16 h light and 8 h dark) for 8 weeks and their inflorescences were detached and held with their cut peduncle in ABA (A), ACC (B), MeJA (C) and SA (D) solutions and incubated in the dark for 3 days. Chlorophyll content is expressed as percentage of day 0 value. Bars indicate the standard error of six biological replicates. One-way ANOVA was performed using Minitab (Version 16). Treatments significantly different from the control were determined using Dunnett's test at **p*=0.05. Residual plots were inspected to check normality and constant variance assumptions. * indicates measurements that were significantly different from that of untreated control.

3.2.1.2 Degreening of detached dark-held leaves is differentially regulated by MeJA concentration

Arabidopsis leaves treated with 33 μM JA showed accelerated senescence (He et al., 2002). However, applying a smaller concentration of MeJA to detached dark-held L*er*-0 immature inflorescences did not accelerate their rate of degreening. Because of this, Arabidopsis leaves were treated with the same MeJA dosages used on the inflorescences to test whether the observed MeJA senescence response was specific to the inflorescences. Cauline leaves were treated with 10 μM, 100 μM, 1 mM, 3 mM and 5 mM MeJA (Fig. 3.2.3). Treatment with 1 mM MeJA accelerated the visible yellowing of the leaves, whereas 3 and 5 mM MeJA delayed it (Fig. 3.2.3A). Like for the detached inflorescences, leaf yellowing was quantified by measuring chlorophyll concentration at day 3 of dark incubation and percentage chlorophyll loss was compared with untreated control (Fig. 3.2.3B). At this time, the leaves of the untreated control had lost ~46% of their chlorophyll concentration. Treatment of leaves with 10 μM MeJA did not significantly change the chlorophyll loss over that observed in the control. However, treatment with 100 μM MeJA increased chlorophyll loss by 13% and when the MeJA concentration was increased to 1 mM the loss was even higher at 39%. By contrast, leaves treated with 3 and 5 mM MeJA retained significantly higher concentrations of chlorophyll (13 and 10%, respectively) than the control. Therefore, like inflorescences, the effect of MeJA on leaf senescence is strongly dependent on the concentration to which the tissue is treated. At lower concentrations, it accelerates whereas at higher concentrations it delays dark-induced leaf senescence.

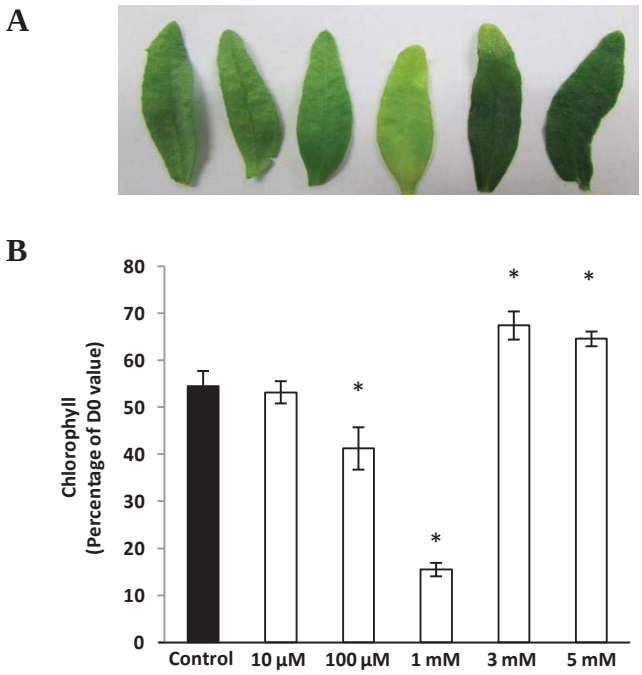

Figure 3.2.3. Effects of different concentrations of MeJA on phenotype and chlorophyll content of detached dark-held Arabidopsis leaves at day 3.

The detached dark-held cauline leaves were incubated in different concentrations of MeJA. A. Phenotype of the leaves on day 3. B. Chlorophyll content is expressed as percentage of day 0 value. Plants were grown in a green house under long day conditions (16 h light and 8 h dark) for 8 weeks and their leaves were detached and placed in the dark. Bars indicate the standard error of six biological replicates. One-way ANOVA was performed using Minitab (Version 16). Treatments significantly different from the control were determined using Dunnett's test at *p=0.05. Residual plots were inspected to check normality and constant variance assumptions. * indicates measurements that were significantly different from that of untreated control.

3.2.1.3 Lower applied concentrations of MeJA significantly accelerated degreening of secondary inflorescences detached from old plants

The significant loss of chlorophyll in the leaves treated with lower concentrations of MeJA suggested an interaction between MeJA and age-associated changes to induce MeJA-mediated early onset of senescence (Jibran et al., 2013). The role of age-associated changes in inducing MeJA-mediated inflorescence senescence was determined by using secondary inflorescences of 55-day-old Arabidopsis plants. The secondary inflorescences were treated with different concentrations of MeJA (10 μM, 100 μM, 1 mM, 3 mM and 5 mM) and incubated in the dark (Fig. 3.2.4). The inflorescence degreening was quantified by measuring chlorophyll concentration at day 3 of their incubation. At this time, the control inflorescences had lost ~70% of their chlorophyll concentration. Treatment with low concentrations of MeJA (10 μM, 100 μM and 1 mM) further accelerated chlorophyll loss by ~5 to 10%, whereas inflorescences treated with 3 and 5 mM MeJA retained ~10% more than control. The data suggests that there is an interaction between age-related changes and effect of MeJA on inflorescence senescence and that the inflorescences used in this study are young.

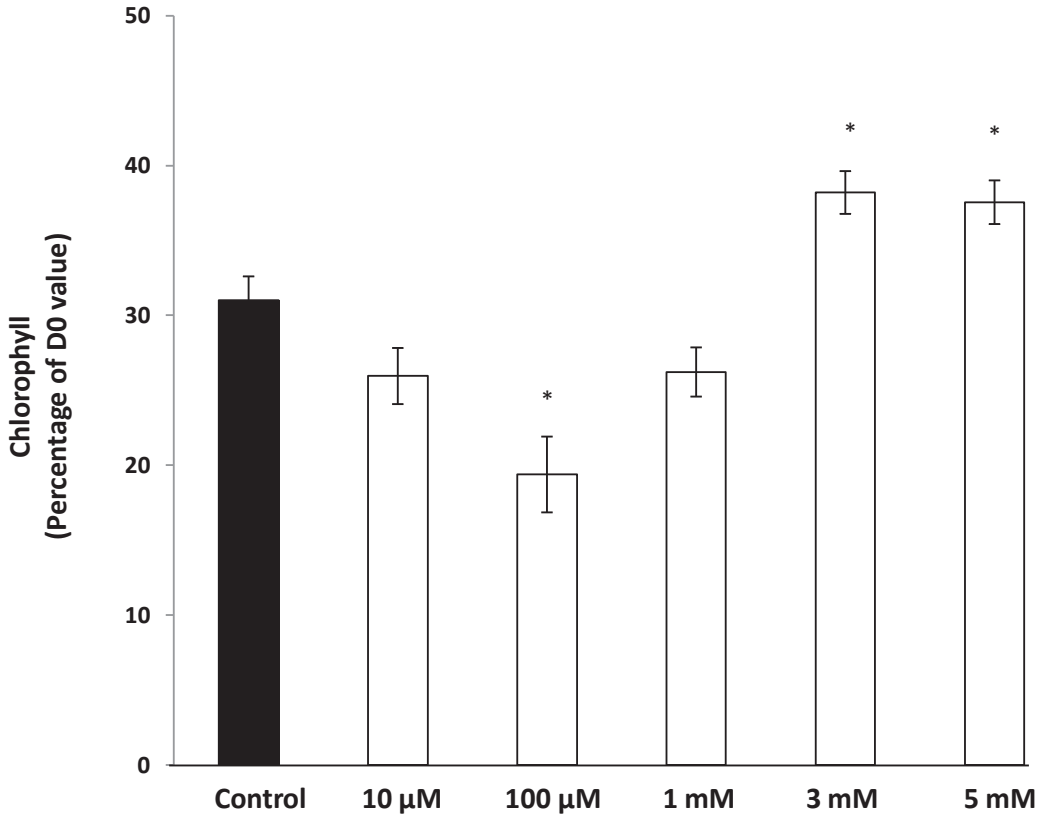

Figure 3.2.4. Effects of different concentrations of MeJA on chlorophyll content of detached dark-held Arabidopsis inflorescences at day 3.

Plants were grown in a green house under long day conditions (16 h light and 8 h dark) for 10-weeks and their inflorescences were detached and placed with their cut peduncle in MeJA solutions and incubated in the dark for 3 days. Chlorophyll content is expressed as percentage of day 0 value. Bars indicate the standard error of six biological replicates. One-way ANOVA was performed using Minitab (Version 16). Treatments significantly different from the control were determined using Dunnett's test at $*p=0.05$. Residual plots were inspected to check normality and constant variance assumptions. * indicates measurements that were significantly different from that of untreated control

3.2.1.4 MeJA treatments differentially regulate mRNA abundance of senescence associated genes

To understand the genetic mechanisms underlying the MeJA-mediated delayed inflorescence senescence phenotype, I quantified the transcript abundance of genes known to show increased mRNA abundance during developmental- and/or artificially-induced leaf and inflorescence senescence. The transcript abundance of *SEN4* (*SENESCENCE 4*), *ATNAP*/*ANAC029* (*ARABIDOPSIS NAC DOMAIN CONTAINING PROTEIN 29*), *ANAC092*, *NAC3* (*NAC DOMAIN CONTAINING PROTEIN 3*, also known as *ANAC019*) and *SAG12* (*SENESCENCE ASSOCIATED GENE 12*) was measured in the inflorescences treated with different concentrations of MeJA and was compared with untreated control.

SEN4 is highly up-regulated during natural- and dark-induced leaf senescence (Park et al., 1998). *ATNAP* is a positive regulator of leaf senescence and its transcript accumulates in senescing leaves and in floral primordia (Guo and Gan, 2006). In addition to causing leaf senescence, *NAC3* also functions as a transcription activator to regulate jasmonate-induced expression of defense and ABA-induced drought tolerance genes (Jiang et al., 2009). *SAG12* is one of the most widely used molecular markers of developmental senescence (e.g., He et al., 2002; Chen et al., 2012).

The transcript abundance of four out of the five senescence-induced genes was suppressed in the 3 and 5 mM MeJA treated inflorescences (Fig. 3.2.5). This was consistent with these concentrations of MeJA delaying the senescence of the detached dark-held inflorescences. The suppression was more than 3-fold for *SEN4*, *ANAC029*, *NAC3* and *SAG12*. Lower concentrations of MeJA (10 and 100 μM) did not significantly alter transcript abundance of three of those four genes. Again, this was consistent with these treatments not significantly altering the chlorophyll content of the inflorescence tissue from that of the untreated control. Although, the increase in transcript abundance of *NAC3* was highest in the inflorescences treated with 1 mM, similar to the other genes its abundance declined in the tissue exposed to the higher MeJA concentrations. In contrast to the other genes, the transcript abundance of *NAC092* was not altered in the inflorescences by any of the MeJA concentrations tested. Furthermore, 1 mM MeJA caused decreased transcript abundance of *SAG12* that is again in agreement with no effects of MeJA on inflorescence

senescence at that concentration. Together the data indicate that high concentrations of exogenously applied MeJA (3 and 5 mM) delays dark-induced inflorescence senescence as suggested by the suppressed transcript abundance of senescence associated genes.

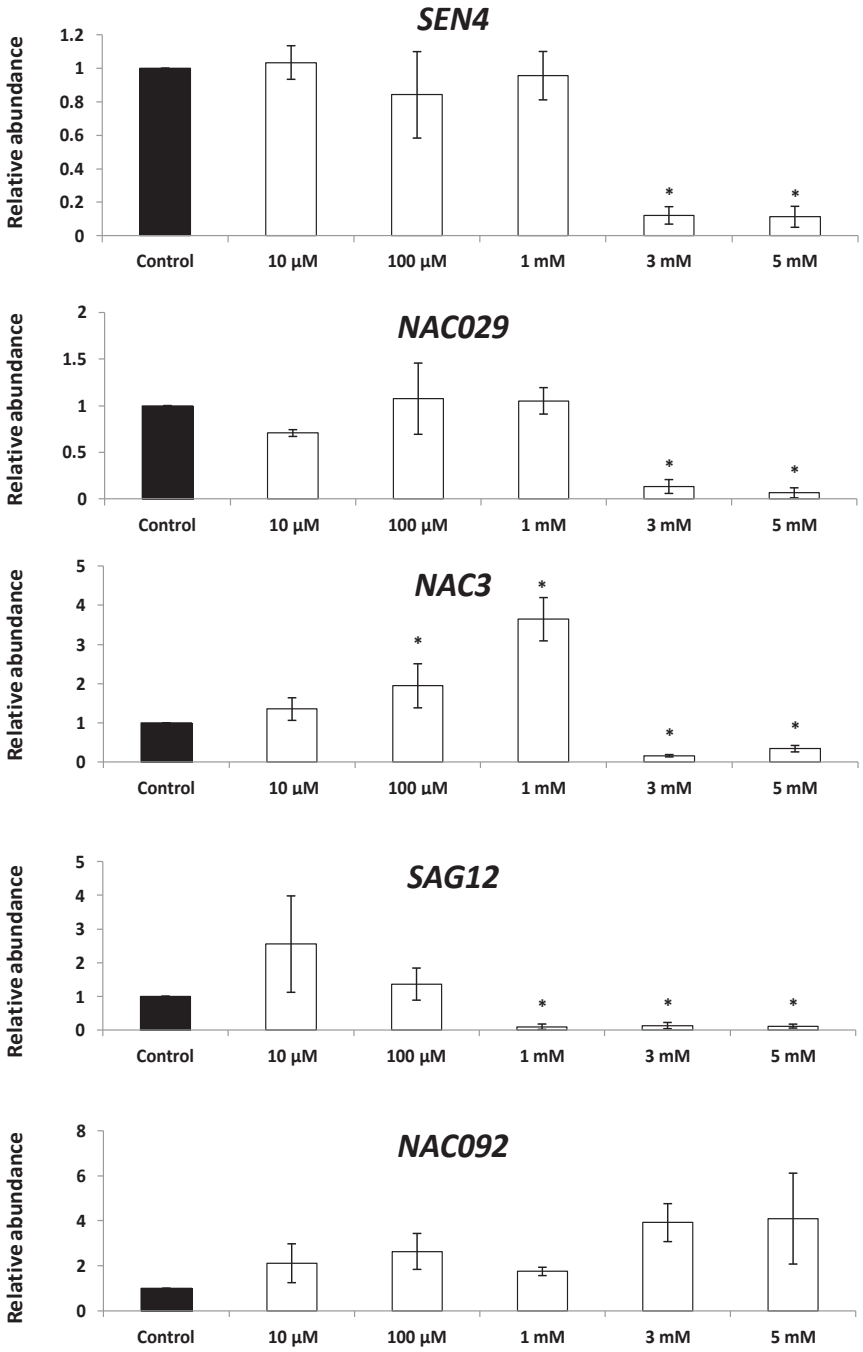

Figure 3.2.5. Transcript abundance of *SEN4, NAC029, NAC3, SAG12* and *NAC092* in detached inflorescences treated with different concentrations of MeJA at day 3 of the dark incubation.

Plants were grown in a green house under long day conditions (16 h light and 8 h dark) for 8 weeks and their inflorescences were detached and placed in the dark for 3 days. Transcript abundance was quantified by RT-PCR and normalised to abundance of *PP2A* (*PHOSPHATASE 2A*). Values were then normalised to control that was designated as 1. Error bars indicate the standard error of three biological replicates. * indicates measurements that were significantly different from that of untreated control ($p<.05$).

3.2.1.5 Exogenously applied MeJA alters the transcript abundance of JA responsive genes

I analysed the mRNA abundance of transcription factors known to be integral to jasmonate signalling to understand whether they had a role in delayed inflorescence senescence caused by higher dosages of MeJA. The genetic components acting downstream of JA include *ERF1* (*ETHYLENE RESPONSE FACTOR 1*), *ERF11*, *ORA59* (APETALA2/Ethylene Response Factor (AP2/ERF)-domain transcription factor), *RAP2.4* (*RELATED TO AP2.4*) and *PDF1.2* (*PLANT DEFENSE 1.2*). In addition to positive regulators of JA responses, the transcript abundance of a jasmonate repressor, *JAZ10* (*JASMONATE-ZIM-DOMAIN PROTEIN 10*) was also determined.

The MeJA treatments significantly increased the transcript abundance of *ERF1*, *ERF11*, *ORA59* and *RAP2.4* in a dosage dependent manner (Fig. 3.2.6). The transcript abundance of both *ERF1* and *RAP2.4* was increased from ~2 fold (by 100 µM MeJA) to ~10 fold (3 mM MeJA). Interestingly, a further increase in MeJA concentration from 3 to 5 mM caused a slight decrease in transcript abundance of *ERF1* and *RAP2.4*. The *ERF11* transcripts were increased by 44 fold in inflorescences treated with higher concentration of MeJA. Similar to *ERF1*, the transcripts of *ERF11* decreased from 44 to 35 fold upon further increase in MeJA concentration. The *ORA59* showed strong induction upon MeJA treatments and its transcripts increased up to 90 fold by 3 mM and 62 fold by 5 mM MeJA treatments. The 5 compared to 3 mM MeJA caused an insignificant decrease in transcript accumulation of *ERF1*, *ERF11*, *ORA59* and *RAP2.4*, which indicates a decreasing trend in the transcript accumulation of these genes at the 5 mM treatments.

By contrast to the above mentioned genes, *JAZ10* responded differentially to the MeJA treatments (Fig. 3.2.6). The 100 µM and 1 mM MeJA treatments increased *JAZ10* mRNA abundance by ~4 fold and ~7 fold, respectively, whereas 3 and 5 mM MeJA treatments decreased its transcript abundance.

PDF1.2 also showed differential response to changes in its transcript accumulation upon MeJA treatments. Apart from the 1 mM MeJA treatment, its lower and higher concentrations both suppressed the transcript abundance of *PDF1.2* (Fig. 3.2.6). The

10 and 100 μM MeJA decreased the transcript abundance of *PDF1.2* to ~2 and ~3 fold, respectively, whereas 3 and 5 mM treatments resulted in undetectable transcripts of the gene.

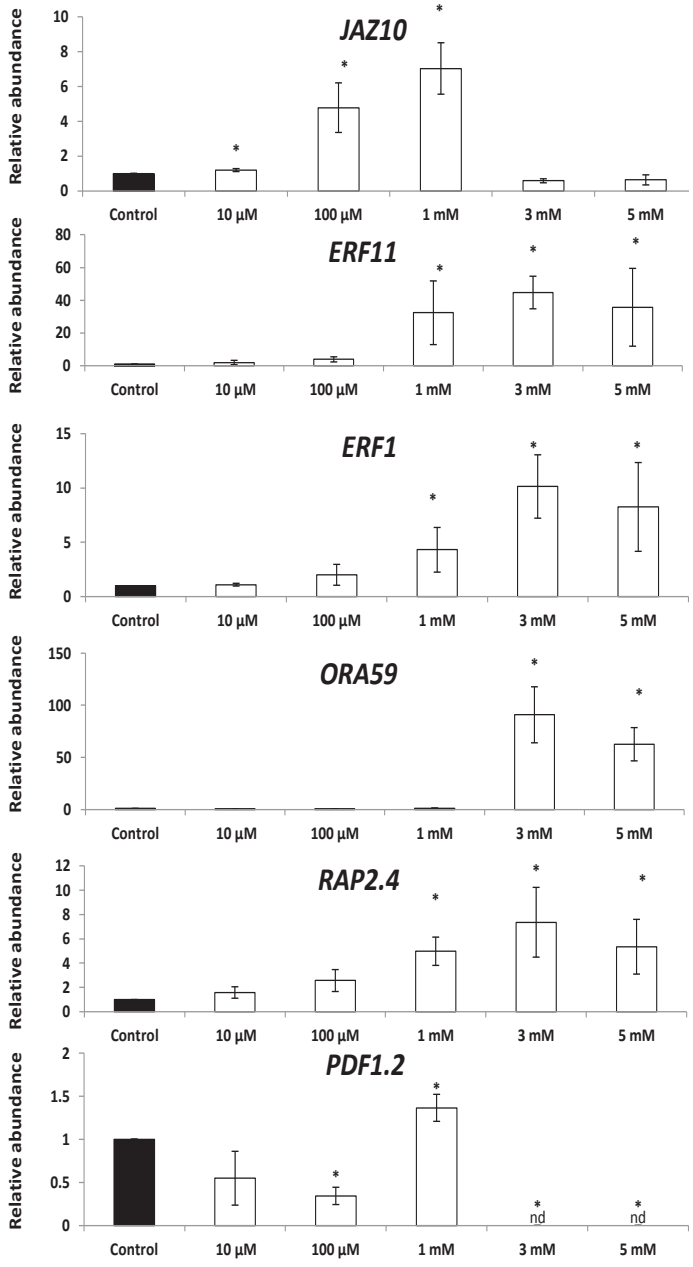

Figure 3.2.6. Transcript abundance of *JAZ10*, *ERF11*, *ERF1*, *ORA59*, *RAP2.4* and *PDF1.2* in detached dark-held inflorescences treated with different concentrations of MeJA.

Plants were grown in a green house under long day conditions (16 h light and 8 h dark) for 8 weeks and their inflorescences were detached and placed in the dark. Transcript abundance was quantified by RT-PCR in inflorescences at day 3 of dark incubation and normalised to abundance of *PP2A* (*PHOSPHATASE 2A*). Values were then normalised to control that was designated as 1. Error bars indicate the standard error of three biological replicates. * indicates measurements that were significantly different from that of untreated control ($p<.05$). nd represents non-detectable transcript abundance.

3.2.1.6 MeJA suppresses the expression of ethylene biosynthesis and signalling genes

JA and ethylene signalling pathways interact synergistically to regulate plant defense responses (Reviewed by Zarie et al., 2011). Exogenously applied JA causes an increase in ACC and ethylene biosynthesis in flowers of dendrobium and petunia (Porat et al., 1993). Therefore, to see the effect of range of MeJA concentrations on ethylene production I quantified transcript accumulation of ethylene biosynthesis and signalling genes in MeJA treated inflorescences. The genes included *ACS2*, *ACS10*, *ACO4*, *EIN2* and *EIN3*. ACC SYNTHASE (ACS) converts S-adenosyl methionine (SAM) into 1-aminocyclopropane-1-carboxylate (ACC) (Yang and Hoffman, 1984), ACC OXIDASE (ACO) converts ACC into ethylene (Yang and Hoffman, 1984) and EIN2 and EIN3 both are components of ethylene signal transduction pathway (Alonso et al., 1999; Potuschak et al., 2003).

The transcript abundance of *ACS10* and *EIN3* was not altered by MeJA treatment (Fig. 3.2.7). The 10 and 100 μM MeJA treatments did not alter transcript abundance of *ACS2* and *ACO4*. The 1 mM MeJA treatment caused significant increase in mRNA abundance of *ACS2* but did not affect *ACO4.* Transcript abundance of *ACO4* and *ACS2* was significantly decreased by higher MeJA treatments. Transcript abundance of *EIN2,* a central regulator of ethylene and JA response (Alonso et al., 1999), was reduced to undetectable levels in the tissue by the 3 and 5 mM MeJA treatments, but the lower concentrations of MeJA had no effect on its transcript abundance. The suppressed transcript abundance of ethylene genes in the inflorescences treated with higher concentration of MeJA suggested that MeJA delays inflorescence senescence by interfering with the ethylene response pathway.

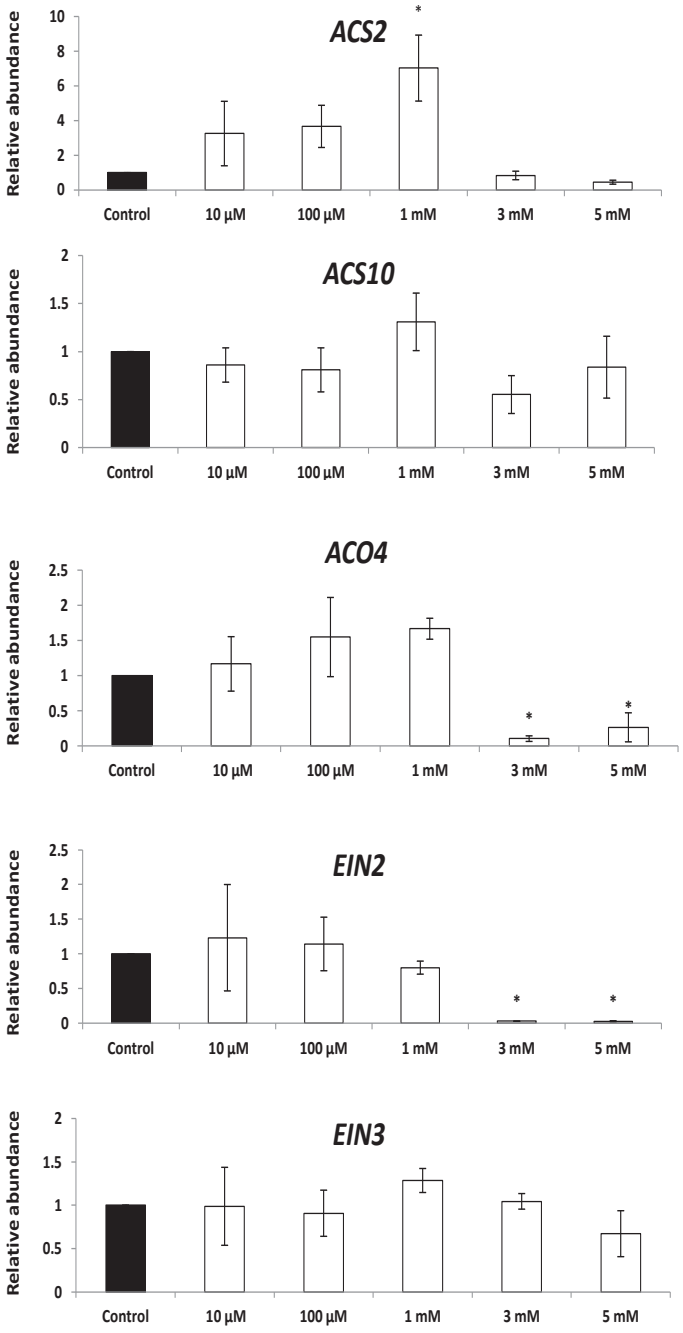

Figure 3.2.7. Transcript abundance of *ACS2*, *ACS10*, *ACO4*, *EIN2* and *EIN3* in detached dark-held inflorescences treated with different concentrations of MeJA.

Plants were grown in a green house under long day conditions (16 h light and 8 h dark) for 8 weeks and their inflorescences were detached and placed in the dark. Transcript abundance was quantified by RT-PCR at day 3 of dark incubation and normalised to abundance of *PP2A* (*PHOSPHATASE 2A*). Values were then normalised to control that was designated as 1. Error bars indicate the standard error of three biological replicates. * indicates measurements that were significantly different from that of untreated control ($p<.05$).

3.2.2 Discussion

Here I examined the effects of hormones applied at a range of concentrations on senescence of detached dark-held Arabidopsis inflorescences. The senescence of the inflorescences was accelerated by exposure to ABA and ACC and delayed by treatment with high (3 to 5 mM) concentrations of MeJA. SA in contrast to the other hormones, did not alter the timing of degreening at any concentrations tested, which is consistent with previous research showing it does not alter senescence of detached dark-held leaves (Morris et al., 2001; Buchanan-Wollaston et al., 2005). To understand the molecular basis of MeJA-mediated delayed inflorescence degreening, we used qRT-PCR technology to quantify transcript accumulation of JA responsive, senescence associated and ethylene biosynthesis and signalling genes. I found that transcript accumulation of JA responsive genes was increased in inflorescences treated with higher concentrations of MeJA, whereas mRNA abundance of senescence-induced and ethylene synthesis and signalling genes, was significantly decreased.

Immature inflorescences treated with 1, 3 and 5 mM ACC show accelerated senescence

Detached dark-held inflorescences held in 1, 3 or 5 mM ACC displayed earlier sepal yellowing than water-held controls (Fig. 3.2.1 and 3.2.2A). This senescence promoting effect of ACC is consistent with previous studies that have shown exogenously applied ethylene or ACC accelerate leaf and flower senescence and induces plant defense responses (Mayak and Halevy, 1972; Nadeau et al., 1993; Payton et al., 1996; Jing et al., 2002; Hunter et al., 2004; Arrom and Munné-Bosch, 2012). The response of the inflorescences to ACC is also consistent with our previous findings that showed ethylene regulates senescence of detached dark-held inflorescences (Trivellini et al., 2012). This was seen by inflorescence degreening being delayed in the ethylene insensitive *ein2* mutant and in finding transcript enrichment for ethylene associated processes in 24 h dark-held inflorescences. For example, transcript abundance of *ACC OXIDASE* was increased ~200 fold, *ACO4* ~2.5 fold, *EIN2* ~2 fold, *EIN3* ~3 fold and *EIL* ~6 fold.

Surprisingly, lower concentrations of ACC (10 & 100 µM), which induced yellowing in detached Arabidopsis leaves, did not accelerate senescence of dark-held detached inflorescences. This different response of the leaves and inflorescences to the lower concentrations of ACC may be explained by the previously identified interaction between age-related changes (ARCs) and ethylene. Ethylene affects timing of leaf senescence by interacting with the leaf age (Hensel et al., 1993; Grbic and Bleecker, 1995; Jing et al., 2005: Jing et al., 2002). Jing et al., (2005) showed that ethylene causes early onset of leaf senescence only when the leaf acquired a certain developmental age. Furthermore, the study of Jing et al., (2005) concluded that during the process of aging the tissues became more susceptible to signals that accelerate senescence. Being an immature tissue the Arabidopsis inflorescence likely does not have enough ARCs to interact with the ethylene produced by lower concentrations of ACC. Thus in the absence of ARCs lower ACC dosages cannot induce senescence in the inflorescences.

However, higher ACC treatments resulted in increased inflorescence degreening. This is consistent with the study of Jing et al., (2005), which showed that when 8-day old Arabidopsis plants were treated with ethylene for 16 h they showed enhanced leaf senescence. The authors proposed that in addition to causing early onset of leaf senescence, ethylene resulted in early occurrence of ARCs in young leaves. Concurrent with this it has been shown that the duration of ethylene treatment varied the onset of ARCs in leaf. Here, I suggest that higher ACC concentrations may be stimulating ARCs to occur early in immature inflorescences and causes accelerated inflorescence senescence.

Lower ABA dosages more effectively accelerate inflorescence senescence than higher dosages

Exogenously applied ABA at all concentrations (10 µM to 5 mM) accelerated senescence of the detached dark-held inflorescences compared with the water-held controls (Fig. 3.2.2A and B). This agrees with other studies that showed exogenously applied ABA accelerates yellowing of oat, rice, maize and Arabidopsis leaves and senescence (wilting) of rose and daffodil flowers (Borochov et al., 1976; Gepstein and Thimann, 1980; Müller et al., 1999; Hunter et al., 2004; Lee et al., 2011).

The accelerated senescence of the inflorescences by ABA may be independent of ethylene signalling. For example, ABA still caused precocious senescence (wilting) of daffodil flowers when the flowers were pretreated with the ethylene action inhibitor 1-methylcyclopropene (Hunter et al., 2004). Similarly, ABA accelerated chlorophyll loss in leaves of the ethylene-insensitive Arabidopsis *ethylene receptor* (*er*) mutant (Zacarias and Reid, 1990). Conversely, other studies have suggested that ABA accelerates senescence through ethylene production or signalling. For example, *ein2* plants that are insensitive to all ethylene responses (Alonso et al., 1999) do not show accelerated leaf senescence when treated with ABA (Kim et al., 2009). Exogenously applied ABA also enhances ethylene production in carnation, cotton, bean and shrubby orache (Lieberman and Kunishi, 1970; Ronen and Mayak, 1981; Hassine and Lutts, 2010). Moreover, in some cases where it inhibited ethylene production, ethylene sensitivity of the tissue was increased e.g., in wheat and rice (Mayak and Halevy, 1972; Wright, 1980; Kao and Yang, 1983).

Interestingly, ABA was less effective in promoting inflorescence senescence at higher than at lower concentrations. This may be due to the fact that ABA at its higher dosages suppresses ethylene production. This is consistent with other studies demonstrating that higher ABA dosages regulate different plant responses by inhibiting ethylene production. For instance, under water limited conditions increased ABA contents are required to suppress ethylene synthesis in maize seedlings (Sharp and LeNoble, 2002). Furthermore, it has been shown that lower dosages of ABA promote and its higher dosages inhibit various plant growth and developmental responses. For examples, leaves of maize seedlings treated with 10 and 100 µM ABA had increased activity of antioxidant enzymes than the leaves of plants exposed to 1 mM ABA concentrations (Jiang et al., 2010).

10 µM to 1 mM MeJA treatments have little effect on inflorescence degreening

Low MeJA concentrations (10 µM to 1 mM) did not accelerate chlorophyll loss of the inflorescences. This differs from other studies where these applied concentrations accelerated leaf yellowing and flower wilting (Ueda and Kato, 1980; Ueda et al., 1981; Hayat et al., 2010; Liu and Howell, 2010). The inability of MeJA to accelerate inflorescence degreening was consistent with its inability to increase transcript abundance of the senescence-associated transcripts *SAG12*, *SEN4*, *NAC029* and *NAC092*. These genes are associated with or cause age-, hormone- and/or stress-induced leaf senescence (Grbic and

Bleecker, 1995; Weaver and Amasino, 2001; Xiao et al., 2004; Guo and Gan, 2006). Transcripts of these genes have previously been shown to be induced by 10 μM JA in tissues where JA accelerated senescence (He et al., 2002; Woo et al., 2001; Woo et al., 2004; Park et al., 1998).

The detached dark-held leaves showed accelerated yellowing when treated with low (100 μM and 1 mM) MeJA concentrations (Fig. 3.2.2). This is consistent with other findings demonstrating that low MeJA treatments were sufficient to accelerate leaf yellowing in Arabidopsis (He et al., 2002; Jibran et al., 2013). However, the detached dark-held L*er*-0 inflorescences of young plants did not degreen in response to the lower MeJA concentrations. This may be due to different levels of the hormone in these tissues with the immature inflorescences having higher MeJA levels than leaves. This would need further study.

ARCs are required for causing hormone-induced senescence, reviewed in (Jibran et al., 2013). In this study to determine the effect of ARCs on inflorescence senescence, the inflorescences of old plants (55-day old) were treated with lower MeJA concentrations (Fig. 3.2.4). These inflorescences showed a significant loss in chlorophyll concentrations compared with untreated controls and inflorescences of young plants. The data suggest that inflorescences of old plants are more competent to respond to lower MeJA concentrations, as the whole plant is experiencing the phenomenon of aging. Furthermore, Jing et al., (2005) showed that ethylene treatment could not affect the senescence of 11-day old Arabidopsis plants, whereas it caused an acceleration of leaf senescence in 21- and 27-day old Arabidopsis plant.

High concentrations of exogenously supplied MeJA (3 and 5 mM) delays inflorescence degreening.

The detached dark-held inflorescences treated with higher MeJA concentrations showed delayed senescence as judged by reduced chlorophyll loss and reduced transcript accumulation of senescence markers (Fig. 3.2.1D & 3.2.5). The decline in transcript abundance of the markers of senescence suggests that the effect of MeJA was not just simply to retard chlorophyll breakdown but was to inhibit the senescence programme.

To my knowledge, I am the first to report that higher MeJA concentrations can delay rather than accelerate chlorophyll loss. However, some studies have demonstrated that low and high jasmonate concentrations differentially regulate plant growth and developmental processes. For example, Ulloa et al., (2002) demonstrated that lower JA concentrations promoted cell expansion and shoot elongation in potato stems cuttings, whereas higher JA concentrations inhibited growth. Similarly, differential effects of lower and higher MeJA concentrations on stomatal closing of fava bean have been reported. Evans (2003) found in guard cell protoplasts that 0.1 μM MeJA activated potassium efflux channels whereas 50 μM MeJA significantly reduced activation of potassium efflux channels.

High concentrations of exogenously supplied MeJA (3 to 5 mM) differentially affect transcript abundance of JA-responsive genes

To understand how MeJA-signalling delayed inflorescence senescence, I quantified transcript abundance of genes involved in regulating JA responses. These genes included *ERF1*, *ERF11*, *ORA59*, *RAP2.4, JAZ10* and *PDF1.2* (Fig. 3.2.6).

JAZ10 transcript abundance increased in the inflorescences as the concentration of applied MeJA increased from 100 μM to 1 mM MeJA (Fig. 6). *JAZ10* is a repressor of jasmonate responses (Chung and Howe, 2009). It has been shown that increased JA signalling induces its own repressors to auto-regulate energy consuming defense responses (Thines et al., 2007). The MeJA-mediated increase in *JAZ10* transcriptional levels in the detached dark-held inflorescences is consistent with studies demonstrating that enhanced jasmonate signalling caused increased expression of *JAZ* repressor genes (Thines et al., 2007; Yan et al., 2007; Chung et al., 2008; Katsir et al., 2008). For example, infection on Arabidopsis plants with *Botrytus cinerea* resulted in increased JA concentrations and transcript abundance of *JAZ10* (Méndez-Bravo et al., 2011). Similarly, *Spodoptera exigua* feeding of Arabidopsis leaves caused an increased transcript abundance of eleven out of twelve *JAZ* genes (Chung et al., 2008). Moreover, mechanical wounding of Arabidopsis seedlings resulted in increased mRNA abundance of *JAZ10* in a COI1-dependent manner (Yan et al., 2007). It is possible that the application of MeJA enhanced the transcript abundance of *JAZ10* to repress JA responses.

Interestingly, inflorescences treated with higher MeJA dosages showed decreased transcript accumulation of *JAZ10* and increased transcript accumulation of JA responsive genes (*ERF1*, *ERF11*, *ORA59* and *RAP2.4*) that are key regulators of ethylene and JA induced defense responses (Lorenzo et al., 2003; Zarei et al., 2011; Zhang et al., 2011a). This is consistent with the role of JAZ10, as a suppressor of JA responsive genes. The increase in expression of JA responsive genes has been shown to be associated with enhanced tolerance to various environmental stresses. For example, Chung et al., (2008) demonstrated that increased expression of *MYC2*, *JAZ1*, *JAZ5*, *OPR3* and *VSP1* were associated with increased resistance in Arabidopsis to *S. exigua* feeding, as determined by the weights of larvae. Furthermore, a study performing an analysis of overall transcript reprogramming in Arabidopsis plants challenged by aphid and *P.syringae* highlighted the significance of *ERFs* in inducing defense responses (Barah et al., 2013). Similarly, the expression of twelve out of thirteen *ERF* transcription factors was enhanced by exogenously applied ET and JA in corollas of senescing petunia flower (Liu et al., 2011).

Here I suggest that MeJA at lower concentrations increased the transcript abundance of *JAZ10* which then repressed jasmonate signalling. Conversely, higher MeJA concentrations decreased the transcript abundance of *JAZ10* that de-repressed jasmonate signalling. This increased jasmonate signalling resulted in delayed inflorescence senescence.

MeJA delayed inflorescence senescence by blocking ethylene responses

Higher concentrations of MeJA resulted in decreased transcript abundance of ethylene biosynthesis (*ACS2* and *AC04*) and signalling genes (*EIN2*) (Fig. 3.2.7). I also found that mutants defective in jasmonate synthesis did not show altered inflorescence senescence phenotype, whereas ethylene signalling mutant of Arabidopsis *ein2* showed delayed inflorescence senescence (Trivellini et al., 2012). This indicates the significance of ethylene signalling in regulating dark-detachment induced inflorescence senescence. Many studies have shown that defects in the ethylene response pathway alter the timing of stress induced senescence, reviewed in Kunkel and Brooks, (2002). For example, under lesion-promoting conditions and pathogen attack, death and defense phenotypes of the *vad1-1* (*vascular associated death*) mutant was found to be dependent on ethylene biosynthesis and signalling pathway (Bouchez et al., 2007). Similarly, over expression of *SUBMERGENCE1A* (*SUB1A*) in rice inhibited dark-induced leaf senescence by decreasing

ethylene production and responsiveness to JA (Fukao et al., 2012). Ethylene signalling regulates plant defense responses and senescence in petunia. When petunia plants expressing the *etr1-1* allele, which causes ethylene insensitivity, were challenged with *Botrytis cinerea* they showed retarded senescence and reduced disease symptoms of detached leaves, flowers and intact plants.

PDF1.2 transcript abundance was abolished at higher MeJA concentrations in the inflorescences showing delayed senescence phenotype (Fig. 3.2.6). Enhanced transcript abundance of *PDF1.2* has been associated with the accelerated senescence of Arabidopsis plants caused by overexpression of the *ARABIDOPSIS A FIFTEEN* (*AAF*) (Chen et al., 2012). The senescence of these plants and increased transcript abundance of *PDF1.2* by *AAF* was also shown to require *EIN2*. This suggests senescence and increased transcript abundance of *PDF1.2* was mediated through the ethylene signalling pathway. My study is consistent with this. Furthermore, it has been shown that transcript abundance of *PDF1.2* is strongly increased by synergistic interaction of both ethylene and jasmonate signalling compared to their application alone (Zarei et al., 2011). The decreased transcripts of *PDF1.2* by higher MeJA treatments suggest that MeJA signalling suppresses ethylene response at its higher concentrations. Increasing amount of data had demonstrated an antagonistic interaction between MeJA and ethylene signalling (Matsushima et al., 2002; Rojo et al., 1999; Kim et al., 2013; Song et al., 2014). Matsushima et al., (2002) showed that ethylene blocked MeJA-induced vegetative storage protein accumulation in Arabidopsis. Rojo et al., (1999) found that Arabidopsis ethylene response mutants showed enhanced accumulation of transcript abundance of genes involved in jasmonate responses. Kim et al., (2013) found that reduced JA levels in *ein2* caused enhanced responsiveness of the mutant to exogenously applied ethylene. Song et al., (2014) showed that the interaction between JA and ethylene is regulated by both MYC2, involved in JA responses, and EIN3, involved in ethylene responses, transcription factors. Taken together this study suggests that increased MeJA signalling causes delayed inflorescence senescence by blocking ethylene signalling.

This study unravels the previously unknown role of jasmonates in delaying dark induced Arabidopsis inflorescence senescence and suggests an antagonistic interaction between jasmonate and ethylene in regulating the process. The increased MeJA signalling delays inflorescence senescence by suppressing transcript accumulation of senescence associated genes and ethylene synthesis and signalling genes. In addition to identifying the

novel role of MeJA, this study has provided a new direction to investigate the biological mechanisms involve in regulating inflorescence senescence. Further research to understand the interaction between age of the tissue at time of harvest, ethylene and jasmonate will be helpful.

Blank page

3.3 Identifying novel genetic lesions that regulate senescence of detached dark-held immature inflorescences

Abstract

Detached dark-held inflorescences with altered timing of degreening were successfully identified by screening inflorescences of 20,000 ethyl methanesulfonate (EMS)-mutagenized Arabidopsis (Landsberg *erecta*) plants. The screen identified 30 potential inflorescence senescence mutants. These were designated *accelerated inflorescence senescence* (*ais*) and *delayed inflorescence senescence* (*dis*) mutants depending on their timing of inflorescence degreening. *ais* inflorescences were more yellow than wild-type at day 3 of dark incubation, whereas *dis* inflorescences were more green than wild-type at day 5 of dark incubation. The degreening of the *ais* and *dis* inflorescences was quantified by chlorophyll analysis. The detached *ais* inflorescences had significantly lower and the *dis* inflorescences significantly higher chlorophyll content than wild-type at day 3 of dark incubation. The detached leaves of the *ais* mutants held in the dark also showed accelerated degreening, but interestingly the detached leaves of the *dis* mutants held in the dark did not show delayed leaf degreening. Taken together, mutants with altered inflorescence senescence timing could be identified from a chemically mutagenized population of plants and the lesions responsible for the delayed senescence phenotypes may be novel. This is because these lesions specifically controlled inflorescence senescence and so would not have been identified in previous leaf senescence screens. This also suggests that there are both similarities and differences between the control of leaf and inflorescence degreening.

3.3.0 Introduction

Forward and reverse genetics approaches are powerful methodologies for studying gene function. In plants, both forward and reverse genetic approaches have been successfully employed to identify genes regulating leaf senescence (Jing et al., 2002; Higgins et al., 2006; Kim et al., 2006; Kim et al., 2011). The forward genetics approach identifies a mutant defective in a biological process and subsequently the genetic lesion causing the phenotype. Populations of mutants for forward genetics approaches can be produced using chemicals, e.g., ethyl methane-sulfonate (EMS) or radiation which induces random lesions in DNA. The resulting mutants containing the genetic lesions are afterward screened for the desired traits of interest. The genetic lesion underlying the traits of interest can be identified either through traditional map-based cloning (Jing et al., 2002) or high-throughput sequencing approaches (Nordström et al., 2013). In the reverse genetics approach the researcher first decides on the gene of interest and then uses approaches to knock out or knock down the expression of the gene in order to elucidate its function (Peters et al., 2003). This may be done for example by disrupting the function of the gene using T-DNA insertion or RNA interference or by overexpressing the gene in genetically modified plants with promoters such as the 35S CaMV promoter (Omirulleh et al., 1993; Wesley et al., 2001; Sessions et al., 2002).

The EMS-based forward genetics screening strategy has successfully identified genetic loci regulating various plant developmental processes including onset of leaf senescence, flower initiation, flower development, hormone signalling and hormone biosynthesis (Merlot and Giraudat, 1997; Penmetsa and Cook, 2000; Jing et al., 2002). EMS-induced mutagenesis causes C/G to T/A single nucleotide substitutions. Studies show that these types of mutations not only cause loss or gain of function of the genes but also produce partial loss of function mutations that help to identify the role of genes whose loss of function can be lethal in plants (Kim et al., 2006; Schippers et al., 2008; Thang et al., 2010). In contrast, gamma-rays induce 4-to 6-bp deletions, which can be non-transmissible because of their lethal nature (Naito et al., 2005). Thus, EMS mutagenesis has emerged as a powerful tool for identifying novel regulators of a range of biological processes.

I used an EMS-based forward genetics approach to identify mutant plants with putative genetic lesions affecting senescence of detached dark-held immature inflorescence in Arabidopsis (Landsberg *erecta*). I quantified their altered timing of inflorescence degreening and tested if the mutant plants also showed altered timing of leaf degreening.

3.3.1 Results

3.3.1.1 EMS-based forward genetic approach identifies Arabidopsis inflorescence senescence mutants

To identify inflorescence senescence mutants, I followed the strategy outlined in Fig. 3.3.1. I first sowed a population of M2 EMS-mutagenized Arabidopsis (Landsberg *erecta*) seeds. The immature inflorescences of the mutant plants were analyzed for an altered timing of degreening as compared to wild-type. Immature inflorescences were detached and held in the dark for 3 (D3), 5 (D5) and 8 (D8) days. Degreening was assessed at D3, D5 and D8 of dark incubation, representing when wild-type inflorescences were green (D3), completely yellow (D5) or had been yellow for 3 days (D8). Mutants whose dark-held detached inflorescences were yellower than wild-type at D3 of dark incubation were designated *accelerated inflorescence senescence* (*ais*), example of *ais3* is presented in Fig. 3.3.2A, whereas mutants whose dark-held detached inflorescences more green than wild-type at D5 of dark incubation were called *delayed inflorescence senescence* (*dis*), example of *dis3* is presented in Fig. 3.3.2B. Screening was stopped at D8 of dark incubation as the inflorescences often began to show visible signs of fungal infection. Initial screening of the M2 EMS-mutagenized Arabidopsis plants identified 122 inflorescence senescence mutants from which half of them (61) were *ais* and the other half (61) were *dis* (Fig. 3.3.1; Table 3.3.1).

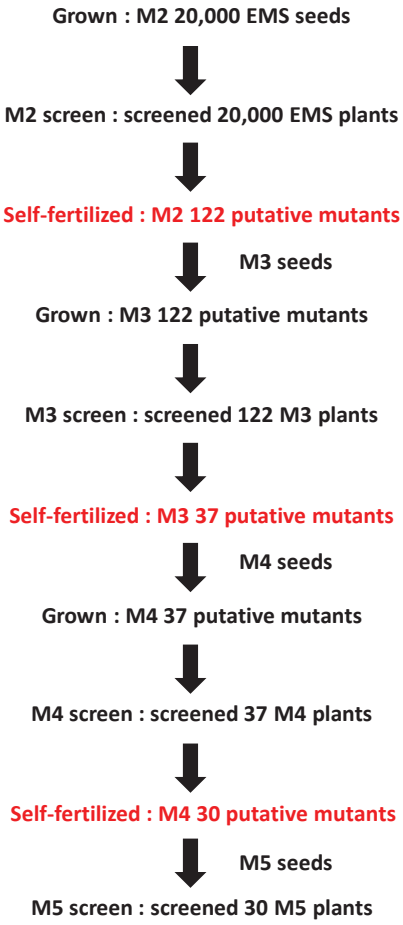

Figure 3.3.1. Strategy for identifying inflorescence senescence mutants.

An M2 population of EMS-mutagenized seeds was sown and allowed to grow. Inflorescences from 20,000 M2 plants were detached and held in the dark at 21°C for 8 days (M2 screen). A total of 122 putative inflorescence degreening mutants were identified, allowed to self-pollinate and seeds were collected (M3 seeds). The 122 M3 seed lines were sown and the inflorescences of the resultant plants rescreened for altered timing of degreening (M3 screen). The number of positives fell to 37 seed lines. These were self-fertilized and seeds collected (M4 seeds). The 37 seed lines were sown and their inflorescences checked again for altered timing of degreening (M4 screen). The number of positives fell to 30. These were self-fertilized, the seeds collected (M5 seeds) and the inflorescence of these seed lines confirmed as altered in their timing of degreening (M5 screen). Plants were grown under long day conditions (16 h light and 8 h dark) in a green house.

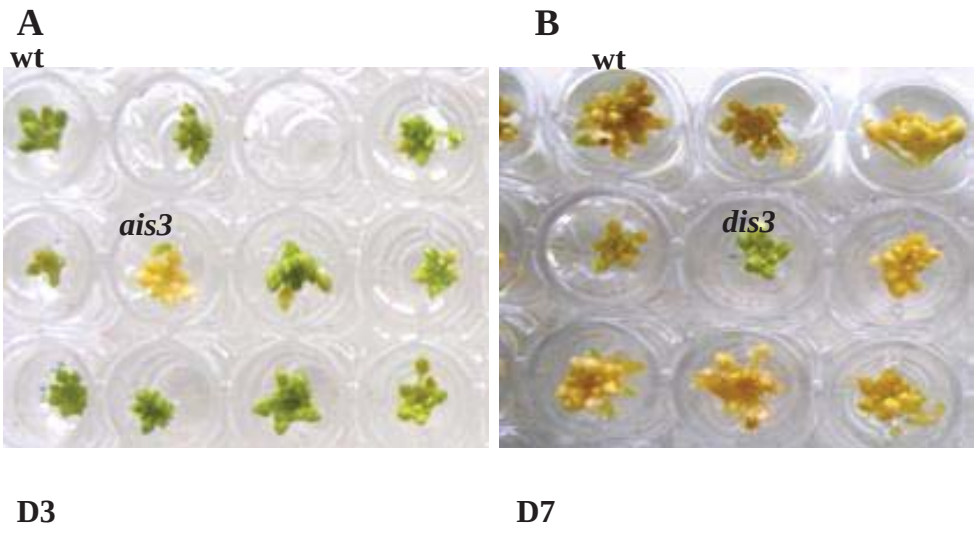

Figure 3.3.2. Screening of immature dark-held detached inflorescences of EMS-mutagenized Arabidopsis plants.

The immature inflorescences of EMS and wild-type (wt) plants were harvested from primary bolts and placed in water at 21°C. All inflorescences are from EMS-mutagenized plants except wild-type where indicated. A. Inflorescence of *ais3* at day 3. B. Inflorescence of *dis*3 at day 7. Plants were grown in long day conditions (16 h light and 8 h dark) in a green house.

3.3.1.2 Stabilization of identified mutations

To remove hypomorphic- (mutation penetration in next generation is less than 100%) or environment-dependent mutations, the 122 M2 mutants were self-fertilized for three successive generations and their inflorescence degreening phenotypes retested in each subsequent progeny (Fig. 3.3.1). The number of mutants confirmed as having inflorescences with altered timing of degreening was lower in two successive generations (M3 and M4) and became stable in the last generation (M5) (Table 3.3.1). Of the 122 M2 mutants, 37 were confirmed in the next (M3) generation. Twenty of them were *dis* and 17 were *ais* mutants. When the M4 generation of these plants were screened, seven of the 17 *ais* mutants no longer showed an accelerated inflorescence senescence phenotype, whereas all the 20 *dis* mutants showed stable phenotype. Thus, the number of stable and potential inflorescence senescence mutants was reduced to 30 in the M4 generation (Fig. 3.3.3A and B). All 30 mutants retained their altered inflorescence degreening phenotype in their next generation (M5 screen). Their whole plant phenotypes are listed in Table 3.3.2.

Eighteen of the 20 *dis* mutants in the M5 generation were not noticeably different from wild-type in their look and growth habit (Table 3.3.2). Two of them, *dis9* and *dis15* differed from wild-type in being stunted (Fig. 3.3.4). In contrast to the *dis* mutants, many of the *ais* mutants were morphologically different in plant phenotype from wild-type, e.g., *ais3*, *ais4* and *ais19* (Fig. 3.3.5). However, certain mutants, such as, *ais20* and *ais26* were similar to wild-type (appendix 3.1). *ais61* showed an *apatela-1* like phenotype in which sepals were converted into bract-like structures and petals were replaced by stamens (Fig. 3.3.6A). In addition to these mutants, an *agamous-like* sterile mutant was also identified during M2 screening (Fig. 3.3.6B), which showed delayed inflorescence senescence phenotype.

Table 3.3.1 Self-pollination of the identified mutants allows the stabilization of mutations causing altered inflorescence senescence phenotypes.

The putative inflorescence mutants were grown in long day conditions (16 h light and 8 h dark) in a green house. Altered inflorescence degreening timing was tested using more than three inflorescences per plant.

# of screen	Mutant generations (# Plants screened)	Positive plants from screening	*# dis* plants	*# ais* plants
1	M2 (~20,000)	122	61	61
2	M3 (122)	37	20	17
3	M4 (37)	30	20	10
4	M5 (30)	30	20	10

Table 3.3.2 Plant phenotypes of M5 *dis* and *ais* mutants.

Mutants were grown in long day conditions (16 h light and 8 h dark) in a green house. More than twelve plants were investigated to compare the plant developmental phenotype with that of the wild-type.

#.	*dis*	Plant Phenotype		Plant Phenotype
1	*dis1*	Normal	*ais3*	Stunted [3]
2	*dis2*	Normal	*ais4*	Bushy[4]
3	*dis3*	Normal	*ais9*	thin stem and small leaves[5]
4	*dis6*	Normal	*ais10*	Normal
5	*dis7*	Normal	*ais12*	Stunted [3]
6	*dis9*	Stunted [1]	*ais16*	Stunted [3]
7	*dis12*	Normal	*ais19*	Stunted [3]
8	*dis15*	Stunted [2]	*ais20*	Normal
9	*dia16*	Normal	*ais26*	Normal
10	*dis21*	Normal	*ais61*	*apetala-1-like*[5]
11	*dis28*	Normal		
12	*dis34*	Normal		
13	*dis39*	Normal		
14	*dis41*	Normal		
15	*dis47*	Normal		
16	*dis48*	Normal		
17	*dis51*	Normal		
18	*dis52*	Normal		
19	*dis58*	Normal		
20	*dis59*	Normal		

[1] *dis9* mutant is stunted (small leaves, small inflorescences) with an increased number of inflorescence branching. [2] *dis15* is stunted plant and appears light green in colour. Its inflorescences are also lighter in colour than wild-type. [3] *ais3, 12, 16 and 19* are stunted. [4] *ais4* has increased branching. [5] *ais61* inflorescences have an *apetala-1*(*ap1*)-like phenotype, in *ap1* mutant sepals are converted into bract-like structures and petals into petal-petal-stamen-bract like mosaic structure.

A

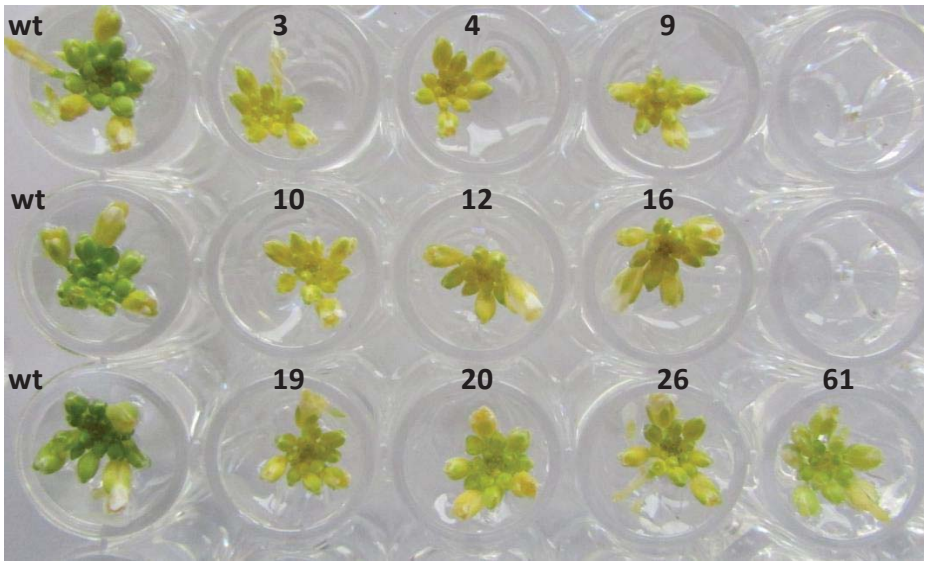

B

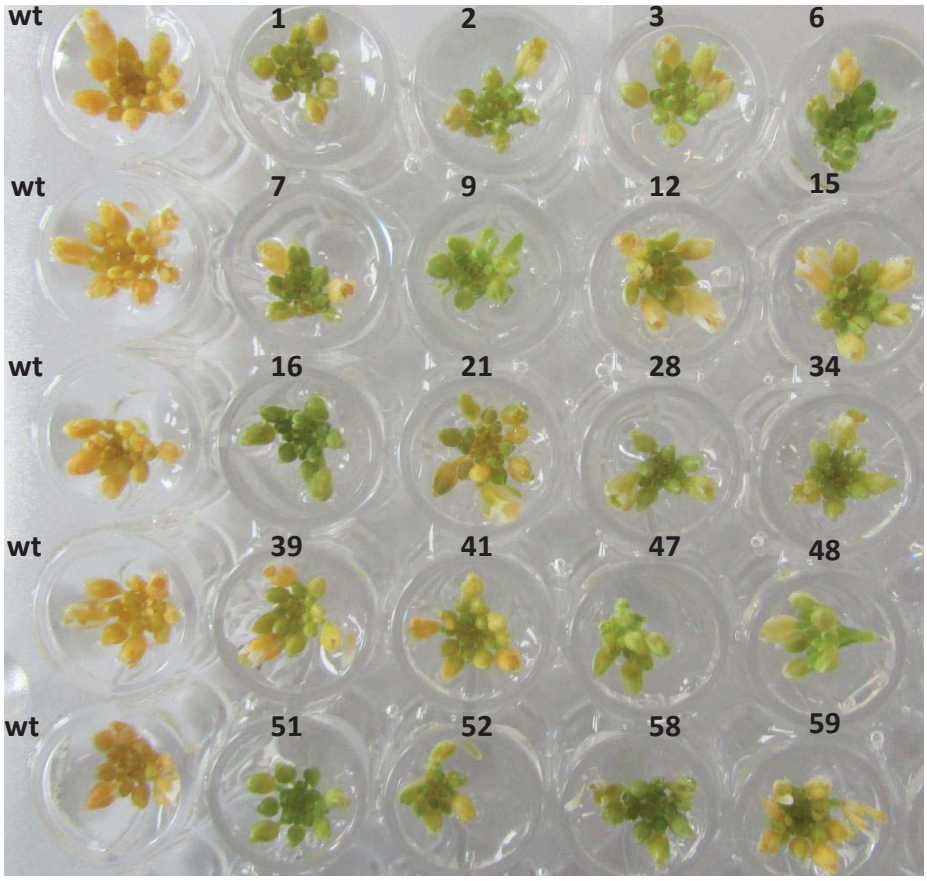

Figure 3.3.3. Visible dark-induced inflorescence degreening of stable inflorescence senescence mutants (M5).

A. Detached dark-held inflorescences of *ais* mutants at day 3. B. Detached dark-held inflorescences of *dis* mutants at day 5. Inflorescences were harvested from the primary bolts of the plants grown in a 16 h photoperiod and placed in the dark with their cut ends in water at 21°C. Numbers above each well indicate mutant number, i.e. 3 in (A) indicates *ais3*. wt indicates wild-type.

Figure 3.3.4. The plant phenotypes of L*er*-0 (wild-type), *dis58, dis9,* and *dis15*.

M5 plants were grown under long day conditions (16 h light and 8 h dark) in a green house for 8 weeks and then photographed. Scale bar space = 1cm.

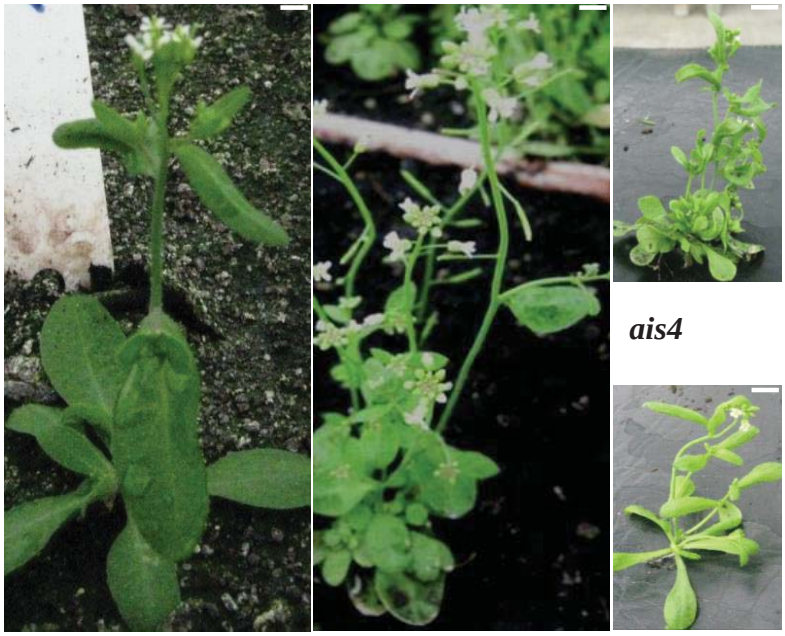

Figure 3.3.5. The plant phenotypes of *ais3, ais4* and *ais19* as compared to L*er*-0 (wild-type) phenotype.

M5 plants were grown under long day conditions (16 h light and 8 h dark) for 8 weeks in a green house and then photographed. Scale bar space = 1cm.

A **B**

Figure 3.3.6. *apetala-1-like* and *ag-1 like* inflorescences identified from the inflorescence senescence screen.

A. Inflorescence of *ais61* mutant (*apetala1*-like). B. Inflorescence of *agamous-like* mutant. The plants were grown in long day conditions (16 h light and 8 h dark) in a green house for 8 weeks and inflorescences were cut and photographed.

3.3.1.3 Quantification of visible degreening of *ais* and *dis* dark-held detached inflorescences

Inflorescence degreening of M5 *ais* and *dis* mutants was quantified by chlorophyll analysis (Fig. 3.3.7). All the *ais* mutants had significantly lower chlorophyll content than wild-type at day 3 of dark incubation (Fig. 3.3.7A), whereas all the *dis* mutants had significantly more chlorophyll content than wild-type (Fig. 3.3.7B). There were also differences within the *ais* and *dis* mutants with respect to how much chlorophyll was lost or retained. Some *ais* mutants such as *ais4* showed greater loss than others, whereas some *dis* mutants, e.g., *dis34* were better at retaining chlorophyll than the other mutants. This demonstrated that the chlorophyll content of the *ais* and *dis* inflorescences was consistent with their visible inflorescence degreening and that there were different genetic lesions responsible for the altered senescence timing.

A

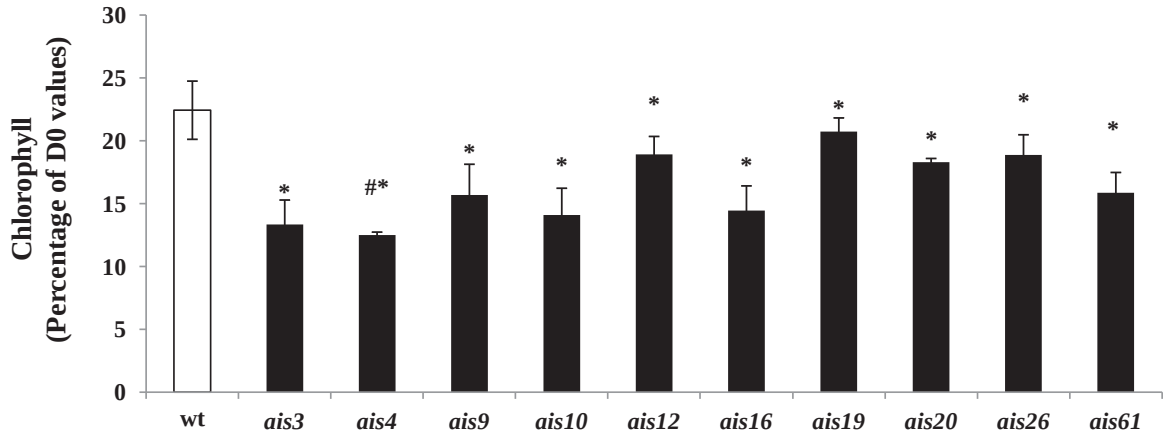

B

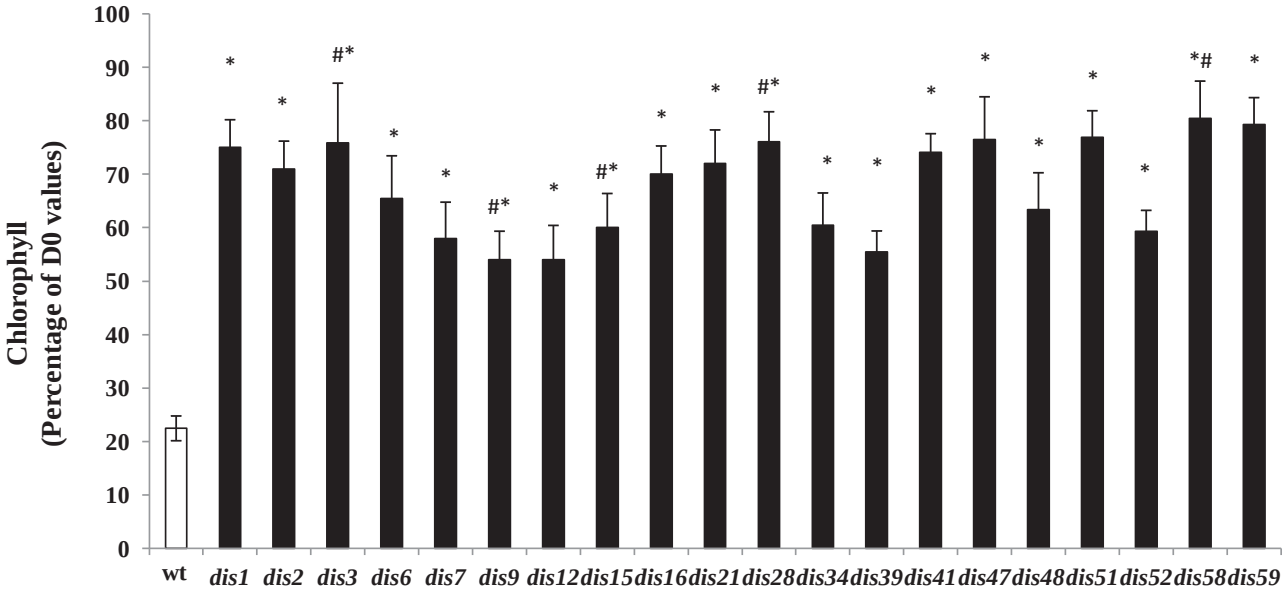

Figure 3.3.7. Percentage chlorophyll content of dark-held detached inflorescences of M5 *ais* and *dis* mutants.

Chlorophyll content of *ais* (A) and *dis* (B) detached inflorescences at day 3 of dark incubation compared with wild-type. Inflorescences were detached from the primary bolts of the plants grown in a 16 h photoperiod and placed with their cut ends in water at 21°C. Chlorophyll content is expressed as percentage of day 0 value. Bars indicate the standard error of six biological replicates. To make the variability more equal logs–base 10-of data is taken. One-way ANOVA was performed using Minitab (Version 16); chlorophyll content of mutants significantly different from the wild-type was determined using Dunnett's test at p=0.05. Overall ANOVA shows significant difference between mutants at * p<0.001. Dunnett's test identifies *ais4*, *ais26*, *dis3*, *dis9*, *dis15*, *dis28* and *dis58* as significantly higher than control indicated by #. Residual plots were inspected to check normality and constant variance assumptions.

3.3.1.4 Quantification of visible degreening of *ais* and *dis* dark-held detached leaves

To investigate whether the putative genetic lesions responsible for the altered inflorescence degreening timing was specific for inflorescence senescence, I determined whether *ais* and *dis* mutants also showed altered timing of leaf degreening. The first cauline leaves of 6-week-old plants were used for analysis to help circumvent problems associated with different aged leaves in the rosettes because leaf age has a substantial effect on timing of dark-induced degreening in Arabidopsis (Jing et al., 2002). Dark-induced senescence of selected *ais* and *dis* detached leaves was quantified by measuring chlorophyll content (Fig. 3.3.8). Mutants with a variable range of inflorescence senescence phenotype (delayed or accelerated) were selected for leaf analysis. The chlorophyll content of leaves of selected *ais* mutants at day 3 of dark incubation was significantly lower than wild-type. Leaves of the *ais* mutants had ~30 to 60% lower chlorophyll content than wild-type at day 3 of dark incubation (Fig. 3.3.8A). Surprisingly, the detached leaves of selected *dis* mutants held in the dark did not show any delay in chlorophyll loss compared to wild type (Fig. 3.3.8B). Instead there was either no difference in the percentage chlorophyll content retained (*dis1*, *13*, *15* and *47*) or they showed significantly more chlorophyll loss than wild-type at day 3 of dark incubation (e.g., *dis3*, *34*, *39* and *58*). Taken together the data indicated that the EMS-based forward genetic screen was a useful tool to identify mutants that are specific for inflorescence senescence. Furthermore, this data emphasizes that although some genetic regulators of inflorescence senescence are common to leaf senescence, inflorescence senescence is also controlled by its own specific genes.

A

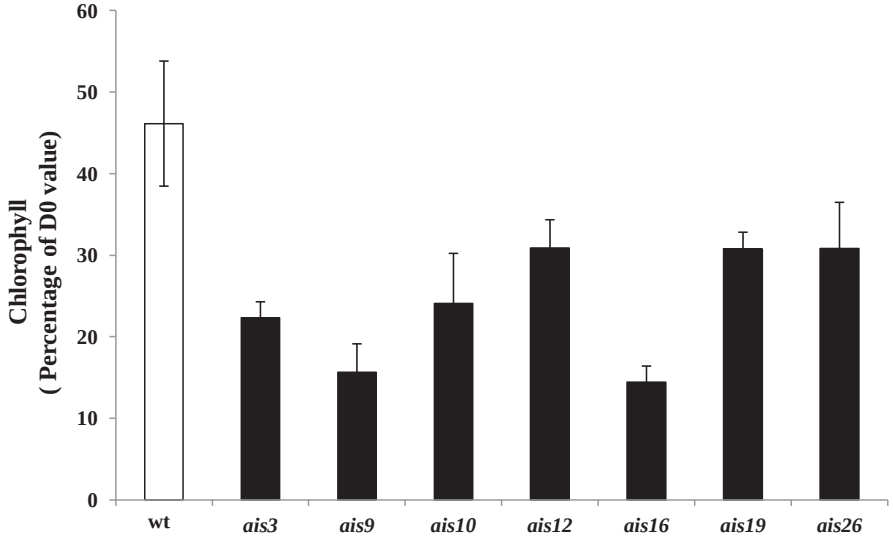

B

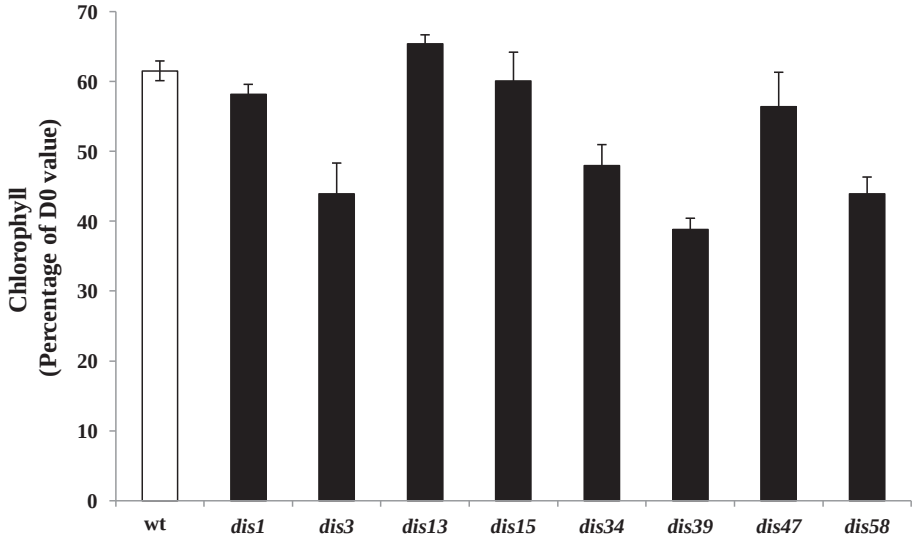

Figure 3.3.8. Percentage chlorophyll content of dark-held detached leaves of *ais* and *dis* mutants.

Chlorophyll content of *ais* (A) and *dis* (B) leaves at day 3 of dark incubation compared with wild-type. Cauline leaves from 6-weeks old plants were harvested from the plants grown in a 16 h photoperiod and placed in water at 21°C. Chlorophyll content is expressed as percentage of day 0 value. Bars indicate the standard error of six biological replicates. To make the variability more equal log – base 10 - of data is taken. One-way ANOVA was performed using Minitab (Version 16); chlorophyll content of mutants significantly different from the wild-type was determined using Dunnett's test at p=0.05. Overall ANOVA shows significant differences between mutants at * p<0.001. Dunnett's test identifies *ais9*, *ais16* and *dis34* as significantly higher than control. Residual plots were inspected to check Normality and constant variance assumptions.

3.3.2 Discussion

Detached dark-held inflorescences having altered timing of degreening were successfully identified by screening inflorescences of 20,000 EMS mutagenized Arabidopsis plants. The mutants were categorized as *accelerated* (*ais*) or *delayed* (*dis*) *inflorescence senescence*, based on the timing of degreening of their dark-held detached inflorescences. The inflorescences of the *ais* mutants were more yellow than wild-type at day 3 of dark incubation, whereas the *dis* mutants were more green than wild-type at day 5. The extent of degreening in the mutants was quantified by chlorophyll analysis. Although *ais* mutants also showed accelerated leaf chlorophyll loss, the *dis* mutants did not show delayed chlorophyll loss in their detached dark-held leaves. This highlights both similarities and differences in the genetic pathways regulating leaf and inflorescence senescence. In addition, finding that the *dis* mutants did not show delayed leaf senescence suggests that the lesions underlying the senescence delay will be novel since traditional leaf senescence screens will not have identified them.

EMS-based forward genetics approach is a successful technique to identify postharvest *inflorescence senescence* mutants

The EMS-based forward genetic approach was successful in identifying 30 inflorescence senescence mutants (Table. 3.3.2; Fig. 3.3.3). This is consistent with the approach having successfully identified novel genes involved in regulating leaf senescence. For example, analysis of the EMS-induced *onset of leaf death* (*old*) mutants identified key genetic regulators of leaf senescence (Jing et al., 2002; Jing et al., 2005; Schippers et al., 2008) and highlighted the importance of age in controlling leaf senescence (Jing et al., 2002; Jing et al., 2005). Similarly, EMS-based mutagenesis was used by Nam and coworkers to generate a number of delayed leaf senescence mutants (*oresara* mutants) (Oh et al., 1997). The genetic lesions for a number of these have now been identified. For example, *oresara12-1* is a gain of function mutation in the cytokinin receptor AHK3 (Kim et al., 2006; Oh et al., 1997).

Stabilization of mutations causes a decrease in identified mutants

Initial screening of the 20,000 inflorescences from the EMS-mutagenized plant population (M2) identified 122 *accelerated* or *delayed inflorescence senescence* mutants (Table. 3.3.1). However, self-fertilization of these mutants over two generations resulted in loss of the inflorescence phenotype in ~70% of them (Table. 3.3.2). This was expected as the frequency of identified mutations is known to decrease in successive generations (Wollaston and Ali, 2007; Batista et al., 2008; Parry et al., 2009; Wu et al., 2012). There can be many reasons for the mutations in the M2 plant population being non-heritable. Mutagenesis approaches by their nature lead to the presence of many genetic lesions additional to the one of interest scattered randomly throughout the genome (Batista et al., 2008). These additional lesions may lead to generalised stress responses that can lead to loss of penetrance of the trait of interest by a wide variety of indirect mechanisms, e.g., altering stress hormone production or sensitivity. These stress responses may occur more or less in the resulting generations depending on which of the additional lesions get by chance locked into the homozygous state of the plants as they self-fertilise. Furthermore, variable environmental conditions may contribute to non-heritable but desired phenotypes in M2 generation. For example, certain mutations are deleterious in some environments but neutral in others and vice versa (Elena and de Visser, 2003; Kishony and Leibler, 2003).

Genes affecting inflorescence degreening regulate novel mechanism of senescence

In this study it was revealed that none of the leaves of the *delayed inflorescence senescence* mutants showed a delayed senescence phenotype and interestingly leaves of some of the mutants e.g., *dis3*, *34*, *39* and *58* actually showed accelerated leaf senescence (Fig. 3.3.8B). This suggests that the *dis* loci act as specific genetic regulators of inflorescence senescence. This was unexpected, as previous reports have indicated that genes that regulate senescence of one plant organ often regulate senescence of other plant organs. For example, lesions in *ein2, anac092, max2* and *ahk3,* which delay leaf senescence (Kim et al., 2006; Kim et al., 2009), also delayed senescence of the detached dark-held immature inflorescences (Trivellini et al., 2012). Similarly, broccoli transformed with antisense *1-*

AMINOCYCLOPROPANE-1-CARBOXYLATE OXIDASE2 (*ACO2*) displayed delayed leaf senescence in both detached leaves and heads (Gapper et al., 2005).

In addition, common genetic pathways are involved in regulating multiple plant growth and developmental processes. For example, non-functional HIF312-BAY (heterogeneous inbred family) not only inhibited accumulation of anthocyanin (Diaz et al., 2006), but caused increased sugar content and accelerated leaf senescence (Wingler et al., 2010). Similarly, decreased expression of *WRKY53* resulted in delayed flowering and leaf senescence in Arabidopsis (Miao et al., 2004). Furthermore, vernalization-dependent and independent flowering pathways regulate senescence of the Arabidopsis rosette (Wingler et al., 2010). Therefore, genes affecting senescence are found to be functionally linked with other plant developmental processes. Here, the results suggest that several *dis* loci appear to be specific inflorescence senescence regulators and may not interact with other plant growth and development processes under favourable plant growth conditions.

The successful identification of putative inflorescence senescence mutants indicates that immature detached Arabidopsis inflorescences are a useful system to study dark-induced senescence of floret tissues as the inflorescences reproducibly senesce with age and they are amenable to genetic analysis. Furthermore, the identification of mutants that are affected in inflorescence senescence and not leaf senescence indicates that there are key differences between these two programmes. The genetic loci that specifically affect inflorescence senescence will be cloned using both conventional (map-based cloning) and modern high-through-put (HRM-PCR and whole genome sequencing) technologies.

Blank page

Blank page

3.4 Mapping of delayed inflorescence senescence genes

Abstract

Senescence screening of detached dark-held immature inflorescences of EMS mutagenized Arabidopsis (L*er*-0) plants identified *accelerated inflorescence senescence* (*ais*) and *delayed inflorescence senescence* (*dis*) mutants (chapter 3.3). Segregating populations for both *ais* and *dis* mutants were created, by backcrossing the mutants with L*er*-0 wild-type, to investigate whether identified mutations are recessive, dominant or co-dominant. To identify *dis* mutations in the genome, recombinants for mapping were generated by outcrossing the mutants with Col-0 wild-type. F1 seeds of the crosses were planted and plants were allowed to self-pollinate and produce F2 seeds. F2 individuals of both segregating and mapping populations were grown and their detached inflorescences were screened for their dark-induced senescence phenotype. The degreening phenotype of the F2 detached dark-held inflorescences was compared with L*er*-0 and Col-0 wild-types. The segregation analysis of 10 *dis* mutants showed that the mutations were recessive in nature F2 recombinants, homozygous for the phenotype, were used for linkage analysis. Linkage analysis of five *dis* mutants was performed by using high-throughput HRM-PCR based on single nucleotide polymorphisms (SNPs) between L*er*-0 and Col-0. Three of the six mutations were mapped to chromosome 4, one was mapped to chromosome 2 and one was mapped to chromosome 3. The study demonstrated that linkage analysis using HRM-based PCR was a reliable and fast approach to map the genetic lesions causing the delayed senescence phenotype.

3.4.0 Introduction

The roles of many genes involved in various biological processes have been identified by creating loss of function and gain of function mutants. Genetic mutations causing altered gene functions can be created either by T-DNA insertions or by various chemicals such as ethyl-methane sulfonate (EMS) (Jander et al., 2002). Although T-DNA insertional mutagenesis has successfully identified the functions of many genes, chemical mutagenesis can be a more powerful approach for identifying novel gene functions. This is because insertional mutagenesis typically creates amorphic (complete loss of wild-type protein activity) knockout mutants; whereas chemical mutagenesis has the potential to create hypomorphic (decreased activity of wild-type protein) knock down mutants. Furthermore, chemical mutagenesis introduces more mutations in the plant genome than insertional mutagenesis. Thus, it can alter the functions of multiple plant genes compared to T-DNA insertions that can create one to three insertions per line (Feldmann et al., 1994). It may produce mutants that result from mutations in multiple genes, which although hard to analyze are potentially very informative.

To date, chemical mutagenesis has effectively identified the functions of many essential genes through hypomorphic mutations (Kreps et al., 1996; Conklin et al., 1999; Schippers et al., 2008). For instance, function of Arabidopsis *VTC1* (*CYT1*), as a potent antioxidant and cellular reductant, was identified by EMS mutagenesis as its null mutant was lethal (Conklin et al., 1999). Furthermore, the majority of the key regulatory steps in biochemical pathways are identified by using chemical mutagenesis. For instance, an EMS-induced G to A transition identified the role of *ANTHRANILATE SYNTHASE* (*AS)* in tryptophan metabolism (Kreps et al., 1996).

Forward genetic approaches depend on identifying plants defective in a particular biological process and subsequent identification of the lesion causing the phenotype (Jander et al., 2002). Genetic lesions causing the mutant phenotype can be identified by constructing a genetic map that determines the genetic distance between the molecular markers and the mutation (Jander et al., 2002). The genetic map is constructed by linkage analysis, which calculates the recombination events between two DNA markers present on two non-sister chromatids of each pair of a homologous chromosome (Jander et al., 2002). The markers

linked to the mutations will have less recombination frequency compared to the un-linked markers. The percentage linkage of the markers will provide the rough position of the mutation in the genome. The genetic distance between genes or molecular markers can be described as centimorgans (cM) or percentage linkage.

Selection of molecular DNA markers used for linkage analysis has been a critical step in map-based cloning. However, the arrival of new high-throughput sequencing technologies has facilitated the identification of reliable molecular markers that can be used for mapping purposes. The combined use of reliable markers and advancement in molecular technologies has accelerated the process of mapping. The technologies that recently have been employed in identifying the mutation include high through-put deep sequencing technologies e.g., re-sequencing, bulk segregant analysis and NIKS (Needle In *K*-Stack) (Mccallum et al., 2000; Clark et al., 2007; Schneeberger et al., 2009; Nordström et al., 2013).

HRM-PCR has been used for high throughput mutation analysis, developing marker maps and genotyping in many plants e.g., wheat, almond and barley (Gundry et al., 2003; Lehmensiek et al., 2008; Wu et al., 2009; Ugo et al., 2010; Matsuda et al., 2012). The dyes fluoresce brightly only when bound to double-stranded DNA molecules. The DNA sample having the variant of interest is first amplified by using standard PCR and subsequently HRM analysis is performed. In HRM analysis, the double stranded amplicons are melted apart and loss of fluorescence is represented in a melt curve. PCR products of different sequences have different melting temperatures and thus different melt peaks. The melting temperature of a DNA sample depends on GC content, length and sequence of DNA (Ugo et al., 2010). Sequence variants even of a single base pair can be inferred from changes in the melting temperature of the PCR product (Ugo et al., 2010). In a heterozygote DNA sample both homoduplexes and heteroduplexes are formed, whereas in a homozygote DNA sample only homoduplexes are formed (Gundry et al., 2003). The presence of both homoduplexes and heteroduplexes in heterozygote will yield a different melting profile than that of the homoduplexes in homozygote. Hence, the homozygote samples will be easily distinguished from heterozygote samples. Furthermore, HRM analysis provides results within hours of the PCR initiation because HRM analysis does not require restriction enzyme digestion and gel electrophoresis.

This study shows that SNP-based HRM-PCR is a fast and reliable technique to perform the segregating analysis in recombinant individuals of L*er*-0 and Col-0. This HRM-based segregation analysis allowed the mapping of five *dis* mutations onto the genome.

3.4.1 Results

3.4.1.1 Identified *dis* mutations were recessive in nature

The heritability of the altered inflorescence senescence traits was tested to determine whether the mutations causing delayed inflorescence senescence were recessive, dominant, or co-dominant. This was done to determine the complexity of the regulation underlying their altered senescence traits and therefore the potential difficulty for mapping the mutants. Ten *dis* M4 mutant plants (Table 3.3.2) were backcrossed to L*er*-0 and F1 seeds collected as illustrated in Fig. 3.4.1. No delayed inflorescence senescence phenotype was observed in any of the F1 individuals demonstrating that mutations are recessive. The F1 seeds of 10 *dis* mutants were allowed to self-pollinate to create F2 seeds. Fifteen to 128 F2 plants for each mutant backcross were screened for their segregation ratio. The mutants *dis1, 3*, *9*, *13*, *15*, *34*, *47*, *48*, *58* and *59* segregated in a 3(wild-type):1(mutant) ratio, characteristic of a monogenic recessive trait (Table 3.4.1). Fig. 3.4.2 shows the segregation ratios of *dis15* and *dis58* F2 individuals obtained from backcrosses of the mutants with L*er*-0.

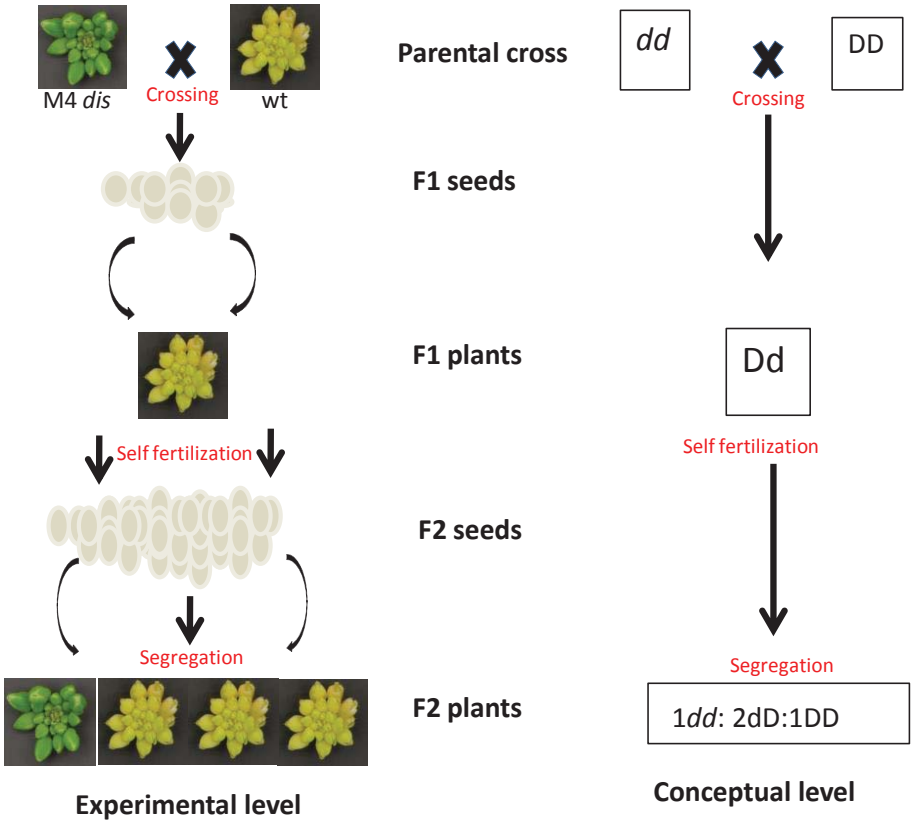

Figure 3.4.1. Schematic representation of backcrossing of identified recessive mutants.

A backcrossing scheme of *dis* recessive mutants backcrossed with L*er*-0 wild-type. Seeds of the backcross are collected (F1 seeds). F1 seeds produce F1 individuals that do not show the *dis* phenotype. F1 individuals are self-pollinated to produce F2 seeds. Subsequently, F2 seeds are planted to generate F2 segregating plant population. In the F2 plant population recessive mutations segregate into 3:1 (wild-type:mutant) phenotypic ratios. The genotype of segregating population is 1:2:1 (1 wild-type:2 heterozygote:1 mutant).

Table 3.4.1. Segregation analysis of F2 individuals obtained from backcrossing mutants with L*er*-0.

The 3:1 ratios of wild-type and mutants were tested and accepted at $P \geq 0.05$ based on their calculated $\chi 2$ values. $\chi 2$ values are based on a 1 degree of freedom. The tabulate $\chi 2$ value at *probability* of 0.05 is 3.84 that is obtained from $\chi 2$ values table available at *http://graphpad.com/quickcalcs/PValue1.cfm*. Plants were grown in long day conditions for 8 weeks (16 h light and 8 h dark) in a green house. The immature inflorescences of F2 individuals were harvested from primary bolts and placed in water at 21°C for at least 8 days. The inflorescence phenotypes were examined at day 3, 5 and 8.

***dis* BC L*er*-0**	**# of plants**	**wild-type**	***dis***	**Observed ratio**	**Calculated $\chi 2$**	**P values**
dis1	36	25	7	5:1	0.125	0.723
dis3	132	100	32	3:1	.04	0.84
dis9	36	31	6	6:1	0.17	0.9
dis13	36	31	5	7:1	2.37	0.1237
dis15	40	29	11	4:1	.1333	0.715
dis34	147	114	33	4:1	.51	0.48
dis47	168	128	40	4:1	0.13	0.72
dis48	48	35	13	4:1	.111	0.7384
dis58	65	50	11	6:1	.10	0.75
dis59	24	15	6	4:1	2	0.1573

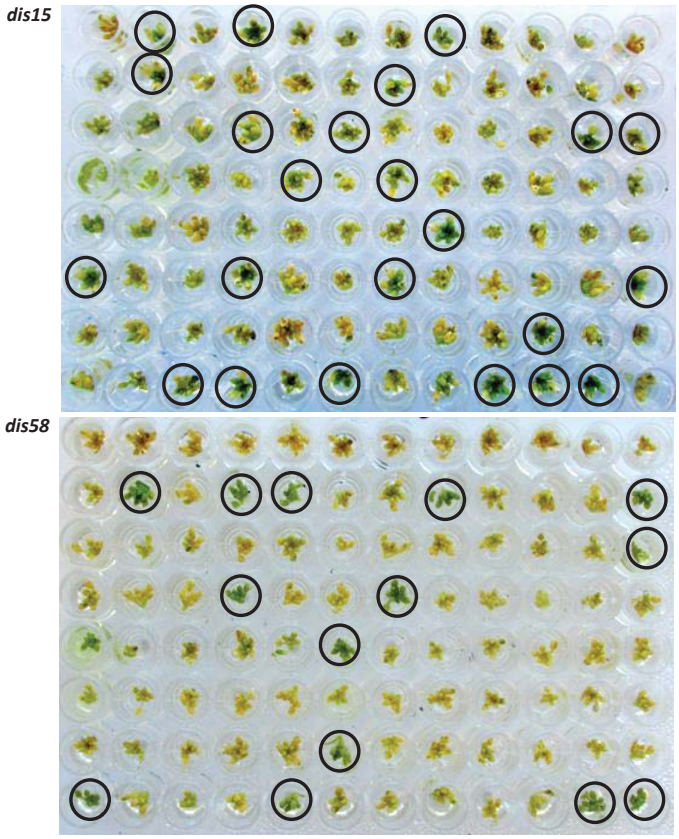

Figure 3.4.2. Inflorescence senescence phenotypes of *dis15* and *dis58* F2 plants obtained from mutants backcross with L*er*-0.

Plants were grown in long day conditions for 8 weeks (16 h light and 8 h dark) in a green house. The immature inflorescences of plants were harvested from the primary bolts and placed in water at 21°C. Plants in each F2 population were identified as mutant if their detached inflorescences were still green at day 5 of dark incubation. Detached dark-held inflorescences that showed delayed inflorescence senescence phenotypes at day 5 are circled in black.

The 10 *ais* and 20 *dis* mutants in L*er*-0 (M4) were outcrossed with Col-0 to raise mapping populations for linkage analysis. F1 seeds of the backcross for seven of the *dis* mutants (*dis 1, 3, 9, 15, 34, 58* and *59*) were sown. Their F1 plants were always found to display the raceme-type inflorescence structure of Col-0, which was expected as the *erecta* mutation is recessive. F1 plants were allowed to self-pollinate to generate F2 seeds. All the F2 recombinants generated by sowing seeds of the F1 selfed plants displayed a segregation ratio of 3(wild-type):1(mutant) (Table 3.4.2), which was independent confirmation of the genetic lesions behind the delayed senescence traits being monogenic recessive. Fig. 3.4.3 shows the segregation ratios of *dis15* and *58* F2 individuals obtained from outcross of the mutants with Col-0.

Table 3.4.2. Segregation analysis of F2 recombinants obtained by mutants outcrossed with Col-0.

The 3:1 ratios of wild-type and mutants were tested and accepted at $P \geq 0.05$ based on their calculated $\chi 2$ values. $\chi 2$ values are based on a 1 degree of freedom. The tabulate $\chi 2$ value at *probability* of 0.05 is 3.84 that are obtained from $\chi 2$ values table available at *http://graphpad.com/quickcalcs/PValue1.cfm*. Plants were grown in long day conditions for 8 weeks (16 h light and 8 h dark) in a green house. The immature inflorescences of F2 individuals were harvested from primary bolts and placed in water at 21°C for at least 8 days. The inflorescence phenotype was examined at day 3, 5 and 8.

dis	**# of plants**	**wild-type**	**mutant**	**Observed ratios**	**Calculated χ^2**	**P values**
dis1	70	53	17	4:1	.019F	0.89
dis3	76	64	12	6:1	3.438	0.354
dis9	72	54	18	4:1	0	1
dis15	96	76	20	5:1	0.888	0.346
dis34	78	60	18	4:1	0.1538	0.6949
dis58	65	50	15	4:1	.1282	0.723
dis59	116	84	32	3:1	1.724	0.52

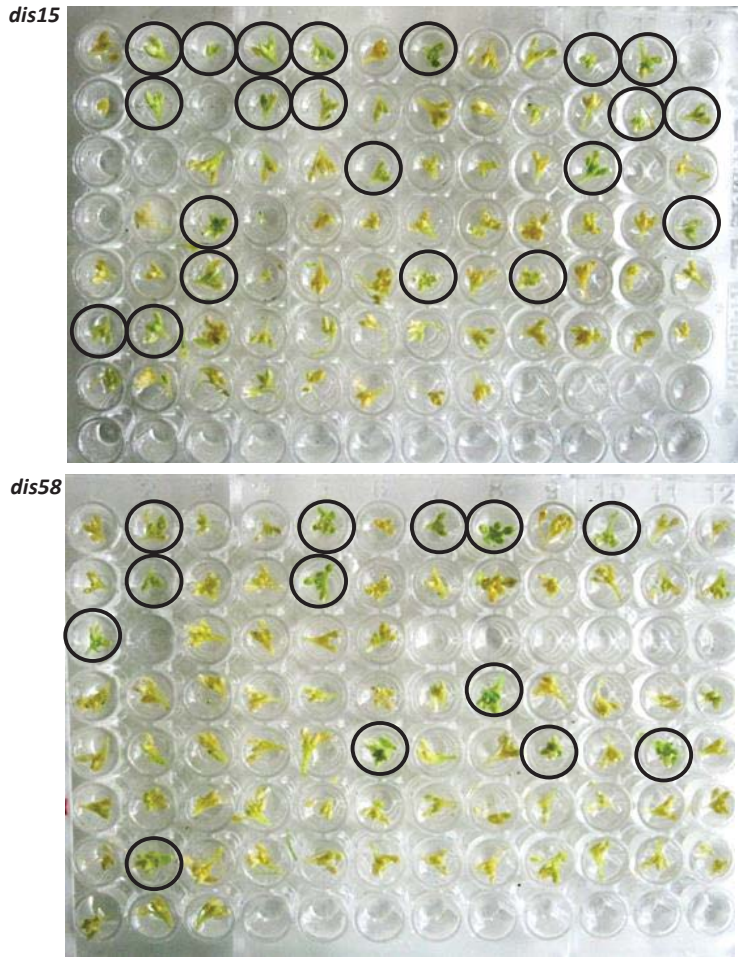

Figure 3.4.3. Inflorescence senescence phenotypes of *dis15* and *58* F2 recombinants obtained by mutants outcrossed with Col-0.

Plants were grown in long day conditions for 8 weeks (16 h light and 8 h dark) in a green house. The immature inflorescences of plants were harvested from primary bolts and placed in water at 21°C. Plants in each F2 population were identified as mutant if their detached inflorescences were still green at day 5 of the dark incubation. Detached dark-held inflorescences that showed delayed inflorescence senescence phenotypes at day 5 are circled in black.

3.4.1.2 Screening of SNP markers using HRM-PCR

Mapping of genetic lesions responsible for the *dis* traits was carried out using high-resolution melt (HRM)-PCR. HRM-PCR is a method that can distinguish between amplicons that differ by only a single nucleotide. Therefore, amplicons encompassing single nucleotide polymorphisms (SNPs) can potentially be used in HRM-PCR to distinguish between different genotypes and associate traits with particular chromosomal locations. 119 SNPs, identified by Warthmann et al., (2007), covering all five chromosomes of the Arabidopsis genome (Table 3.4.3), were tested for mapping by HRM-PCR. To be useful, the melt profiles needed to distinguish between the L*er*-0/L*er*-0 homoduplexes, Col-0/Col-0 homoduplexes and L*er*-0/Col-0 heteroduplexes. Based on how easily their melt curves distinguished the homo- and hetero-duplexes, the SNPs were categorized as good (G) and not good (NG) markers (Table 3.4.3). For example, the SNP 44607824 and 44606664 are good marker as their amplicon melt profiles clearly differentiated between homozygous (Col and L*er*) and heterozygous genotypes (Fig 3.4.4A and B). By contrast, the SNP 21607590 and 21607336 are not good markers because the difference in profiles between Col-0 and L*er*-0 was indistinguishable (Fig. 3.4.4C and D). Of the 119 SNP-targeted amplicons tested, approximately 70% gave melt profiles, which could identify whether the SNP was homozygous for L*er*-0, homozygous for Col-0 and heterozygous for L*er*-0 and Col-0 in a particular F2 plant (Table 3.4.3). Based on their ability to differentiate the different genotypes in HRM-PCR, 4 to 6 markers per chromosome were initially chosen for mapping of the genetic lesions responsible for the delayed senescence traits (Table 3.4.4). The positions of the SNP markers chosen for HRM analysis is shown in Fig. 3.4.5.

Table 3.4.3. SNPs usefulness in mapping.

A total of 119 SNP-targeted amplicons were tested in HRM-PCR to see whether their melt profiles could distinguish different genotypes. The marker number used, as described by Warthmann et al., 2007, is indicated in each chromosome (Chr) column. The SNP markers were categorized as good (G) and not good (NG) based on whether their amplicon melt profiles could easily distinguish between the homoduplexes of L*er*-0 and Col-0 and the heteroduplexes that result from outcrosses of mutants (in L*er*-0 background) with Col-0. M = Markers, chr = chromosome, R = Quality of markers.

#	M of Chr1	R	M of Chr1	R	M of Chr2	R	M of Chr3	R	M of Chr4	R	M of Chr5	R
1	21607386	G	44607693	G	44606769	G	21607250	G	21607184	G	214606110	G
2	21607648	G	44608060	G	21607038	G	21607479	G	21607598	G	21606996	G
3	44606313	G	44606256	NG	44606142	G	44606427	G	44606493	G	44606574	G
4	44606794	G	44606362	NG	44606419	G	44607348	G	44606615	G	44607038	G
5	44607225	G	44606232	NG	44606533	G	44607718	G	44606851	G	4460648	G
6	44606973	G	44606411	NG	44606598	G	44606102	G	44607079	G	44606745	G
7	21607336	NG	21607411	NG	44606322	G	44606436	G	44607545	G	44607234	G
8	21607463	G	44606867	NG	44606444	G	44607578	G	21607200	G	21607402	G
9	21607590	NG	44606981	NG	44606664	G	44607987	G	21607631	G	44606639	G
10	21607700	G	21606988	NG	44607824	G	44606908	NG	44606558	G	44607046	G
11	44606126	G			44607930	G	44607283	NG	21607750	G	44607193	G
12	44606248	G			44606802	NG	44607735	NG	44606680	G	44607242	G
13	44606370	G			44607332	NG	21607675	NG	44606916	G	44607413	G
14	44606517	G			21607259	NG	44606273	NG	44607291	G	44607808	G
15	44606525	G			4606590	NG	44606721	NG	44607405	G	44606159	NG
16	44606883	G			44606989	NG	44606957	NG	44607751	G	44607800	NG
17	44607217	G			44607627	NG	21607573	NG	44607792	G	44606566	NG
18	44607258	G			44607898	NG	44606379	NG	44607751	G	44606826	NG
19	44607315	G			21607488	NG	44607087	NG	44607759	NG	44607676	NG
20	44607421	G			44606940	NG	44607120	NG	44606216	NG	44607160	NG
21	44607520	G			44606997	G			44606688	NG		
22	44607536	G			44607503	G			44607816	NG		
23	44607602	G							21607733	NG		
24	44607611	G							44608028	NG		

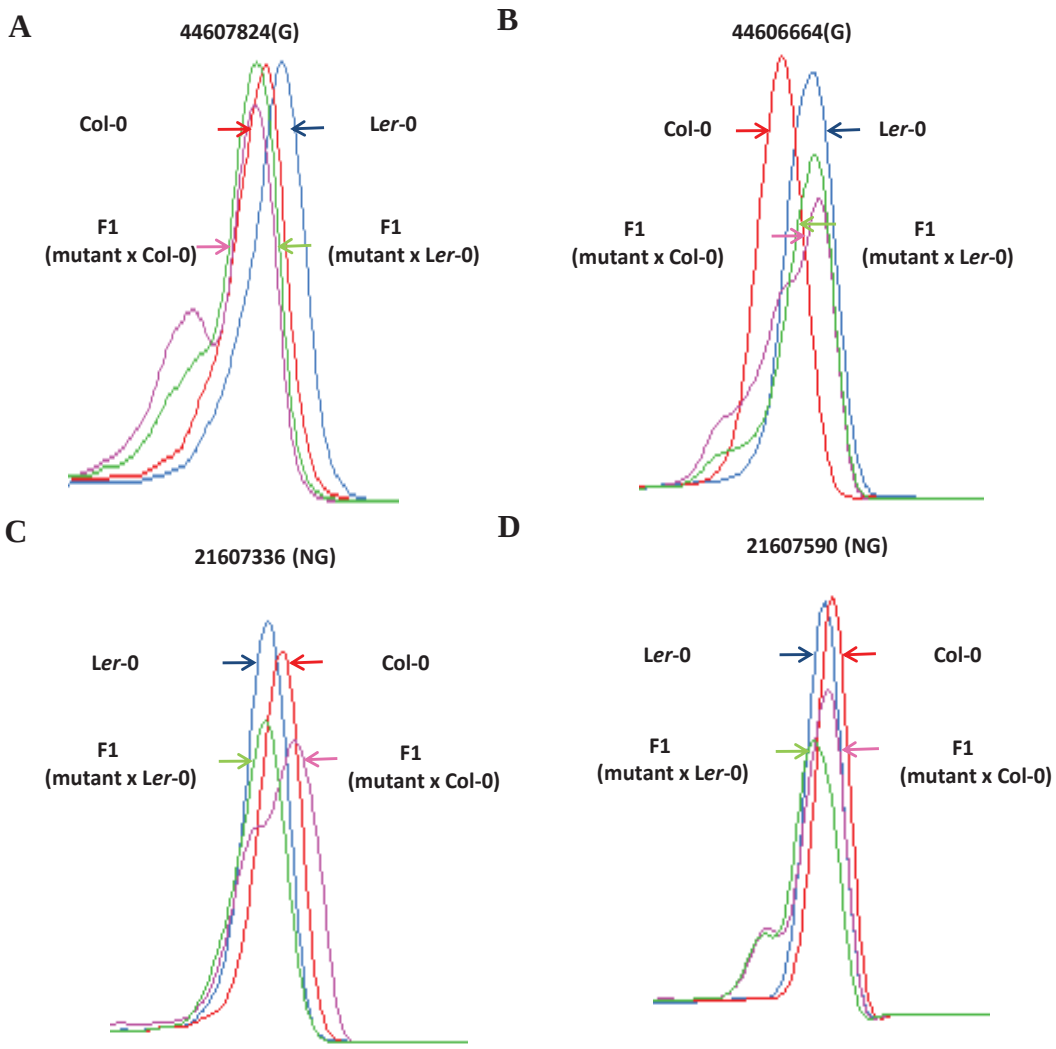

Figure 3.4.4. Melt profiles of SNP-targeted amplicons obtained in HRM analysis.

A and B Good (G) markers and C and D Not Good (NG) markers. The markers were categorized based on whether their amplicon melt profiles could easily distinguish between L*er*-0/L*er*-0 homoduplexes, Col-0/Col-0 homoduplexes and the heteroduplexes resulting from outcrossing mutants (L*er*-0 background) with Col-0. Numbers represent the name of the markers. Blue colour represents L*er*-0 peaks, red colour represents Col-0 peaks, pink colour represents F1 peaks (mutant outcrossed Col-0), green colour represents F1 peaks (mutant backcross L*er*-0). HRM analysis was performed by using LightCycler 480 SW 1.5 software.

Table 3.4.4. SNP-based markers used in HRM-PCR for preliminary linkage analysis.

Most of the SNP markers used for HRM-segregation analysis were identified by Warthmann et al (2007). Additional SNP markers are shown in red. Each SNP was given a two-digit identifier for easy reference to the chromosome it is a marker for. The first digit of the name represents the chromosome to which it belongs and the second digit is the primer number. The position of markers for chromosomes is represented with respect to the L*er*-0 genome.

#	Marker	Position on chr.	#	Marker	Position on chr.
1-1	44607520	5,929,39	4-20	44606493	4,903,963
1-2	44606126	11,466,003	4-21	7,365,693	7,365,693
1-3	44606794	20,083,812	4-22	44606851	7,362,775
1-4	44606525	26,787,537	4-23	7,517,029	7,517,029
2-5	44606322	801,880	4-24	7,555,037	7,555,037
2-6	44606989	13140388	4-25	44606916	7,783,449
2-7	21607038	2,287,176	4-26	7,796,989	7,796,989
2-8	44606664	9,148,329	4-27	44606558	8,003,049
2-9	44607914	9,367,662	4-28	44607545	10,150,635
2-10	44607701	9,148,329	4-29	44607792	11,849,009
2-11	44607824	12,122,750	4-30	21607184	12,729,400
2-12	21607013	19,240,187	4-31	44606615	13,510,330
2-13	44606533	19,240,187	4-32	44607751	13,725,319
3-14	21607479	580,747	5-33	44606639	6,708,014
3-15	44606957	2,228,040	5-34	44607038	13,917,965
3-16	44607987	3,884,290			
3-17	44607718	9,292,157			
3-18	21607675	16,213,412			
3-19	21607250	20.930,705			

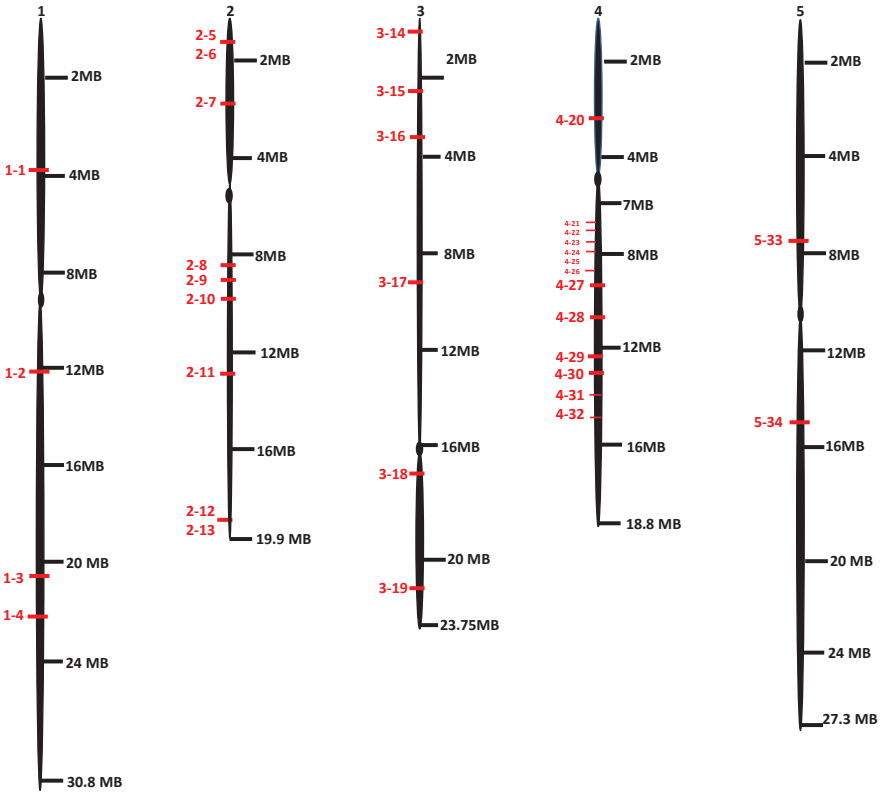

Figure 3.4.5. Approximate chromosomal positions of SNP markers in the Arabidopsis genome.

The numbers 1, 2, 3, 4 and 5 correspond to five chromosomes in Arabidopsis. Numbering of SNPs is from north (up) to south (down) on the chromosomes according to their positions in L*er*-0 genome (as mentioned in Table 3.4.4). MB = Megabases. The SNP markers are labelled in red. The first digit of the SNP markers represents the chromosome to which it belongs and the second digit is the primer number.

3.4.1.3 Mapping of the genetic lesions responsible for the *dis* phenotypes

Five *dis* mutants (*dis1, 9, 15, 34* and *58*) were selected for mapping by HRM-PCR. Mapping was carried out by determining the percentage linkage of the SNPs to the delayed degreening trait. The primer sequences used for HRM-PCR are presented in Appendix 3.4.1. The percentage recombination of four SNPs on chromosomes 1, 2, 3 and 4 and 2 SNPs on chromosome 5 was examined in 9-30 F2 recombinants. As shown in Table 3.4.1, genetic lesions underlying the delayed senescence traits of the *dis* plants were inherited in a recessive manner. This meant that all the F2 individuals of the mapping population showing delayed inflorescence senescence were homozygous for the L*er*-0 sequence at the genetic lesion. Therefore, HRM-PCR was performed only on the F2 plants visually confirmed to have the delayed degreening trait (homozygous plants). The percentage recombination was determined using the formula described in Chapter 2. The lower percentage recombination suggests a stronger linkage of the SNP to the delayed degreening trait.

Nine F2 plants homozygous for the *dis1* genetic lesion were initially used for linkage analysis using the markers shown in Table 3.4.5. The chromosome 1 markers including 1-1, 1-2, 1-3 and 1-4 showed 50, 50, 50 and 38% recombination, respectively. This indicated that these markers are not linked to *dis1* phenotype. Similarly, no linkage was observed for the markers present on chromosome 2, 3 and 5. Thus, *dis1* could not be on chromosome 1, 2, 3 and 5. However, the percentage recombination was lowest for the markers on chromosome 4 (i.e., 33% for 4-27, 16% for 4-30, 16% for 4-31 and 38% for 4-32) which suggested that the genetic lesion responsible for *dis1* was located on chromosome 4 (Table 3.4.5). The genotypic analysis of F2 recombinants revealed that this mutation could be present 16 cM north or south of marker 4-32 and 27 cM north or south of marker 4-30 (Fig. 3.4.6). For example, the genetic makeup of plant # 2, 5 and 8 highlighted in red predicted that the mutation was either north or south of marker 4-32 (Table 3.4.5).

Table 3.4.5. Genetic analysis of *dis1* recombinants.

HRM-PCR was performed to investigate linkage of 19 SNP markers across the whole genome to *dis1* delayed degreening phenotype. Order of the SNP markers from left to right corresponds to north (up) to south (down) of chromosomes (Fig. 3.4.6). The plants highlighted in red are used to predict the position of mutation. Recombinant # is the unique identifier for that plant in the F2 population tested. LL = homozygous L*er*-0, CC = homozygous Col-0, LC = heterozygous

#	*dis1* F2	1-1	1-2	1-3	1-4	2-5	2-7	2-9	2-13	3-15	3-16	3-17	3-18	3-19	4-27	4-30	4-31	4-32	5-33	5-34
1	1	LC	LL	LL	LL	LL	LL	LL	LC	LL	LC	LL	LC	LC	LL	LL	LL	LL	LC	LC
2	2	LC	CC	CC	LL	LL	LL	LL	LC	LC	LL	LC	CC	LC	CC	CC	CC	LC	CC	LC
3	3	CC	LC	LC	LC	LC	LC	CC	CC	LC	LL	LC	LC	LL	LL	LL	LL	LL	LC	CC
4	4	CC	LC	LC	LC	LC	LC	LC	LL	CC	CC	CC	LC	CC	LL	LL	LL	LL	LC	CC
5	5	LL	LC	LC	LC	LC	LC	LC	LC	LC	CC	LC	LC	LC	LL	LL	LL	LC	LC	LL
6	6	LC	LC	LC	CC	LC	LL	LL	LL	LC	LC	LC	LC	LC	CC	LL	LL	LL	CC	LC
7	8	CC	CC	LC	LL	LC	LL	LL	LC	LC	LC	LC	LL	LL	LC	LL	LL	LL	LC	CC
8	9	LL	LL	LC	LC	CC	CC	LC	LC	LL	LC	LL	LL	LL	LC	LC	LC	LC	LC	LL
9	10	LL	CC	LC	LC	CC	CC	CC	CC	LC	CC	LC	LL	LC	LL	LL	LL	LL	LC	LL
	L*er*		2	1	3	3	4	4	2	2	2	2	3	3	5	7	**7**	**6**	0	0
	Col		3	1	1	2	2	2	2	1	3	1	1	1	2	2	**1**	**0**	2	4
	Het		4	7	5	5	3	3	5	6	4	6	5	5	2	1	**1**	**3**	7	7
	% linkage	**50**	**55**	**50**	**38**	**50**	**38**	**38**	**50**	**44**	**55**	**44**	**38**	**38**	**33**	**16**	**16**	**38**	**64**	**61**

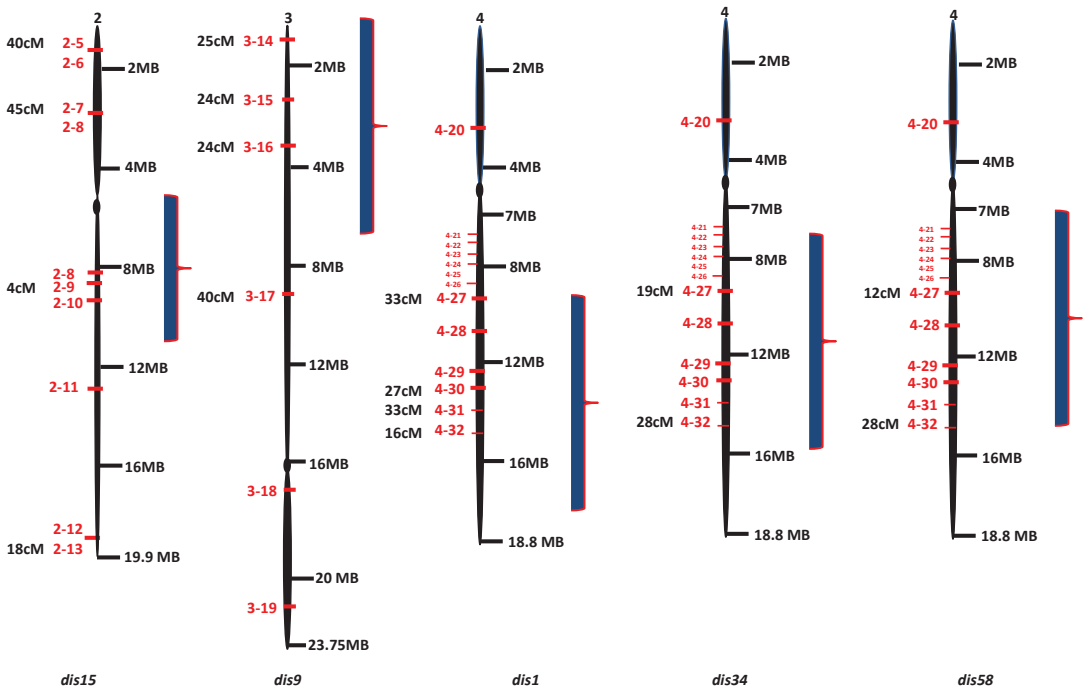

Figure 3.4.6. Rough mapping of *dis1*, *9*, *15*, *34* and *58*.

The numbers 2, 3 and 4 at the bottom of the figure correspond to chromosome 2, 3 and 4 in Arabidopsis. The markers highlighted in red were used for initial rough mapping of the mutants. SNPs markers were numbered according to their relative positions from north (up) to south (down) on the chromosomes as mentioned in Table 3.4.4. The predicted locations of genetic lesions are highlighted by blue lines. MB = Megabases.

The *dis9* genetic lesion was mapped to chromosome 3 using 27 F2 recombinant plants homozygous for the *dis9* lesion (Appendix 3.4.2 and Fig. 3.4.6). Markers 3-14 and 3-16 were 25 and 24% linked with the *dis9* locus, respectively. The genotypic analysis of the F2 plants revealed that the *dis9* mutation was south of 3-14 and north of 3-16. For example, plant number 18, 19 and 20 describes that the mutation is north of 3-16.

The *dis15* genetic lesion was mapped to chromosome 2 using 11 F2 plants homozygous for the lesion. Markers 2-9 and 2-13 were positioned at genetic distances of 4 cM and 18 cM, respectively from the lesion (Appendix 3.4.3 and Fig. 3.4.6). The genotypic analysis of the F2 plants revealed that the lesion was north of 2-9; however to explain the location of the *dis15* gene around 2-13, more recombinants and markers were required.

The *dis34* genetic lesion was found to be linked to markers 4-27 and 4-32 at genetic distance of 19cM and 28cM, respectively (Appendix 3.4.4 and Fig. 3.4.6). The *dis58* genetic lesion was mapped to chromosome 4 by markers 4-27 and 4-32. These markers were present at a genetic distance of 12 and 27cM, respectively (Appendix 3.4.5 and Fig 3.4.6). At this stage, it was difficult to predict whether *dis34* and *58* mutations are present either north or south of the markers.

3.4.1.4 Fine mapping of *dis* mutants

The preliminary linkage analysis helped identify the approximate positions of the *dis* mutations in the genome. More F2 recombinants were used to further map *dis15, 34* and *58* on the respective chromosomes.

3.4.1.4.1 Further mapping of *dis15*

The *dis15* genetic lesion was rough mapped to chromosome 2 at 4 cM north and south of 2-9 (appendix 3.4.3). To more closely map to the mutation, linkage analysis was performed on 81 F2 recombinant individuals homozygous for the genetic lesion using markers 2-9 and 2-11 (Table 3.4.6). The linkage analysis revealed that the *dis15* mutation is located 37 cM south of 2-8 and 11 cM north/south of 2-11 (Table 3.4.6 and Fig. 3.4.7). The physical distance between these two markers is ~2.5MB.

Table 3.4.6. Genetic analysis of *dis15* recombinants.

Linkage analysis of *dis15* was performed using chromosome 2 markers. Order of the markers from left to right corresponds to north to south of chromosome (Fig. 3.4.8). Recombinant number is the unique identifier for that plant in the F2 population tested. LL = homozygous L*er*-0, CC = homozygous Col-0, LC = heterozygous

#	*dis15* F2	2-8	2-11	#	*dis15* F2	2-8	2-11
1	57	LC	LL	42	121	LC	LC
2	58	LC	LL	43	132	LL	LL
3	63	LL	LL	44	133	LC	LC
4	64	LL	LL	45	71	LC	LC
5	81	LC	LL	46	72	LC	LC
6	82	LL	LL	47	69	LL	LL
7	92	LC	LL	48	70	LC	LC
8	93	LL	LL	49	87	LL	LL
9	104	LL	LL	50	88	LL	LL
10	105	LL	LL	51	87	LC	LC
11	116	LL	LC	52	98	LL	LC
12	117	LC	LL	53	99	CC	LL
13	128	LL	LL	54	110	LL	CC
14	129	LL	LL	55	111	CC	LL
15	59	LC	LL	56	122	LC	LL
16	60	LC	LL	57	123	LC	LL
17	65	LL	LL	58	73	LC	LL
18	66	LC	LL	59	74	LC	LL
19	83	LL	LL	60	77	LC	LL
20	84	LC	LC	61	78	LL	LL
21	83	LL	LL	62	134	CC	LL
22	84	LL	LC	63	88	LC	LL
23	94	LC	LL	64	89	LC	LL
24	95	LC	LL	65	100	LC	LL
25	106	LC	LL	66	101	CC	LL
26	107	LC	LL	67	112	LL	LC
27	118	LL	LL	68	113	CC	LL
28	119	LL	LL	69	124	CC	LL
29	130	LC	LL	70	75	LC	LC
30	131	LL	LL	71	76	LC	LL
31	61	LC	LL	72	79	LC	LL
32	62	LC	LL	73	80	LC	LC
33	67	LC	LL	74	135	LC	LL
34	68	LC	LL	75	136	CC	LL
35	85	LL	LL	76	90	LC	LL
36	86	LC	LC	77	91	LC	LL
37	96	LL	LL	78	102	CC	LL
38	97	LC	LC	79	115	LL	LL
39	108	LL	LL	80	126	LL	LC
40	109	LC	LC	81	127	CC	LL
41	**120**	**LL**	**LL**				
					Marker	**2-8**	**2-11**
					L*er*-0	**30**	**63**
					Col-0	**8**	**1**
					Het	**42**	**17**
					%Linkage	**37**	**11**

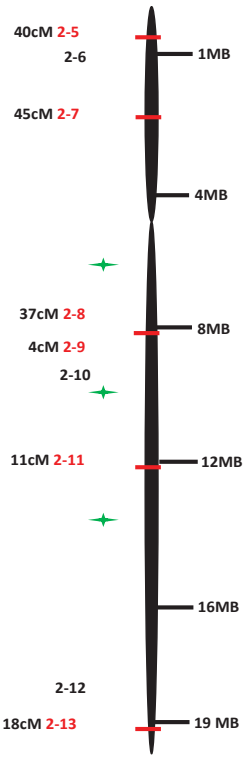

Figure 3.4.7. Mapping of *dis15* on chromosome 2.

SNPs markers were numbered according to their relative positions from north (up) to south (down) on the chromosome as mentioned in Table 3.4.4. The green asterisk represents the predicted location of genetic lesion on chromosome 2. cM = centimorgan, MB = Megabases.

3.4.1.4.2 Further mapping of *dis34*

Rough mapping had indicated that markers 4-27 and 4-32 were linked to the *dis34* (Appendix 3.4.4). The physical distance between these two markers was almost 6 Mb. Fine mapping was carried out by using markers 4-20, 4-22, 4-25, 4-28 and 4-29 over the distance of 10 Mb in the vicinity of markers 4-27 and 4-28 (Table 3.4.7 & Fig. 3.4.8). The recombination analysis was performed on 69 additional recombinants homozygous for the *dis34* lesion. This shows that *dis34* genetic lesion is present at a genetic distance of 22 cM from marker 4-22 and 29 cM from marker 4-25. The genetic analysis of F2 recombinants revealed that the *dis34* mutation is located south of 4-21 and north or south of 4-25.

Table 3.4.7. Genetic analysis of *dis34* F2 recombinants.

Linkage analysis of *dis34* was performed using chromosome 4 markers. Order of the markers from left to right corresponds to north to south of chromosome (Fig. 3.4.8). Recombinant number is the unique identifier for that plant in the F2 population tested. LL = homozygous L*er*-0, CC = homozygous Col-0, LC = heterozygous

#	*dis34* F2	4-20	4-22	4-25	4-28	4-29
1	65	LC	LL	LC	LC	LC
2	67	CC	LL	LC	LC	LC
3	68	LL	LL	LL	LC	LC
4	72	LC	LL	LC	LL	LL
5	69	LC	LC	LL	LL	LC
41	73	LC	LL	LL	LL	LL
42	70	LC	LL	LL	LL	LL
43	62	LL	LL	LL	LL	LL
44	71	LL	LL	LC	LL	LL
45	63	LC	LL	LL	LC	LC
46	53	LL	LL	LL	LL	LC
47	64	LL	LL	LL	LL	LL
48	54	LL	LL	LL	LL	LL
49	55	LC	LL	LL	LL	LL
50	46	LL	LL	LC	LL	LL
51	56	LC	LL	LL	LC	LC
52	47	LL	LL	LC	CC	CC
53	57	LC	LC	LL	LC	LC
54	48	LC	LL	LC	LL	LL
55	59	LL	CC	LC	LC	LC
56	49	CC	LL	LC	CC	LC
57	60	LC	LL	LC	LL	LL
58	50	LC	LC	LL	LC	LC
59	61	LC	LL	LL	LL	LL
60	51	LC	LL	LL	LL	LL
61	44	LL	LL	LL	LL	LL
62	52	LC	LL	LL	LL	LL
63	45	LL	LL	LL	LL	LL
64	62	LL	LL	LL	LL	LL
65	74	LC	LL	LL	LL	LL
66	82	CC	LL	LC	LC	LC
67	75	LC	LC	LC	LC	LC
68	83	LC	LL	LL	LL	LL
69	76	CC	CC	CC	CC	CC
70	70	LL	LL	LL	LL	LL
71	77	LC	CC	CC	CC	LC
72	71	LL	LL	LL	LL	LC
73	78	CC	CC	CC	CC	CC
74	72	LL	LL	LL	LC	LC
75	79	LL	LL	LL	LL	LL
76	73	LL	LL	LL	LL	LL
77	80	LC	CC	LC	LC	LL
78	75	LC	LL	LL	LL	LL
79	81	LL	LC	LC	LC	LC
80	76	LL	LL	LL	LL	LL
81	85	LC	LC	LC	LC	LC
82	86	LL	LL	LL	LL	LL
83	97	CC	LC	LL	CC	CC
84	98	LL	LL	LC	LC	LC
85	87	LL	LL	LL	LL	LL
86	88	LL	LL	LL	LL	LL
87	99	LL	LL	LL	LL	LL
88	100	LC	LC	LC	LC	LC
89	89	CC	CC	CC	CC	CC
90	90	CC	CC	CC	CC	CC
91	101	LL	LL	LL	LC	LC
92	102	CC	LC	LC	LC	LC
93	91	CC	LL	LC	LC	LC
94	92	LC	LC	LC	LC	LC
95	103	LC	LL	LL	LL	LL
96	104	LC	LC	LC	LC	LC
97	93	LL	LL	CC	LC	CC
98	94	LC	LC	LC	LL	LL
99	105	CC	CC	LC	LC	LC
100	106	LL	LL	LL	CC	LL
101	95	LL	LL	CC	LL	LL
102	96	LC	LC	LC	LL	LL
103	107	LC	LL	LL	LL	LL
104	108	CC	LC	LC	LC	CC
	L*er*-0	28	46	36	35	35
	Col-0	**12**	**8**	**8**	**9**	**8**
	Het	**29**	**15**	**25**	**25**	**26**
	% linkage	**38%**	**22%**	**29%**	**31%**	**30%**

3.4.1.4.3 Fine mapping of *dis58*

The *dis58* mutation was roughly present at genetic distance of 12 cM and 28 cM either south or north of markers 4-27 and 4-32, respectively (Fig. 3.4.6). The physical difference between 4-19 and 4-28 is approximately 6 MB. Markers for fine mapping were used that cover an approximately 10 MB region including 4 MB sequence upstream of 4-19. This additional 4 MB area was used because genotypic analysis of F2 plants revealed that the mutated locus is either north or south of the 4-27 marker. Fine mapping was started with 50 positive recombinants (Table 3.4.8). Percentage recombination showed that *dis58* is 1% linked to marker 4-22 and 5% linked to marker 4-25 (Table 3.4.8). The physical distance between these two markers (4-21 and 4-25) is ~420 kb. Furthermore, the genetic analysis of the recombinants suggests that *dis58* is present south of 4-22 and north of 4-25.

To further map *dis58*, the 420 kb regions of L*er*-0 and Col-0 genome were assembled and subsequently scanned to identify the SNPs in the region. The identified SNPs markers present in the mapped region were tested on new *dis58* F2 recombinants (Table 3.4.9 and Fig. 3.4.9). HRM analysis revealed that *dis58* genetic lesion was located either north or south of marker 4-23 and 4-24 at a genetic distance of ~4cM and ~5.7cM, respectively. The physical distance between these two markers is ~40 kb.

Table 3.4.8. Genetic analysis of *dis58* F2 recombinants.

Linkage analysis of *dis58* was performed using chromosome 4 markers. Order of the markers from left to right corresponds to north to south of chromosome (Fig. 3.4.8). Recombinant number is the unique identifier for that plant in the F2 population tested. LL = homozygous L*er*-0, CC = homozygous Col-0, LC = heterozygous

#	***dis58* F2**	**4-20**	**4-22**	**4-25**	**4-28**	**4-29**
1	32	LL	LL	LL	LC	LC
2	33	LL	LL	LL	LL	LL
3	34	LL	LL	LL	LL	LL
4	27	LL	LL	LL	LL	LC
5	35	CC	LL	LL	LL	LL
6	28	LL	LL	LL	LL	LL
7	36	LC	LL	LL	LL	LC
8	29	LC	LL	LL	LC	LL
9	37	LL	LL	LL	LL	LL
10	30	LL	LL	LL	LL	LL
11	38	LC	LL	LL	LL	LL
12	31	LL	LL	LL	LL	LL
13	39	LL	LL	LL	LL	LC
14	40	LL	LL	LL	LL	LL
15	48	LL	LL	LL	LL	LC
16	41	LL	LL	LL	LC	LC
17	49	LL	LL	LL	LC	LL
18	42	CC	LC	LL	LL	CC
19	51	LL	LL	LL	LL	LC
20	43	LL	LL	LC	LC	LC
21	52	LL	LL	LL	LL	LL
22	44	LL	LL	LL	LL	LL
23	53	LC	LL	LL	LL	LL
24	45	LL	LL	LL	LL	LL
25	59	LL	LL	LL	LL	LC
26	46	LL	LL	LC	LC	LL
27	47	LL	LL	LC	LC	LC
28	44b	LL	LL	LL	LC	LC
29	47b	LC	LL	LL	LL	LL
30	59b	LC	LL	LL	LL	LL
31	45b	LL	LL	LL	LL	LC
32	60b	LL	LL	LL	LL	LC
33	46b	LC	LL	LL	LC	LC
34	61b	LC	LL	LL	LL	LL
35	47b	LC	LL	LL	LL	LL
36	62b	LC	LL	LL	LC	LC
37	55b	LC	LL	LL	LL	LL
38	63b	LL	LL	LL	LC	LC
39	56b	LL	LL	LL	LC	LC
40	64b	LC	LL	LL	LC	LC
41	57b	LL	LL	LL	LL	LC
42	65b	LC	LL	LL	LL	LL
43	58b	LC	LL	LL	LL	LC
44	66b	LC	LL	LL	LL	LL
45	67b	LL	LL	LL	LL	LC
46	68b	LL	LL	LL	LL	LL
47	69b	LC	LL	LL	LL	LL
48	42b	LL	LL	LL	LL	LL
49	43b	LL	LL	LC	LC	LC
	L*er*-0	**29**	**48**	**44**	**36**	**26**
	Col-0	**2**	**0**	**0**	**0**	**1**
	Het	**18**	**1**	**5**	**11**	**20**
	% linkage	**22%**	**1.02%**	**5.1%**	**11%**	**22%**

Table 3.4.9. Genetic analysis of *dis58* F2 recombinants.

Linkage analysis of *dis58* was performed using chromosome 4 markers. Order of the markers from left to right corresponds to north to south of chromosome (Fig. 3.4.8). Recombinant number is the unique identifier for that plant in the F2 population tested. LL = homozygous L*er*-0, CC = homozygous Col-0, LC = heterozygous.

#	*dis58 F2*	4-22	4-21	4-23	4-24	4-26	#	*dis58 F2*	4-21	4-23	4-24	4-26
1	105a	LC	LC	LC	LL	LC	134	142	LC	LL	LL	LC
2	106a	LL	LC	LL	LL	CC	135	153	LC	LL	LL	LC
3	103	LL	LL	LL	LL	LL	136	154	LL	LL	LL	LL
4	104	LL	LL	LL	LL	LL	137	166	LL	LL	LL	LL
5	116	LL	LL	LL	LL	LL	138	167	LL	LL	LL	LL
6	117	LL	LL	LL	LL	LL	139	173	LL	LL	LL	LL
7	128	LC	LC	LL	LL	LC	140	174	LC		LL	LC
8	129	LL	LL	LL	LL	LL	141	143	LL	LL	LL	LL
9	107a	LL	LL	LL	LL	LL	142	144	LL	LL	LL	LL
10	108a	LL	LL	LL	LL	LL	143	155	LL	LL	LL	LL
11	105	LL	LL	LL	LL	LL	144	157	LC	LL	LL	LC
12	106	LC	LC	LC	LL	LC	145	168	LL	LL	LL	LL
13	118	LL	LL	LL	LL	LL	146	169	LL	LL	LL	LL
14	119	LL	LL	LL	LL	LL	147	177	LL	LL	LL	LL
15	130	LC	LC	LL	LL	LC	148	178	LL		LL	LL
16	131	LL	LL	LL	LL	LL	149	145	LC	LL	LL	LC
17	141	LC	CC	LL	LL	LC	150	146	LC	LL	LL	LC
18	109a	LL	LL	LL	LL	LL	151	158	LL	LL	LL	LL
19	110a	LL	LL	LL	LL	LL	152	159	LL	LL	LL	LL
20	107	LL	LL	LL	LL	LL	153	170	LL	LL	LL	LL
21	108	LLL	LL	LL	LL	LL	154	171	LL	LL	LL	LL
22	120	LL	LL	LL	LL	LL	155	179	LL	LL	LL	LL
23	121	LL	LL	LL	LL	LL	156	180	LL	LL	LL	CC
24	132	LL	LL	LL	LL	LL	157	147	LC	LL	LL	LC
25	133	LL	LL	LL	LL	LL	158	148	LC	LL	LL	LC
26	111a	LL	LC	LC	LL	LC	159	160	LL	LL	LL	LL
27	112a	LL	LL	LL	LL	LL	160	161	LL	LL	LL	LL
28	109	LL	LL	LL	LL	LL	161	172	LC	LL	LL	LC
29	110	LL	LL	LL	LL	LL	162	173	LL	LL	LL	LL
30	122	LL	LL	LL	LL	LL	163	181	LL	LL	LL	LL
31	123	LL	LL	LL	LL	LL	164	182	LL	LL	LL	LL
32	134	LL	LL	LL	LL	LL	165	149	LC	LC	LL	LC
33	135	LC	LC	LL	LL	LC	166	150	LC	LC	LL	LC
34	113	LL	LL	LL	NA	LL	167	162	LL	LL	LL	LL
35	114	LL	LL	LL	LL	LL	168	163	LL	LL	LL	LL
36	111	LL	LL	LL	LL	LL	169	174	LC	LC	LC	LC
37	112	LL	LL	LL	LL	LL	170	175	LL	LL	LL	LL
38	124	LL	LL	LL	LL	LL	171	183	LL	LL	LL	LL
39	125	LL	LL	LL	LL	LL	172	184	LC		LL	LC
40	137	LC	LC	LC	LL	LC	173	151	LC		LL	LC
41	138	LC	LC	LC	LL	LC	174	152	LC		LL	LL
42	115a	LL	LL		LL	LL	175	164	LL		LL	LL
43	116a	LL	LL		LL	LL	176	165	LL		LL	CC
44	113	LL	LL		LL	LL	177	175	LL		LL	
45	115	LL	LC		LL	LC	178	176	LL		LL	
46	126	LL	LC		LL	LC	179	185	LL	LC	LL	CC
47	127	LL	LL		LL	LL	180	186	LL		LL	
48	139	LC	LC		LL	LC						
49	140	LC	LL		LL	LL						
					4-21	**4-22**	**4-23**	**4-24**	**4-26**			
				L*er*-0	**68**	**39**	**69**	**95**	**64**			
				Col-0	**1**	**0**	**0**	**0**	**4**			
				Het	**27**	**10**	**9**	**1**	**26**			
				%linkage	**15.1**	**10.2**	**4**	**5.7**	**17.7**			

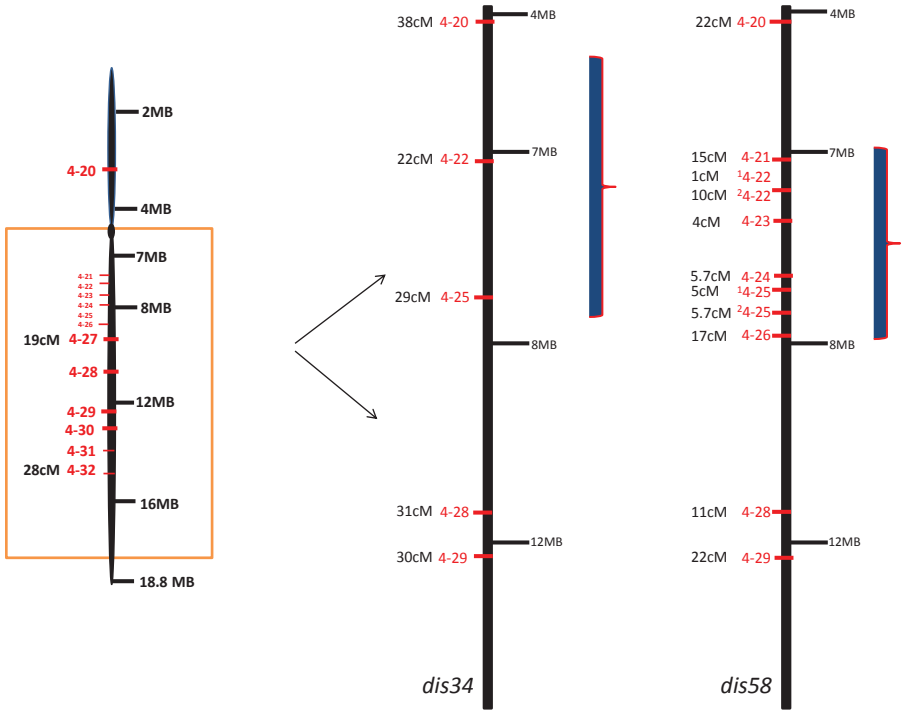

Figure 3.4.8. Schematic diagram for fine mapping of *dis34* and *dis58*.

SNPs markers were numbered according to their relative positions from north (up) to south (down) on the chromosome as mentioned in Table 3.4.4. The predicted locations of genetic lesions on chromosome 4 are highlighted by blue lines. [1] and [2] represent genetic distances calculated by the same marker in a separate HRM analysis. cM = centimorgan, MB = Megabytes.

3.4.2 Discussion

Creating and subsequent identification of mutations, which cause a defect in a particular biological process, is often straightforward. However, the isolation of the genetic lesion causing the phenotype can be different. In the last decade, introduction of high-throughput technologies for differentiating between sequence variants (e.g., HRM) (Lehmensiek et al., 2008) and deep sequencing technologies (e.g., Illumina sequencing system) (Reis-Filhoto and Jorge, 2009) to sequence the whole genome of the organisms has tremendously reduced the time required to identify single base pair mutations.

The tested *dis* mutations are recessive in nature

All the tested *dis* mutations were recessive in nature (Table 3.4.1). The reason for this is that the majority of the wild-type alleles are dominant over the mutated alleles (Haldane, 1930; Fisher., 1934; S.Wright, 1934; Wright, 1956; Nanjundiah, 1993; Bourguet, 1999; Fisher, 1999). However, a long-debated question is why most mutations are recessive to the wild-type. To explain this many hypotheses have been proposed. For example, Fisher, (1934) anticipated that the force of natural selection favours the dominance of wild-type allele over the mutated one. This is because heterozygotes, having one wild-type and one mutant allele, can survive better than the homozygotes that have two mutated alleles. However, the process of selection of dominant mutations differs from the recessive mutations. Dominant deleterious mutations are eliminated from the population as soon as they arise, whereas the dominant advantageous mutations can eliminate previous wild-types and can be selected for (Haldane, 1930). Conversely, Wright, (1934) asserted that dominance of wild-type allele is the consequence of metabolism rather than act of natural selection.

Nanjundiah, (1993) analyzed the genetic evidence to investigate whether the dominance of wild-type is the act of either force of natural selection or enzyme-mediated metabolic pathways. He concluded that dominance of wild-type is the outcome of both evolution and metabolic processes. Kacser and Burns, 1981 proposed that the abundance of enzymes is higher than the substrates and enzyme can function well below saturation. Thus, the decreased amount of protein in the cell produced by one wild-type allele (while the

mutated allele has stopped producing functional proteins) is sufficient to perform normal functions.

An alternative explanation for dominance of wild-type is that the cellular constituents are buffered against the variations in DNA sequences (Chandra and Nanjundiah, 1990). For examples, transcription factors regulating genes transcription by binding to the particular *cis* elements act on particular sets of DNA sequences. However, in some instances it is also found that recessive mutations show a phenotype in the heterozygote form. This happens when two mutated alleles of two different genes controlling the same phenotype come together in the heterozygote (Campos-Ortega and Knust, 1990).

SNP-based HRM PCR is a successful method for linkage analysis

In this study, HRM-PCR performed on F2 recombinants of *dis1*, *9*, *15*, *34* and *58* (Fig. 3.4.7) proved useful for coarse mapping the genetic lesions responsible for the delayed senescence phenotypes. HRM is a very sensitive method that can easily distinguish differences of even a single base pair between different samples. HRM-PCR based segregation analysis is faster than traditional mapping techniques because it does not require additional steps of restriction digestion and gel-electrophoresis. In HRM analysis, the results can be obtained within two hours of the PCR initiation. However, because it relies on subtle changes in the melt profiles of amplicon, the success of the procedure relies on many parameters, including amplicon size, primer specificity, buffer composition and DNA concentration and quality (White and Potts, 2006; Lehmensiek et al., 2008; Martín-Núñez et al., 2012). For example, White and Potts (2006) concluded that amplicons with sizes greater than 300 bp produced more errors compared to amplicons of smaller sizes (e.g., 50- 300 bp). To avoid these errors, I used high quality DNA (see Chapter 2) with amplicon sizes ranging from 70-150 bps.

The mutants in the L*er*-0 background were outcrossed to the Col-0 accession for mapping the mutations. The single nucleotide polymorphisms (SNPs) between the two ecotypes were used for HRM-based linkage analysis. The success of HRM analysis depends on the molecular markers that can distinguish between homozygous L*er*-0, homozygous Col-0 and heterozygous (progeny of *dis* mutants outcrossed with Col-0) DNA samples. Due to difficulties mentioned in the previous paragraph, identifying good HRM markers is critical.

Hence, first I identified HRM molecular markers that can be useful for mapping. Approximately 68% of the SNPs tested yielded melt profiles that were able to distinguish between L*er*-0 homoduplexes, Col-0 homoduplexes and heteroduplexes formed between L*er*-0 and Col-0 DNA strands in heterozygotes. These markers also provide a useful resource for future HRM-PCR based mapping studies for L*er*-0 and Col-0 accessions.

Approximately 32% of the SNPs tested could not be used for mapping because L*er*-0 and Col-0 homozygous HRM-melt profiles were inconclusive, as they overlapped (Fig. 3.4.4C and D). In HRM analysis the melt peak of distinct DNA samples differs according to the melting temperature of the amplicons. Therefore, it is possible that despite the presence of an SNP between the two wild types, the markers failed to distinguish between them as both DNA duplexes had similar melting temperature. However, for these primers the melt profiles of heterozygote samples were distinguishable from the wild-types homozygotes. This is because both homoduplexes and heteroduplexes were formed in the heterozygotes DNA sample, whereas in homozygotes only homoduplexes were formed.

Mapping success is affected by recombination events, selection of false positives and epistatic interactions

Mapping can be complicated by low frequency of recombination. For example, Laitinen et al., (2010) could not narrow down the mutation causing a dwarf phenotype in Arabidopsis accession Krotzenburg (Kro-0). They attributed this to the presence of a 116.5 kb region of polymorphic repetitive DNA which was suppressing recombination. Interestingly, it appears that in the genomic region where the *dis58* mutation is present the recombination frequency is probably high, as ~200 recombinants allowed the fine mapping to an ~40 kb region. This is consistent with the study by Drouaud et al., (2006), who demonstrated the existence of meiotic recombination "hot spots" on chromosome 4 of Arabidopsis. The authors found 12 to 14 crossover breakpoints within a region 20 kb apart. Further, the work of Drouaud et al., (2006) demonstrated that the region between 6 to 8 MB on chromosome 4 was also found as a hot spot for crossover events. The high number of double recombination events suggested in the mapping of *dis58* in the 7 to 8 MB region of chromosome 4 (Table 3.4. 7 and 3.4.8) further supports this region as a hotspot for recombination. Other researchers have also found that certain regions within chromosome 2 and 4 are hotspots for recombination, which can lead to multiple crossovers when mapping

(Lam et al., 2005; Drouaud et al., 2006). However, the caveat is that the double crossover events observed in HRM analysis of *dis58* can be due to selection of false positive or mistakes in HRM analysis.

Many genes can regulate a particular biological process. Thus, an identified phenotype could be due to defects in functions of more than one gene. When many genetic loci contribute to the phenotype of a particular trait then this genetic interaction is called epistatic, which can be synergistic or antagonistic. Mapping of such epistatic interactions is difficult and labor intense because to identify the combination of lesions causing the phenotype requires substantial screening of F2 recombinants.

It is also possible that during mutant screening some wild-type plants are also selected as mutants. This can happen when the mutant phenotype differs subtly from that of the wild-type. Furthermore, linkage analysis assumes that molecular markers are independent of the phenotype. However, any association between mapping markers and the phenotype will introduce errors in the mapping (Kang et al., 2008).

Taken together the mapping of *dis15* to ~2.5 MB and *dis58* to ~40 kb mutants demonstrates that HRM-PCR based linkage analysis is reliable tool for mapping the mutations in the genome.

Blank page

3.5 Identification of a novel non-coding RNA that regulates Arabidopsis inflorescence senescence

Abstract

HRM-based linkage analysis of SNP markers mapped the *dis15* and *58* mutations to chromosome 2 and 4, respectively. To identify their exact location in the two chromosomes whole genome sequencing (WGS) was performed on both mutants. Eight putative SNPs containing G/C to A/T transitions were identified in the mapped region for *dis15*, whereas only one SNP was present in the mapped region of *dis58*. Of the eight putative *dis15* SNPs, three were in coding regions and of these, only one caused a non-synonymous amino acid change. This change converted a phenylalanine to leucine in a eukaryotic aspartyl protease encoded by locus AT2G28030. The SNP in *dis58* was in a region annotated as an intron of a non-coding RNA at locus AT4G13495. Transformation of *dis58* with a 5.6 kb DNA fragment containing the non-coding RNA complemented the phenotype. This suggests that *DIS58* is a non-coding RNA that regulates inflorescence senescence in Arabidopsis.

3.5.0 Introduction

In the past, map-based cloning has been a labour intensive approach because it required that the causal mutations be identified by mapping to a physical distance of ~100 to 300 kb. The mapped region was then subsequently interrogated by Sanger sequencing to identify the causal mutation. Advancements in next generation sequencing (NGS) technologies have replaced the more laborious and costly Sanger approach (Sturre et al., 2009; Schneeberger and Weigel, 2011). In some instances it has even become more cost/time effective to sequence whole genomes rather than just the mapped regions. This is particularly true for plants with small genomes such as Arabidopsis. Here I report on using whole genome sequencing (WGS) to identify the genetic lesions causing the *dis15* and *58* phenotypes. In *dis15,* a G to A mutation was found in eukaryotic aspartyl protease encoded by AT2G28030. In *dis58*, the SNP was found in a non-coding RNA encoded by the AT4G13495 locus. The *dis58* mutant transformed with wild-type DNA fragment complemented the delayed senescence phenotype suggesting that non-coding RNA is involved in regulating inflorescence senescence.

3.5.1 Results

3.5.1.1 Identifying the putative genetic lesions of *dis15* and *58* by whole genome sequencing

The *dis15* and *58* lesions that had been mapped by HRM-PCR to ~2.5 MB region of chromosome 2 and to ~40 kb region of chromosome 4, respectively, were analysed further by whole genome sequencing (WGS). WGS was performed by sequencing 100 bp paired-end reads through Illumina next-generation sequencing (NGS) technology. Genomes of the two mutants were sequenced at an average of ~80-fold genome coverage. Both *dis15* and *58* WGS trimmed raw reads were first assembled to the L*er*-0 wild type sequence (kindly provided by Richard Mott); *dis15* reads to the ~3 Mb region of chromosome 2 and *dis58* reads to a 100 kb region of chromosome 4, which HRM-PCR indicated to contain the causal SNP. It was possible to use each mutant as a second reference for each other to further filter out background differences because the causal senescence delaying SNPs in each mutant were on different chromosomes. G/C to A/T transitions found in these regions were focused on as these were the types of changes expected from the EMS mutagenesis procedure.

3.5.1.1.1 The putative *dis15* lesion is in a gene encoding a eukaryotic ASPARTYL PROTEASE (AT2g28030)

dis15 WGS raw reads assembled to the ~3 MB mapped region of L*er*-0 chromosome 2 were compared with *dis58* WGS sequencing data assembled to L*er*-0 over the same region. Sequence analysis of the two assemblies (mutant cf. L*er*-0 and mutant cf. *dis58*) revealed the presence of eight SNPs showing a G to A transition in the 3 Mb region of *dis15* that were not present in the L*er*-0 or *dis58* genome. Of the eight SNPs identified, three were in open reading frames. One was present in CYTOCHROME P450 encoded by AT2G23190 and the other in a SERINE CARBOXYPEPTIDASE encoded by AT2G22980. Both of these lesions did not change the amino acid sequence encoded. However, the third in AT2G28030 locus caused a non-synonymous amino acid change from phenylalanine to leucine (F20L) in the encoded eukaryotic ASPARTYL PROTEASE family protein.

3.5.1.1.1 The putative *dis58* lesion is in a at4g13495 encoding non-coding RNA and micro-RNA

Compared to *dis15*, *dis58* was mapped to a relatively small 40 kb region of chromosome 4, however instead of sequencing the 40 kb mapped region, the *dis58* WGS sequence was performed because it is a less laborious and time consuming method. Trimmed raw reads of *dis58* WGS data were assembled to a 100 kb region of wild-type (L*er*-0) spanning both sides of the two most closely linked markers (Fig. 3.4.9). The raw reads of *dis15* WGS data were also assembled to the wild type L*er*-0 genome over the same 100 kb region to filter out the background mutations that were present due to natural variations in the sequence of L*er*-0 plants. To further confirm that the lesions identified were true SNPs, the putative SNPs were also checked to confirm their absence in *dis15.* The comparison of both *dis58* and *dis15* raw reads assembled against L*er*-0 revealed a single G to A transition in the AT4G13495 locus of *dis58* that was not present in the *dis15* sequence.

The AT4G13495 locus encodes a non-coding RNA according to TAIR10 annotation. The G to A transition in the *dis58* mutant was found in a region of AT4G13495 annotated as an intron at 1502 bp from the annotated start site of the gene (Fig. 3.5.1A). The SNP in the *dis58* mutant was confirmed by Sanger sequencing of *dis58* and wild-type (Fig. 3.5.1B and C, primers are listed in Appendix 3.5.1). The EST database revealed that the region of AT4G13495 containing the mutation is transcriptionally expressed. To determine the exact size of the transcript, RT-PCR (Reverse transcriptase) was used. According to the EST data, the length of the AT4G13495 RNA fragment was ~945 bp. I was able to amplify ~784 bp of the AT4G13495 sequence from cDNA (Fig. 3.5.1D, primers are listed in Appendix 3.5.1), which contained the site of the *dis58* SNP. The data demonstrated that *dis58* mutation is in a transcribed region of AT4G13495 and not in an intron as annotated.

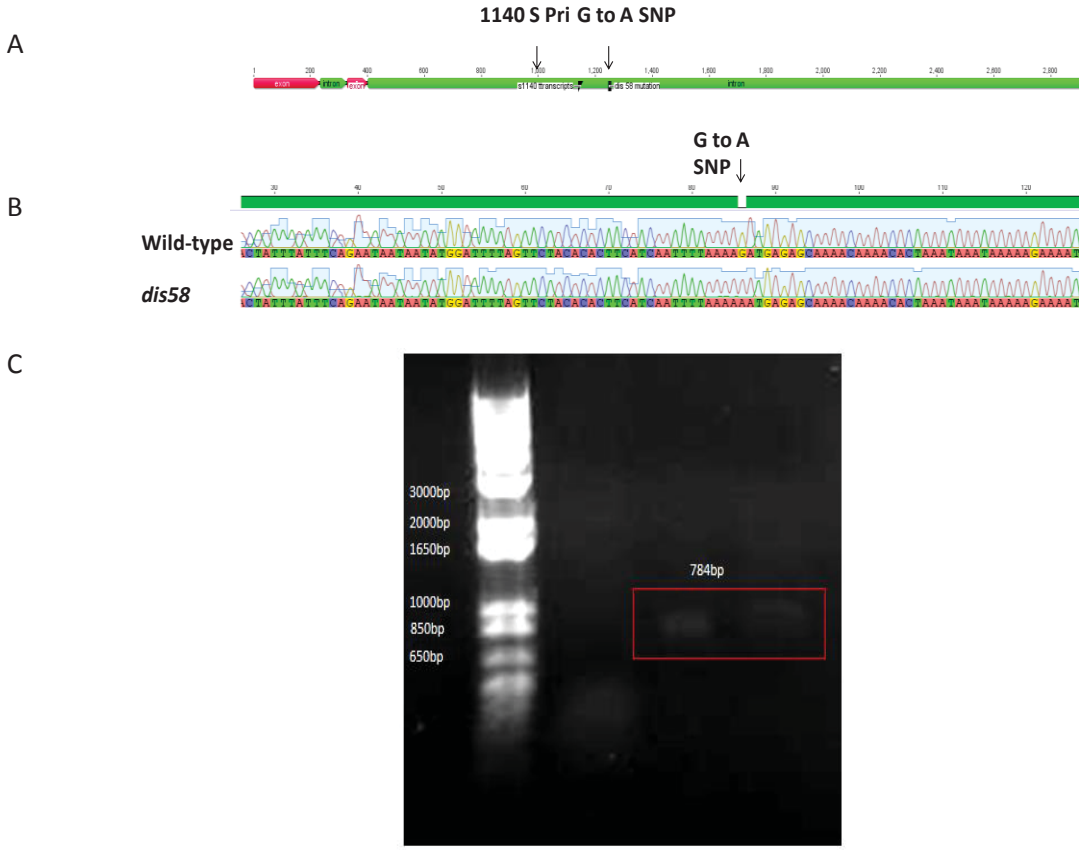

Figure 3.5.1. Confirmation of the *dis58* SNP.

A. AT4G13495 genomic DNA (~3.5 kb) showing site of *dis58* SNP and the 1140s sequencing primer that was used for confirmation of the SNP. B. Traces of wild-type and *dis58* sequences over the site of *dis58* SNP. C. Amplified cDNA containing *dis58* mutation. The arrows in (A) represent primers used for sequencing. The arrow in (B) indicates G to A transition in *dis58*. Red box highlights the fragment amplified by reverse transcriptase PCR.

3.5.1.2 AT4G13495 T-DNA mutant show delayed dark-induced inflorescence senescence

The detached inflorescences of three T-DNA insertion lines of AT4G13495 (SALK 092164.46, SALK 144395 and SALK 139539) were investigated for delayed dark-induced senescence (Fig. 3.5.2A). The detached inflorescences of all three SALK lines showed delayed dark-induced senescence (Fig. 3.5.2B). The SALK 092164.46 line was further characterised. It has a T-DNA insertion in the annotated intron of AT4G13495 at 2000 bp from the annotated start site of the gene (Fig. 3.5.2A). The presence of the T-DNA in this SALK line was confirmed by PCR amplifying a ~500 bp sequence from the genomic DNA of four plants and wild-type (used as a control) with one primer specific for the left border of the T-DNA (LBP) and another one specific for the gene (RP) (Primers are listed in Appendix 3.5.1). To differentiate between the plants that were heterozygote or homozygote for the T-DNA insertion an ~1100 bp PCR fragment was amplified with two gene specific primers (LP and RP, Primers are listed in Appendix 3.5.1) that flanked the T-DNA insertion site. As expected the PCR primer pair the T-DNA (LBP and RP) that was specific for did not amplify ~500 bp product from wild-type control sample, whereas the pair amplified the PCR product from four plants of T-DNA segregating line (Fig 3.5.2C). This confirmed that these four segregating plants were positive for the insertion. The primer pair LP and RP was used to differentiate between homozygous and heterozygous T-DNA plant lines. This pair was able to amplify the PCR product from wild-type control, plant # 3 and 4 but could not amplify the product from plant # 1 and 2. This showed that plant # 1 and 2 are homozygous for the insertion, whereas 3 and 4 are heterozygous (Fig 3.5.2C). Interestingly, all four plants showed delayed inflorescence senescence (Fig. 3.5.2D). This suggests that absence of one allele of the non-coding RNA is sufficient to cause the delayed inflorescence senescence phenotype.

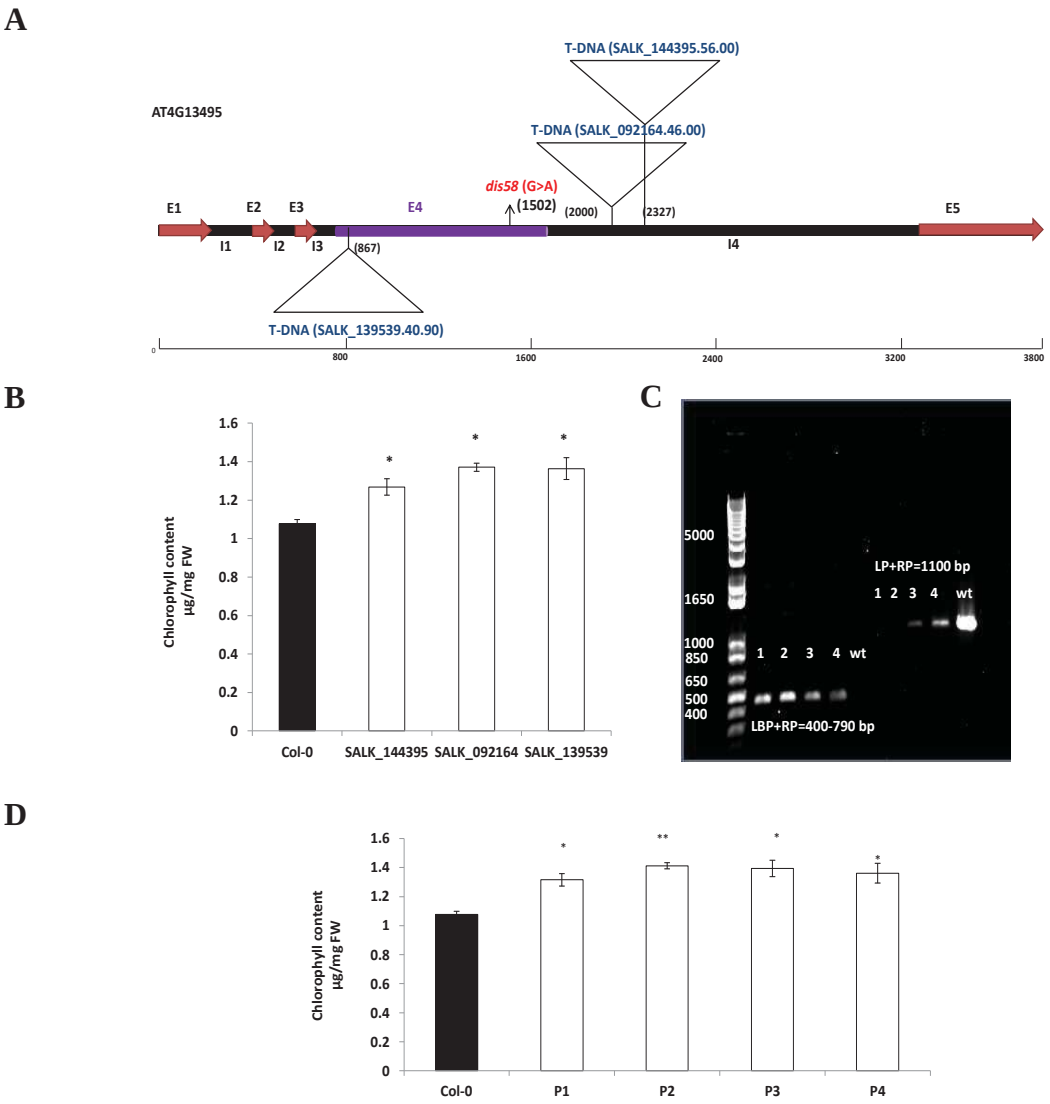

Figure 3.5.2. Molecular and physiological characterization of AT4G13495 T-DNA mutants.

A. Schematic diagram of AT4G13495 in L*er*-0. B. Chlorophyll contents of SALK-lines with T-DNA insertions in AT4G13495. C. Genotyping of segregating T-DNA insertion lines to identify homozygous individuals. D. Chlorophyll contents of segregating plants of SALK 092164.46 and Col-0 (wild-type). Plants were grown in a green house under long day conditions (16 h light and 7 h dark) for 8 weeks. Inflorescences were detached and incubated in the dark for 3 days at 21°C. Red arrows indicate exons, purple line represents EST, black lines represent putative introns, black arrow indicates site of the *dis58* SNP and triangles indicate the sites of T-DNA insertions. I = Intron, E = Exon.

3.5.1.3 Cloning of wild-type *DIS58* 5.6 kb genomic fragment containing the putative *dis58* genetic lesion

To complement the putative lesion in *dis58*, a 5.6 kb genomic fragment encompassing the AT4G13495 gene was cloned. Primers (Primers are listed in Appendix 3.5.1) were used to amplify the 5.6 kb fragment, which consisted of 3558 bp of the AT4G13495 sequence, a 2 kb promoter region and 200 bp of DNA sequence downstream of the 3′ region of AT4G13495 according to The Arabidopsis Information Resource database (http://www.arabidopsis.org/) (Fig. 3.5.3A). To confirm the cloning of the 5.6 kb fragment into pGEM®-T Easy the cloned fragment was digested with *Eco*R1. Based on *in silico* digestion of the L*er*-0 reference sequence, six fragments of sizes 527, 734, 1332, 1527,1561 and 3018 bp were expected (Construct is shown in appendix 3.5.2). However, the bottom two fragments of 734 and 527 were not seen. To clarify whether the correct sequence had been cloned into pGEM®-T Easy, the fragment was sequenced. Sequencing confirmed the presence of the AT4G13495 sequence and on inspection it was found that there was two *Eco*R1 site missing in the cloned sequence which explained why the *in silico* digestion results did not agree with the gel result. This fragment was amplified from L*er*-0 genomic DNA, whereas the *in silico* cloned fragment was from Col-0. When the L*er*-0 fragment was cloned into pGreen0229 (construct is shown in Appendix 3.5.3) and the plasmid digested with *Eco*R1, fragments of 1332, 1561 and 7183 were obtained which agreed with what was expected from the *in silico* digestion.

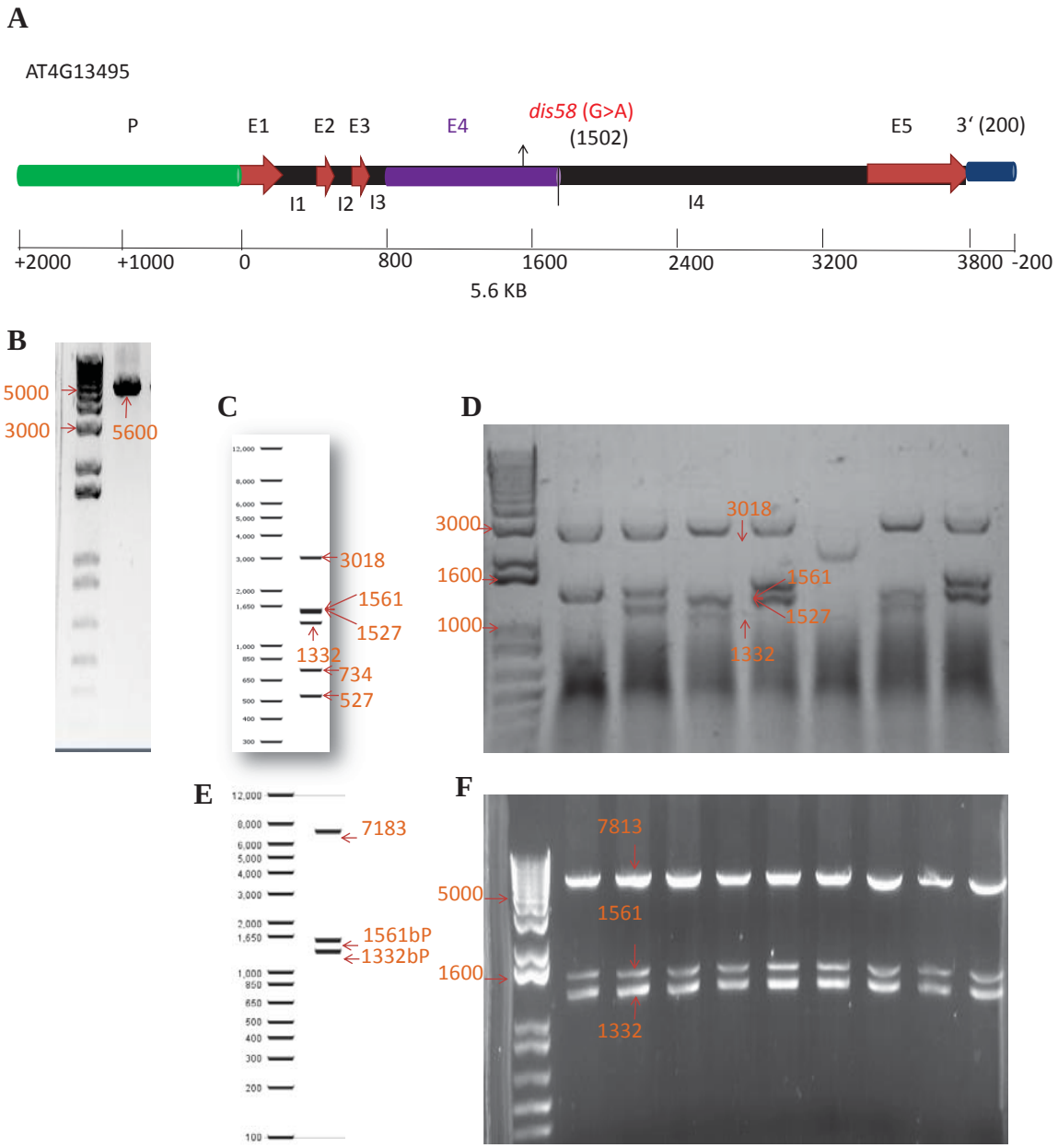

Figure 3.5.3. Cloning of *DIS58*.

A. Schematic presentation of the *DIS58* genomic fragment. B. PCR amplified 5.6 kb fragment of AT4G13495 from L*er*-0. C. *In silico Eco*R1 digestion of positive pGEM T-Easy constructs. D. Screening of positive pGEM T-Easy plasmids by *Eco*R1 restriction digestion. E. *In silico Eco*R1 digestion of positive pGreen0229 construct. F. Screening of positive pGreen0229 constructs by *Eco*R1 restriction digestion. The numbers represent the sizes of the DNA fragments in base pairs. .

3.5.1.4 Genetic complementation of *dis58*

Molecular complementation of *dis58* with the wild-type (L*er*-0) 5.6 kb genomic fragment containing the AT4G13495 gene driven by its native promoter was undertaken to confirm whether the wild type version of the AT4G13495 region would revert the delayed senescence phenotype back to wild type. Of the 14 T0 lines selected on BASTA, 13 showed absence of the *dis58* phenotype (Fig. 3.5.4A). However, the transformed BASTA positive plants showed partial complementation, as inner whorls of detached dark-held inflorescences were greener than the wild-type inflorescences that became completely yellow at day 5 of the incubation (Fig. 3.5.4A). PCR showed that the 13 lines that had the plants showing the intermediate inflorescence senescence type (less senescent than wild type, but more than *dis58*) were positive for the BASTA resistance gene (Fig. 3.5.4B). Thus, the data indicated that *dis58* phenotype is due to defects in function of AT4G13495.

T0 transgenic lines were allowed to self-pollinate and the resulting T1 progeny of four transgenic lines 2, 9, 11 and 15 was further tested for segregation of the *dis58* phenotype. Interestingly, at day 5 of the dark incubation detached immature inflorescences of T2 segregating lines showed three different phenotypes, delayed degreening (like *dis58* mutant), intermediate degreening and complete degreening. The segregating phenotype of *dis58*-complemented plants # 2, 9 and 11 is shown in Fig. 3.5.5. χ^2 analysis shows that the ratio of complete degreening:intermediate degreening:delayed degreening in each line is consistent with a 1:14:1 segregation ratio (Table 3.5.2). This suggests that these transgenic lines each have two independent T-DNA integrations, such that in 1 out of 15 plants no T-DNA is present, resulting in the *dis58* phenotype. Moreover, it suggests that two homozygous T-DNA insertions are required to fully complement the *dis58* phenotype. The reason for this is not clear at the moment, but it could be that the T-DNA insertions are in genomic locations that are relatively low expressed, or that the *DIS58* gene is located in a region that is relatively highly expressed. Nevertheless, the data shows that the *dis58* phenotype can be fully complemented with the wild type *DIS58* construct, providing strong evidence that *DIS58* is AT4G13495.

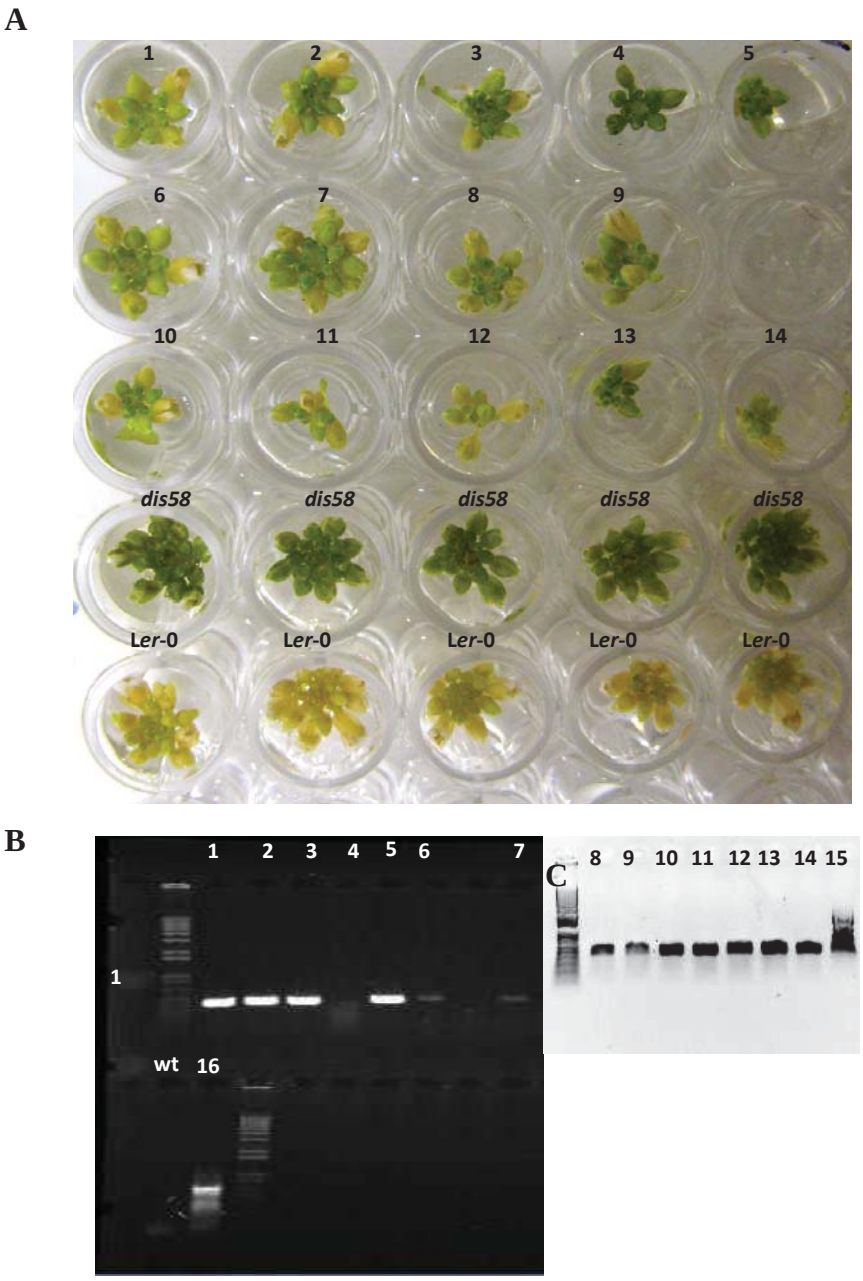

Figure 3.5.4. Genetic complementation of *dis58*.

A. Detached dark-held inflorescences of 14 *dis58* Basta-selected positive plants. B and C. PCR amplification of Basta-resistance gene in *dis58* complemented and wild-type (wt) plants and in the pGreeen0229 plasmid containing the cloned fragment. Numbers from 1 to 14 represent 14 *dis58* complemented plants, numbers 15 and 16 represent pGreen0229 plasmids containing the cloned fragment and wt represents L*er*-0. The 1kb+ DNA ladder is also shown. The photograph of detached dark-held inflorescences were taken at day 5. Plants were grown in long day conditions (16 h light and 8 h dark) for 8 weeks and inflorescences detached for degreening analysis.

Table 3.5.1. Segregation analysis of T2 segregation progeny of *dis58*-complemented plants.

The 1:14:1 ratios of complete, intermediate and delayed degreening were tested and accepted at P≥0.05 based on their calculated χ^2 values. χ^2 values are based on 2 degrees of freedom. The tabulated value is 5.99 at *probability* of 0.05. Plants were grown in long day conditions for 8 weeks (16 h light and 8 h dark) in a green house. The immature inflorescences of F2 individuals were harvested from primary bolts and placed in water at 21°C for at least 8 days. The inflorescence phenotype was examined at day 3, 5 and 8.

T2 lines	# of plants	wild-type	intermediate	mutant	ratio	Calculated χ^2	P values
# 2	32	4	26	2	16:1	1.25	0.723
# 9	55	4	47	4	14:1	0.14	0.84
# 11	61	8	49	4	15:1	0.80	0.9
# 15	61	5	53	3	20:1	0.51	0.1237

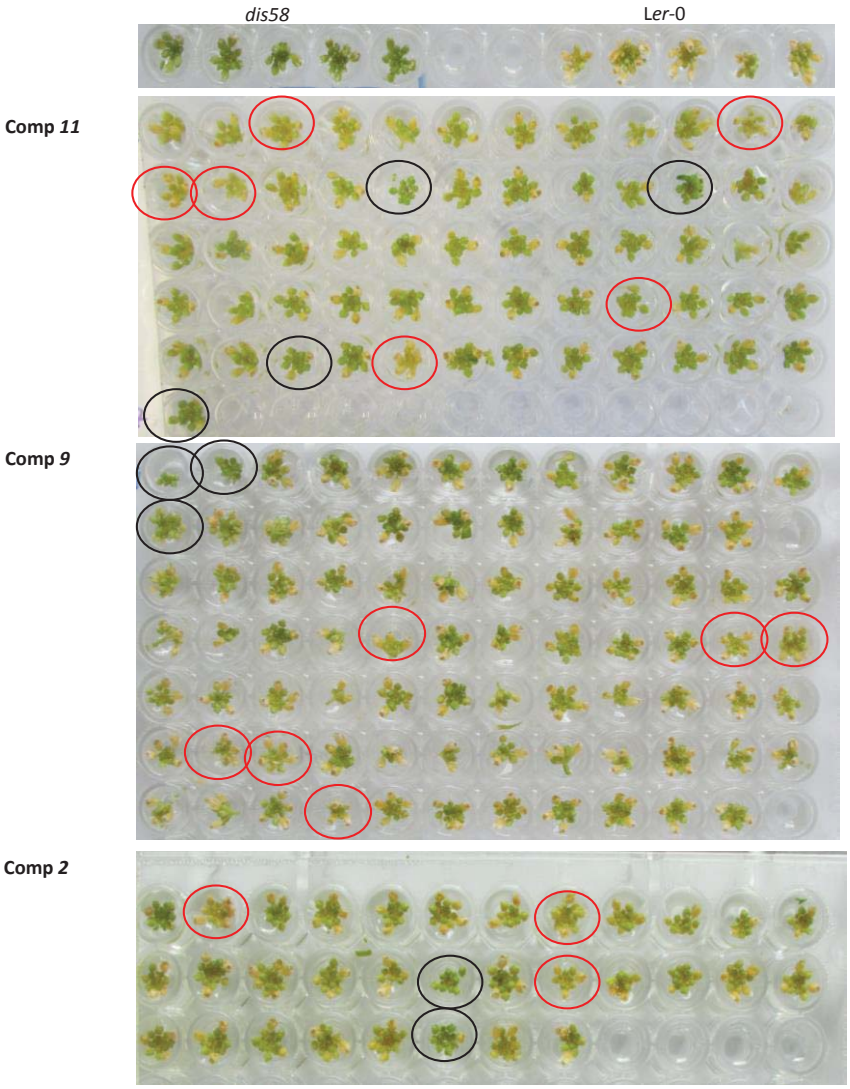

Figure 3.5.5. T2 segregating plants of *dis58*-complemented lines.

A. *dis58*-complemented plant # *11*. B. *dis58*-complemented plant # *9*. C. *dis58*-complemented plant # *2*. The plants were grown in long day conditions (16 h light and 8 h dark) for 8 weeks and inflorescences were detached for senescence analysis. The inflorescences from wild-type potential plants are indicated by red circles and from potential *dis58* mutants are indicated by black circles. All other inflorescences belong to the potential heterozygote plants.

3.5.2 Discussion

HRM-based linkage analysis of SNP markers placed the *dis15* and *58* mutations to chromosome 2 and 4, respectively. To identify the genetic lesions underlying the phenotypes, whole genomes of these mutants were sequenced by high-through put Illumina sequencing technology. The comparison of raw reads of *dis15* and *58* mapped regions to the reference L*er*-0 genome and with each other's genomes revealed eight G to A transitions in ~3 MB *dis15* and one SNP in ~100 kb *dis58* assembled regions. In *dis15* the SNP that caused non-synonymous amino acid change was in eukaryotic aspartyl protease (encoded by AT2G28030 locus). Interestingly, the *dis58* SNP was in non-coding RNA encoded by AT4G13495 locus. The *dis58* transformation with a ~5.6 kb DNA fragment of wild-type non-coding RNA complemented the phenotype suggesting the identified ncRNA regulates inflorescence senescence in Arabidopsis.

Combination of conventional and deep genome sequencing methods identifies potential *dis* mutations

Map-based cloning has frequently been used to identify genetic lesions underlying the altered plant phenotypes (Jander et al., 2002). Before the arrival of next generation sequencing technologies, the candidate genes identified by MAP-based cloning were sequenced one by one using Sanger sequencing until the genetic lesion causing the phenotype was identified (Jander et al., 2002). This process was time consuming and labor intensive. Next generation sequencing (NGS) technologies have replaced this laborious Sanger-based sequencing approach (Sturre et al., 2009; Schneeberger and Weigel, 2011). The quality and depth of the sequencing data obtained in single run by using NGS technology has enhanced the speed to sequence the region mapped for underlying mutations. However, this high-through put sequencing approach still requires PCR-amplification of the mapped regions often using overlapping amplicons of ~10 kb and can miss the mutations due to problems related to amplifying the region or PCR-based sequencing errors. Therefore, PCR-based genome sequencing step was omitted and *dis58* and *15* whole genomes were sequenced and integrated in the region the HRM-PCR had indicated to contain the causal SNPs. This approach has been used by Laitinen et al, (2010) for identifying a spontaneous mutation in a wild Arabidopsis accession Krotzenburg (Kro-0;CS1301). The authors narrowed down the

dwarf phenotype of the plant to 530 kb interval on chromosome 1 by using 1,900 F2 plants. They identified the mutation by comparing deep sequencing data of the mutant genome with the parental line within the 530 kb interval using WGS.

In the future, with the rapid advances in NGS technologies combined with their lower cost, the initial mapping procedures will likely be completely circumvented with the NGS technologies themselves being solely used to do the mapping. For example, bulked segregant analysis (Schneeberger et al., 2009; Cuperus et al., 2010) and NIKS (needle in the *k*-stack) (Nordström et al., 2013) were successfully used to identify a genetic lesion causing an altered plant phenotype in Arabidopsis. Bulk-segregant analysis identifies the mutation by aligning the pooled recombinant genomes obtained through deep sequencing to the reference genome (Schneeberger et al., 2009; Cuperus et al., 2010). Interestingly, NIKS identifies the genetic lesions based on homozygous differences between highly related genomes without the need of a reference genome. Thus, these advanced technologies are providing a fast and accurate way to identify the genetic lesions causing the altered plant phenotype by eliminating the requirement for outcrossing, reference genome and genetic maps.

DIS15 is a putative pepsin-like aspartyl protease family protein

The process of proteolysis controls abundance, trafficking and activities of cellular proteins (Van der Hoorn et al., 2004). Hence, it regulates many aspects of plant growth and development including disease resistance, starvation, stress response and senescence (Hortensteiner and Feller, 2002; Coupe et al., 2003; Schwechheimer and Schwager, 2004; Eason et al., 2005). The *dis15* SNP causes a non-synonymous amino acid change in a protein belonging to a pepsin-like aspartyl protease family of eukaryotes (Beers et al., 2004). Although the role of these proteases in plant growth and development is not clear yet, certain findings suggest their involvement in plant disease resistance and cell death (Beers et al., 2004). Here the finding that *dis15* has a SNP causing a non-synonymous change in an aspartyl protease suggests the role of this uncharacterized protein in inflorescence senescence. However, to confirm this, the *dis15* mutant phenotype needs to be complemented by the wild-type gene.

***DIS58* encodes a non-coding RNA**

The genetic lesion causing the *dis58* delayed inflorescence senescence phenotype was identified in a sequence that was annotated as an intron of gene at locus AT4G13495 that encodes non-coding RNA (ncRNA) of un-known function. ncRNA genes encode RNA molecules rather than producing proteins (Eddy, 2001). Many ncRNA have mRNA-like characteristics such as the presence of a poly A tail and splice variants (Eddy, 2001). They are of two types, small ncRNA (~22 nucleotides) and long ncRNA (> 200 nucleotides) (Brosnan and Voinnet, 2009).

ncRNA transcriptionally and post-transcriptionally regulates the expression of many genes under various biotic and abiotic stresses. Often this happens by the stresses reducing the expression of the ncRNAs to relieve suppression of the stress-related genes. For example, in the absence of stress miR398 keeps the activity of the superoxide (O_2^-) scavenging proteins CU-ZN SUPEROXIDE DISMUTASE (CSD1) and CSD2 low by post-transcriptionally degrading their transcripts (Sunkar et al., 2006). However, imposition of stress causes transcript abundance of miR398 to decrease. This in turn prevents the ncRNA from degrading the *CSD1* and *2* transcripts therefore allowing their proteins to accumulate to scavenge the higher amounts of superoxides produced by the stress, which is vital for plant resistance. Other examples of ncRNA that are suppressed by stress are *CR20* ncRNA (Teramoto et al., 1995) and *Mt4* in medicago (Burleigh and Harrison, 1998).

Thus, *DIS58* non-coding RNA may be involved in regulating the expression of genes causing inflorescence senescence. It is likely that *DIS58* is a positive regulator of inflorescence senescence as complementation of *dis58* mutants with wild type *DIS58* caused enhanced inflorescence degreening. The significance of non coding genes during senescence is further supported by a recent finding indicating that EIN3 causes developmental leaf senescence by directly supressing transcription of *miR164* (Li et al., 2013).

The role of this *DIS58* ncRNA during inflorescence senescence is further independently confirmed by the delayed senescence phenotype of detached dark-held inflorescences of AT4G13495 T-DNA lines (Fig. 3.5.2). Segregating plants of the TDNA lines that were either heterozygous or homozygous for the T-DNA line showed delayed inflorescence senescence phenotype. This is unexpected as *dis58* is a recessive mutation and

to delay the inflorescence senescence in T-DNA knock out both allele of the gene should be knockout. Thus, the only T-DNA plants that should show delayed inflorescence senescence would be homozygous for the insertion. This can be explained as different alleles of the same gene can respond differently. For example, both recessive and dominant alleles of the *ACS5* genes were found by Vogel et al., (1998). The loss of function recessive allele (*cin5*) in *ACS5* resulted in disruption of cytokinin-induced ethylene biosynthesis, whereas the dominant allele (*eto2*) caused ethylene over production.

The study shows that *DIS58* is a novel ncRNA regulates senescence of detached dark-held inflorescences in Arabidopsis. This discovery has provided a new direction to understand RNA-guided regulatory mechanisms during inflorescence senescence.

Blank page

3.6 Defects in homeotic genes cause altered senescence of dark-held detached Arabidopsis inflorescences

Abstract

A homeotic delayed inflorescence senescence mutant was identified in the EMS-based inflorescence senescence screen (section 3.3.1.2). The mutant was sterile due to homeotic conversion of stamens into petals and carpels into a new flower to give a sepal-petal-petal phenotype. This phenotype was similar to the *ag-1* mutant (Bowman et al., 1999). The sterility of the mutant prevented identification of the genetic lesion causing the *agamous-like* (*agl*) phenotype. However, its morphological similarity with *ag-1* led me to investigate whether the detached inflorescences of *ag-1* and other homeotic mutants would also show altered senescence when held in the dark. The detached dark-held inflorescences of all tested homeotic mutants, *leafy-4* (*lfy-4)*, *leafy-5* (*lfy-5*), *apetala1-1* (*ap1-1)*, *apetala2-1* (*ap2-1*), *apetala3* (*ap3*), *pistillata* (*pi*), *agamous-1* (*ag-1*), *sepallata1/sepallata2/sepallata3* (*sep1/sep2/sep3*) and *early extra petals* (*eep*), showed altered timing of senescence. This suggests that the activity of homeotic genes or the consequence of their activity regulates in part energy deprivation-driven senescence response.

3.6.0 Introduction

The ABCDE conceptual model of flower development elaborates how floral homeotic genes interact with each other to specify floral organ identity (Theißen, 2001) (Fig. 3.6.1). Floral homeotic genes are categorised into five functional classes: A (e.g., *APETALA1* and *APETALA2*), B (e.g., *APETALA3* and *PISTILLATA*), C (e.g., *AGAMOUS*), D (e.g., *FLORAL-BINDING PROTEIN 7* and *FBP11*) and E (e.g., *SEPALLATA1*, *SEPALLATA2*, *SEPALLATA3* and *SEPALLATA4*) (Pelaz et al., 2000; Honma and Goto, 2001; Theißen, 2001; Smaczniak et al., 2012). The genes in each class determine the identities of the four whorls of a flower in an overlapping manner. To determine organ identity, the homeotic proteins of each class form higher-order complexes with each other. For example, the class A protein AP1 specifies sepal identity by making a complex (AP1-AP1-UNKNOWN-UNKNOWN) with other unknown transcription factors. Similarly, the C AGAMOUS (AG) and E SEPALLATA (SEP3) class proteins determine carpel identity by making a complex AG-AG-SEP3-SEP3. Petals and stamens are initiated by interactions of A and C proteins together with B including APETALA (AP3) and PISILLATA (PI) and E class proteins (Honma and Goto, 2001; Immink et al., 2010). Petals are specified when APETALA1 (AP1) interacts with AP3-PI hetero-dimers and SEP3 to make an AP1-AP3-PI-SEP complex. Stamens are determined when AP3-PI hetero-dimers interact with both SEP3 and AG homo-dimers to give a PI-AP3-AG-SEP complex (Theißen, 2001).

In addition to interacting synergistically, the organ identity genes also act antagonistically. For example, A class proteins suppress the activities of C class in whorls 1 and 2, whereas C class proteins antagonize the activities of A class in whorls 3 and 4. Hence, a cascade of floral homeotic genes works in a concert to regulate the identities of four whorls of a flower (Theißen, 2001).

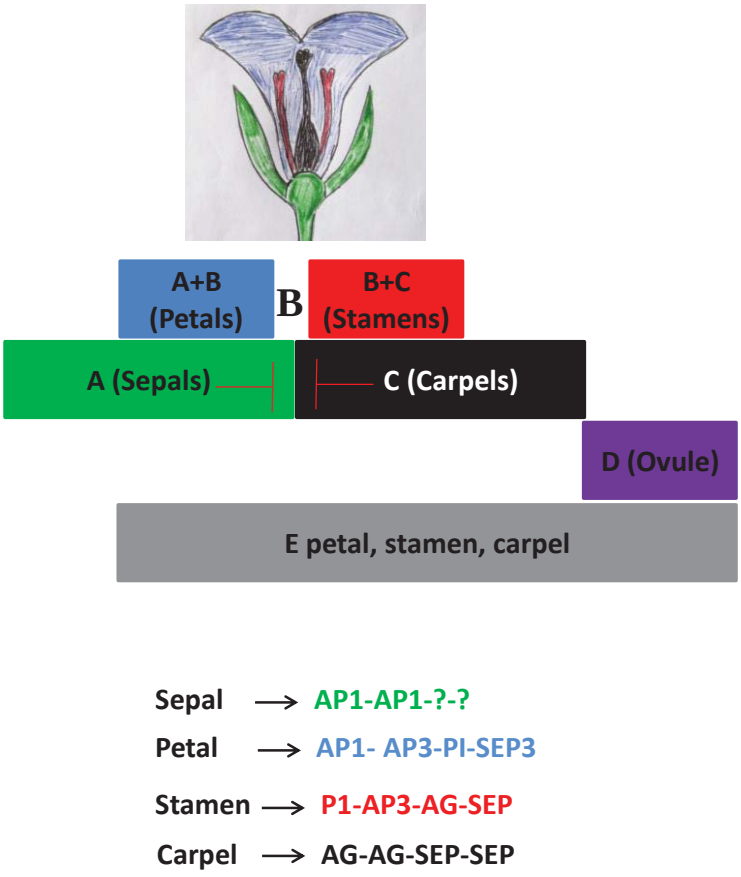

Figure 3.6.1. ABCDE conceptual model of flower development.

The model adapted from Theißen, (2001) explains how the five classes of homeotic genes A, B, C, D and E specify floral organ identity in an overlapping manner**.** A and unknown proteins (indicated by a question mark in the figure) specify sepals in whorl 1; three classes A, B and E determine petal identity in whorl 2; three classes B, C and E specify stamen identity in whorl 3; and two classes C and E specify carpel identity in whorl 4. Class A represses activities of class C in whorls 1 and 2 and C suppresses the activity of A in whorls 3 and 4. Antagonistic interactions are indicated by barred lines and hyphen indicates heterodimer formation. ? symbolises unknown proteins.

Defects in the functions of organ identity genes cause homeotic abnormalities in developmental patterns of the floral organs (Irish and Sussex, 1990). The abnormalities are the replacement of a normal floral organ with another floral organ (Weigel and Meyerowitz, 1993). For example, complete loss of A activity in *ap1* and *ap2* mutants causes homeotic transformation of sepals into leaf-like structures or carpels in the first whorl and of petals into stamens in the second whorl. In B class mutants (e.g., *ap3* and *pi*), petals are converted into sepals and stamens into carpels. The loss of C activity (e.g., in *ag-1*) transforms stamens into petals in the third whorl and carpels into sepals in the fourth whorl of a flower (Theißen, 2001). The main function of the A class proteins is to establish the floral meristem identity and repress AG in the outer whorls, which results in perianth development (Litt, 2007).

As part of my study to identify delayed dark-induced inflorescence senescence mutants, I found a sterile mutant with floral homeotic abnormalities. The identified mutant had a sepal-petal-petal flower phenotype similar to the *ag-1* mutant first described by Bowman et al., (1989). The sterility of the mutant meant its genetic lesion could not be identified. I investigated the role of *AG* and other homeotic genes during senescence of detached dark-held inflorescences by using floral homeotic mutants. This mutant-based genetic approach was used to specifically remove or alter particular floral structures in the florets of the inflorescences to determine whether: a) the absence of particular floral organs, b) the replacement of organs for another type, or c) the underlying genetic response was the cause of the delayed senescence.

3.6.1 Results

3.6.1.1 An *agamous-like* delayed inflorescence senescence mutant was identified from an EMS-based inflorescence senescence screen

Screening detached inflorescences of seedlings from an EMS-mutagenized population of Arabidopsis seeds (Chapter. 3.3) for delayed senescence led to the identification of a sterile mutant that resembled the *ag-1* mutant. Flowers of the identified mutant showed a sepal-petal-petal mosaic phenotype (Fig. 3.6.2C) in contrast to the wild-type (L*er*-0) flower which has sepals, petals, stamens and two fused carpels (Fig. 3.6.2A). Although the sterility of the *agamous-like* (*agl*) mutant prevented further work on it, I analyzed other floral homeotic mutants as part of trying to understand the mechanism behind the senescence delay of the *agl* mutant.

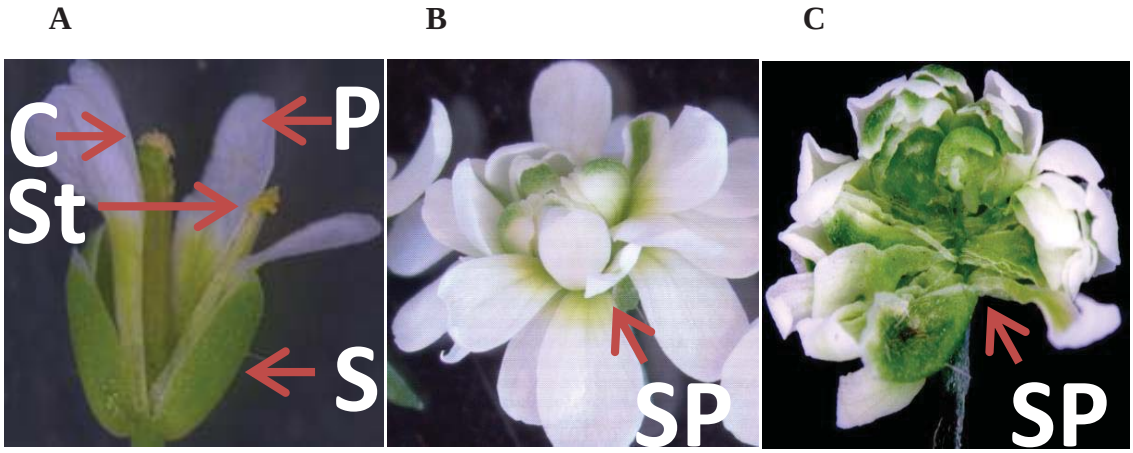

Figure 3.6.2. Wild-type (L*er*-0), *agamous-like* and *ag-1* flower.

A. Wild type (L*er*-0) flower. B. *ag-1* flower. C. *agamous-like* flower. Plants were grown in long day conditions (16 h light and 8 h dark) for 8 weeks in a green house and the flowers were detached and photographed. The arrows indicate sepals (S), petals (P), stamens (St), carpel (C) and sepal-petal (SP) mosaic.

3.6.1.2 Homeotic mutants show delayed or accelerated dark-induced senescence of detached inflorescences

Immature detached inflorescences of floral homeotic mutants (Table. 3.6.1) were incubated in the dark for up to eight days. Interestingly, the inflorescences of all the homeotic mutants, except *early extra petal* (*eep*), degreened slower than wild-type (Fig. 3.6.3). The detached inflorescences of *eep*, by contrast, were completely yellow at day 3 of dark incubation. The chlorophyll data demonstrated that the L*er*-0 wild-type inflorescences had lost ~77% of their initial chlorophyll content at day 3 of dark incubation (Fig. 3.6.4A). The homeotic mutants *lfy-4*(intermediate-allele), *lfy-5*(weak-allele), *ap1-1*(strong-allele), *ap2-1* (weak-allele), *ap3*, *pi* and *ag-1* in the L*er*-0 background had lost ~64, 60, 64, 67, 58, 73% and 30% of their chlorophyll respectively over this same time period. At day 5 of the dark treatment, the detached inflorescences of the *ag-1* mutant had retained ~30% of its chlorophyll content. All other mutants had retained ~10%, in contrast to wild-type, which had retained only ~5% of its initial chlorophyll content (Fig. 3.6.4A). Another homeotic mutant examined was the *sep1/sep2/sep3* triple mutant, which had only sepals in its flower. The mutant was in the Col-0 background. The *sep1/sep2/sep3* detached dark-held inflorescence retained ~23% more chlorophyll content than wild-type Col-0 at day 3 of dark incubation and ~30% more at day 5 (Fig. 3.6.4B).

Table 3.6.1. Inflorescence senescence phenotype of floral homeotic mutants.

The inflorescences were detached and placed in the dark and their senescence phenotype determined based on the loss of chlorophyll content compared to wild-type at day 5. Plants were grown in long day conditions (16 h light and 8 h dark) for 8 weeks in a green house. S = sepals, P = petals, St = stamens, C = carpels, L = leaves, P-St = petal-stamen mosaic.

Mutants	**Flower phenotype**	**Homeotic conversions**	**Senescence**
leafy-5 (*lfy-5*)	Lacks sepals and petals and stamens are reduced (Weak-allele)	S into L or C P into St or P-St	delayed
leafy-4 (*lfy-4*)	Lacks sepals and petals and stamens are reduced (Intermediate-allele)	S into L or C P into St or P-St	delayed
apetala1-1 (*ap1-1*)	Lacks petals and sepals Strong-allele	S into L or C P into St or P-St	delayed
Apetala2-1 (*ap2-1*)	Lacks petals, sepals are converted in to bract-leaf (Weak-allele)	S into L or C P into St or P-St	delayed
apetala3-1 (*ap3-1*)	Lacks petals and stamens	P into S St into C	delayed
pistillata (*pi*)	Lacks petals and stamens	P into S St into C	delayed
agamous-1 (ag-1)	Lacks stamens and carpels	St into P C into S	delayed
sepellata1/sepellata2/sepellata3 (*sep1/sep2/sep3*)	Lacks petals, stamens and carpel	P into S St into S C into S	delayed
extra early petals (*eep*)	Early extra petals	No conversions	accelerated

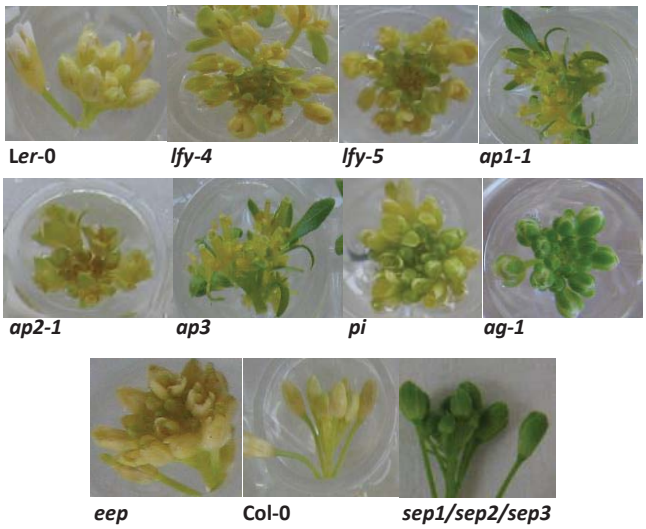

Figure 3.6.3. Detached dark-held immature inflorescences of L*er*-0, Col-0, *lfy-4*, *lfy-5*, *ap1-1*, *ap2-1*, *ap3*, *pi*, *ag-1*, *sep1/sep2/sep3* and *eep*.

Plants were grown in long day conditions for 8 weeks (16 h light and 8 h dark) in a green house. The inflorescences were subsequently detached from primary bolts and their cut ends placed in water for eight days at 21°C. All the mutants are in L*er*-0 background, except the *sep1/sep2/sep3* triple mutant, which is in Col-0 background. The photograph of *eep* was taken at day 3 of the dark incubation, whereas for other homeotic mutants, L*er*-0 and Col-0 photographs were taken at day 5.

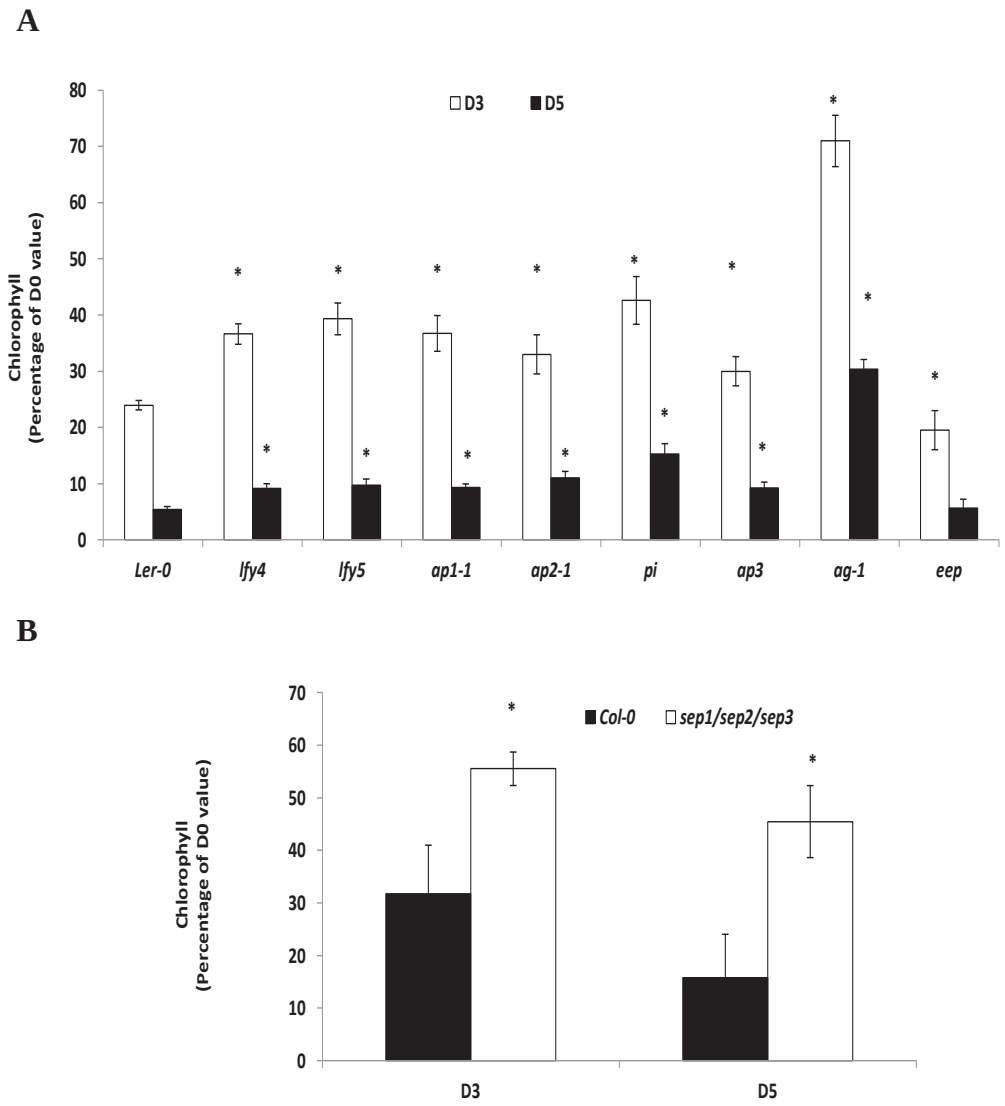

Figure 3.6.4. Inflorescence chlorophyll content of the floral homeotic mutants.

A. Chlorophyll content of wild-type (L*er*-0), *lfy4*, *lfy5*, *ap1-1*, *ap2-1*, *pi*, *ag-1* and *eep* at day 3 and 5 of the dark incubation. B. Chlorophyll content of wild-type (Col-0) and *sep1/sep2/sep3* at day 3 and 5 of the dark incubation. The inflorescences were detached from primary bolts of plants that were grown in long day conditions for 8 weeks (16 h light and 8 h dark) in a green house. Any opened florets were removed and their cut ends placed in water for 5 days at 21°C. Chlorophyll content is expressed as percentage of day 0 value. The error bars indicate standard errors of 6 biological replicates. Statistically significant differences in percentage chlorophyll content values between the wild-types and mutants using Student's *t*-test are indicated (*$P < 0.05$).

3.6.3 Discussion

A sterile mutant with a delayed inflorescence senescence phenotype was identified from an EMS-mutagenized Arabidopsis (Landsberg *erecta)* plant population (section 3.3.1.2). The mutant had homeotic conversion of stamens into petals and carpels into a new flower to give a repeating pattern of sepal-petal-petal, which was similar to the *ag-1* mutant. To determine whether the delayed senescence phenotype was specific for the *ag-1* type phenotype or whether it was simply due to sterility or loss of particular organ structures I tested a range of homeotic mutants in the floral senescence system. The detached dark-held inflorescences of selected homeotic mutants showed delayed senescence suggesting that homeotic genes regulate dark-induced senescence of detached immature Arabidopsis inflorescences.

Lack of A class activity may regulate inflorescence senescence by organogenesis or by regulating senescence genes

Detached dark-held inflorescences of *lfy-5* and *lfy-4* showed delayed senescence (Fig. 3.6.3 and 3.6.4). LEAFY (LFY) is a positive regulator of *AG* expression (Busch et al., 1999; Moyroud et al., 2011; Winter et al., 2011). Therefore, the delayed senescence observed in the *lfy* mutants may be due to their lowered AG content in the inflorescences. It should be noted that the delay in *lfy-5* and *lfy-4* is not as strong as that seen in *ag-1*. This may be explained by these mutants not completely abolishing AG activity in the central portion of the flower (Weigel and Meyerowitz, 1993). This has been attributed to functional redundancy among LFY and WUSCHEL (Lohmann et al., 2001) in positively regulating *AG* expression. Alternatively, the delayed inflorescence senescence phenotype of the *lfy* mutants could be due to conversion of sepals into leaf-like structures as detached dark-held leaves lose their chlorophyll content more slowly than the inflorescences (see chapter 3.3, Fig. 3.3.7 and 3.3.8).

Detached dark-held inflorescences of *ap1-1* and *ap2-1* showed delayed senescence (Fig. 3.6.3 and 3.6.4). AP1 and AP2 are negative regulators of AG activity in the first two whorls of the flower (Wollmann et al., 2010). Thus, if decreased AG activity is causing the delayed inflorescence senescence then increased AG activity in *ap1* and *ap2*

mutants would result in accelerated and not the observed delayed inflorescence senescence. Similar as described above for *lfy* mutants, this discrepancy may be explained by the sepals in the *ap1-1* and *ap2-1* mutants being converted to leaves, which we have found to show a slower loss of chlorophyll than sepals when held in the dark (Fig. 3.3.7 and 3.3.8).

LFY, *AP1* and *AP2* are meristem identity genes as absence of their activity results in partial or complete reversion of the flower meristem into an inflorescence meristem (Weigel and Nilsson, 1995; Yanofsky, 1995; Liljegren et al., 1999). Thus, it can be hypothesized that delayed senescence of detached dark-held inflorescences of the *lfy* and *apetala* mutants is maybe due to increased cytokinin content that presumably is associated with transformation of the flower meristem into multiple meristematic regions. Furthermore, it has been demonstrated that WUSCHEL (a positive regulator of *AG*) directly represses the transcription of *ARABIDOPSIS RESPONSE REGULATOR* genes (*ARR5*, *ARR6*, *ARR7* and *ARR15*) (Leibfried et al., 2005) indicating the regulation of senescence inhibiting hormone cytokinin by homeotic genes. *ARABIDOPSIS RESPONSE REGULATOR* genes act in the negative-feedback loop of cytokinin signalling (Leibfried et al., 2005). The role of cytokinins as a negative regulator of senescence has been documented by many molecular and genetic studies (Jibran et al., 2013). For example, exogenously applied dihydrozeatin (cytokinin) caused delayed senescence in cut carnation flowers (Bosse and Van Staden, 1989). Furthermore, the senescence specific expression of *IPT* (*ISOPENTENYL TRANSFERASE*), a gene involved in cytokinin biosynthesis, resulted in delayed leaf senescence in transgenic Arabidopsis plants (Gan and Amasino, 1995). Thus, delayed dark-induced senescence of detached *lfy-4*, *lfy-5*, *ap1-1* and *ap2-1* inflorescences could be due to higher cytokinin contents in their meristematic regions. However, additional experiments are required to test this hypothesis.

Lack of B class activity may regulate inflorescence senescence by organogenesis or by regulating senescence genes

Detached dark-held inflorescences of the *ap3* and *pi* mutants showed delayed senescence (Fig. 3.6.3 and 3.6.4). *AP3* and *PI* hetero-dimers (AP3/PI) interact with *AP1* homo-dimers to specify petal identities and with *AG* homo-dimers to specify stamens identities (Riechmann et al., 1996). *AP3* and *P1* loss-of-function mutants have carpeloid

organs instead of petals and sepals instead of stamens (Bowman et al., 1989; Hill and Lord, 1989). Tian et al., (1995) reported that physically removing stamens from immature broccoli florets delayed senescence of the broccoli heads. This would be consistent with the delayed senescence of *ap3* and *pi* that lack stamens. Interestingly, it was found that *SENESCENCE-ASSOCIATED1* (*SEN1*) and two senescence-associated genes encoding lipases were down-regulated in *pi-1* and *ap3-3* loss-of-function mutants (Oh et al., 1996; Wagstaff et al., 2002; Zik and Irish, 2003). This suggests that AP3 and PI might be involved in regulating senescence-associated genes. Furthermore, expression of an Arabidopsis NAC gene called *NAP* (*ANAC029*) was directly activated by a heterodimer of the APETALA 3 and PISTILLATA proteins (Zik and Irish, 2003). ANAC029 regulates leaf senescence in Arabidopsis (Guo et al., 2006). Thus, taken together it is hypothesised that AP3 and PI may control dark-induced inflorescence senescence by regulating senescence genes.

Lack of C activity causes delayed senescence of detached dark-held inflorescences

Detached dark-held inflorescences of the *ag-1* mutant showed delayed senescence (Fig. 3.6.3 and 3.6.4). The role of AG in regulating sepal senescence is consistent with role of other *AGMOUS-LIKE* genes in regulating perianth senescence. For instance, Fernandez et al., (2000) demonstrated that overexpression of *AGL15* resulted in delayed sepal and petal senescence as well as transition to flowering and fruit maturation. Similarly, it was found that increased activity of *AGL42* (*AGAMOUS-LIKE 42*) resulted in an ethylene-mediated delay in sepal senescence and perianth abscission (Chen et al., 2011). Interestingly, decreased AG and increased AGL15 and AGL42 activities caused the delayed senescence. Consistent with this I found that detached *ag-1* inflorescences showed ~7-fold increase in transcript abundance of *AGL42* and ~2-fold increase in transcript abundance of *AGL15* (data not shown). Thus, AG may be causing the delayed developmental sepal and dark-induced inflorescence senescence by interacting with these homeotic genes.

Lack of E class activity causes delayed senescence of detached dark-held inflorescences

Detached dark-held *sep1/sep2/sep3* triple mutant inflorescences showed delayed senescence (Fig. 3.6.3 and 3.6.4). *SEPALLATA1 (AGL2), SEPALLATA2 (AGL4)* and *SEPALLATA3 (AGL9)* are involved in specifying floral meristem and organ identities (Pelaz et al., 2000; Favaro et al., 2003). SEP1 (AGL2), SEP2 (AGL4) and SEP3 (AGL9) redundantly regulate the expression of target genes by making ternary complexes with other MADS-box transcription factors including *AP3*, *PI* and *AG* (Honma and Goto, 2001; Jack, 2004). The *sep1/sep2/sep3* triple mutant showed sepals in all four whorls of the flower indicating that these genes are involved in determining petals, stamens and carpel identities. Interestingly, the phenotype of the *sep1/sep2/sep3* triple mutant is similar to the phenotype of the *ap3/ag* and *pi/ag* double mutants (Pelaz et al., 2000). This indicates that in *sep1/sep2/sep3* mutants floral homeotic B and C proteins are not working, although these genes are not required for the initial expression of B and C class genes (Pelaz et al., 2000). Hence, the delayed inflorescence senescence phenotype of the *sep1*/*sep2*/*sep3* triple mutant could be due to decreased activity of both B and C class genes.

The *eep* mutant has accelerated inflorescence senescence due to increased levels of CUC1 and CUC2

In contrast to other homeotic mutants, the *eep* mutant showed accelerated inflorescence senescence (Fig. 3.6.3 and 3.6.4). The mutant has increased transcript abundance of *CUC1* and *CUC2* (*CUP SHAPED COTYLEDON*), which is due to decreased levels of *miR164c,* a repressor of these genes (Olsen et al., 2005). CUC1 and CUC2 positively regulate the expression of NAC transcription factors including *NAC1*, *NAC80* and *NAC100*. Interestingly, Kim et al., (2009) demonstrated that *ORE1*/*NAC092* that positively regulates leaf senescence is repressed by miR164. Therefore, it is more likely that instead of presence of extra petals, the increased levels of the NAC genes, particularly *NAC092* is the cause of accelerated inflorescence senescence in *eep* inflorescences.

The chlorophyll analysis of detached dark-held inflorescences in which different floral organs were genetically replaced by other organs suggests that absence (e.g., stamens

and carpels in the *ag-1*), presence (e.g., extra petals in *eep*), or replacement of particular flower organs (e.g., sepals into leaves in *ap1-1*, *ap2-1*, *lfy-4* and *lfy-5*) may not be involved in regulating the programme. Furthermore, the regulation of senescence associated genes e.g., *NAP* (ANAC029) by AP3-PI heterodimer (Zik and Irish, 2003) and *ARR*s by WUSCHEL (Leibfried et al., 2005) suggests that floral homeotic genes control inflorescence senescence directly by regulating genes involved in the regulation of senescence.

Blank page

3.7 AGAMOUS causes developmental sepal senescence and abscission by regulating JA biosynthesis

Abstract

Floral homeotic genes determine inflorescence, flower and floral organ meristem identities. Several floral homeotic mutants show *in planta* delayed sepal senescence and perianth abscission suggesting an additional role for the homeotic genes in controlling senescence processes (chapter 3.6). A homeotic *ag-like* EMS mutant that was delayed in dark-induced inflorescence senescence was found in a mutagenized Arabidopsis (L*er*-0) plant population (chapter 3.6). To investigate the basis of this delay we used the *ag-1* mutant. The *ag-1* mutant showed a delay in both developmentally-induced sepal senescence and abscission and dark-induced inflorescence senescence. The *ag-1* inflorescences, like wild-type (Landsberg *erecta*), showed accelerated degreening when treated with ACC, MeJA, ethrel and ABA suggesting that the delayed senescence was not caused by defects in ethylene, jasmonate or ABA signalling. To determine whether the delayed senescence was caused by reduced synthesis of the hormones, endogenous concentrations of ACC, ethylene, JA, ABA and SA were measured in the freshly detached sepals and whole inflorescences. Compared to wild-type, *ag-1* tissues had trace amount of JA but otherwise there was no significant difference in concentrations of ACC, ethylene, ABA and SA. Although the *ag-1* mutant was almost devoid of JA, the JA deficient mutants, *dde2* and *dad1*, did not show delayed senescence of detached dark-held inflorescences. Interestingly, similar to *ag-1*, *dde2* showed delayed developmental sepal senescence and abscission. Furthermore, exogenously applied MeJA to the *ag-1* plant accelerated sepal yellowing, abscission and flower opening. Taken together the data suggests that reduced JA in the *ag-1* detached dark-held inflorescences is not the cause of the delayed senescence but is the cause of the delayed *in planta* sepal senescence.

.

3.7.0 Introduction

Increasing amounts of data suggest that floral homeotic proteins not only regulate various aspects of flower development, but also control other plant growth and developmental processes including the timing of senescence (Fernandez et al., 2000; Breeding et al., 2011; Chen et al., 2011; Zheng et al., 2013). For example, *AGAMOUS LIKE 15* (*AGL15*) was found to regulate somatic embryogenesis, sepal senescence and perianth abscission in Arabidopsis (Fernandez et al., 2000; Zheng et al., 2013). Chen et al., (2011) showed that ectopically expressed *AGAMOUS-LIKE 42* (*AGL42*) delayed flower senescence in transgenic Arabidopsis plants by suppressing components of the ethylene signalling pathway. Furthermore, transgenic Arabidopsis plants with increased activity of *NTAG1* (*CHINESE NARCISSUS AGAMOUS HOMOLOGUE1*), showed early flowering and accelerated leaf senescence (Breeding et al., 2011). Thus, it appears that homeotic proteins are involved in almost all the aspects of flower development ranging from specifying flower organ identities to their senescence and abscission.

Interestingly, AG regulates the production of senescence-controlling hormones in the Arabidopsis flower. For example, *AGAMOUS* positively regulates transcription of a JA biosynthesis gene, *DEFECTIVE IN ANTHER DEHISCENCE 1* (*DAD1)* (Ito et al., 2007) and a gene involved in cytokinin degradation, *CYTOKININ OXIDASE/DEHYDROGENASE 6* (*CKX6*) (Ó'Maoiléidigh et al., 2013). Compared to the well-characterized role of cytokinins in delaying senescence, the role of endogenous JA in causing plant senescence remains questionable (Jibran et al., 2013). This is because although exogenously applied MeJA or JA accelerates senescence of detached leaves in many plant species, JA biosynthesis mutants such as *allene oxide synthase* (*aos*) (Park et al., 2002) and *oxophytodienoate reductase3* (*opr3*) (Schommer et al., 2008) do not show delayed leaf senescence. It was proposed that JA and other yet unknown pathways regulate leaf senescence in parallel but in an independent manner (Schommer et al., 2008). Nevertheless, a recent study on the *coronatine insensitive 1–37* (*coi1-37*) mutant has clearly demonstrated that JA plays a key role in regulating *in planta* perianth abscission of Arabidopsis flowers (Kim et al., 2013).

Here I uncover a previously unknown role for AGAMOUS in regulating developmental sepal senescence and abscission. The study suggests that delayed developmental sepal senescence in *ag-1* is due to decreased JA concentrations.

3.7.1 Results

3.7.1.1 *ag-1* flowers show *in planta* delayed sepal senescence and abscission

Compared with wild-type flowers, flowers of *ag-1* were delayed in sepal senescence and abscission. To more clearly compare senescence and abscission events between *ag-1* and wild-type plants, I used the numbering system of Bleecker and Patterson, (1997), which defines the positions of the flowers on an inflorescence stalk by counting down from the first flower at the top of the inflorescence with visible white petals. Using this system, sepal yellowing was found to be greatly delayed in the *ag-1* flowers compared to L*er*-0 wild-type flowers (Fig. 3.7.1). In the *ag-1* flower sepal yellowing occurred at position 12, compared to position 4 of wild-type.

Sepal senescence was quantified by measuring sepal chlorophyll content of the *ag-1* and wild-type opened flowers at position 2 (Fig. 3.7.1) and comparing it back to the chlorophyll content of un-opened floral buds present at the outer periphery of inflorescence (Fig. 3.7.2A and B). The data showed that percentage drop in chlorophyll content of sepals of wild-type flowers was significantly higher (~40%) compared to *ag-1* flowers (~6%) (Fig. 3.7.2C). Furthermore, abscission in the *ag-1* sepals was also delayed, *ag-1* sepals abscised at position 14, whereas wild-type sepals abscised at position 6 (Fig. 3.7.1).Taken together the data shows that the *ag-1* mutant is delayed in developmental sepal senescence and abscission.

Figure 3.7.1. *In planta* sepal senescence and abscission.

A. Wild-type flowers. B. *ag-1* flowers. Plants were grown in long day conditions for 8 weeks (16 h light and 8 h dark) in a green house and flowers were detached and photographed. The arrows indicate flowers with senesced and abscised sepals. The flowers were numbered according to the numbering system of Bleecker and Patterson (1997).

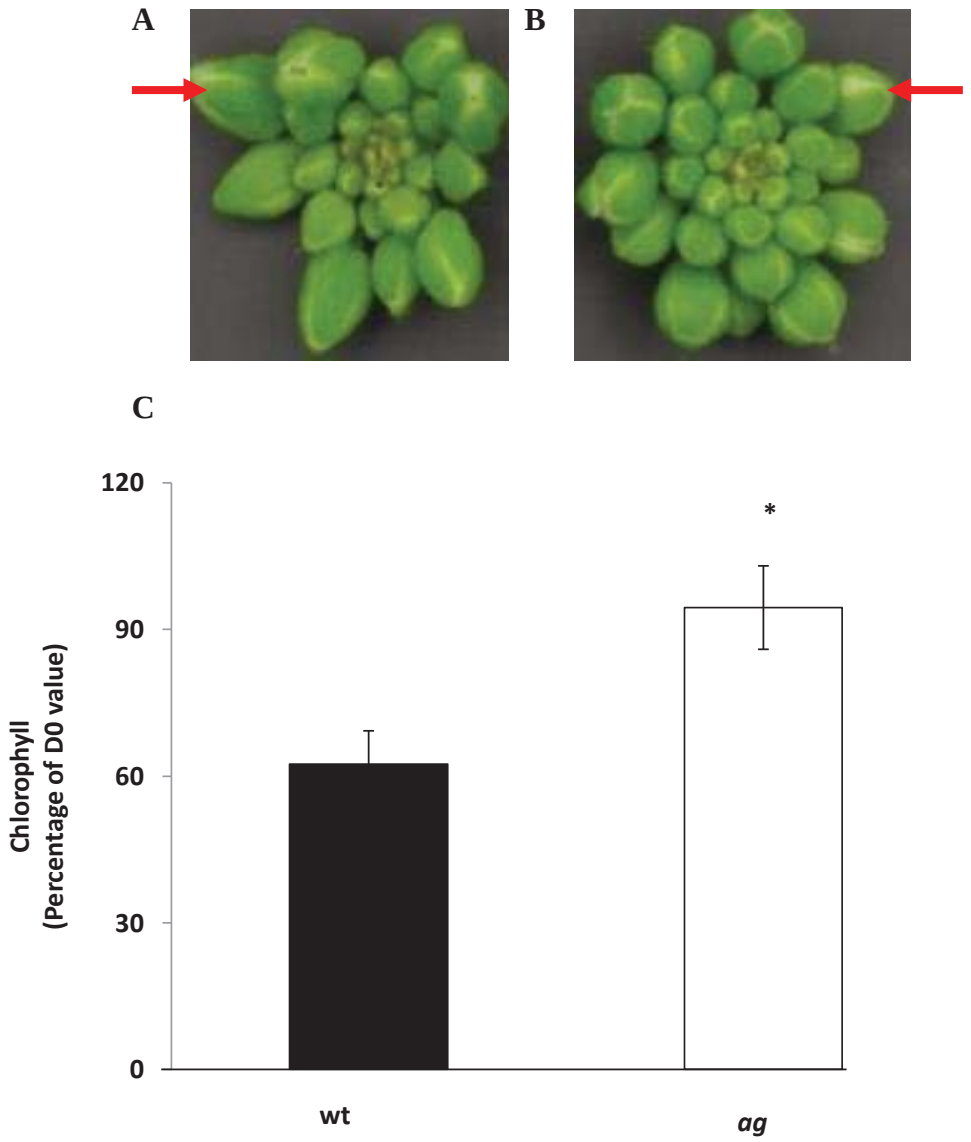

Figure 3.7.2. *In planta* sepal senescence quantification.

A. Wild-type (L*er*-0) inflorescence. B. *ag-1*(*ag*) inflorescence. C. Percentage chlorophyll content of L*er*-0 (wt) and *ag-1* sepals at position 2, as compared to sepals from unopened flowers. The percentage chlorophyll was calculated by comparing the chlorophyll content at position 2 (Fig. 3.7.1) to sepals from unopened buds (arrows). Plants were grown in long day conditions for 8 weeks (16 h light and 8 h dark) in a green house and their inflorescences were detached. The error bars indicate standard errors of 6 biological replicates. Statistically significant differences in percentage chlorophyll content values between the L*er*-0 and *ag-1* using Student's *t*-test are indicated (*$P < 0.05$).

3.7.1.2 Detached dark-held immature *ag-1* inflorescences show delayed senescence

Detached dark-held wild-type (L*er*-0) inflorescences degreened more rapidly (Fig. 3.7.3A) than the *ag-1* inflorescences (Fig. 3.7.3B). Quantification of chlorophyll content at day 3 of dark incubation revealed that *ag-1* inflorescences had retained ~80% of their initial total chlorophyll content compared with ~55% for wild-type inflorescences (Fig. 3.7.3C). Furthermore, to investigate whether the delayed dark-induced senescence of detached immature inflorescences was specific to *ag-1* in the L*er*-0 ecotype, a T-DNA insertion *ag-T1* (CS302905) mutant in Col-0 background was used. The data demonstrated that detached dark-held inflorescences of *ag-T1* retained more chlorophyll content than Col-0 wild-type (Fig. 3.7.3D). These results show that the delayed senescence of the *ag-1* and *ag-T1* mutants is due to disruption in AG function.

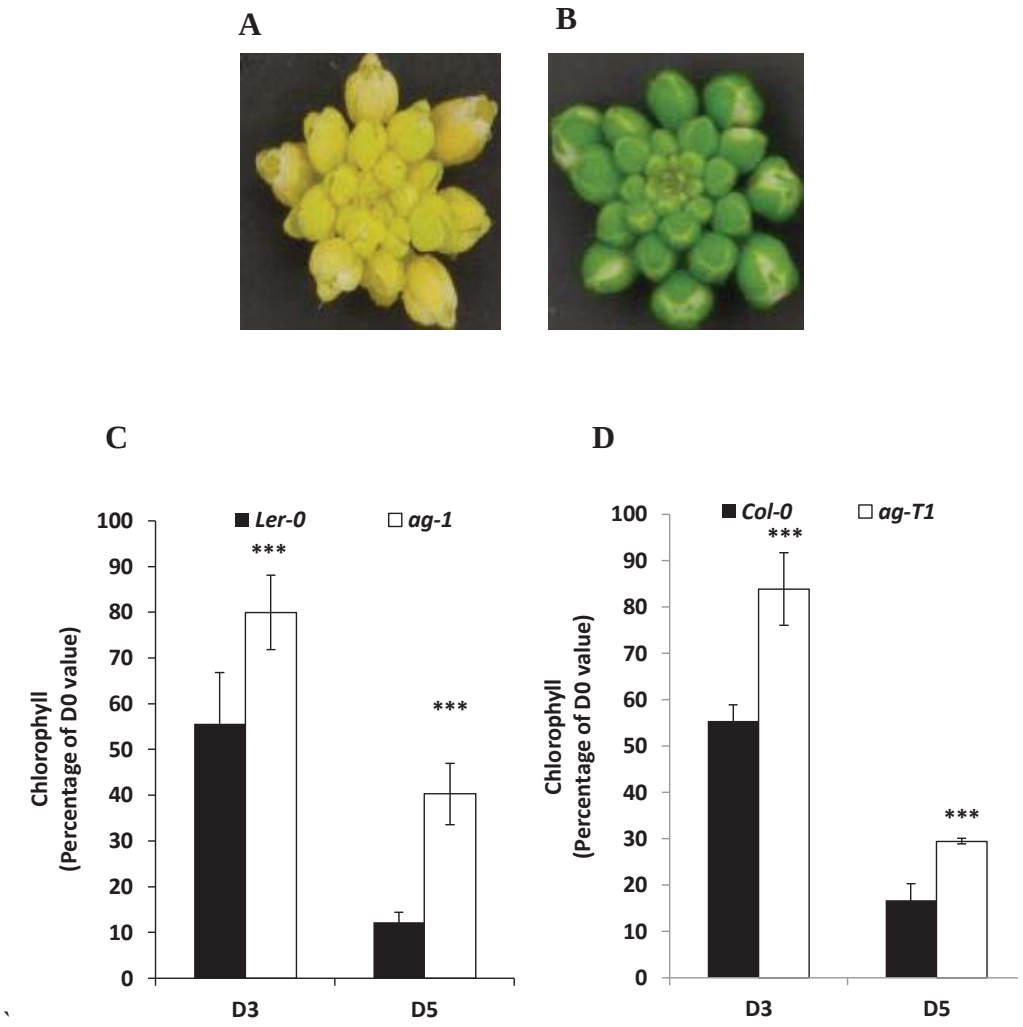

Figure 3.7.3. Dark-induced senescence of detached immature inflorescences.

A. Wild-type (L*er*-0) inflorescence at day 5 of the dark incubation. B. *ag-1* inflorescence at day 5 of the dark incubation. C. Percentage chlorophyll content of detached *ag-1* and L*er*-0 inflorescences at day 3 and 5 of the dark incubation. D. Percentage chlorophyll content of *ag-T1* and wild-type (Col-0) inflorescences at day 3 and 5 of the dark incubation. Plants were grown in long day conditions for 8 weeks (16 h light and 8 h dark) in a green house. The inflorescences were detached from the primary bolts of the plants and their cut ends were placed in water at 21°C for 5 days. Chlorophyll content is expressed as percentage of day 0 value. The error bars indicate standard errors of 6 biological replicates. Statistically significant differences in percentage chlorophyll content values between the wild-type and *ag-1* using Student's *t*-test are indicated (***$P < 0.05$). D3, day 3; D5, day 5.

3.7.1.3 Sterile mutants do not show delayed dark-induced inflorescence senescence

Dark-incubation of detached Arabidopsis inflorescences may result in sugar starvation-induced inflorescence senescence (section 3.1.1.2). Thus, I hypothesized that dark-induced senescence of sepals in wild-type inflorescences occurs because they may have become a source to provide nutrients for maintenance of reproductive organs. Therefore, in *ag-1* inflorescences the lack of reproductive organs (sink) may be the cause of the delayed inflorescence senescence in the dark. To investigate this, sepals of wild-type and the *ag-1* inflorescences were dissected and placed in the dark for five days. The *ag-1* sepals showed delayed degreening compared to wild-type (Fig. 3.7.4A), suggesting that delayed sepal senescence in the *ag-1* does not depend on sepal attachment to the inflorescence and that the delay in inflorescence senescence in *ag-1* is regulated by a source-sink independent pathway.

To investigate further whether delayed senescence of the *ag-1* inflorescences is due to lack of functions of reproductive organs, I quantified the inflorescence senescence of male (*ms5* and *dde2)* and female (*reb1-1* and *ant5)* sterile mutants in the dark (Fig. 3.7.4B). Although the average value of chlorophyll content of sterile mutants was higher than wild-types at day 3, the difference was insignificant. The chlorophyll content in L*er*-0 and Col-0 wild-type inflorescences was decreased to ~55 and 58%, respectively. The detached dark held inflorescences of *rbe1-1*, *ant5*, *ms5* and *dde2* mutant showed a reduction of ~49, 47, 45 and 54% in chlorophyll content, respectively. However, detached dark-held *ag-1* inflorescences showed a decrease of only ~20% in their chlorophyll content at day 3 of the dark incubation (Fig. 3.7.3C). Furthermore, at day 5 of dark incubation, the sterile mutants had the same amount of chlorophyll content as wild-type (data not shown). By contrast, *ag-1* inflorescences retained almost double the amount of chlorophyll content at day 5 in the dark compared to wild-type (Fig. 3.7.3C). Therefore, based on the data it is concluded that sepal senescence of detached dark-held *ag-1* inflorescences is not controlled by pollination- and fertilization-associated events.

Interestingly, the *dde2* mutant showed *in planta* delayed sepal senescence and abscission. The wild-type (Col-0) sepals senesced at position 6 and abscised at position 8 (Fig. 3.7.4C), whereas *dde2* sepals senesced at position 13 and abscised at position 15 (Fig.

3.7.4D). Furthermore, *ms5*, *dde1* and *ant5* also showed *in planta* delayed sepal senescence and abscission (data not shown). This suggests that *in planta* sepal senescence and abscission may be regulated by reproductive growth.

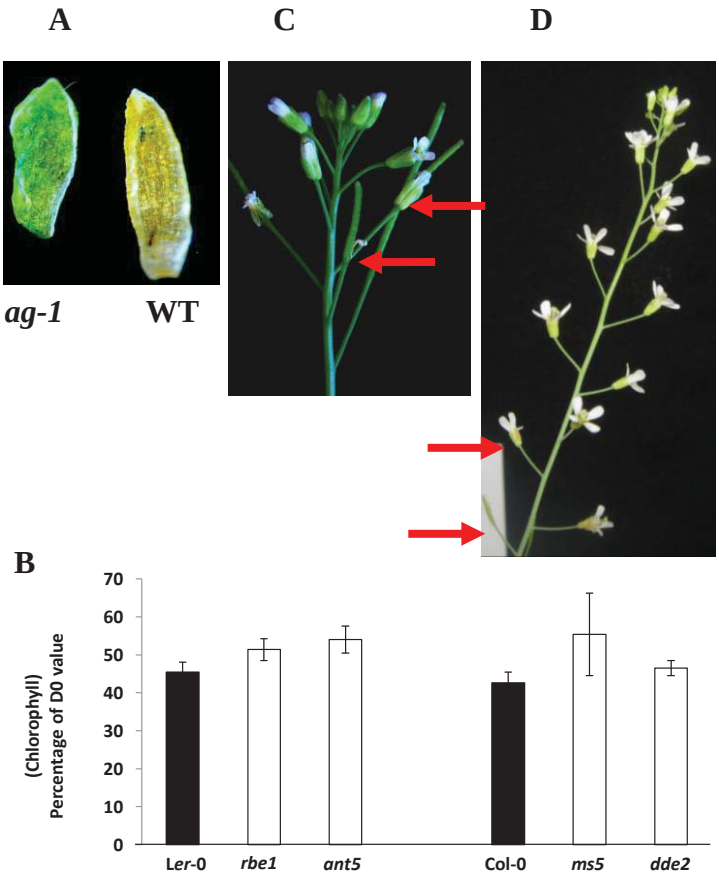

Figure 3.7.4. Dark-induced and *in planta* senescence of floral tissues.

A. Detached dark-held wild-type (L*er*-0) and *ag-1* sepals at day 5. B. Percentage chlorophyll content of detached dark-held inflorescences of male (in Col-0 background) and female (in L*er*-0 background) sterile mutants at day 3 of the dark incubation. C. Wild-type (Col-0) inflorescence stalk. D. *dde2* inflorescence stalk. Plants were grown in long day conditions for 8 weeks (16 h light and 8 h dark) in a green house and were photographed. The inflorescences were detached from the primary bolts of the plants and their cut ends placed in water at 21°C for 3 days. The error bars indicate standard errors of 6 biological replicates. The arrows indicate flowers with senesced and abscised sepals.

3.7.1.4 Exogenously applied ACC, ethrel, MeJA and ABA causes accelerated dark-induced senescence in *ag-1* detached inflorescences

The majority of ethylene synthesis occurs in the stamens and carpel of harvested broccoli heads (Tian et al. 1994). The *ag-1* inflorescence could have reduced ethylene production, due to lack of stamen and carpel tissue. Furthermore, AG directly regulates the transcription of *DEFECTIVE IN ANTHER DEHISCENCE1* (*DAD1*) to produce JA in anthers (Ito et al., 2007). Although the role of JA in senescence is not clear, it has been implicated by many studies (reviewed by Schippers et al., 2007; Jibran et al., 2013). Jasmonic acid (JA) is required for pollen maturation and stamen development in Arabidopsis (Stintzi et al., 2001). Thus, I hypothesized that delayed inflorescence senescence in *ag-1* is due to defects in hormone signalling or synthesis. To investigate this, detached dark-held wild-type and *ag-1* inflorescences were treated with ACC, ethrel (chlorethephon), MeJA and ABA (Fig. 3.7.5).

At day 3 of the dark incubation, wild-type and *ag-1* inflorescences lost ~70 and 46% chlorophyll content, respectively (Fig. 3.7.5A). 1mM ACC treated wild-type and *ag-1* inflorescences lost ~82 and 75% of their chlorophyll content, respectively. Although 1 mM ACC caused accelerated degreening both in wild-type and *ag-1* inflorescences, 100 μM ACC did not affect the degreening in wild-type inflorescences. Interestingly, the same ACC concentration of 100 μM caused an ~82% drop in chlorophyll content of the *ag-1* detached dark-held inflorescences. This suggests that *ag-1* inflorescences are more sensitive to exogenously applied ACC.

Exogenously applied ethrel, MeJA and ABA enhanced senescence both in wild-type and *ag-1* detached dark-held inflorescences (Fig. 3.7.5B). At day 3 of the dark incubation, untreated wild-type and *ag-1* inflorescences lost ~88 and 45% chlorophyll content, respectively.

Ethrel treated wild-type and *ag-1* inflorescences lost ~94 and 87% chlorophyll content, respectively (Fig. 3.7.5B). Thus, exogenously applied ethrel accelerated chlorophyll decrease in the *ag-1* inflorescences to 87% similar to the ~88% drop observed in the untreated wild-type control. Student *t* test demonstrated that there was no significant

difference in wild-type untreated inflorescences and ethrel treated *ag-1* inflorescences. This suggests that ethylene has a key role during dark-induced inflorescence senescence.

MeJA treated wild-type and *ag-1* inflorescences had both lost ~90% of their chlorophyll content at day 3 (Fig. 3.7.5B). MeJA could accelerate only 3% chlorophyll degradation in the wild-type inflorescences suggesting that MeJA is not the key regulator of dark-induced inflorescence senescence. However, MeJA treated *ag-1* inflorescences became similar to the untreated wild-type control. Furthermore, this also suggests that *ag-1* inflorescences may have decreased MeJA levels. Student *t* test demonstrated no significant difference between wild-type untreated inflorescences and MeJA treated *ag-1* inflorescences, or between MeJA treated *ag-1* and wild type inflorescences.

Interestingly, ABA treated wild-type and *ag-1* detached dark-held inflorescences both lost ~95% of their chlorophyll content. This data suggests that *ag-1* inflorescences are more sensitive to ABA treatments as ABA complemented the *ag-1* delayed senescence phenotype to ABA treated wild-type inflorescences.

Taken together the data suggests that the *ag-1* inflorescences are not defective in hormone-signalling pathways because they still respond to the hormones. The results also suggest that the *ag-1* inflorescences are hypersensitive to exogenously applied MeJA, ABA and ACC because treatment with those hormones caused a greater drop in chlorophyll levels in the *ag-1* mutant than in the wild type. However, this could also be the result of a decreased synthesis of these hormones.

A

B

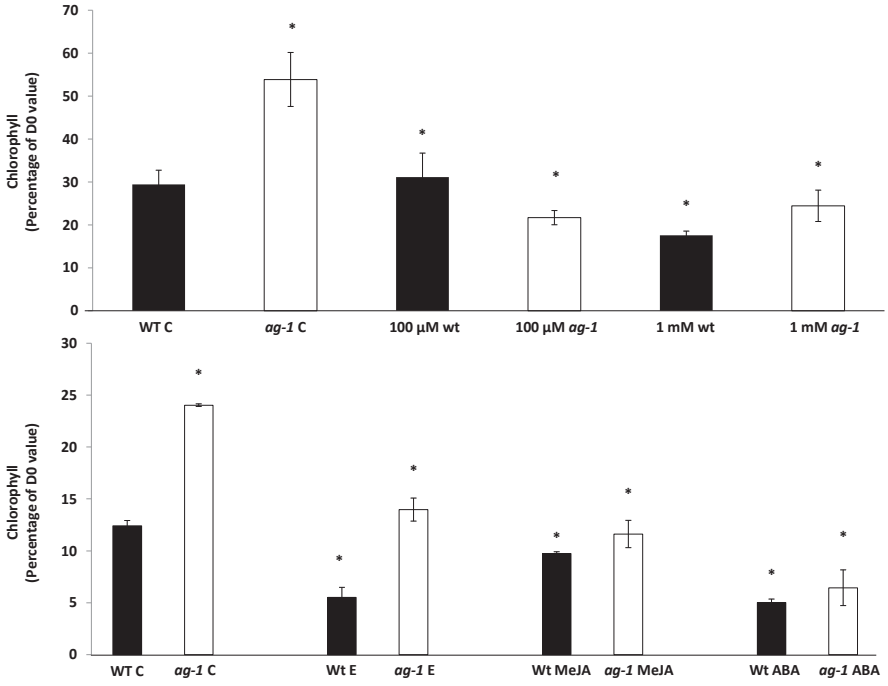

Figure 3.7.5. Detached dark-held wild-type and *ag-1* inflorescences treated with ACC, ethrel, MeJA and ABA.

A. Detached dark-held wild-type and *ag-1* inflorescences treated with 100 µM and 1 mM ACC. B. Detached dark-held wild-type and *ag-1* inflorescences treated with 20 ppm Ethrel (E), 100 µM MeJA and 1 mM ABA**.** Plants were grown in long day conditions for 8 weeks (16 h light and 8 h dark) in a green house. The inflorescences were detached from primary bolts of the plants and their cut ends placed in water or chemicals for 3 days at 21°C. Chlorophyll content is expressed as percentage of day 0 value. The error bars indicate standard errors of 6 biological replicates. Statistically significant differences in percentage chlorophyll content between the wild-type control inflorescences and hormone-treated wild type inflorescences and between *ag-1* control and hormone-treated *ag-1* inflorescences using Student's *t*-test are indicated (*$P < 0.05$).

3.7.1.5 Detached *ag-1* sepals and inflorescences show decreased JA concentration

To investigate whether delayed senescence of detached dark-held inflorescences in *ag-1* is due to defects in hormones biosynthesis pathways, concentrations of JA, ACC (precursor of ethylene), ABA and SA were measured in detached sepals and inflorescences of wild-type and *ag-1* (Fig. 3.7.6). The data showed that *ag-1* sepals (Fig. 3.7.6A) and inflorescences (Fig. 3.7.6B) had un-detectable JA concentrations compared to wild-type sepals, whereas there was no significant difference in ACC, ABA and SA concentrations both in wild-type and *ag-1* detached sepals and inflorescences. Furthermore, ethylene evolution in detached *ag-1* and wild-type inflorescences was also measured (Fig. 3.7.6C). The data demonstrated that there was no significant difference in ethylene production in *ag-1* detached inflorescences as compared to wild-type inflorescences. Taken together the data show that detached *ag-1* sepals and inflorescences have decreased JA concentrations.

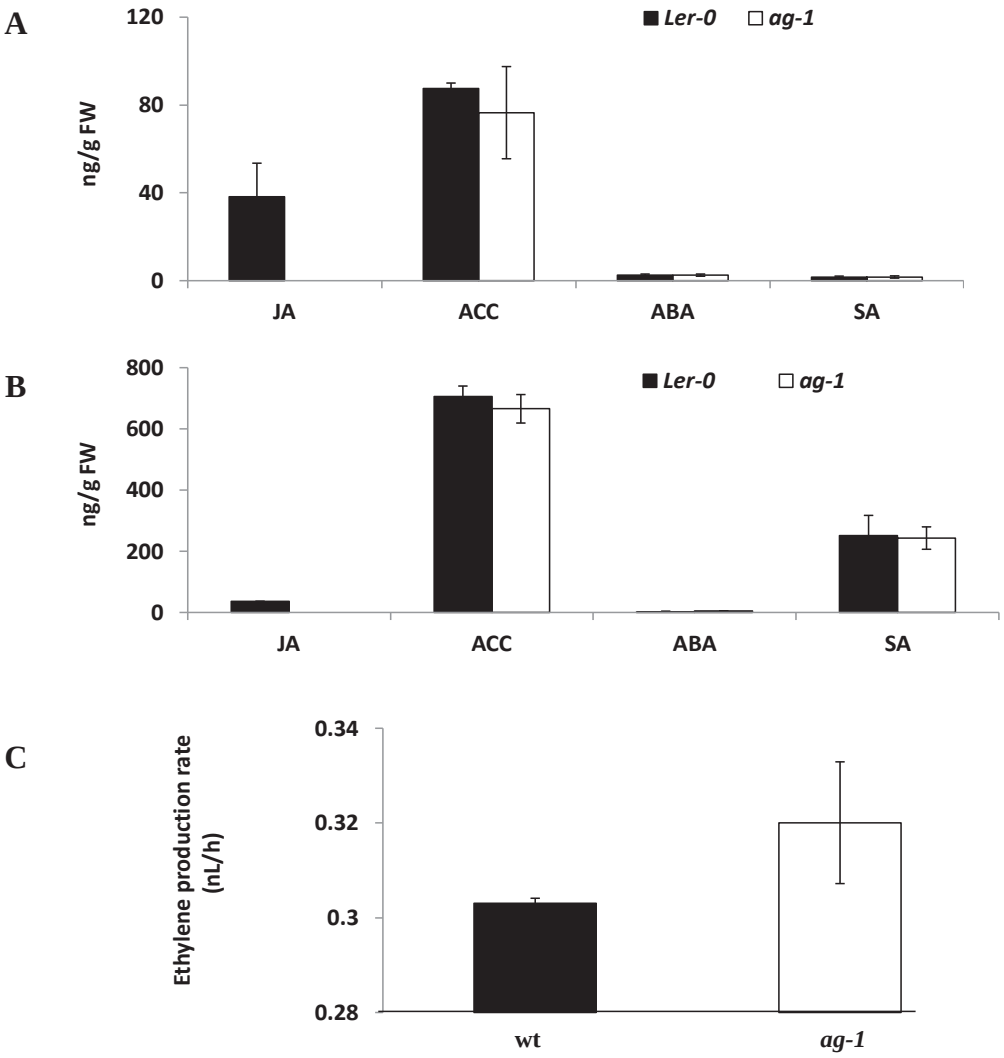

Figure 3.7.6. Endogenous concentrations of hormones in detached wild-type and *ag-1* sepals and inflorescences.

A. Endogenous levels of hormones in detached sepals. B. Endogenous levels of hormones in detached inflorescences. C. Ethylene production in detached inflorescences. Plants were grown in long day conditions for 8 weeks (16 h light and 8 h dark) in a green house and their sepals and inflorescences detached for hormone analysis. JA, ACC, ABA and SA concentrations were measured by using LCMS. Ethylene production rate was measured in nL/h with an ETD-300 Ethylene Detector. The error bars represent standard errors of 2 biological replicates.

3.7.1.6 *dad1* and *dde2* do not show a delay in dark-induced senescence of detached inflorescences

Detached *ag-1* inflorescences are defective in JA synthesis (Fig. 3.7.6B) and senesced early when treated with 100 μM MeJA (Fig. 3.7.5). Therefore, it was possible that delayed inflorescence senescence in detached dark-held *ag-1* inflorescences was due to decreased JA concentrations. To test the role of JA in regulating inflorescence senescence, I investigated dark-induced senescence of detached immature inflorescences of *dad1* and *dde2* mutants, which are defective in JA synthesis (Ito et al., 2007). The JA content in detached inflorescences of the *dde2* mutant was undetectable (data not shown). Interestingly, detached dark-held inflorescences of these JA deficient mutants did not show a significant difference in chlorophyll loss compared to the wild-type (Fig. 3.7.7). This suggests that JA is not involved in regulating dark-induced senescence of the immature detached Arabidopsis inflorescences.

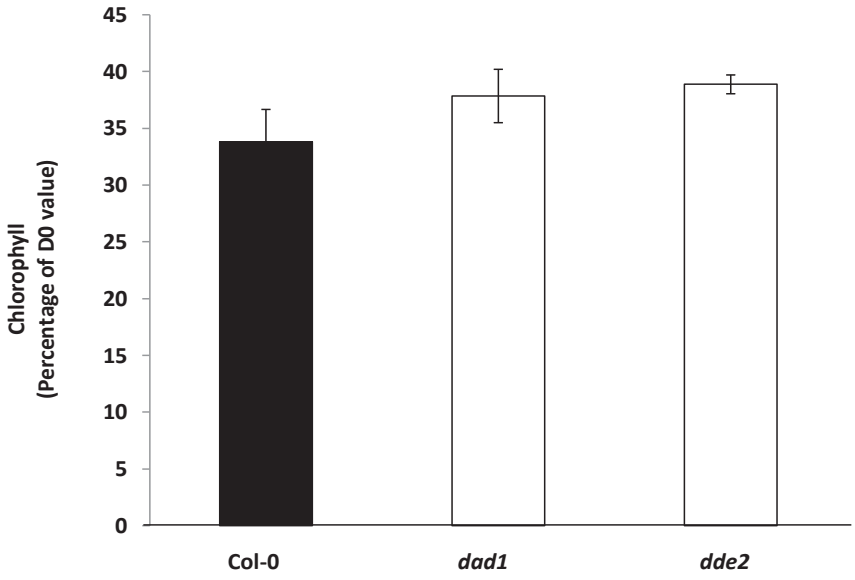

Figure 3.7.7. Percentage chlorophyll content of detached dark-held inflorescences of Col-0, *dad1* and *dde2* at day 3.

Plants were grown in long day conditions for 8 weeks (16 h light and 8 h dark) in a green house. The inflorescences were detached from primary bolts of the plants and their cut ends placed in water for 3 days at 21°C. The error bars indicate standard errors of 6 biological replicates.

3.7.1.7 Exogenously applied MeJA enhances *in planta* sepal senescence and abscission of the *ag-1*

Next, I investigated whether AG regulates developmental sepal senescence by controlling the biosynthesis of JA. The *ag-1* plants were sprayed with 100 μM MeJA each day for three days. Control plants were sprayed with 1% ethanol and water. To investigate senescence and abscission events the numbering system of Bleecker and Patterson (1997) was used. The sepals of mock-treated *ag-1* flowers degreened at position 12 and abscised at position 14 (Fig. 3.7.8A). Exogenously applied MeJA accelerated the yellowing of sepals from position 12 to 7 and the sepals were abscised at position 9 compared to position 12 (Fig. 3.7.8B). Furthermore, MeJA treatment enhanced the flower opening of *ag-1* plant compared to mock-treated control (Fig. 3.7.9). Hence, the data suggest that exogenously applied MeJA can accelerate sepal senescence, abscission and flower opening in *ag-1*.

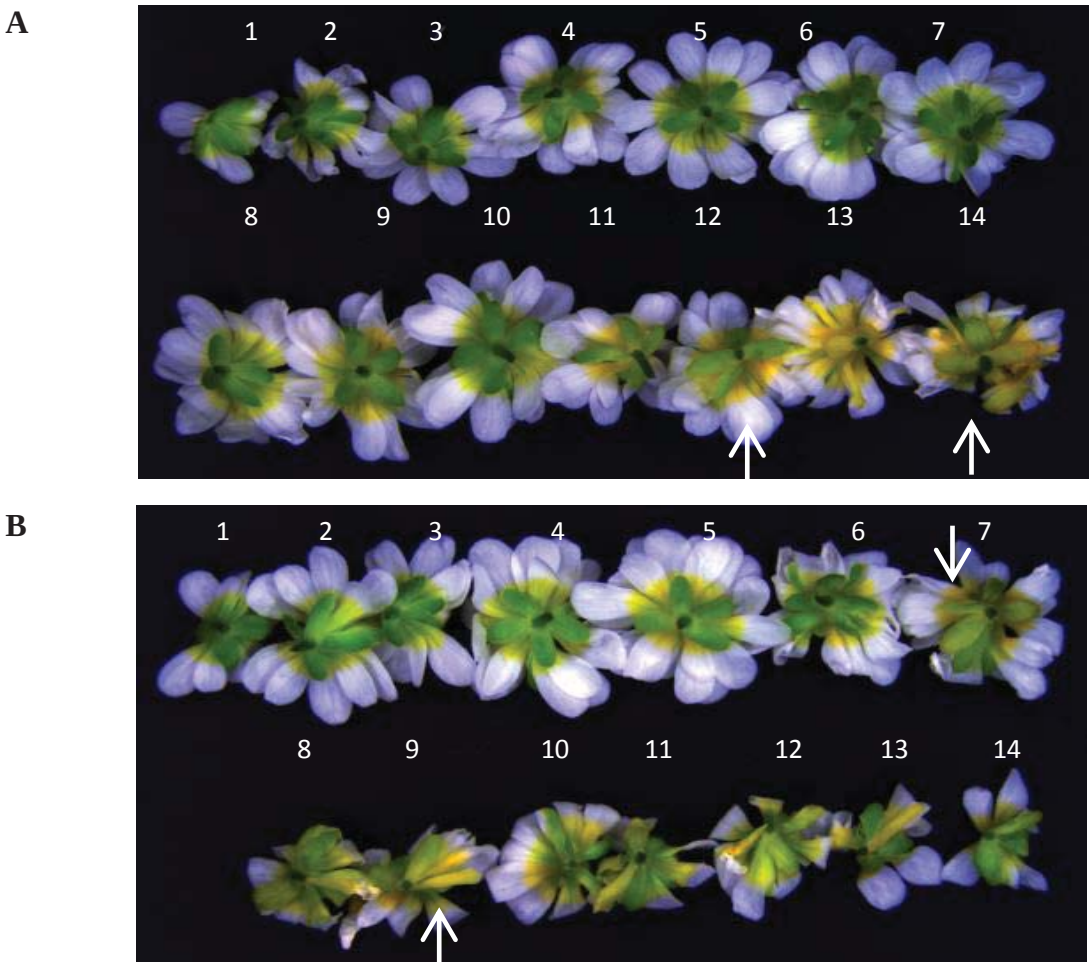

Figure 3.7.8. MeJA-treated *ag-1* plant.

A. Mock-treated *ag-1* flowers. B. MeJA-treated *ag-1* flowers. Plants were grown in long day conditions for 8 weeks (16 h light and 8 h dark) in a green house, sprayed with MeJA for three days and flowers were detached and photographed. The arrows indicate flowers with senesced and abscised sepals. The flowers are numbered according to the system of Bleecker and Patterson (1997).

Figure 3.7.9. MeJA treatments enhance flower opening in *ag-1* plants.

A. Mock-treated *ag-1* plants at day 1. B. Mock-treated *ag-1* plants at day 3. C. 100 µM MeJA-treated *ag-1* plants at day 1. D. 100 µM MeJA-treated *ag-1* plants at day 3. Plants were grown in long day conditions for 8 weeks (16 h light and 8 h dark) in a green house and sprayed with 100 µM MeJA for 3 days. Photographs were taken at day 1 and 3 of MeJA treatment.

3.7.2 Discussion

In this chapter, I investigated how defects in AGAMOUS led to delayed *in planta* sepal senescence, abscission and dark-induced senescence of detached immature inflorescences in Arabidopsis. It was possible that the delayed senescence of the detached dark-held *ag-1* was due to sterility of the flower. This would be consistent with the senescence of many flowers being under the control of pollination (van Doorn and Woltering, 2008). However, detached dark-held *ant5*, *rbe1*, *dde2* and *ms5* inflorescences that had complete flowers but were sterile due to defects in carpel and stamen maturation did not show delayed dark-induced senescence (Fig. 3.7.4B). Moreover, in detached dark-held inflorescences pollination and fertilization does not occur as development is arrested rapidly in the dark (section 3.1.1.1). Therefore, it is unlikely that absence of pollination- or fertilization-associated molecular events (e.g., ethylene burst) was the cause of the delayed senescence of the dark-held *ag-1* inflorescences.

It was plausible that the delayed senescence of the *ag-1* flowers was caused by defects in signalling of the senescence promoting hormones, ethylene, JA, or ABA. However, the detached dark held *ag-1* inflorescences showed enhanced senescence when treated with ACC, ethrel, MeJA and ABA (Fig. 3.7.5). This suggests that defects in signalling of these hormones are not the cause of delayed senescence in detached dark held *ag-1* inflorescences.

It was also possible that the delayed senescence of the *ag-1* inflorescences was due to reduced production of ACC, ethylene, ABA or JA. Although it does not seem to be because of reduced ethylene production as the concentrations of endogenous ACC and ethylene in the detached *ag-1* and L*er*-0 inflorescences were similar (Fig. 3.7.6), *ag-1* inflorescences were more sensitive to lower concentration of ACC compared to wild-type. Endogenous ABA concentrations were also similar in *ag-1* and wild type inflorescences again indicating that the delayed senescence in the *ag-1* inflorescences was not because they produced less ABA. It was interesting however, that exogenously applied ABA was better at accelerating degreening of the *ag-1* than wild type inflorescences. This raises the possibility that delayed senescence in *ag-1* could be in part due to the inflorescences having reduced sensitivity to ACC and ABA. An alternative explanation could be that although the hormone levels in

wild-type and *ag-1* inflorescences are the same, the spatial distribution of the hormones may have been disturbed in the mutant.

In contrast to ABA and ethylene, the JA content of the *ag-1* inflorescences and detached sepals was significantly lower than in wild type tissues (Fig. 3.7.6A and B). Many studies have demonstrated a role for exogenously applied JA in inducing leaf senescence (reviewed by Jibran et al., 2013). Furthermore, *coi1* and *dde2*, which are defective in JA signalling or devoid in JA respectively, have recently been found to have delayed *in planta* sepal senescence and perianth abscission (Kim et al., 2013). Exogenously applied MeJA also suppresses the delay in senescence of the *ag-1* inflorescences suggesting that lack of MeJA in the *ag-1* tissue could have a role in delaying the dark-held senescence. Interestingly exogenously applied MeJA in *ag-1* plant caused enhanced flower opening (Fig. 3.7.9). This is consistent with the study of (Ishiguro et al., 2001), which demonstrated that exogenously sprayed JA resulted in enhanced flower opening in *dad1*.

JA appears to have a role in controlling *in planta* flower senescence of Arabidopsis as *dde2* plants that are deficient in jasmonates due to a lesion in the *AOS* gene show delayed perianth senescence and abscission. This is reversed when the inflorescences are sprayed with MeJA (Kim et al., 2013). *ag-1* plants also showed delayed *in planta* sepal yellowing and abscission compared to wild type and this was prevented at least in part by spraying the inflorescences with MeJA (Fig. 3.7.8).

MeJA might affect senescence of the inflorescences by working in concert with the ethylene senescence-associated hormonal pathway. It is well established that JA mediates plant pathogen response by affecting EIN3 activity. This is through degrading JAZ proteins that repress EIN3 function (Chao et al., 1997; Lorenzo et al., 2003; Zhu et al., 2011). Defects in *EIN3* also delay inflorescence senescence (data not shown) raising the possibility that senescence is through cooperative activity of JA and ethylene like reported for pathogen response.

This view does, however, have to be tempered with the finding that the JA biosynthesis mutants, *dad1* and *dde2*, did not show delayed dark-induced inflorescence senescence. This may mean that dark-induced senescence of detached inflorescences is regulated differently from *in planta* senescence. It may be that AGAMOUS affects the

expression of other genes that in turn controls the senescence in the dark. One such candidate gene may be *CYTOKININ OXIDASE/DEHYDROGENASE 6* (*CKX6*), which AGAMOUS positively regulates (Ó'Maoiléidigh et al., 2013). *CKX6* catalyzes cytokinin degradation (Schmulling et al., 2003) and cytokinins are potent inhibitors of dark induced degreening including that of the dark-held inflorescences (Jibran et al., 2013; Trivellini et al., 2012).

In conclusion, the study suggests that reduced jasmonate production in *ag-1* causes *in planta* delayed sepal senescence and abscission. However, the delayed senescence seen in the detached dark-held *ag-1* inflorescences is may be through another non-MeJA mechanism.

Chapter 4

Blank page

Chapter 4 Summary, outlook and future work

This research work was performed to understand the molecular and genetic mechanisms underlying dark-induced senescence of detached immature inflorescences. Arabidopsis was used because of the research advantages it provided over commercially relevant plant species. The results from this research have increased our understanding of the mechanisms associated with energy-deprivation-driven senescence of detached plant tissues.

The senescence system used in this thesis was based on detaching immature inflorescences and investigating how they responded to prolonged dark incubation. The response of the inflorescences to darkness was distinct from that of those held in the light. In the light, the inflorescences continued to develop to produce siliques suggesting that given sufficient energy input the detached immature inflorescences could act as an autonomous unit and develop independently of the rest of the plant. By contrast, the developmental arrest seen in the dark-held inflorescences suggested assimilation of carbon was becoming limiting and this was further supported by exogenously applied sugar phenocopying growth in the light. The addition of sugar to the holding solution also inhibited degreening of the dark-held inflorescences indicating that loss of chlorophyll is caused by signals associated with either lack of light or lack of carbon.

The timing of senescence in a carbon-deprived environment is affected by plant hormones.

Exogenously applied ACC, Ethrel, MeJA and ABA applied at 10 µM to 1 mM hastened senescence of the detached dark-held Arabidopsis inflorescences. This is consistent with the role of these chemicals in accelerating both age-related and dark-induced senescence (Jibran et al., 2013; Lim et al., 2007). Thus, these hormones may also have a role in the natural timing of senescence of the dark-held inflorescences.

Surprisingly, the detached dark-held inflorescences treated with 3 or 5 mM MeJA concentrations showed less degreening than wild-type. Finding that these inflorescences had decreased transcript abundance of SAGs (senescence-associated genes) including *SEN4*,

ANAC029, *NAC3* and *SAG12* suggested that the comparatively high MeJA concentrations were retarding degreening by inhibiting the senescence programme. This may be through its effect on ethylene production or sensing as the MeJA treated inflorescences had lower transcript abundance of *ACS2, ACO4* and *EIN2.* Despite the unexpected effects of the relatively high concentrations of MeJA on inhibiting inflorescence senescence, the hormone appeared to still be influencing physiologically relevant processes in the inflorescences as it also induced known JA responsive genes *ERF11, ORA59* and *RAP2.4.*

Unravelling the regulatory mechanisms underlying inflorescence senescence using a forward genetics strategy

To further understand the regulation of senescence under energy deprived conditions, I screened inflorescences of plants derived from chemically mutagenized seeds for those which had altered timing of degreening when held in the dark. This led to identification of 10 *accelerated* (*ais*) and 20 *delayed* (*dis*) *inflorescence senescence* mutants. The accelerated senescence of the *ais* mutants was seen in both detached leaves and inflorescences, whereas the delayed senescence of most *dis* mutants appeared specific for the inflorescences. Therefore, characterization of this mutant collection offers a unique opportunity to understand the genetic response of plant tissues under energy limiting conditions.

In addition to the above mutants, the screen also identified a delayed inflorescence senescence sterile homeotic *ag-1 like* mutant (*agl*). The *agl* delayed inflorescence senescence mutant prompted me to investigate whether mutations in other homeotic genes would affect the timing of dark-induced inflorescence senescence. The immature detached dark-held inflorescences of *ag-1*, *lfy4*, *lfy*5, *ap1-1*, *ap1-2*, *ap3*, *pi* and *sep1/sep2/sep3* showed delayed degreening suggesting that floral homeotic genes regulate the inflorescence senescence process. To further investigate the mechanism by which homeotic genes might regulate inflorescence senescence I focused on *ag-1.* Finding substantially lower endogenous concentrations of JA, but not ACC, ABA and SA in the detached inflorescences and sepals of *ag-1* suggested that the delayed senescence was through lack of JA. This was consistent with observing accelerated sepal senescence when the detached dark-held inflorescences were treated with low concentrations of MeJA and when the *ag-1* plants were

sprayed with 100 μM MeJA. It was also in agreement with finding delayed *in planta* sepal senescence in the JA deficient mutant *dde2*. However, intriguingly the JA-deficient mutants *dde2* and *dad1* did not show delayed dark-induced inflorescence senescence. This therefore indicates that the delayed *in planta* sepal senescence in *ag-1* plants is due to decreased JA concentrations, but the delayed senescence of the dark-held *ag-1* inflorescences is due to an as yet un-known non-JA pathway. The differential importance of JA in regulating natural and dark-induced senescence and the effects of homeotic genes on *in planta* and dark-induced sepal senescence has highlighted their importance in this process and merits further study.

The genetic lesions underlying the delayed senescence of some of the identified mutants were mapped using HRM-PCR and WGS. Use of these technologies uncovered a novel regulator of inflorescence senescence. The genetic lesion in *dis58* was in a non-coding RNA encoded by the AT4G13495 locus. ncRNA genes encode RNA molecules rather than proteins and they have been found to regulate expression of defense-associated genes during various biotic and abiotic stresses. Here I have shown that a ncRNA is involved in regulating dark-induced inflorescence senescence. Interestingly, transformation of *dis58* with the wild-type AT4G13495 DNA fragment caused full complementation only if the construct was present in more than one copy. This suggests that the ncRNA differentially controls the phenotype in a dosage dependent manner. Nevertheless, important questions remain to be addressed to understand the role of ncRNA during inflorescence senescence. For example, identifying other genetic lesions or lesions involved in *dis58* delayed inflorescence senescence phenotype. Furthermore, complete characterization of *dis58* and the other most delayed senescence mutants could provide new insights for understanding the genetic components regulating inflorescence senescence.

Translation of research into commercially relevant vegetables

Complete characterisation of the mutants identified in this study will greatly contribute to a full understanding of the key control points that regulate deterioration of harvested dark-held produce. This fundamental knowledge when translated into commercially relevant vegetables will likely help maintain their quality postharvest and help to minimize the significant food losses currently experienced in food supply chain. The obvious initial target is broccoli because of the close relatedness of Arabidopsis with broccoli and the type of screen that was used. The findings could be translated into broccoli through

TILLING (Kurowska et al., 2011) or by using the new genome editing strategies (e.g., Zinc Finger, TALEN, CRISPR-Cas) that enable researchers to specifically target and alter genomic regions in plants (Wood et al., 2011; Shan et al., 2013).

Chapter 5 Appendices

Blank page

Appendix 3.4.1. List of primers used for HRM-PCR. Most of the SNP markers used for HRM-segregation analysis were identified by Warthmann et al (2007). Additional SNP markers are shown in red. Each SNP was given a two-digit identifier for easy reference to the chromosome it is a marker for. The first digit of the number represents the chromosome to which it belongs and the second digit is the primer number. The position of markers for chromosomes is represented with respect to L*er*-0 genome.

#	SNP Marker	Sense-primer	Anti-sense primer
1-1	44607520	CGAATTGAGAAATGGATGGAG	CCAGAAGAAACGGAGGAAGA
1-2	44606126	ACACTGGTCCTCCTCCTGTT	CCGAAGAGCTTGTGACTCCT
1-3	44606794	CAGACCTCACATCAAAGCACA	CAATGCAAACCCCATTATCC
1-4	44606525	ACGATATTGGGGACTCTGCT	TCGAAGAGGTTCATTGCTGTT
2-5	44606322	AATTGTGCAGTGATGGGTTG	TCTGGAGGGTCTTCAAATGG
2-6	44606989	GATCGTCATCAAGGTTTACTCTGT	TTACGCTCATCGGGAATAGG
2-7	21607038	GGCACTGAAACCACAACTCC	TGCCTCCAAGTCCACTGATT
2-8	44606664	CTGACGATGAATTGCCCTTT	GAATCTCTCTCTTCTCTCCATAACA
2-9	44607914	GACTGCGAGGAGTTTACAGGA	GACGCAACGATAGCCGATT
2-10	44607701	CGAAATTGCAGATCCTGAGAC	GCTACTCGGGCCTTCTTCTT
2-11	44607824	CACACATAACAACAGACCCACTTC	CAACTTTGAGCCAGTTTGGT
2-12	21607013	CGTTACCGTTTTAGCGTTTCTC	TAGCTCCGCCGTCATTTATC
2-13	44606533	GAGCCGACAGGGGATTAGTT	GCAGCGTTTGAGCTGTTACTT
3-14	21607479	TTAATTCCGGCTGGTTTGTT	TGATTCCTTCAGGCAAAGGT
3-15	44606957	AAAGGCAGAGAGAAAGCACA	TGGTTTGGTTGATGATGAGG
3-16	44607987	ATCCAGTTCACCTTCCATCC	GAACAATTACGGATATGACTTCCAG
3-17	44607718	CTGAGACAAAGGGAAAAGTGAA	ACGGTGTTGATTCTGGAGTG
3-18	21607675	ATTGGTTTTTGGAGCCCTTT	TGGTGATGAACAAGCGAAGT
3-19	21607250	GGCCCAAGAAGAAGGAAACA	TACTACATGGCTCCCGAGGT
4-20	44606493	TTGCGGCTAACCTTTTTCA	CGGAAACACAATTCGGAGA
4-21	7365693	CGGGTCTGACACATCTGCTT	TTGGTGCAAGAGTCACCATC
4-22	44606851	CCTGTCCTGTCTTCTCCATCT	TGAATTAGCAACCGCTACAA
4-23	7517029	CGATGCTACAAAGCTAGAACGA	TGCATTGGTGTGCAAATACG
4-24	7555037	GGTCGTGCATCGTTGTGTTCA	GAGCTTTTATCCTATGTCCCTTTGTGT
4-25	44606916	TGCTTTGCTACAACCTTCTGTT	AGTCATCCACCTGCTTCGTC
4-26	7796989	CTTTGCAGTGTCTGGCGTATC	AATTGCCTTGTCCCTCCAC
4-27	44606558	GAATTACAGAGGTGGACACTGG	TACCACGAGAAGAGCGTTGA
4-28	44607545	GACGAGCTTCCTCCAACAGA	GCCGTCGAAGAGATGGTAAG
4-29	44607792	GTGAAACCAATCTTCTCAAACTTCC	ATTGTGGGTGAGGGAAAACA
4-30	21607184	GGAGGAAGAAACAAGAAACGAA	ATCCTTGCAGCTTGGTATGG
4-31	44606615	TCTGCTTACTCTGCACCATCA	TAGCTCATGCCTCTGCTTCA
4-32	44607751	ATACCTTGCCGTTTGGGTCT	GTCTCCTTATGCGCCATCTC
5-33	44606639	CCCTTTTATCTCCACCACATT	CAAAACGAGTCTTCAGGATGG
5-34	4,460,7038	CAACATCATACATCGTAACTTCCAG	CCTTTACTTCCAAGAACGAGTCA

Appendix 3.4.2. Genetic analysis of *dis9* recombinants. HRM-PCR was performed to investigate linkage of 19 SNP markers across the whole genome to *dis9* delayed degreening phenotype. Order of the SNP markers from left to right corresponds to north (up) to south (down) of chromosomes (Fig. 3.4.6). Recombinant number is the unique identifier for that plant in the F2 population tested. LL = homozygous L*er*-0, CC = homozygous Col-0, LC = heterozygous

#	*dis9 F2*	1-2	1-3	1-4	2-5	2-7	2-8	2-13	3-14	3-16	3-17	3-19	4-27	4-32	5-33
1	1	LC	LC	LC	CC	LC	LC	LL	LL	LL	LL	LL	LC	LC	LL
2	3	LC	LC	LC	LC	LC	LC	LC	LC	LC	LL	LL	LC	LC	LL
3	5	LL	CC	LC	LC	LC	LL	LC	CC	LL	LL	LL	CC	LC	LL
4	7	LC	CC	LC	CC	CC	CC	LC	CC	LL	LL	LL	LL	LC	LL
5	9	LC	CC	LC	CC	CC	LC	LL	CC	LL	LC	LC	LL	LC	CC
6	11	LC	CC	LL	LL	LL	LL	LL	LL	LL	LL	LL	LC	LC	CC
7	2	LC	LC	LC	LL	LL	LL	LC	LL	LL	LC	LC	LC	CC	LC
8	4	LC	LC	LL	LL	LL	CC	LC	LL	LL	LC	LC	CC	LC	LC
9	6	LC	CC	CC	LL	LC	LC	CC	LC	LC	LC	CC	CC	CC	LC
10	8	CC	CC	CC	LL	LC	CC	LC	LL	LL	LL	LL	LC	CC	LC
11	10	LC	LC	LC	LC	LC	LC	LC	LL	LC	LL	LC	LC	LC	CC
12	12	LL	LC	LC	LL	LC	LC	LC	LL	LL	LC	LL	LC	CC	CC
13	13	CC	CC	LC	LC	LC	LC	LL	LL	LC	LL	LC	LC	LC	LL
14	15	LC	CC	CC	CC	CC	LC	LL	LC	LL	CC	LC	LL	LC	LC
15	17	LC	CC	CC	LL	LL	LL	CC	CC	CC	CC	CC	LC	LC	LL
16	19	LL	LC	LC	CC	LC	CC	CC	LC	LL	LC	LL	LL	LL	LL
17	21	LL	LL	LL	LC	LC	LC	LC	LL	LL	LL	LL	LC	LC	CC
18	23	LC	LL	LC	LL	LL	LC	LC	LL	LC	CC	LC	LC	LC	CC
19	14	LC	CC	LC	CC	LC	LC	LC	LL	CC	CC	CC	LC	LC	LC
20	16	CC	LC	LC	CC	LC	CC	CC	LL	LC	CC	LC	LC	LC	LC
21	18	LC	LC	CC	LL	LL	LC	CC	LL	LL	LL	CC	LC	LC	LC
22	20	LL	CC	CC	CC	CC	CC	LC	LL	LC	LL	LC	CC	CC	LC
23	22	LC	LC	CC	LC	LC	LC	LC	LL	LL	LC	CC	LL	CC	CC
24	24	LL	LC	CC	CC	LL	LL	LC	LL	LL	LC	LL	LC	LC	LC
25	25	LC	CC	CC	LC	LC	LC	CC	LL	LL	CC	CC	LC	CC	LC
26	27	LL	LL	LL	LL	LL	LL	CC	LL	LC	LC	LC	CC	LL	LC
27	26	CC	CC	LC	LC	LC	LC	CC	LC	LL	LC	LL	LC	LL	LL
	L*er*-0	**7**	**3**	**4**	**10**	**8**	**6**	**6**	**18**	**16**	**11**	**7**	**4**	**3**	**8**
	Col-0	**4**	**14**	**8**	**9**	**4**	**6**	**8**	**4**	**2**	**6**	**6**	**5**	**7**	**7**
	Het	**16**	**10**	**14**	**8**	**15**	**15**	**13**	**5**	**9**	**10**	**10**	**18**	**17**	**12**
	% linkage	**44**	**70**	**55**	**48**	**42**	**50**	**53**	**25**	**24**	**40**	**40**	**52**	**57**	**48**

Appendix 3.4.3. Genetic analysis of *dis15* recombinants. HRM-PCR was performed to investigate linkage of 19 SNP markers across the whole genome to *dis15* delayed degreening phenotype. Order of the SNP markers from left to right corresponds to north (up) to south (down) of chromosomes (Fig. 3.4.6). Recombinant number is the unique identifier for that plant in the F2 population tested. LL = homozygous L*er*-0, CC = homozygous Col-0, LC = heterozygous

#	*dis15 F2*	1-1	1-2	1-3	1-4	2-5	2-7	2-9	2-13	3-15	3-16	3-17	3-19	4-27	4-30	4-31	4-32	5-33	5-34
1	5	LL	LL	LC	LC	LC	LC	LL	LL	LC	CC	LC	CC	LL	LL	LL	LL	LC	LL
2	6	LC	LC	CC	LC	LL	LL	LL	LL	LC	CC	LC	CC	LL	CC	CC	LC	LC	LL
3	7	CC	CC	CC	CC	CC	CC	LC	LL	LC	CC	LL	CC	LC	CC	CC	LC	CC	LC
4	8	LC	CC	LC	LC	CC	CC	LL	LC	LC	LC	LC	CC	LL	CC	CC	LC	CC	LC
5	1	LC	CC	CC	CC	LC	LC	LL	LL	LC	CC	LC	LL	LC	LC	CC	LC	LC	LC
6	9	CC	CC	LC	LC	LC	LC	LL	LL	LL	CC	CC	CC	CC	LC	LL	CC	CC	LC
7	2	LL	LL	LC	LC	LC	LC	LL	LL	LC	CC	LC	LL	LC	LL	LL	LL	LC	LC
8	10	LC	LC	CC	LC	LC	LC	LL	LC	LL	LC	LC	LC	LC	CC	CC	LC	LC	LC
9	3	LL	LL	LC	LC	LL	LC	LL	LC	LC	LC	CC	LC	CC	LC	LC	CC	CC	CC
10	11	LC	LC	CC	LC	LL	LL	LL	LL	LC	LC	LC	LC	LC	LL	LL	LL	CC	CC
11	4	LL	LC	LC	LC	LL	LL	LL	LC	LL	LC	LC	LC	LL	LL	LL	LL	LC	LC
	L*er-0*	**4**	**3**	**0**	**0**	**4**	**3**	**10**	**7**	**3**	**0**	**1**	**2**	**4**	**4**	**5**	**4**	**0**	**2**
	Col	**2**	**3**	**4**	**2**	**2**	**2**	**0**	**0**	**0**	**6**	**2**	**5**	**2**	**4**	**5**	**2**	**5**	**2**
	Het	**5**	**7**	**6**	**9**	**5**	**6**	**1**	**4**	**8**	**5**	**8**	**4**	**5**	**3**	**1**	**5**	**6**	**7**
	% linkage	**40**	**50**	**63**	**59**	**40**	**45**	**4**	**18**	**36**	**77**	**54**	**63**	**40**	**50**	**50**	**40**	**72**	**61**

Appendix 3.4.4. Genetic analysis of *dis34* recombinants. HRM-PCR was performed to investigate linkage of 19 SNP markers across the whole genome to *dis34* delayed degreening phenotype. Order of the SNP markers from left to right corresponds to north (up) to south (down) of chromosomes (Fig. 3.4.6). Recombinant number is the unique identifier for that plant in the F2 population tested. LL = homozygous L*er*-0, CC = homozygous Col-0, LC = heterozygous

#	*dis34* F2	1-2	1-3	1-4	2-5	2-7	2-9	2-13	3-15	3-16	3-17	4-27	4-32	5-33	5-34
1		CC	CC	LC	LL	LL	LL	LC	LC	LC	LC	CC	CC	CC	LC
2	6	LC	CC	CC	LC	LC	LC	LL	LL	LL	LL	LL	LC	LC	LC
3	8	LC	CC	LC	LC	LC	LC	LC	LC	CC	LC	LL	LC	CC	LC
4	3	LC	LC	LC	LC	LC	LL	LL	LL	CC	LC	LC	LC	LC	LC
5	5	LC	CC	CC	LC	LC	LC	LC	CC	CC	CC	LL	LC	CC	LC
6	7	LC	LC	CC	CC	CC	CC	LC	CC	LL	LL	LL	LL	CC	LL
7	9	LC	LC	LC	LC	LC	LC	LC	LC	LC	LC	LL	LL	LC	LC
8	10	LC	LC	LC	LC	LC	LL	LC	LC	LC	LC	LL	LC	CC	LC
9	12	LC	LC	CC	CC	CC	CC	LC	LL	CC	LC	LC	LC	LL	LC
10	14	CC	LC	LC	LC	LC	LC	LC	LL	LL	LL	LL	LL	LC	LC
11	16	LC	LC	LL	LL	LL	LC	CC	LL	LC	LC	CC	LC	CC	LC
12	18	LL	LL	LL	LC	LC	LC	LC	LC	LC	LC	LL	LL	CC	CC
13	21	LC	LL	LC	CC	LC	LL	LL	LC	LC	LL	LL	LC	CC	LL
14	11	LC	LC	LC	CC	CC	LC	LC	LL	LC	LC	LL	LL	LL	CC
15	13	LC	LL	LC	LC	CC	CC	LL	CC	LC	CC	LL	LC	CC	LC
16	15	CC	LC	LC	LC	LL	LL	LL	LC	CC	LC	LL	LL	CC	LC
17	19	LC	CC	LL	LC	LC	LC	LL	LC	CC	LC	LL	LL	CC	LC
18	22	CC	LC	CC	LC	LC	LC	LL	LC	LL	LL	LC	CC	CC	LC
19	23	LC	LC	LC	LC	LL	LL	LC	LC	LC	CC	LC	LC	LC	CC
20	25	LC	LL	CC	LC	LC	LC	LL	LC	LL	CC	LL	LL	CC	CC
21	27	CC	LC	LC	LC	CC	CC	CC	LL	LL	CC	LL	LL	CC	LC
22	30	LC	LC	CC	LL	LL	LL	LL	LC	CC	LC	LC	CC	LC	LL
23	32	LC	LC	LL	LC	LC	LL	LC	LL	LL	LL	CC	LC	CC	CC
24	34	LC	LC	LC	LL	LL	LL	LL	CC	CC	CC	LL	CC	LC	LC
25	24	LC	LL	LC	LC	LC	LL	LC	LC	CC	LC	LL	LL	LC	LC
26	26	LL	LC	CC	LC	LC	CC	CC	LC	LC	CC	LL	LC	LC	LC
27	28	LC	LC	CC	LC	LC	CC	LC	LC	LC	LC	LL	LC	CC	CC
28	31	LL	LC	LC	CC	LC	LC	LC	LC	CC	LC	LC	LC	LC	LC
29	33	CC	LC	LC	LC	LC	LC	LC	LC	LC	LC	LL	LL	LC	LL
30	37	CC	LL	LL	LL	LL	LL	LL	LC	LC	LC	LL	LL	LC	LC
31	38	CC	LC	LC	LL	LC	LL	LL	CC	CC	CC	LL	LL	LL	LC
32	40	LC	LC	CC	LL	LL	LL	CC	LC	LC	LC	LL	LL	LC	LC
33	43	CC	CC	LC	CC	CC	CC	LC	LC	CC	CC	LL	LL	LC	LC
34	39	LL	LL	CC	CC	CC	LC	LC	CC	LC	LC	LL	LL	LC	LC
35	42	LC	LC	LC	LL	LL	LL	CC	LL	CC	CC	LL	LL	LC	LC
	L*er*-0	**6**	**7**	**5**	**8**	**9**	**14**	**12**	**9**	**6**	**7**	**25**	**18**	**2**	**4**
	col	**9**	**6**	**12**	**7**	**7**	**7**	**5**	**6**	**14**	**9**	**4**	**3**	**16**	**6**
	Het	**20**	**22**	**18**	**20**	**19**	**14**	**18**	**20**	**15**	**19**	**5**	**13**	**17**	**25**
	% linkage	**54**	**48**	**60**	**48**	**47**	**40**	**40**	**45**	**61**	**52**	**19**	**28**	**70**	**52**

Appendix 3.4.5. Genetic analysis of *dis58* recombinants. HRM-PCR was performed to investigate linkage of 19 SNP markers across the whole genome to *dis58* delayed degreening phenotype. Order of the SNP markers from left to right corresponds to north (up) to south (down) of chromosomes (Fig. 3.4.6). Recombinant number is the unique identifier for that plant in the F2 population tested. LL = homozygous L*er*-0, CC = homozygous Col-0, LC = heterozygous

#	*dis58* F2	1-1	1-2	1-3	1-4	2-5	2-7	2-9	2-13	3-15	3-16	3-17	4-27	4-32	5-33	5-34
1	1	CC	CC	LC	LL	LC	LC	LL	LL	CC	LC	CC	LC	LL	LC	LL
2	2	LC	CC	CC	LC	LL	LL	LC	LL	LC	LC	LC	LL	LL	LC	CC
3	4	CC	LC	CC	LC	CC	LC	LC	LC	CC	CC	CC	LL	LL	CC	CC
4	8	LC	LL	LC	LC	LC	LC	CC	CC	LC	CC	CC	LC	CC	LC	CC
5	12	LC	LL	LL	LC	LC	LC	LC	LL	LL	LC	CC	LL	LC	LC	LC
6	14	LC	LC	LC	CC	LC	CC	LC	LC	LL	LC	LL	LL	LC	LL	LC
7	17	LC	LC	LC	LC	CC	CC	CC	LC	LL	LC	LC	LL	LC	LC	LL
8	19	CC	LC	LC	LC	LC	LC	LC	LC	LC	LC	LC	LC	LL	CC	CC
9	6	LL	CC	LC	CC	CC	CC	LC	LC	CC	LC	CC	LL	LL	LC	CC
10	11	LL	LC	LC	LL	LL	LL	LL	LC	LC	CC	LC	LL	LC	CC	CC
11	13	CC	CC	LC	LL	LC	LL	LL	LL	LL	LC	LC	LL	LC	CC	LC
12	15	CC	LC	LC	LL	LC	LC	CC	CC	LC	LC	LC	LL	LC	LL	CC
13	18	CC	LC	LC	LC	LC	LC	LC	LC	LL	LC	LL	LL	LC	CC	CC
14	21	LC	LL	LL	LC	LC	LC	LC	LC	LC	LC	LC	LL	LL	LC	CC
15	22	LC	LL	LL	LC	LL	LL	LC	CC	LC	CC	LC	LC	LL	CC	LC
16	8b	CC	CC	CC	CC	LL	LC	LC	LC	LC	LC	LC	LL	LC	LC	LC
17	14b	LL	LL	CC	CC	LC	LC	CC	LC	LC	LC	CC	LL	LC	LL	CC
18	16b	LL	LL	LL	LL	LC	LC	LL	LC	LC	LC	LC	LL	LC	LC	LC
19	19b	CC	LC	CC	LC	LC	LC	LC	LL	LL	LC	LC	LC	LL	LC	LC
20	3b	CC	LC	CC	LL	LL	LL	LL	LL	LC	LC	LC	LL	LL	CC	LL
21	2b	LL	LC	CC	LC	LL	LC	LC	LC	LL	LC	LL	LL	LC	CC	LC
22	12b	LC	LL	LL	LL	LC	LC	CC	LC	LC	LC	LC	LL	LC	CC	CC
23	15b	LC	LL	LL	LL	CC	LC	LL	LL	LC	CC	LC	LL	LL	LL	LC
24	17b	CC	LC	CC	CC	LC	LC	LC	LC	LC	LL	CC	LL	LC	LL	LC
25	1b	LC	CC	CC	CC	LC	LC	LC	CC	LC	LC	LC	LC	CC	CC	LC
26	8b	LC	LC	LC	CC	LC	LC	LL	LL	LC	LC	LL	LL	LC	CC	CC
	L*er*-o	**5**	**8**	**6**	**7**	**6**	**6**	**7**	**8**	**7**	**1**	**4**	**20**	**14**	**5**	**3**
	Col-0	**10**	**6**	**9**	**6**	**4**	**2**	**5**	**4**	**3**	**5**	**7**		**2**	**11**	**12**
	Het	**11**	**12**	**11**	**13**	**16**	**18**	**14**	**14**	**16**	**20**	**15**	**6**	**10**	**10**	**11**
	% linkage	**59**	**46**	**55**	**47**	**46**	**42**	**40**	**42**	**42**	**57**	**55**	**12**	**27**	**61**	**67**

Appendix 3.5.1. List of primers used for cloning sequencing and RT-PCR.

utilization	Name	Sense-primer	Anti-sense primer
dis58 Sanger sequencing	*AT4G13495S1140*	*TATCTTTTAACCGTATTCT*	
dis58 reverse transcriptase PCR	*A470S-1254AS*	*GGTTAGATAGAAACTGATTAGATCTGAGAC*	*ATTTAGTGTTTTGTTTTGCTCTCA*
reverse-strand primer KS-DT		*CGGTACCGATAAGCTTGATTTTTTTTTTTTTTTTT*	
SALK_092164 genotyping	*LF+RP*	*GGAGGTTTTATATGGGAACGG*	*CATATTACCACCGCATATGGC*
	LBb1.3+RP	*ATTTTGCCGATTTCGGAAC*	*CAATGCAAACCCCATTATCC*
dis58 cloning	*864S-6505AS*	*ggcCTGCAGGTTGTGGAATAATCTCTTGTCAGG*	*cgcGCGGCCGCCCAGATAAGGCAAGTGTAGGATTC*
BASTA resistance gene	*BAR*	*GAAGTCCAGCTGCCAGAAAC*	*TCGTCAACCACTACATCCAGAC*
qRT-PCR	*PP2A*	*GTTCTCCACAACCGCTTGGT*	*TAACGTGGCCAAAATGATGC*
qRT-PCR	*EIN2*	*ATCATGGCGATTTCGAAGGTCTG*	*AGGAAGCCCTAACAGAGCAACC*
qRT-PCR	*SAG12*	*GCTCCTTCAATAGCCGCAACCG*	*CGTTTCTTCTGGTGCTTTGCCG*
qRT-PCR	*ACO1*	*TAATGCACCGTGTGATGACCCAGA*	*GTCCCACTCTCAACAGTCGTCACTTTAC*
qRT-PCR	*AtNAP*	*TGAACCGCTGTGAATGGCTTTGT*	*GACCCATGGCAATTACCCGAGAA*
qRT-PCR	*JAZ10*	*TCGAGAAGCGCAAGGAGAGATTAG*	*TCGTTTAGGCCGATGTCGGATAG*
qRT-PCR	*ERF1*	*CCTTCAACGAGAACGACTCAGAGG*	*AGGTTTGTTGCGTGGACTGCTC*
qRT-PCR	*ORA59*	*CTTGTTCTCTTTGCTGCTTTCGAC*	*CTCGCACAACTTCTGTGCTTCC*
qRT-PCR	*EIN3*	*AACTGGCATGTCCACATCGAGAC*	*ATGAAACCTGGATGGTGCTGCTC*
qRT-PCR	*PDF1.2*	*ATCAGGCGGCTTTCGCTTTG*	*CTTCCGGAGAGATTCTTCAACGAC*
qRT-PCR	*SEN4*	*GTTCGACCCAACCGCCAATTTC*	*GGTGTGTCATCGACGGTCAATATG*
qRT-PCR	*ACO4*	*GATCTCGACGACGATTACAGAACG*	*TCTCGCACAGCAGATCCAGTAG*
qRT-PCR	*ACS2*	*ACTCCGTGTTCTCCCGGATATG*	*TCGATCAAGCACGACCATCGAC*
qRT-PCR	*RAP2.4*	*TTGTCGGAGCTGACGTTTGGTG*	*GCTTTGCGTCGACAGAGGAATG*
qRT-PCR	*ERF11*	*GGTGGTGCAGAACAACAAACGC*	*AATAACCCGCCGCCAAAGTCAC*
qRT-PCR	*NAC3*	*CGTCGAAATGGAAGCACCAAGC*	*TGTCGACGAACCATTGTTGCTG*
qRT-PCR	*NAC092*	*TCGGGTATTTCCGGTCTCTCAC*	*CTTACCATGGAAGGCTAAGATGGG*

Appendix 3.5.2. Genetic map of 5.6 kb AT4G13495 genomic DNA fragment in pGEM®-T Easy Vector.

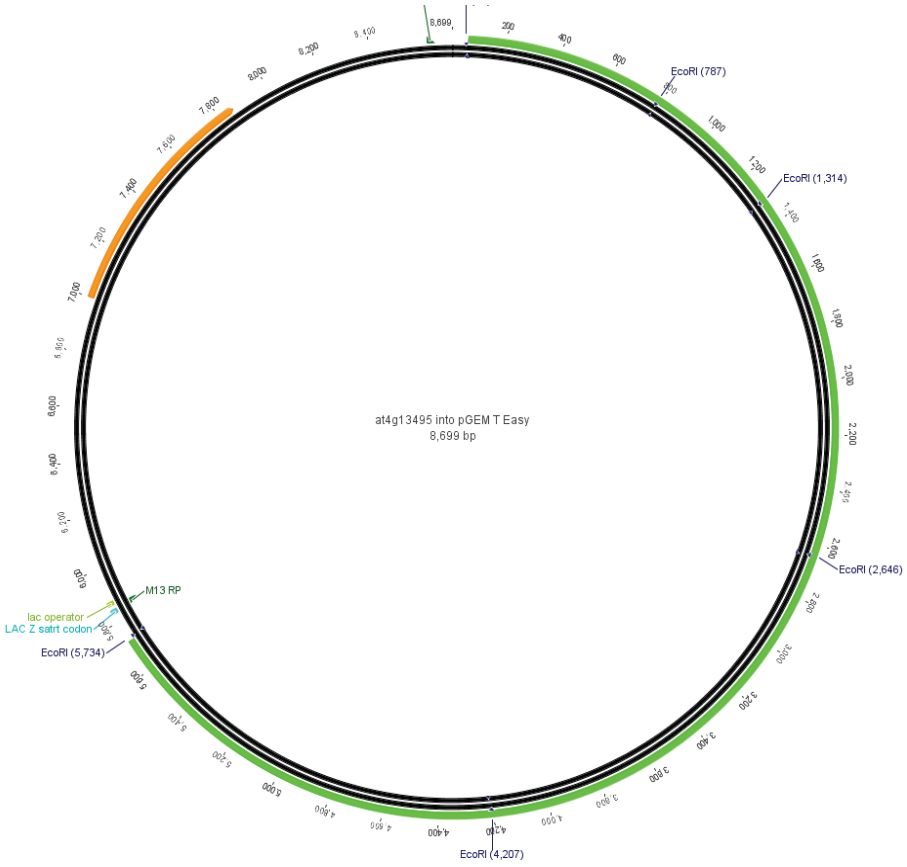

Appendix 3.5.3. Genetic map of 5.6 kb AT4G13495 genomic DNA fragment in pGreen 0229.

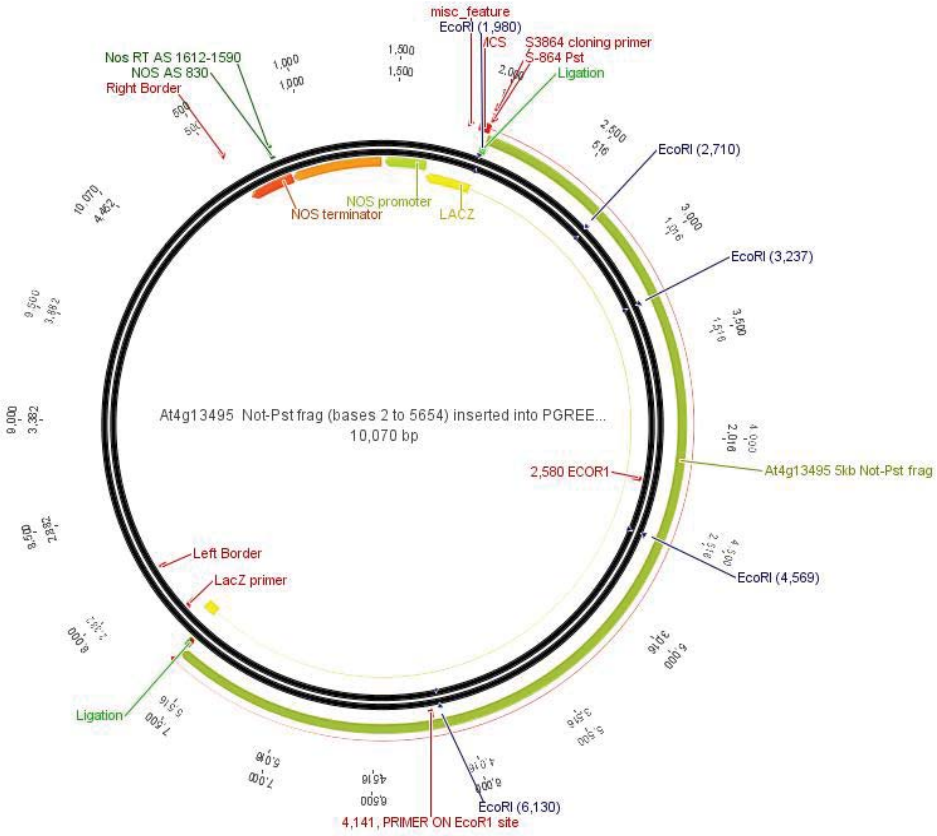

Bibliography

Aiamla-or, S., Nakajima, T., Shigyo, M. and Yamauchi, N. (2012). Pheophytinase activity and gene expression of chlorophyll-degrading enzymes relating to UV-B treatment in postharvest broccoli (*Brassica oleracea* Italica Group) florets. Postharvest Biology and Technology **63,** 60-66.

Alonso, J.M., Hirayama, T., Roman, G., Nourizadeh, S. and Ecker, J.R. (1999). EIN2, a bifunctional transducer of ethylene and stress responses in Arabidopsis. Science **284,** 2148-2152.

Amir-Shapira, D., Goldschmidt, E.E. and Altman, A. (1987). Chlorophyll catabolism in senescing plant tissues: in vivo breakdown intermediates suggest different degradative pathways for citrus fruit and parsley leaves. Proceedings of the National Academy of Sciences of the United States of America **84,** 1901-1905.

Arrom, L. and Munné-Bosch, S. (2012). Hormonal regulation of leaf senescence in Lilium. Plant Physiology 169,1542-50.

Azumi, Y. and Watanabe, A. (1991). Evidence for a senescence-associated gene induced by darkness. Plant Physiology **95,** 577-583.

Baena-González, E. (2010). Energy signalling in the regulation of gene expression during stress. Molecular Plant **3,** 300-313.

Baena-González, E. and Sheen, J. (2008). Convergent energy and stress signalling. Trends Plant Science **13,** 474-482.

Baena-González, E., Rolland, F., Thevelein, J.M. and Sheen, J. (2007). A central integrator of transcription networks in plant stress and energy signalling. Nature **448,** 938-942.

Balazadeh, S., Riaño-Pachón, D. and Mueller-Roeber, B. (2008). Transcription factors regulating leaf senescence in *Arabidopsis thaliana*. Plant Biology **10,** 63-75.

Balazadeh, S., Kwasniewski, M., Caldana, C., Mehrnia, M., Zanor, M.I., Xue, G.P. and Mueller-Roeber, B. (2011). ORS1, an H_2O_2-responsive NAC transcription factor, controls senescence in *Arabidopsis thaliana*. Molecular Plant **4,** 346-360.

Balazadeh, S., Siddiqui, H., Allu, A.D., Matallana-Ramirez, L.P., Caldana, C., Mehrnia, M., Zanor, M.I., Köhler, B. and Mueller-Roeber, B. (2010). A gene regulatory network controlled by the NAC transcription factor ANAC092/AtNAC2/ORE1 during salt-promoted senescence. Plant Journal **62,** 250-264.

Barah, P., Winge, P., Kusnierczyk, A., Tran, D.H. and Bones, A.M. (2013). Molecular signatures in *Arabidopsis thaliana* in response to insect attack and bacterial infection. Plos One **8,** e58987.

Bariola, P.A., Howard, C.J., Taylor, C.B., Verburg, M.T., Jaglan, V.D. and Green, P.J. (1994). The Arabidopsis ribonuclease gene Rns1 is tightly controlled in response to phosphate limitation. Plant Journal **6,** 673-685.

Bassham, D.C., Laporte, M., Marty, F., Moriyasu, Y., Ohsumi, Y., Olsen, L.J. and Yoshimoto, K. (2006). Autophagy in development and stress responses of plants. Autophagy **2,** 2-11.

Bate, N.J., ROTHSTEIN, S.J. and THOMPSON, J.E. (1991). Expression of nuclear and chloroplast photosynthesis-specific genes during leaf senescence. Journal of Experimental Botany **42,** 801-811.

Batista, R., Saibo, N., Lourenço, T. and Oliveira, M.M. (2008). Microarray analyses reveal that plant mutagenesis may induce more transcriptomic changes than transgene insertion. Proceedings of the National Academy of Sciences of the United States of America **105,** 3640-3645.

Becker, W. and Apel, K. (1993). Differences in gene-expression between natural and artificially induced leaf senescence. Planta **189,** 74-79.

Beddington, S.J. (2011). The future of food and farming. International Journal of Agricultural Management **1,** 2-6.

Beers, E.P., Jones, A.M. and Dickerman, A.W. (2004). The S8 serine, C1A cysteine and A1 aspartic protease families in Arabidopsis. Phytochemistry **65,** 43-58.

Besseau, S., Li, J. and Palva, E.T. (2012). WRKY54 and WRKY70 co-operate as negative regulators of leaf senescence in *Arabidopsis thaliana*. Journal of Experimental Botany **63***,* 2667–2679.

Bhattacharjee, S. (2005). Reactive oxygen species and oxidative burst: Roles in stress, senescence and signal transduction in plants. Current Science **89,** 1113-1121.

Bichet, A., Desnos, T., Turner, S., Grandjean, O. and Höfte, H. (2001). BOTERO1 is required for normal orientation of cortical microtubules and anisotropic cell expansion in Arabidopsis. The Plant Journal **25,** 137-148.

Biddinger, E.J., Liu, C., Joly, R.J. and Raghothama, K. (1998). Physiological and molecular responses of aeroponically grown tomato plants to phosphorus deficiency. Journal of the American. Society for Horticultural Sciences **123,** 330-333.

Bleecker, A.B. and Patterson, S.E. (1997). Last exit: senescence, abscission and meristem arrest in Arabidopsis. The Plant Cell **9,** 1169.

Borochov, A., Mayak, S. and Halevy, A.H. (1976). Combined effects of abscisic acid and sucrose on growth and senescence of rose flowers. Physiologia Plantarum **36,** 221-224.

Bosse, C. and Van Staden, J. (1989). Cytokinins in cut carnation flowers. V. Effects of cytokinin type, concentration and mode of application on flower longevity. Plant Physiology **135,** 155-159.

Bouchez, O., Huard, C., Lorrain, S., Roby, D. and Balague, C. (2007). Ethylene is one of the key elements for cell death and defense response control in the Arabidopsis lesion mimic mutant vad1. Plant Physiology **145,** 465-477.

Bourguet, D. (1999). The evolution of dominance. Heredity **83,** 1-4.

Bowman, J.L., Smyth, D.R. and Meyerowitz, E.M. (1989). Genes directing flower development in Arabidopsis. The Plant Cell **1,** 37-52.

Breeding, M.P., Deng, X., Xiong, L., Wang, Y. and Li, X. (2011). Ectopic expression of an AGAMOUS homolog NTAG1 from Chinese narcissus accelerated earlier flowering and senescence in Arabidopsis. Molecular Plant Breeding **2,** 00424.

Breeze, E., Harrison, E., McHattie, S., Hughes, L., Hickman, R., Hill, C., Kiddle, S., Kim, Y.S., Penfold, C.A., Jenkins, D., Zhang, C., Morris, K., Jenner, C., Jackson, S., Thomas, B., Tabrett, A., Legaie, R., Moore, J.D., Wild, D.L., Ott, S., Rand, D., Beynon, J., Denby, K., Mead, A. and Buchanan-Wollaston, V. (2011). High-resolution temporal profiling of transcripts during Arabidopsis leaf senescence reveals a distinct chronology of processes and regulation. The Plant Cell **23,** 873-894.

Brosnan, C.A. and Voinnet, O. (2009). The long and the short of noncoding RNAs. Current Opinion. in Cell Biology. **21,** 416-425.

Brychkova, G., Alikulov, Z., Fluhr, R. and Sagi, M. (2008). A critical role for ureides in dark and senescence-induced purine remobilization is unmasked in the Atxdh1 Arabidopsis mutant. The Plant Journal **54,** 496-509.

Buchanan-Wollaston, V., Page, T., Harrison, E., Breeze, E., Lim, P.O., Nam, H.G., Lin, J.F., Wu, S.H., Swidzinski, J., Ishizaki, K. and Leaver, C.J. (2005). Comparative transcriptome analysis reveals significant differences in gene expression and signalling pathways between developmental and dark/starvation-induced senescence in Arabidopsis. The Plant Journal **42,** 567-585.

Burleigh, S.M. and Harrison, M.J. (1998). Characterization of the Mt4 gene from *Medicago truncatula*. Gene **216,** 47-53.

Busch, M.A., Bomblies, K. and Weigel, D. (1999). Activation of a floral homeotic gene in Arabidopsis. Science **285,** 585-587.

Campos-Ortega, J.A. and Knust, E. (1990). Molecular analysis of a cellular decision during embryonic development of *Drosophila melanogaster*: epidermogenesis or neurogenesis. European Journal of Biochemistry **190,** 1-10.

Cao, W.H., Liu, J., He, X.J., Mu, R.L., Zhou, H.L., Chen, S.Y. and Zhang, J.S. (2007). Modulation of ethylene responses affects plant salt-stress responses. Plant Physiology **143,** 707-719.

Chandra, H.S. and Nanjundiah, V. (1990). The evolution of genomic imprinting. Development **108,** 47-53.

Chao, Q., Rothenberg, M., Solano, R., Roman, G., Terzaghi, W. and Ecker, J.R. (1997). Activation of the ethylene gas response pathway in Arabidopsis by the nuclear protein ETHYLENE-INSENSITIVE3 and related proteins. Cell **89,** 1133-1144.

Chen, C.T., Li, C.C. and Kao, C.H. (1991). Senescence of rice leaves XXXI. Changes of chlorophyll, protein and polyamine contents and ethylene production during senescence of a chlorophyll-deficient mutant. Journal of Plant Growth Regulation. **10,** 201-205.

Chen, G.-H., Liu, C.-P., Chen, S.-C.G. and Wang, L.-C. (2012). Role of ARABIDOPSIS A-FIFTEEN in regulating leaf senescence involves response to reactive oxygen species and is dependent on ETHYLENE INSENSITIVE2. Journal of Experimental Botany. **63,** 275-292.

Chen, L.-F.O., Hwang, J.-Y., Charng, Y.-Y., Sun, C.-W. and Yang, S.-F. (2001). Transformation of broccoli (*Brassica oleracea* var. *italica*) with isopentenyltransferase gene via Agrobacterium tumefaciens for post-harvest yellowing retardation. Molecular Breeding **7,** 243-257.

Chen, L.-F.O., Huang, J.-Y., Wang, Y.-H., Chen, Y.-T. and Shaw, J.-F. (2004). Ethylene insensitive and post-harvest yellowing retardation in mutant ethylene response sensor (boers) gene transformed broccoli (*Brassica olercea* var. *italica*). Molecular Breeding. **14,** 199-213.

Chen, L.-F.O., Lin, C.-H., Kelkar, S.M., Chang, Y.-M. and Shaw, J.-F. (2008). Transgenic broccoli (*Brassica oleracea* var. *italica*) with antisense chlorophyllase (*BoCLH1*) delays postharvest yellowing. Plant Science **174,** 25-31.

Chen, M.K., Hsu, W.H., Lee, P.F., Thiruvengadam, M., Chen, H.I. and Yang, C.H. (2011). The MADS box gene, FOREVER YOUNG FLOWER, acts as a repressor controlling floral organ senescence and abscission in Arabidopsis. The Plant Journal **68,** 168-185.

Chiba, A., Ishida, H., Nishizawa, N.K., Makino, A. and Mae, T. (2003). Exclusion of ribulose-1,5-bisphosphate carboxylase/oxygenase from chloroplasts by specific bodies in naturally senescing leaves of wheat. Plant and Cell Physiology **44,** 914-921.

Cho, Y.-H., Sheen, J. and Yoo, S.-D. (2010). Low glucose uncouples hexokinase1-dependent sugar signalling from stress and defense hormone abscisic acid and C2H4 responses in Arabidopsis. Plant Physiology **152,** 1180-1182.

Chung, D.W., Pružinská, A., Hörtensteiner, S. and Ort, D.R. (2006). The role of pheophorbide a oxygenase expression and activity in the canola green seed problem. Plant Physiology **142,** 88-97.

Chung, H.S. and Howe, G.A. (2009). A critical role for the TIFY motif in repression of jasmonate signalling by a stabilized splice variant of the JASMONATE ZIM-domain protein JAZ10 in Arabidopsis. The Plant Cell **21,** 131-145.

Chung, H.S., Koo, A.J., Gao, X., Jayanty, S., Thines, B., Jones, A.D. and Howe, G.A. (2008). Regulation and function of Arabidopsis JASMONATE ZIM-domain genes in response to wounding and herbivory. Plant Physiology **146,** 952-964.

Clark, R.M., Schweikert, G., Toomajian, C., Ossowski, S., Zeller, G., Shinn, P., Warthmann, N., Hu, T.T., Fu, G. and Hinds, D.A. (2007). Common sequence polymorphisms shaping genetic diversity in *Arabidopsis thaliana*. Science **317,** 338-342.

Clarke, S.F., Jameson, P.E. and Downs, C. (1994). The influence of 6-benzylaminopurine on post-harvest senescence of floral tissues of broccoli (*Brassica oleracea* var *Italica*). Plant Growth Regulation **14,** 21-27.

Clough, S.J. and Bent, A.F. (1998). Floral dip: a simplified method for Agrobacterium-mediated transformation of *Arabidopsis thaliana*. The Plant Journal **16,** 735-743.

Clouse, S.D., Langford, M. and McMorris, T.C. (1996). A brassinosteroid-insensitive mutant in *Arabidopsis thaliana* exhibits multiple defects in growth and development. Plant Physiology **111,** 671-678.

Conklin, P.L., Norris, S.R., Wheeler, G.L., Williams, E.H., Smirnoff, N. and Last, R.L. (1999). Genetic evidence for the role of GDP-mannose in plant ascorbic acid (vitamin C) biosynthesis. Proceedings of the National Academy of Sciences of the United States of America **96,** 4198-4203.

Coupe, S.A., Sinclair, B.K., Watson, L.M., Heyes, J.A. and Eason, J.R. (2003). Identification of dehydration-responsive cysteine proteases during post-harvest senescence of broccoli florets. Joural of Experimental Botany **54,** 1045-1056.

Craftsbrandner, S.J., Below, F.E., Harper, J.E. and Hageman, R.H. (1984). Effects of pod removal on metabolism and senescence of nodulating and nonnodulating soybean isolines enzymes and chlorophyll. Plant Physiology **75,** 318-322.

Cuperus, J.T., Montgomery, T.A., Fahlgren, N., Burke, R.T., Townsend, T., Sullivan, C.M. and Carrington, J.C. (2010). Identification of MIR390a precursor processing-defective mutants in Arabidopsis by direct genome sequencing. Proceedings of the National Academy of Sciences of the United States of America **107,** 466-471.

Dai, N., Schaffer, A., Petreikov, M., Shahak, Y., Giller, Y., Ratner, K., Levine, A. and Granot, D. (1999). Overexpression of Arabidopsis hexokinase in tomato plants inhibits growth, reduces photosynthesis and induces rapid senescence. Plant Cell **11,** 1253-1266.

Davies, P. and Gan, S. (2012). Towards an integrated view of monocarpic plant senescence. Russian Journal of Plant Physiology **59,** 467-478.

Davies, P.J. (1995). The plant hormones: their nature, occurrence and functions. In Plant hormones Plant Hormones Physiology, Biochemistry and Molecular Biology, Kluwer Academic Publishers, Dordrecht (1995), pp. 1‑12.

Dellaporta, S.L., Wood, J. and Hicks, J.B. (1983). A plant DNA minipreparation: version II. Plant Molecular Biology Reporter **1,** 19-21.

Diaz, C., Saliba-Colombani, V., Loudet, O., Belluomo, P., Moreau, L., Daniel-Vedele, F., Morot-Gaudry, J.-F. and Masclaux-Daubresse, C. (2006). Leaf yellowing and anthocyanin accumulation are two genetically independent strategies in response to nitrogen limitation in *Arabidopsis thaliana*. Plant and Cell Physiology. **47,** 74-83.

Dixit, R. and Cyr, R. (2004). The cortical microtubule array: from dynamics to organization. The Plant Cell **16,** 2546-2552.

Doelling, J.H., Walker, J.M., Friedman, E.M., Thompson, A.R. and Vierstra, R.D. (2002). The APG8/12-activating enzyme APG7 is required for proper nutrient recycling and senescence in *Arabidopsis thaliana*. The Journal of Biological Chemistry **277,** 33105-33114.

Doi, M. and Reid, M.S. (1995). Sucrose improves the postharvest life of cut flowers of a hybrid *Limonium*. HortScience **30,** 1058-1060.

Douglas, S.J., Chuck, G., Dengler, R.E., Pelecanda, L. and Riggs, C.D. (2002). KNAT1 and ERECTA regulate inflorescence architecture in Arabidopsis. The Plant Cell **14,** 547-558.

Downs, C.G., Somerfield, S.D. and Davey, M.C. (1997). Cytokinin treatment delays senescence but not sucrose loss in harvested broccoli. Postharvest Biology and Technology **11,** 93-100.

Drouaud, J., Camilleri, C., Bourguignon, P.-Y., Canaguier, A., Bérard, A., Vezon, D., Giancola, S., Brunel, D., Colot, V. and Prum, B. (2006). Variation in crossing-over rates across chromosome 4 of *Arabidopsis thaliana* reveals the presence of meiotic recombination “hot spots”. Genome Research **16,** 106-114.

Eason, J., Ryan, D., Watson, L., Hedderley, D., Christey, M., Braun, R. and Coupe, S. (2005). Suppression of the cysteine protease, aleurain, delays floret senescence in *Brassica oleracea*. Plant Molecular Biology **57,** 645-657.

Eastmond, P.J. and Graham, I.A. (2003). Trehalose metabolism: a regulatory role for trehalose-6-phosphate? Currebt Opinion in Plant Biology **6,** 231-235.

Eddy, S.R. (2001). Non–coding RNA genes and the modern RNA world. Nature Reviews in Genetics **2,** 919-929.

Elena, S.F. and de Visser, J.A.G. (2003). Environmental stress and the effects of mutation. Journal of Biology **2,** 12.

Engqvist, M.K.M., Kuhn, A., Wienstroer, J., Weber, K., Jansen, E.E.W., Jakobs, C., Weber, A.P.M. and Maurino, V.G. (2011). Plant D-2-hydroxyglutarate dehydrogenase participates in the catabolism of lysine especially during senescence. The Journal of Biological Chemistry **286,** 11382-11390.

Eulgem, T., Rushton, P.J., Robatzek, S. and Somssich, I.E. (2000). The WRKY superfamily of plant transcription factors. Trends in Plant Sciences **5,** 199-206.

Evans, N.H. (2003). Modulation of guard cell plasma membrane potassium currents by methyl jasmonate. Plant Physiology **131,** 8-11.

Eveland, A.L. and Jackson, D.P. (2012). Sugars, signalling and plant development. Journal of Experimental Botany **63,** 3367-3377.

Fan, L., Zheng, S.Q. and Wang, X.M. (1997). Antisense suppression of phospholipase D alpha retards abscisic acid- and ethylene-promoted senescence of postharvest Arabidopsis leaves. The Plant Cell **9,** 2183-2196.

Favaro, R., Pinyopich, A., Battaglia, R., Kooiker, M., Borghi, L., Ditta, G., Yanofsky, M.F., Kater, M.M. and Colombo, L. (2003). MADS-box protein complexes control carpel and ovule development in Arabidopsis. The Plant Cell **15,** 2603-2611.

Feldman, P.L., Griffith, O.W., Hong, H. and Stuehr, D.J. (1993). Irreversible inactivation of macrophage and brain nitric-oxide synthase by l-n(g)-methylarginine requires nadph-dependent hydroxylation. Journal of Medicinal Chemistry **36,** 491-496.

Feldmann, K.A., Malmberg, R.L. and Dean, C. (1994). Mutagenesis in Arabidopsis. Cold Spring Harbor Monograph Archive **27,** 137-172.

Feller, U. anders, I. and Mae, T. (2008). Rubiscolytics: fate of Rubisco after its enzymatic function in a cell is terminated. Journal of Experimental Botany **59,** 1615-1624.

Fernandez, D.E., Heck, G.R., Perry, S.E., Patterson, S.E., Bleecker, A.B. and Fang, S.-C. (2000). The embryo MADS domain factor AGL15 acts postembryonically: Inhibition of perianth senescence and abscission via constitutive expression. The Plant Cell **12,** 183-197.

Finnemann, J. and Schjoerring, J.K. (2000). Post-translational regulation of cytosolic glutamine synthetase by reversible phosphorylation and 14-3-3 protein interaction. The Plant Journal **24,** 171-181.

Fischer-Kilbienski, I., Miao, Y., Roitsch, T., Zschiesche, W., Humbeck, K. and Krupinska, K. (2010). Nuclear targeted AtS40 modulates senescence associated gene expression in *Arabidopsis thaliana* during natural development and in darkness. Plant Molecular Biology **73,** 379-390.

Fisher, R.A. (1999). The genetical theory of natural selection: a complete variorum edition. Oxford University Press.

Fisher., R.A. (1934). Professor Wright on the theory of dominance. The American Naturalist 68:370-374.

Friedrich, J.W. and Huffaker, R.C. (1980). Photosynthesis, leaf resistances and ribulose-1,5-bisphosphate carboxylase degradation in senescing barley leaves. Plant Physiology **65,** 1103-1107.

Fröhlich, V. and Feller, U. (1991). Effect of phloem interruption on senescence and protein remobilization in the flag leaf of field-grown wheat. Biochemie und Physiologie der Pflanzen **187,** 139-147.

Fujiki, Y., Ito, M., Nishida, I. and Watanabe, A. (2000). Multiple signalling pathways in gene expression during sugar starvation. Pharmacological analysis of DIN gene expression in suspension-cultured cells of Arabidopsis. Plant Physiology **124,** 1139-1148.

Fukao, T., Yeung, E. and Bailey-Serres, J. (2012). The submergence tolerance gene SUB1A delays leaf senescence under prolonged darkness through hormonal regulation in rice. Plant Physiology **160,** 1795-1807.

Gan, S. and Amasino, R.M. (1995). Inhibition of leaf senescence by autoregulated production of cytokinin. Science **270,** 1986-1988.

Gan, S.S. and Amasino, R.M. (1997). Making sense of senescence - Molecular genetic regulation and manipulation of leaf senescence. Plant Physiology **113,** 313-319.

Gapper, N.E., Coupe, S.A., McKenzie, M.J., Scott, R.W., Christey, M.C., Lill, R.E., McManus, M.T. and Jameson, P.E. (2005). Senescence-associated down-regulation of 1-aminocyclopropane-1-carboxylate (ACC) oxidase delays harvest-induced senescence in broccoli. Functional Plant Biology 32, 891-901.

Gepstein, S. and Thimann, K.V. (1980). Changes in the abscisic acid content of oat leaves during senescence. Proceedings of the National Academy of Sciences of the United States of America **77,** 2050-2053.

Gepstein, S. and Glick, B.R. (2013). Strategies to ameliorate abiotic stress-induced plant senescence. Plant Molecular Biology **82, 623-633**.

Gepstein, S., Sabehi, G., Carp, M.J., Hajouj, T., Nesher, M.F.O., Yariv, I., Dor, C. and Bassani, M. (2003). Large-scale identification of leaf senescence-associated genes. The Plant Journal **36,** 629-642.

Gómez-Lobato, M.E., Hasperué, J.H., Civello, P.M., Chaves, A.R. and Martínez, G.A. (2012). Effect of 1-MCP on the expression of chlorophyll degrading genes during senescence of broccoli (*Brassica oleracea*). Scientia Horticulturae **144,** 208-211.

Gomez-Lobato, M.E., Civello, P.M. and Martínez, G.A. (2012). Effects of ethylene, cytokinin and physical treatments on BoPaO gene expression of harvested broccoli. Journal of the Science of Food and Agriculture **92,** 151-158.

Graham, I.A. and Eastmond, P.J. (2002). Pathways of straight and branched chain fatty acid catabolism in higher plants. Progress in Lipid Research **41,** 156-181.

Grbic, V. and Bleecker, A.B. (1995). Ethylene regulates the timing of leaf senescence in Arabidopsis. The Plant Journal **8,** 595-602.

Gregersen, P., Holm, P. and Krupinska, K. (2008). Leaf senescence and nutrient remobilisation in barley and wheat. Plant Biology **10,** 37-49.

Gundry, C.N., Vandersteen, J.G., Reed, G.H., Pryor, R.J., Chen, J. and Wittwer, C.T. (2003). Amplicon melting analysis with labeled primers: a closed-tube method for differentiating homozygotes and heterozygotes. Clinical Chemistry **49,** 396-406.

Guo, F.Q. and Crawford, N.M. (2005). Arabidopsis nitric oxide synthase1 is targeted to mitochondria and protects against oxidative damage and dark-induced senescence. The Plant Cell **17,** 3436-3450.

Guo, Y. and Gan, S. (2006). AtNAP, a NAC family transcription factor, has an important role in leaf senescence. The Plant Journal **46,** 601-612.

Guo, Y., Cai, Z. and Gan, S. (2004). Transcriptome of Arabidopsis leaf senescence. Plant, Cell and Environment. **27,** 521-549.

Guo, Y.F. and Gan, S.S. (2012). Convergence and divergence in gene expression profiles induced by leaf senescence and 27 senescence-promoting hormonal, pathological and environmental stress treatments. Plant, Cell and Environment **35,** 644-655.

Hajouj, T., Michelis, R. and Gepstein, S. (2000). Cloning and characterization of a receptor-like protein kinase gene associated with senescence. Plant Physiology **124,** 1305-1314.

1.2.1 **Haldane, J.B.** (1930). A note on Fisher's theory of the origin of dominance and on a correlation between dominance and linkage. The American Naturalist **64**, 87-90.

Hamada, T. (2007). Microtubule-associated proteins in higher plants. Journal of Plant Research **120,** 79-98.

Hanaoka, H., Noda, T., Shirano, Y., Kato, T., Hayashi, H., Shibata, D., Tabata, S. and Ohsumi, Y. (2002). Leaf senescence and starvation-induced chlorosis are accelerated by the disruption of an Arabidopsis autophagy gene. Plant Physiology **129,** 1181-1193.

Harrington, G.N. and Bush, D.R. (2003). The bifunctional role of hexokinase in metabolism and glucose signalling. The Plant Cell **15,** 2493-2496.

Hashimoto, H., Kura-Hotta, M. and Katoh, S. (1989). Changes in protein content and in the structure and number of chloroplasts during leaf senescence in rice seedlings. Plant and Cell Physiology **30,** 707-715.

Hashimoto, T. and Kato, T. (2006). Cortical control of plant microtubules. Current Opinion in Plat Biology **9,** 5-11.

Hassine, A.B. and Lutts, S. (2010). Differential responses of saltbush *Atriplex halimus* exposed to salinity and water stress in relation to senescing hormones abscisic acid and ethylene. Plant Physiologyogy **167,** 1448-1456.

Hayat, Q., Hayat, S., Irfan, M. and Ahmad, A. (2010). Effect of exogenous salicylic acid under changing environment: A review in Environmental and Experimental Botany **68,** 14-25.

He, K., Gou, X., Yuan, T., Lin, H., Asami, T., Yoshida, S., Russell, S.D. and Li, J. (2007). BAK1 and BKK1 regulate brassinosteroid-dependent growth and brassinosteroid-independent cell-death pathways. Current Biology **17,** 1109-1115.

He, Y. and Gan, S. (2002). A gene encoding an acyl hydrolase is involved in leaf senescence in Arabidopsis. The Plant Cell **14,** 805-815.

He, Y.H., Fukushige, H., Hildebrand, D.F. and Gan, S.S. (2002). Evidence supporting a role of jasmonic acid in Arabidopsis leaf senescence. Plant Physiology **128,** 876-884.

Henkel, T., Machleidt, T., Alkalay, I., Krönke, M., Ben-Neriah, Y. and Baeuerle, P.A. (1993). Rapid proteolysis of IκB-α is necessary for activation of transcription factor NF-κB.Nature **365**, 182-185.

Higgins, J., Newbury, H., Barbara, D., Muthumeenakshi, S. and Puddephat, I. (2006). The production of marker-free genetically engineered broccoli with sense and antisense ACC synthase 1 and ACC oxidases 1 and 2 to extend shelf-life. Molecular Breeding **17,** 7-20.

Hill, J.P. and Lord, E.M. (1989). Floral development in *Arabidopsis thaliana*: a comparison of the wild type and the homeotic pistillata mutant. Canadian Journal of Botany **67,** 2922-2936.

Himelblau, E. and Amasino, R.M. (2001). Nutrients mobilized from leaves of *Arabidopsis thaliana* during leaf senescence. Plant Physiology **158,** 1317-1323.

Hoeberichts, F.A., van Doorn, W.G., Vorst, O., Hall, R.D. and van Wordragen, M.F. (2007). Sucrose prevents up-regulation of senescence-associated genes in carnation petals. Journal of Experimental Botany **58,** 2873-2885.

Honma, T. and Goto, K. (2001). Complexes of MADS-box proteins are sufficient to convert leaves into floral organs. Nature **409,** 525-529.

Hortensteiner, S. and Feller, U. (2002). Nitrogen metabolism and remobilization during senescence. journal of Experimental Botany **53,** 927-937.

Hörtensteiner, S. (2006). Chlorophyll degradation during senescence. Annual Review of Plant Biology **57,** 55-77.

Hörtensteiner, S. (2009). Stay-green regulates chlorophyll and chlorophyll-binding protein degradation during senescence. Trends in Plant Sciences **14,** 155-162.

Hu, H., Dai, M., Yao, J., Xiao, B., Li, X., Zhang, Q. and Xiong, L. (2006). Overexpressing a NAM, ATAF and CUC (NAC) transcription factor enhances drought resistance and salt tolerance in rice. Proceedings of the National Academy of Sciences of the United States of America **103,** 12987-12992.

Hung, K.T. and Kao, C.H. (2004). Hydrogen peroxide is necessary for abscisic acid-induced senescence of rice leaves. Journal of Plant Physiology **161,** 1347-1357.

Hunter, D.A., Ferrante, A., Vernieri, P. and Reid, M.S. (2004). Role of abscisic acid in perianth senescence of daffodil (*Narcissus pseudonarcissus* "Dutch Master"). Physiologia Plantarum **121,** 313-321.

Immink, R.G., Kaufmann, K. and Angenent, G.C. (2010). The 'ABC'of MADS domain protein behaviour and interactions. Seminars in Cell & Developmental Biology (Elsevier), pp. 87-93.

Irish, V.F. and Sussex, I.M. (1990). Function of the apetala-1 gene during Arabidopsis floral development. The Plant Cell **2,** 741-753.

Ishida, H., Yoshimoto, K., Izumi, M., Reisen, D., Yano, Y., Makino, A., Ohsumi, Y., Hanson, M.R. and Mae, T. (2008). Mobilization of Rubisco and stroma-localized fluorescent proteins of chloroplasts to the vacuole by an ATG gene-dependent autophagic process. Plant Physiology **148,** 142-155.

Ishiguro, S., Kawai-Oda, A., Ueda, J., Nishida, I. and Okada, K. (2001). The DEFECTIVE IN ANTHER DEHISCENCE1 gene encodes a novel phospholipase A1 catalyzing the initial step of jasmonic acid biosynthesis, which synchronizes pollen maturation, anther dehiscence and flower opening in Arabidopsis. The Plant Cell **13,** 2191-2209.

Ito, T., Ng, K.-H., Lim, T.-S., Yu, H. and Meyerowitz, E.M. (2007). The homeotic protein AGAMOUS controls late stamen development by regulating a jasmonate biosynthetic gene in Arabidopsis. The Plant Cell **19,** 3516-3529.

Izumi, M. and Ishida, H. (2011). The changes of leaf carbohydrate contents as a regulator of autophagic degradation of chloroplasts via rubisco-containing bodies during leaf senescence. Plant signalling & behavior **6,** 685-687.

Izumi, M., Wada, S., Makino, A. and Ishida, H. (2010). The autophagic degradation of chloroplasts via Rubisco-containing bodies is specifically linked to leaf carbon status but not nitrogen status in Arabidopsis. Plant Physiology **154,** 1196-1209.

Jack, T. (2004). Molecular and genetic mechanisms of floral control. The Plant Cell **16,** S1-S17.

Jander, G., Norris, S.R., Rounsley, S.D., Bush, D.F., Levin, I.M. and Last, R.L. (2002). Arabidopsis map-based cloning in the post-genome era. Plant Physiology **129,** 440-450.

Jang, J.-C., León, P., Zhou, L. and Sheen, J. (1997). Hexokinase as a sugar sensor in higher plants. The Plant Cell **9,** 5-19.

Jiang, C.J., Shimono, M., Sugano, S., Kojima, M., Yazawa, K., Yoshida, R., Inoue, H., Hayashi, N., Sakakibara, H. and Takatsuji, H. Molecular Plant-Microbe Interactions **23,** 791-798.

Jiang, H., Li, H., Bu, Q. and Li, C. (2009). The RHA2a-interacting proteins ANAC019 and ANAC055 may play a dual role in regulating ABA response and jasmonate response. Plant Signalling & Behavior **4,** 464-466.

Jibran, R., Hunter, D.A. and Dijkwel, P.P. (2013). Hormonal regulation of leaf senescence through integration of developmental and stress signals. Plant Molecular Biology **82,** 547-561.

Jing, H.C., Sturre, M.J.G., Hille, J. and Dijkwel, P.P. (2002). Arabidopsis onset of leaf death mutants identify a regulatory pathway controlling leaf senescence. The Plant Journal **32,** 51-63.

Jing, H.C., Schippers, J.H., Hille, J. and Dijkwel, P.P. (2005). Ethylene-induced leaf senescence depends on age-related changes and OLD genes in Arabidopsis. Journal of Experimental Botany **56,** 2915-2923.

Jing, H.C., Hebeler, R., Oeljeklaus, S., Sitek, B., Stuhler, K., Meyer, H.E., Sturre, M.J., Hille, J., Warscheid, B. and Dijkwel, P.P. (2008). Early leaf senescence is associated with an altered cellular redox balance in Arabidopsis cpr5/old1 mutants. Plant Biology **10 Suppl 1,** 85-98.

Jing, S., Zhou, X., Song, Y. and Yu, D. (2009). Heterologous expression of OsWRKY23 gene enhances pathogen defense and dark-induced leaf senescence in Arabidopsis. Plant Growth Regulation **58,** 181-190.

Joung., J.K. and Sander., J.D. (2012). TALENs: a widely applicable technology for targeted genome editing. Molecular Cell Biology 14, 49–55**.**

Ju, C., Yoon, G.M., Shemansky, J.M., Lin, D.Y., Ying, Z.I., Chang, J., Garrett, W.M., Kessenbrock, M., Groth, G. and Tucker, M.L. (2012). CTR1 phosphorylates the central regulator EIN2 to

control ethylene hormone signalling from the ER membrane to the nucleus in Arabidopsis. Proceedings of the National Academy of Sciences of the United States of America **109,** 19486-19491.

Kamachi, K., Yamaya, T., Hayakawa, T., Mae, T. and Ojima, K. (1992). Vascular bundle-specific localization of cytosolic glutamine synthetase in rice leaves. Plant Physiology **99,** 1481-1486.

Kang, H.M., Zaitlen, N.A., Wade, C.M., Kirby, A., Heckerman, D., Daly, M.J. and Eskin, E. (2008). Efficient control of population structure in model organism association mapping. Genetics **178,** 1709-1723.

Kao, C.H. and Yang, S.F. (1983). Role of ethylene in the senescence of detached rice leaves. Plant Physiology **73,** 881-885.

Kato, Y., Yamamoto, Y., Murakami, S. and Sato, F. (2005). Post-translational regulation of CND41 protease activity in senescent tobacco leaves. Planta **222,** 643-651.

Katsir, L., Schilmiller, A.L., Staswick, P.E., He, S.Y. and Howe, G.A. (2008). COI1 is a critical component of a receptor for jasmonate and the bacterial virulence factor coronatine. Proceedings of the National Academy of Sciences of the United States of America **105,** 7100.

Keech, O., Pesquet, E., Gutierrez, L., Ahad, A., Bellini, C., Smith, S.M. and Gardeström, P. (2010). Leaf senescence is accompanied by an early disruption of the microtubule network in Arabidopsis. Plant Physiology **154,** 1710-1720.

Khanna-Chopra, R. (2012). Leaf senescence and abiotic stresses share reactive oxygen species-mediated chloroplast degradation. Protoplasma **249,** 469-481.

Kim, H.J., Ryu, H., Hong, S.H., Woo, H.R., Lim, P.O., Lee, I.C., Sheen, J., Nam, H.G. and Hwang, I. (2006). Cytokinin-mediated control of leaf longevity by AHK3 through phosphorylation of ARR2 in Arabidopsis. Proceedings of the National Academy of Sciences of the United States of America **103,** 814-819.

Kim, J., Dotson, B., Rey, C., Lindsey, J., Bleecker, A.B., Binder, B.M. and Patterson, S.E. (2013). New clothes for the jasmonic acid receptor coi1: delayed abscission, meristem arrest and apical dominance. PloS ONE **8,** e60505.

Kim, J.H., Chung, K.M. and Woo, H.R. (2011). Three positive regulators of leaf senescence in Arabidopsis, ORE1, ORE3 and ORE9, play roles in crosstalk among multiple hormone-mediated senescence pathways. Genes & Genomics **33,** 373-381.

Kim, J.H., Woo, H.R., Kim, J., Lim, P.O., Lee, I.C., Choi, S.H., Hwang, D. and Nam, H.G. (2009). Trifurcate feed-forward regulation of age-dependent cell death involving miR164 in Arabidopsis. Science **323,** 1053.

Kim J, Patterson SE, Binder BM (2012) Reducing jasmonic acid levels causes ein2 mutants to become ethylene responsive. Federation of European Biochemical Societies Letters 587: 226-230.

King, G.A. and Morris, S.C. (1994a). Early compositional changes during postharvest senescence of broccoli. Journal of the American Society for Horticultural Science **119,** 1000-1005.

King, G.A. and Morris, S.C. (1994b). Physiological changes of broccoli during early postharvest senescence and through the preharvest-postharvest continuum. Journal of the American Society for Horticultural Science **119,** 270-275.

Kinoshita, T., Cano-Delgado, A.C., Seto, H., Hiranuma, S., Fujioka, S., Yoshida, S. and Chory, J. (2005). Binding of brassinosteroids to the extracellular domain of plant receptor kinase BRI1. Nature **433,** 167-171.

Kishony, R. and Leibler, S. (2003). Environmental stresses can alleviate the average deleterious effect of mutations. Journal of Biology **2,** 14.

Kobe, B. and Kajava, A.V. (2001). The leucine-rich repeat as a protein recognition motif. Current Opionins in Structural Biology. **11,** 725-732.

Kreps, J.A., Ponappa, T., Dong, W. and Town, C.D. (1996). Molecular basis of [alpha]-methyltryptophan resistance in amt-1, a mutant of *Arabidopsis thaliana* with altered tryptophan metabolism. Plant Physiology **110,** 1159-1165.

Kukavica, B. and Jovanovic, S.V. (2004). Senescence-related changes in the antioxidant status of ginkgo and birch leaves during autumn yellowing. Physiologiae Plantarum **122,** 321-327.

Kummu, M., De Moel, H., Porkka, M., Siebert, S., Varis, O. and Ward, P. (2012). Lost food, wasted resources: Global food supply chain losses and their impacts on freshwater, cropland and fertiliser use. Science of The Total Environment **438,** 477-489.

Kunkel, B.N. and Brooks, D.M. (2002). Cross talk between signalling pathways in pathogen defense. Current Opinion in Plat Biology **5,** 325-331.

Kurowska M, Daszkowska-Golec A, Gruszka D, Marzec M, Szurman M, Szarejko I, Maluszynski M (2011) TILLING - a shortcut in functional genomics. Journal of Applied Genetics **52:** 371-390

Laitinen, R.A., Schneeberger, K., Jelly, N.S., Ossowski, S. and Weigel, D. (2010). Identification of a spontaneous frame shift mutation in a nonreference Arabidopsis accession using whole genome sequencing. Plant Physiology **153,** 652-654.

Lam, H.-M., Peng, S.S. and Coruzzi, G.M. (1994). Metabolic regulation of the gene encoding glutamine-dependent asparagine synthetase in *Arabidopsis thaliana*. Plant Physiology **106,** 1347-1357.

Lam, S.Y., Horn, S.R., Radford, S.J., Housworth, E.A., Stahl, F.W. and Copenhaver, G.P. (2005). Crossover interference on nucleolus organizing region-bearing chromosomes in Arabidopsis. Genetics **170,** 807-812.

Lee, I.C., Hong, S.W., Whang, S.S., Lim, P.O., Nam, H.G. and Koo, J.C. (2011). Age-dependent action of an ABA-inducible receptor kinase, RPK1, as a positive regulator of senescence in Arabidopsis leaves. Plant and Cell Physiology **52,** 651-662.

Lee, T.A., Vande Wetering, S.W. and Brusslan, J.A. (2013). Stromal protein degradation is incomplete in *Arabidopsis thaliana* autophagy mutants undergoing natural senescence. BMC Research Notes **6,** 17.

Lehmensiek, A., Sutherland, M.W. and McNamara, R.B. (2008). The use of high resolution melting (HRM) to map single nucleotide polymorphism markers linked to a covered smut resistance gene in barley. Theoretical and Applied Genetics **117,** 721-728.

Leibfried, A., To, J.P., Busch, W., Stehling, S., Kehle, A., Demar, M., Kieber, J.J. and Lohmann, J.U. (2005). WUSCHEL controls meristem function by direct regulation of cytokinin-inducible response regulators. Nature **438,** 1172-1175.

Leshem, Y.Y. (1996). Nitric oxide in biological systems. Plant Growth Regulation **18,** 155-159.

Levine, B. and Klionsky, D.J. (2004). Development by self-digestion: Molecular mechanisms and biological functions of autophagy. Developmental Cell **6,** 463-477.

Lewandowski, I. and Heinz, A. (2003). Delayed harvest of miscanthus - influences on biomass quantity and quality and environmental impacts of energy production. European Journal of Agronomy **19,** 45-63.

Li, Q., Li, P., Sun, L., Wang, Y.P., Ji, K., Sun, Y.F., Dai, S.J., Chen, P., Duan, C.R. and Leng, P. (2012a). Expression analysis of beta-glucosidase genes that regulate abscisic acid homeostasis during watermelon (*Citrullus lanatus*) development and under stress conditions. Plant Physiology. **169,** 78-85.

Li, Y., Lee, K.K., Walsh, S., Smith, C., Hadingham, S., Sorefan, K., Cawley, G. and Bevan, M.W. (2006). Establishing glucose- and ABA-regulated transcription networks in Arabidopsis by microarray analysis and promoter classification using a Relevance Vector Machine. Genome Research **16,** 414-427.

Li, Z., Peng, J., Wen, X. and Guo, H. (2012b). Gene network analysis and functional studies of senescence-associated genes reveal novel regulators of arabidopsis leaf senescence. Journal of Integrative Plant Biology **54**, 526-539

Li, Z., Peng J, Wen, X., and Guo, H. 2013. *ETHYLENE-INSENSITIVE3* is a senescence-associated gene that accelerates age-dependent leaf senescence by directly repressing *miR164* transcription in Arabidopsis. The Plant Cell 25, 3311–3328.

Lieberman, M. and Kunishi, A. (1970). Thoughts on the role of ethylene in plant growth and development. In Plant Growth Substances 1970, Springer-Verlag, Berlin, pp. 549-560.

Liew M, Pryor R, Palais R, Meadows C, Erali M, Lyon E, et al. (2004). Genotyping of single-nucleotide polymorphisms by high-resolution melting of small amplicons. Clinical Chemistry 50, 1156–64.

Liljegren, S.J., Gustafson-Brown, C., Pinyopich, A., Ditta, G.S. and Yanofsky, M.F. (1999). Interactions among APETALA1, LEAFY and TERMINAL FLOWER1 specify meristem fate. The Plant Cell **11,** 1007-1018.

Lim, P.O., Woo, H.R. and Nam, H.G. (2003). Molecular genetics of leaf senescence in Arabidopsis. Trends in Plant Sciences **8,** 272-278.

Lim, P.O., Kim, H.J. and Gil Nam, H. (2007). Leaf senescence. Annual Review of Plant Biology**58,** 115-136.

Lin, J.F. and Wu, S.H. (2004). Molecular events in senescing Arabidopsis leaves. The Plant Journal **39,** 612-628.

Litt, A. (2007). An evaluation of A-function: evidence from the APETALA1 and APETALA2 gene lineages. International journal of plant sciences **168,** 73-91.

Liu, J.X. and Howell, S.H. (2010). bZIP28 and NF-Y transcription factors are activated by ER stress and assemble into a transcriptional complex to regulate stress response genes in Arabidopsis. The Plant Cell **22,** 782-796.

Liu, M.-S., Li, H.-C., Chang, Y.-M., Wu, M.-T. and Chen, L.-F.O. (2011). Proteomic analysis of stress-related proteins in transgenic broccoli harboring a gene for cytokinin production during postharvest senescence. Plant Sciences **181,** 288-299.

Lloyd, C. and Hussey, P. (2001). Microtubule-associated proteins in plants—why we need a MAP. Nature Reviews in Molecular Cell Biology **2,** 40-47.

Lohmann, J.U., Hong, R.L., Hobe, M., Busch, M.A., Parcy, F., Simon, R. and Weigel, D. (2001). A molecular link between stem cell regulation and floral patterning in Arabidopsis. Cell **105,** 793-803.

Lorenzo, O., Piqueras, R., Sánchez-Serrano, J.J. and Solano, R. (2003). ETHYLENE RESPONSE FACTOR1 integrates signals from ethylene and jasmonate pathways in plant defense. The Plant Cell **15,** 165-178.

Love, A.J., Milner, J.J. and Sadanandom, A. (2008). Timing is everything: regulatory overlap in plant cell death. Trends in Plant Sciences **13,** 589-595.

Lundqvist, J., de Fraiture, C. and Molden, D. (2008). Saving water: from field to fork. Curbing losses and wastage in the food chain. In SIWI Policy Brief. Stockholm, Sweden: SIWI.

Mae, T., Kai, N., Makino, A. and Ohira, K. (1984). Relation between ribulose bisphosphate carboxylase content and chloroplast number in naturally senescing primary leaves of wheat. Plant and Cell Physiology **25,** 333-336.

Makrides, S.C. and Goldthwaite, J. (1981). Biochemical changes during bean leaf growth, maturity and senescence. Journal of Experimental Botany **32,** 725-735.

Martín-Núñez, G.M., Gómez-Zumaquero, J.M., Soriguer, F. and Morcillo, S. (2012). High resolution melting curve analysis of DNA samples isolated by different DNA extraction methods. Clinica Chimica Acta **413,** 331-333.

Masclaux, C., Valadier, M.H., Brugiere, N., Morot-Gaudry, J.F. and Hirel, B. (2000). Characterization of the sink/source transition in tobacco (*Nicotiana tabacum*) shoots in relation to nitrogen management and leaf senescence. Planta **211,** 510-518.

Matile, P., Hortensteiner, S., Thomas, H. and Krautler, B. (1996). Chlorophyll breakdown in senescent leaves. Plant Physiology **112,** 1403-1409.

Matsuda, R., Iehisa, J.C. and Takumi, S. (2012). Application of real-time PCR-based SNP detection for mapping of Net2, a causal D-genome gene for hybrid necrosis in interspecific crosses between tetraploid wheat and Aegilops tauschii. Genes and Genetic Systems **87,** 137-143.

Matsushima, R., Hayashi, Y., Kondo, M., Shimada, T., Nishimura, M. and Hara-Nishimura, I. (2002). An endoplasmic reticulum-derived structure that is induced under stress conditions in Arabidopsis. Plant Physiology **130,** 1807-1814.

Mayak, S. and Halevy, A. (1972). Interrelationships of ethylene and abscisic acid in the control of rose petal senescence. Plant Physiology **50,** 341-346.

Mccallum, C.M., Comai, L., Greene, E.A. and Henikoff, S. (2000). Targeted screening for induced mutations. Nature Biotechnology **18,** 455-457.

Méndez-Bravo, A., Calderón-Vázquez, C., Ibarra-Laclette, E., Raya-González, J., Ramírez-Chávez, E., Molina-Torres, J., Guevara-García, A.A., López-Bucio, J. and Herrera-Estrella, L. (2011). Alkamides activate jasmonic acid biosynthesis and signalling pathways and confer resistance to Botrytis cinerea in Arabidopsis thaliana. PloS ONE **6,** e27251.

Merlot, S. and Giraudat, J. (1997). Genetic analysis of abscisic acid signal transduction. Plant Physiology **114,** 751.

Miao, Y., Laun, T., Zimmermann, P. and Zentgraf, U. (2004). Targets of the WRKY53 transcription factor and its role during leaf senescence in Arabidopsis. Plant Molecular Biology **55,** 853-867.

Miller, G., Shulaev, V. and Mittler, R. (2008). Reactive oxygen signalling and abiotic stress. Physiologiae Plantarum **133,** 481-489.

Mishina, T.E., Lamb, C. and Zeier, J. (2007). Expression of a nitric oxide degrading enzyme induces a senescence program in Arabidopsis. Plant, Cell and Environment **30,** 39-52.

Moore, B., Zhou, L., Rolland, F., Hall, Q., Cheng, W.H., Liu, Y.X., Hwang, I., Jones, T. and Sheen, J. (2003). Role of the Arabidopsis glucose sensor HXK1 in nutrient, light and hormonal signalling. Science **300,** 332-336.

Mor, Y. and Reid, M.S. (1980). Isolated petals-a useful system for studying flower senescence. In II International Symposium on Post-harvest Physiology of Cut Flowers 113, pp. 19-26.

Morris, K., Mackerness, S.A.H., Page, T., John, C.F., Murphy, A.M., Carr, J.P. and Buchanan-Wollaston, V. (2000). Salicylic acid has a role in regulating gene expression during leaf senescence. The Plant Journal **23,** 677-685.

Morris, K., Mackerness, S.A.H., Page, T., John, C.F., Murphy, A.M., Carr, J.P. and Buchanan-Wollaston, V. (2001). Salicylic acid has a role in regulating gene expression during leaf senescence. The Plant Journal **23,** 677-685.

Moyroud, E., Minguet, E.G., Ott, F., Yant, L., Posé, D., Monniaux, M., Blanchet, S., Bastien, O., Thévenon, E. and Weigel, D. (2011). Prediction of regulatory interactions from genome sequences using a biophysical model for the Arabidopsis LEAFY transcription factor. The Plant Cell **23,** 1293-1306.

Müller, R., Stummann, B.M.,Ersen, A.S. and Serek, M. (1999). Involvement of ABA in postharvest life of miniature potted roses. Plant Growth Regulation **29,** 143-150.

Nadeau, J.A., Zhang, X.S., Nair, H. and O'Neill, S.D. (1993). Temporal and spatial regulation of 1-aminocyclopropane-1-carboxylate oxidase in the pollination-induced senescence of orchid flowers. Plant Physiology **103,** 31-39.

Naito, K., Kusaba, M., Shikazono, N., Takano, T., Tanaka, A., Tanisaka, T. and Nishimura, M. (2005). Transmissible and nontransmissible mutations induced by irradiating *Arabidopsis thaliana* pollen with γ-rays and carbon ions. Genetics **169,** 881-889.

Nanjundiah, V. (1993). Why are most mutations recessive? Journal of Genetics **72,** 85-97.

Niu, Y.H. and Guo, F.Q. (2012). Nitric oxide regulates dark-induced leaf senescence through EIN2 in Arabidopsis. Journal of Integrative Plant Biology **54***,* 516–525.

Noodén, L. (1988). The phenomena of senescence and aging. Whole plant senescence. *In* L Noodén, A Leopold, eds, Senescence and Aging in Plants. Academic Press, San Diego, CA, pp 1-50, 391-439.

Nooden, L.D. and Penney, J.P. (2001). Correlative controls of senescence and plant death in Arabidopsis thaliana (Brassicaceae). Journal of Experimental Botany **52,** 2151-2159.

Noodén, L.D., Guiamét, J.J. and John, I. (1997). Senescence mechanisms. Physiologiae Plantarum **101,** 746-753.

Nordström, K.J., Albani, M.C., James, G.V., Gutjahr, C., Hartwig, B., Turck, F., Paszkowski, U., Coupland, G. and Schneeberger, K. (2013). Mutation identification by direct comparison of whole-genome sequencing data from mutant and wild-type individuals using k-mers. Nature Biotechnology **31,** 325-330.

O'Hara, L.E., Paul, M.J. and Wingler, A. (2013). How do sugars regulate plant growth and development? New insight into the role of trehalose-6-phosphate. Molecular Plant **6,** 261-274.

Ó'Maoiléidigh, D.S., Wuest, S.E., Rae, L., Raganelli, A., Ryan, P.T., Kwaśniewska, K., Das, P., Lohan, A.J., Loftus, B. and Graciet, E. (2013). Control of reproductive floral organ identity specification in arabidopsis by the c function regulator AGAMOUS. The Plant Cell **25**, 2482-2503.

Oh, S.A., Lee, S.Y., Chung, I.K., Lee, C.-H. and Nam, H.G. (1996). A senescence-associated gene of *Arabidopsis thaliana* is distinctively regulated during natural and artificially induced leaf senescence. Plant Molecular Biology **30,** 739-754.

Oh, S.A., Park, J.H., Lee, G.I., Paek, K.H., Park, S.K. and Nam, H.G. (1997). Identification of three genetic loci controlling leaf senescence in *Arabidopsis thaliana*. The Plant Journal **12,** 527-535.

Olsen, A.N., Ernst, H.A., Lo Leggio, L. and Skriver, K. (2005). NAC transcription factors: structurally distinct, functionally diverse. Trends in Plant Sciences **10,** 79-87.

Omirulleh, S., Ábrahám, M., Golovkin, M., Stefanov, I., Karabev, M.K., Mustárdy, L., Mórocz, S. and Dudits, D. (1993). Activity of a chimeric promoter with the doubled CaMV 35S enhancer element in protoplast-derived cells and transgenic plants in maize. Plant Molecular Biology **21,** 415-428.

Ono, K., Nishi, Y., Watanabe, A. and Terashima, I. (2001). Possible mechanisms of adaptive leaf senescence. Plant Biology **3,** 234-243.

Ono, Y., Wada, S., Izumi, M., Makino, A. and Ishida, H. (2013). Evidence for contribution of autophagy to Rubisco degradation during leaf senescence in *Arabidopsis thaliana*. Plant, Cell and Environment **36,** 1147-1159.

Otegui, M.S., Noh, Y.S., Martinez, D.E., Vila Petroff, M.G. andrew Staehelin, L., Amasino, R.M. and Guiamet, J.J. (2005). Senescence-associated vacuoles with intense proteolytic activity develop in leaves of Arabidopsis and soybean. The Plant Journal **41,** 831-844.

Overmyer, K., Tuominen, H., Kettunen, R., Betz, C., Langebartels, C., Sandermann, H. and Kangasjarvi, J. (2000). Ozone-sensitive Arabidopsis rcd1 mutant reveals opposite roles for ethylene and jasmonate signalling pathways in regulating superoxide-dependent cell death. The Plant Cell **12,** 1849-1862.

Page, T., Griffiths, G. and Buchanan-Wollaston, V. (2001). Molecular and biochemical characterization of postharvest senescence in broccoli. Plant Physiology **125,** 718-727.

Pageau, K., Reisdorf-Cren, M., Morot-Gaudry, J.-F. and Masclaux-Daubresse, C. (2006). The two senescence-related markers, GS1 (cytosolic glutamine synthetase) and GDH (glutamate dehydrogenase), involved in nitrogen mobilization, are differentially regulated during pathogen attack and by stress hormones and reactive oxygen species in Nicotiana tabacum L. leaves. Journal of Experimental Botany **57,** 547-557.

Parfitt, J., Barthel, M. and Macnaughton, S. (2010). Food waste within food supply chains: quantification and potential for change to 2050. Philosophical Transactions of the Royal Society B: Biological Sciences **365,** 3065-3081.

Park, J.-H., Oh, S.A., Kim, Y.H., Woo, H.R. and Nam, H.G. (1998). Differential expression of senescence-associated mRNAs during leaf senescence induced by different senescence-inducing factors in Arabidopsis. Plant Molecular Biology **37,** 445-454.

Park, J.H., Halitschke, R., Kim, H.B., Baldwin, I.T., Feldmann, K.A. and Feyereisen, R. (2002). A knock-out mutation in allene oxide synthase results in male sterility and defective wound signal transduction in Arabidopsis due to a block in jasmonic acid biosynthesis. The Plant Journal **31,** 1-12.

Parlitz, S., Kunze, R., Mueller-Roeber, B. and Balazadeh, S. (2011). Regulation of photosynthesis and transcription factor expression by leaf shading and re-illumination in *Arabidopsis thaliana* leaves. Plant Physiology **168,** 1311-1319.

Parry, M.A., Madgwick, P.J., Bayon, C., Tearall, K., Hernandez-Lopez, A., Baudo, M., Rakszegi, M., Hamada, W., Al-Yassin, A. and Ouabbou, H. (2009). Mutation discovery for crop improvement. Journal of Experimental Botany **60,** 2817-2825.

Passardi, F., Dobias, J., Valério, L., Guimil, S., Penel, C. and Dunand, C. (2007). Morphological and physiological traits of three major *Arabidopsis thaliana* accessions. Plant Physiology **164,** 980-992.

Paul, M.J., Primavesi, L.F., Jhurreea, D. and Zhang, Y. (2008). Trehalose metabolism and signalling. Annual Reviews in Plant Biology **59,** 417-441.

Payton, S., Fray, R.G., Brown, S. and Grierson, D. (1996). Ethylene receptor expression is regulated during fruit ripening, flower senescence and abscission. Plant Molecular Biology **31,** 1227-1231.

Pelaz, S., Ditta, G.S., Baumann, E., Wisman, E. and Yanofsky, M.F. (2000). B and C floral organ identity functions require SEPALLATA MADS-box genes. Nature **405,** 200-203.

Penmetsa, R.V. and Cook, D.R. (2000). Production and characterization of diverse developmental mutants of Medicago truncatula. Plant Physiology **123,** 1387-1398.

Peters, J.L., Cnudde, F. and Gerats, T. (2003). Forward genetics and map-based cloning approaches. Trends in Plant Sciences **8,** 484-491.

Polge, C. and Thomas, M. (2007). SNF1/AMPK/SnRK1 kinases, global regulators at the heart of energy control? Trends in Plant Sciences **12,** 20-28.

Porat, R., Borochov, A. and Halevy, A. (1993). Enhancement of petunia and dendrobium flower senescence by jasmonic acid methyl ester is via the promotion of ethylene production. Plant Growth Regulation **13,** 297-301.

Potuschak, T., Lechner, E., Parmentier, Y., Yanagisawa, S., Grava, S., Koncz, C. and Genschik, P. (2003). EIN3-dependent regulation of plant ethylene hormone signalling by two arabidopsis f box proteins-EBF1 and EBF2. Cell **115,** 679-690.

Pourtau, N., Jennings, R., Pelzer, E., Pallas, J. and Wingler, A. (2006). Effect of sugar-induced senescence on gene expression and implications for the regulation of senescence in Arabidopsis. Planta **224,** 556-568.

Pourtau, N., Mares, M., Purdy, S., Quentin, N., Ruel, A. and Wingler, A. (2004). Interactions of abscisic acid and sugar signalling in the regulation of leaf senescence. Planta **219,** 765-772.

Pružinská, A., Tanner, G. Anders, I., Roca, M. and Hörtensteiner, S. (2003). Chlorophyll breakdown: pheophorbide a oxygenase is a Rieske-type iron–sulfur protein, encoded by the accelerated cell death 1 gene. Proceedings of the National Academy of Sciences of the United States of America **100,** 15259-15264.

Qiao, H., Chang, K.N., Yazaki, J. and Ecker, J.R. (2009). Interplay between ethylene, ETP1/ETP2 F-box proteins and degradation of EIN2 triggers ethylene responses in Arabidopsis. Genes Devlopment **23,** 512-521.

Quirino, B.F., Normanly, J. and Amasino, R.M. (1999). Diverse range of gene activity during Arabidopsis thaliana leaf senescence includes pathogen-independent induction of defense-related genes. Plant Molecular Biology **40,** 267-278.

Quirino, B.F., Noh, Y.S., Himelblau, E. and Amasino, R.M. (2000). Molecular aspects of leaf senescence. Trends in Plant Sciences **5,** 278-282.

Raab, S., Drechsel, G., Zarepour, M., Hartung, W., Koshiba, T., Bittner, F. and Hoth, S. (2009). Identification of a novel E3 ubiquitin ligase that is required for suppression of premature senescence in Arabidopsis. The Plant Journal **59,** 39-51.

Reguera, B., Velo-Suarez, L., Raine, R. and Park, M.G. (2012). Harmful *Dinophysis* species: A review Harmful Algae **14,** 87-106.

Riechmann, J.L., Krizek, B.A. and Meyerowitz, E.M. (1996). Dimerization specificity of Arabidopsis MADS domain homeotic proteins APETALA1, APETALA3, PISTILLATA and AGAMOUS. Proceedings of the National Academy of Sciences of the United States of America **93,** 4793-4798.

Riechmann, J.L., Heard, J., Martin, G., Reuber, L., Jiang, C.Z., Keddie, J., Adam, L., Pineda, O., Ratcliffe, O.J., Samaha, R.R., Creelman, R., Pilgrim, M., Broun, P., Zhang, J.Z., Ghandehari, D., Sherman, B.K. and Yu, C.L. (2000). Arabidopsis transcription factors: Genome-wide comparative analysis among eukaryotes. Science **290,** 2105-2110.

Robatzek, S. and Somssich, I.E. (2001). A new member of the Arabidopsis WRKY transcription factor family, AtWRKY6, is associated with both senescence-and defense-related processes. The Plant Journal **28,** 123-133.

Robatzek, S. and Somssich, I.E. (2002). Targets of AtWRKY6 regulation during plant senescence and pathogen defense. Genes Devlopment **16,** 1139-1149.

Robson, P., Mos, M., Clifton-Brown, J. and Donnison, I. (2012). Phenotypic variation in senescence in miscanthus: towards optimising biomass quality and quantity. Bioenergy Research **5,** 95-105.

Roca, M., James, C., Pružinská, A., Hörtensteiner, S., Thomas, H. and Ougham, H. (2004). Analysis of the chlorophyll catabolism pathway in leaves of an introgression senescence mutant of *Lolium temulentum*. Phytochemistry **65,** 1231-1238.

Rockel, P., Strube, F., Rockel, A., Wildt, J. and Kaiser, W.M. (2002). Regulation of nitric oxide (NO) production by plant nitrate reductase *in vivo* and *in vitro*. Journal of Experimental Botany **53,** 103-110.

Rogers, H.J. (2006). Programmed cell death in floral organs: how and why do flowers die? Annual of Botany **97,** 309-315.

Rogers, H.J. (2012). From models to ornamentals: how is flower senescence regulated? Plant Molecular Biology.**82,** 563-574.

Rohwer, C. and Erwin, J. (2008). Horticultural applications of jasmonates: a review. The Journal of Horticultural Science and Biotechnology **83,** 283-304.

Rojo, E., León, J. and Sánchez-Serrano, J.J. (1999). Cross-talk between wound signalling pathways determines local versus systemic gene expression in *Arabidopsis thaliana*. The Plant Journal **20,** 135-142.

Rolland, F., Moore, B. and Sheen, J. (2002). Sugar sensing and signalling in plants. The Plant Cell **14,** S185-S205.

Rolland, F., Baena-Gonzalez, E. and Sheen, J. (2006). Sugar sensing and signalling in plants: conserved and novel mechanisms. Annual Reviews of Plant Biology **57,** 675-709.

Rolle, R. (2006). Improving postharvest management and marketing in the Asia-Pacific region: issues and challenges. In Postharvest management of fruit and vegetables in the Asia-Pacific Region. Reports of the APO Seminars on Reduction of postharvest losses of fruits and vegetables, India, 5-11 October, 2004 and Marketing and food safety: challenges in postharvest management of agricultural/horticultural products, Islamic Republic of Iran, 23-28 July, 2005. Asian Productivity Organization (APO), pp. 23-31.

Rolny, N., Costa, L., Carrión, C. and Guiamet, J.J. (2011). Is the electrolyte leakage assay an unequivocal test of membrane deterioration during leaf senescence? Plant Physiology and Biochemistry **49,** 1220-1227.

Ronen, M. and Mayak, S. (1981). Interrelationship between abscisic acid and ethylene in the control of senescence processes in carnation flowers. Journal of Experimental Botany **32,** 759-765.

Rossano, R., Larocca, M. and Riccio, P. (2011). 2-D zymographic analysis of Broccoli *Brassica oleracea*. var. *Italica*) florets proteases: Follow up of cysteine protease isotypes in the course of post-harvest senescence. Plant Physiology. **168,** 1517-1525.

Rushing, J.W. (1990). Cytokinins affect respiration, ethylene production and chlorophyll retention of packaged broccoli florets. HortScience **25,** 88-90.

Sato, Y., Morita, R., Katsuma, S., Nishimura, M., Tanaka, A. and Kusaba, M. (2009). Two short-chain dehydrogenase/reductases, NON-YELLOW COLORING 1 and NYC1-LIKE, are required for chlorophyll b and light-harvesting complex II degradation during senescence in rice. The Plant Journal **57,** 120-131.

Schelbert, S., Aubry, S., Burla, B., Agne, B., Kessler, F., Krupinska, K. and Hörtensteiner, S. (2009). Pheophytin pheophorbide hydrolase (pheophytinase) is involved in chlorophyll breakdown during leaf senescence in Arabidopsis. The Plant Cell **21,** 767-785.

Schippers, J.H.M., Jing, H.C., Hille, J. and Dijkwel, P.P. (2007). Developmental and hormonal control of leaf senescence. In Senescence Processes in Plants, S. Gan, ed (Blackwell), pp. 145-170.

Schippers, J.H.M., Nunes-Nesi, A., Apetrei, R., Hille, J., Fernie, A.R. and Dijkwel, P.P. (2008). The Arabidopsis onset of leaf death5 mutation of quinolinate synthase affects nicotinamide adenine dinucleotide biosynthesis and causes early ageing. The Plant Cell **20,** 2909-2925.

Schluepmann, H. and Paul, M. (2009). Trehalose metabolites in Arabidopsis—elusive, active and central. The Arabidopsis book/American Society of Plant Biologists **7**, e0122.

Schluepmann, H., Berke, L. and Sanchez-Perez, G.F. (2012). Metabolism control over growth: a case for trehalose-6-phosphate in plants. Journal of Experimental Botany **63,** 3379-3390.

Schmulling, T., Werner, T., Riefler, M., Krupkova, E. and Manns, I.B.Y. (2003). Structure and function of cytokinin oxidase/dehydrogenase genes of maize, rice, Arabidopsis and other species. Journal of Plant Research. **116,** 241-252.

Schneeberger, K. and Weigel, D. (2011). Fast-forward genetics enabled by new sequencing technologies. Trends in Plant Sciences **16,** 282-288.

Schneeberger, K., Ossowski, S., Lanz, C., Juul, T., Petersen, A.H., Nielsen, K.L., Jørgensen, J.-E., Weigel, D. and Andersen, S.U. (2009). SHOREmap: simultaneous mapping and mutation identification by deep sequencing. Nature Methods **6,** 550-551.

Schommer, C., Palatnik, J.F., Aggarwal, P., Chetelat, A., Cubas, P., Farmer, E.E., Nath, U. and Weigel, D. (2008). Control of jasmonate biosynthesis and senescence by miR319 targets. PLoS Biology **6,** e230.

Schwechheimer, C. and Schwager, K. (2004). Regulated proteolysis and plant development. Plant Cell Reports **23,** 353-364.

Sessions, A., Burke, E., Presting, G., Aux, G., McElver, J., Patton, D., Dietrich, B., Ho, P., Bacwaden, J. and Ko, C. (2002). A high-throughput Arabidopsis reverse genetics system. The Plant Cell **14,** 2985-2994.

Shahri, W. and Tahir, I. (2011). Flower senescence-strategies and some associated events. The Botanical Review **77,** 152-184.

Sharp, R.E. and LeNoble, M.E. (2002). ABA, ethylene and the control of shoot and root growth under water stress. Journal of Experimental Botany **53,** 33-37.

Shan Q, Wang Y, Li J, Zhang Y, Chen K, Liang Z, Zhang K, Liu J, Xi JJ, Qiu J-L (2013) Targeted genome modification of crop plants using a CRISPR-Cas system. Nature biotechnology **31:** 686-688

Shi, Y., Tian, S., Hou, L., Huang, X., Zhang, X., Guo, H. and Yang, S. (2012). Ethylene signalling negatively regulates freezing tolerance by repressing expression of CBF and type-A ARR genes in Arabidopsis. The Plant Cell **24,** 2578-2595.

Shiu, S.H. and Bleecker, A.B. (2001). Plant receptor-like kinase gene family: diversity, function and signalling. Science Signalling **2001,** re22.

Skulachev, V.P. and LONGO, V.D. (2005). Aging as a mitochondria-mediated atavistic program: can aging be switched off? Annals of the New York Academy of Sciences **1057,** 145-164.

Smaczniak, C., Immink, R.G., Muiño, J.M., Blanvillain, R., Busscher, M., Busscher-Lange, J., Dinh, Q.P., Liu, S., Westphal, A.H. and Boeren, S. (2012). Characterization of MADS-domain transcription factor complexes in Arabidopsis flower development. Proceedings of the National Academy of Sciences of the United States of America **109,** 1560-1565.

Smalle, J. and Vierstra, R.D. (2004). The ubiquitin 26S proteasome proteolytic pathway. Annual Reviews in Plant Biology **55,** 555-590.

Smart, C.M. (1994). Tansley review no. 64. Gene expression during leaf senescence. New Phytology **126,** 419-448.

Smith, A.M. and Stitt, M. (2007). Coordination of carbon supply and plant growth. Plant, Cell and Environment **30,** 1126-1149.

Somers, D.E. and Fujiwara, S. (2009). Thinking outside the F-box: novel ligands for novel receptors. Trends in Plant Sciences **14,** 206-213.

Song, S., Qi, T., Fan, M., Zhang, X., Gao, H., Huang, H., Wu, D., Guo, H., and Xie, D. (2013b). The bHLH subgroup IIId factors negatively regulate jasmonate-mediated plant defense and development. PLoS Genetics 9: e1003653.

Soudry, E., Ulitzur, S. and Gepstein, S. (2005). Accumulation and remobilization of amino acids during senescence of detached and attached leaves: in planta analysis of tryptophan levels by recombinant luminescent bacteria. Journal of Experimental Botany **56,** 695-702.

Stasolla, C., Katahira, R., Thorpe, T.A. and Ashihara, H. (2003). Purine and pyrimidine nucleotide metabolism in higher plants. Plant Physiology. **160,** 1271-1295.

Stessman, D., Miller, A., Spalding, M. and Rodermel, S. (2002). Regulation of photosynthesis during Arabidopsis leaf development in continuous light. Photosynthesis Research **72,** 27-37.

Stintzi, A., Weber, H., Reymond, P. and Farmer, E.E. (2001). Plant defense in the absence of jasmonic acid: The role of cyclopentenones. Proceedings of the National Academy of Sciences of the United States of America **98,** 12837.

Stone, J.M. and Walker, J.C. (1995). Plant protein-kinase families and signal-transduction. Plant Physiology **108,** 451-457.

Stuart, T. (2009). Uncovering the global food scandal (Penguin, London).

Sturre, M.J., Shirzadian-Khorramabad, R., Schippers, J.H., Chin-A-Woeng, T.F., Hille, J. and Dijkwel, P.P. (2009). Method for the identification of single mutations in large genomic regions using massive parallel sequencing. Molecular Breeding **23,** 51-59.

Sunkar, R., Kapoor, A. and Zhu, J.-K. (2006). Posttranscriptional induction of two Cu/Zn superoxide dismutase genes in Arabidopsis is mediated by downregulation of miR398 and important for oxidative stress tolerance. The Plant Cell **18,** 2051-2065.

Swidzinski, J.A., Sweetlove, L.J. and Leaver, C.J. (2002). A custom microarray analysis of gene expression during programmed cell death in *Arabidopsis thaliana*. The Plant Journal **30,** 431-446.

Taylor, C.B. and Green, P.J. (1995). Identification and characterization of genes with unstable transcripts (GUTs) in tobacco. Plant Molecular Biology **28,** 27-38.

Taylor, C.B., Bariola, P.A., Delcardayre, S.B., Raines, R.T. and Green, P.J. (1993). Rns2 - a senescence-associated rnase of arabidopsis that diverged from the S-Rnases before speciation. Proceedings of the National Academy of Sciences of the United States of America **90,** 5118-5122.

Taylor, L., Nunes-Nesi, A., Parsley, K., Leiss, A., Leach, G., Coates, S., Wingler, A., Fernie, A.R. and Hibberd, J.M. (2010). Cytosolic pyruvate, orthophosphate dikinase functions in nitrogen remobilization during leaf senescence and limits individual seed growth and nitrogen content. The Plant Journal **62,** 641-652.

Teramoto, H., Toyama, T., Takeba, G. and Tsuji, H. (1995). Changes in expression of two cytokinin-repressed genes, CR9 and CR20, in relation to aging, greening and wounding in cucumber. Planta **196,** 387-395.

Thang, N.B., Wu, J., Zhou, W. and Shi, C. (2010). The screening of mutants and construction of mutant library for *Oryza sativa* cv. Nipponbare via ethyl methane sulphonate inducing. Biologia **65,** 660-669.

Theißen, G. (2001). Development of floral organ identity: stories from the MADS house. Current Opinion in Plat Biology **4,** 75-85.

Thines, B., Katsir, L., Melotto, M., Niu, Y., Mandaokar, A., Liu, G., Nomura, K., He, S.Y. and Howe, G.A. (2007). JAZ repressor proteins are targets of the SCFCOI1 complex during jasmonate signalling. Nature **448,** 661-665.

Thoenen, M., Herrmann, B. and Feller, U. (2007). Senescence in wheat leaves: is a cysteine endopeptidase involved in the degradation of the large subunit of Rubisco? Acta Physiologiae Plantarum **29,** 339-350.

Thomas, H. (1976). Delayed senescence in leaves treated with the protein synthesis inhibitor MDMP. Plant Science Letters **6,** 369-377.

Thomas, H. (2013). Senescence, ageing and death of the whole plant. New Phytology **197,** 696-711.

Thomas, H. and Stoddart, J.L. (1980). Leaf senescence. Annual Review of Plant Physiology **31,** 83-111.

Thomas, H., Ougham, H., Canter, P. and Donnison, I. (2002). What stay-green mutants tell us about nitrogen remobilization in leaf senescence. Journal of Experimental Botany **53,** 801-808.

Thomas, H., Huang, L., Young, M. and Ougham, H. (2009). Evolution of plant senescence. BMC Evol. Biol. **9**. 163.

Thompson, A.R., Doelling, J.H., Suttangkakul, A. and Vierstra, R.D. (2005). Autophagic nutrient recycling in Arabidopsis directed by the ATG8 and ATG12 conjugation pathways. Plant Physiology **138,** 2097-2110.

Thompson, J., Legge, R. and Barber, R. (1987). The role of free radicals in senescence and wounding. New Phytology **105,** 317-344.

Thompson, J.E., Froese, C.D., Madey, E., Smith, M.D. and Hong, Y.W. (1998). Lipid metabolism during plant senescence. Progress in Lipid Research **37,** 119-141.

Thomson, W.W. and Platt-Aloia, K.A. (1987). Ultrastructure and senescence in plants. Plant Senescence: Its Biochemistry and Physiology. American Society of Plant Physiologists, Rockville, MD, pp 20-30.

Tian, M., Downs, C., Lill, R. and King, G. (1994). A role for ethylene in the yellowing of broccoli after harvest. Journal of the American Society for Horticultural Science **119,** 276-281.

Tian, M., Davies, L., Downs, C., Liu, X. and Lill, R. (1995). Effects of floret maturity, cytokinin and ethylene on broccoli yellowing after harvest. Postharvest Biology and Technology **6,** 29-40.

Tripathi, S.K. and Tuteja, N. (2007). Integrated signalling in flower senescence: an overview. Plant Signalling and Behavior **2,** 437-445.

Trivellini, A., Jibran, R., Watson, L.M., O'Donoghue, E.M., Ferrante, A., Sullivan, K.L., Dijkwel, P.P. and Hunter, D.A. (2012). Carbon deprivation-driven transcriptome reprograming in detached developmentally arresting Arabidopsis inflorescences. Plant Physiology **160,** 1357-1372.

Trobacher, C.P.T.C.P. (2009). Ethylene and programed cell death in plants. Botany **87,** 757-769.

Ueda, J. and Kato, J. (1980). Isolation and identification of a senescence-promoting substance from wormwood (Artemisia absinthium L.). Plant Physiology **66,** 246-249.

Ueda, J., Kato, J., Yamane, H. and Takahashi, N. (1981). Inhibitory effect of methyl jasmonate and its related compounds on kinetin-induced retardation of oat leaf senescence. Physiologiae Plantarum **52,** 305-309.

Ugo, V., Tondeur, S., Menot, M.-L., Bonnin, N., Le Gac, G., Tonetti, C., Mansat-De Mas, V., Lecucq, L., Kiladjian, J.-J. and Chomienne, C. (2010). Interlaboratory development and validation of a HRM method applied to the detection of JAK2 exon 12 mutations in polycythemia vera patients. PloS ONE **5,** e8893.

Ulloa, R.M., Raíces, M., MacIntosh, G.C., Maldonado, S. and Téllez-Iñón, M.T. (2002). Jasmonic acid affects plant morphology and calcium-dependent protein kinase expression and activity in Solanum tuberosum. Physiologiae Plantarum **115,** 417-427.

Usadel, B., Bläsing, O.E., Gibon, Y., Retzlaff, K., Höhne, M., Günther, M. and Stitt, M. (2008). Global transcript levels respond to small changes of the carbon status during progressive exhaustion of carbohydrates in Arabidopsis rosettes. Plant Physiology **146,** 1834-1861.

van der Graaff, E., Schwacke, R., Schneider, A., Desimone, M., Flugge, U.I. and Kunze, R. (2006). Transcription analysis of arabidopsis membrane transporters and hormone pathways during developmental and induced leaf senescence. Plant Physiology **141,** 776-792.

Van der Hoorn, R.A., Leeuwenburgh, M.A., Bogyo, M., Joosten, M.H. and Peck, S.C. (2004). Activity profiling of papain-like cysteine proteases in plants. Plant Physiology **135,** 1170-1178.

Van Doorn, W.G. (2008). Is the onset of senescence in leaf cells of intact plants due to low or high sugar levels? Journal of Experimental Botany **59,** 1963-1972.

van Doorn, W.G. and Woltering, E.J. (2008). Physiology and molecular biology of petal senescence. Journal of Experimental Botany **59,** 453-480.

Varshavsky, A. (2005). Ubiquitin fusion technique and related methods. In ubiquitin and protein degradation, Pt B, R.J. Deshaies, ed, pp. 777-799.

Vogel, J.P., Woeste, K.E., Theologis, A. and Kieber, J.J. (1998). Recessive and dominant mutations in the ethylene biosynthetic gene ACS5 of Arabidopsis confer cytokinin insensitivity and ethylene overproduction, respectively. Proceedings of the National Academy of Sciences of the United States of America **95,** 4766-4771.

von Saint Paul, V., Zhang, W., Kanawati, B., Geist, B., Faus-Kessler, T., Schmitt-Kopplin, P. and Schaffner, A.R. (2011). The Arabidopsis Glucosyltransferase UGT76B1 Conjugates Isoleucic Acid and Modulates Plant Defense and Senescence. The Plant Cell **23,** 4124-4145.

Wada, S., Ishida, H., Izumi, M., Yoshimoto, K., Ohsumi, Y., Mae, T. and Makino, A. (2009). Autophagy plays a role in chloroplast degradation during senescence in individually darkened leaves. Plant Physiology **149,** 885-893.

Wagstaff, C., Yang, T.J., Stead, A.D., Buchanan-Wollaston, V. and Roberts, J.A. (2009). A molecular and structural characterization of senescing Arabidopsis siliques and comparison of transcriptional profiles with senescing petals and leaves. The Plant Journal **57,** 690-705.

Wagstaff, C., Leverentz, M.K., Griffiths, G., Thomas, B., Chanasut, U., Stead, A.D. and Rogers, H.J. (2002). Cysteine protease gene expression and proteolytic activity during senescence of Alstroemeria petals. Journal of Experimental Botany **53,** 233-240.

Wang, C. (1977). Effect of aminoethoxy analog of rhizobitoxine and sodium benzoate on senescence of broccoli. HortScience **12**, 54-56.

Wang, Z.Y., Seto, H., Fujioka, S., Yoshida, S. and Chory, J. (2001). BRI1 is a critical component of a plasma-membrane receptor for plant steroids. Nature **411,** 219-219.

Warthmann, N., Fitz, J. and Weigel, D. (2007). MSQT for choosing SNP assays from multiple DNA alignments. Bioinformatics **23,** 2784-2787.

Weaver, L.M. and Amasino, R.M. (2001). Senescence is induced in individually darkened Arabidopsis leaves, but inhibited in whole darkened plants. Plant Physiology **127,** 876-886.

Weaver, L.M., Gan, S.S., Quirino, B. and Amasino, R.M. (1998). A comparison of the expression patterns of several senescence-associated genes in response to stress and hormone treatment. Plant Molecular Biology **37,** 455-469.

Weigel, D. and Meyerowitz, E.M. (1993). Activation of floral homeotic genes in Arabidopsis. Science **261,** 1723-1726.

Weigel, D. and Nilsson, O. (1995). A developmental switch sufficient for flower initiation in diverse plants. Nature **377,** 495-500.

Wesley, S.V., Helliwell, C.A., Smith, N.A., Wang, M., Rouse, D.T., Liu, Q., Gooding, P.S., Singh, S.P., Abbott, D. and Stoutjesdijk, P.A. (2001). Construct design for efficient, effective and high-throughput gene silencing in plants. The Plant Journal **27,** 581-590.

White, H. and Potts, G. (2006). Mutation scanning by high resolution melt analysis. Evaluation of rotor-gene 6000 (Corbett Life Science), HR-1 and 384-well lightscanner (Idaho Technology). National Genetics Reference Laboratory (Wessex 2006).

Wingler, A., Masclaux-Daubresse, C. and Fischer, A.M. (2009). Sugars, senescence and ageing in plants and heterotrophic organisms. Journal of Experimental Botany **60,** 1063-1066.

Wingler, A., Von Schaewen, A., Leegood, R.C., Lea, P.J. and Quick, W.P. (1998). Regulation of leaf senescence by cytokinin, sugars and light effects on NADH-dependent hydroxypyruvate reductase. Plant Physiology **116,** 329-335.

Wingler, A., Purdy, S.J., Edwards, S.A., Chardon, F. and Masclaux-Daubresse, C. (2010). QTL analysis for sugar-regulated leaf senescence supports flowering-dependent and-independent senescence pathways. New Phytology **185,** 420-433.

Wingler, A., Delatte, T.L., O'Hara, L.E., Primavesi, L.F., Jhurreea, D., Paul, M.J. and Schluepmann, H. (2012). Trehalose 6-phosphate is required for the onset of leaf senescence associated with high carbon availability. Plant Physiology **158,** 1241-1251.

Wink, D.A., Cook, J.A., Pacelli, R., Liebmann, J., Krishna, M.C. and Mitchell, J.B. (1995). Nitric oxide (NO) protects against cellular damage by reactive oxygen species. Toxicology Letters **82-3,** 221-226.

Winter, C.M., Austin, R.S., Blanvillain-Baufume, S., Reback, M.A., Monniaux, M., Wu, M.-F., Sang, Y., Yamaguchi, A., Yamaguchi, N. and Parker, J.E. (2011). LEAFY target genes reveal floral regulatory logic *cis* motifs and a link to biotic stimulus response. Devlopmental Cell **20,** 430-443.

Wintermans, J. and De Mots, A. (1965). Spectrophotometric characteristics of chlorophylls *a* and *b* and their phenophytins in ethanol. Biochimica et Biophysica Acta (BBA)-Biophysics including Photosynthesis **109,** 448-453.

Wittenbach, V.A. (1978). Breakdown of ribulose bisphosphate carboxylase and change in proteolytic activity during dark-induced senescence of wheat seedlings. Plant Physiology **62,** 604-608.

Wollaston, V. and Ali, S. (2007). Characterization of EMS induced leaf senescing mutants in Arabidopsis. Sarhad Journal of Agriculture **23**.

Wollmann, H., Mica, E., Todesco, M., Long, J.A. and Weigel, D. (2010). On reconciling the interactions between APETALA2, miR172 and AGAMOUS with the ABC model of flower development. Development **137,** 3633-3642.

Woo, H.R., Kim, J.H., Nam, H.G. and Lim, P.O. (2004). The delayed leaf senescence mutants of Arabidopsis, ore1, ore3 and ore9 are tolerant to oxidative stress. Plant and Cell Physiology. **45,** 923-932.

Woo, H.R., Goh, C.H., Park, J.H., de la Serve, B.T., Kim, J.H., Park, Y.I. and Nam, H.G. (2002). Extended leaf longevity in the ore4-1 mutant of Arabidopsis with a reduced expression of a plastid ribosomal protein gene. The Plant Journal **31,** 331-340.

Woo, H.R., Chung, K.M., Park, J.H., Oh, S.A., Ahn, T., Hong, S.H., Jang, S.K. and Nam, H.G. (2001). ORE9, an F-box protein that regulates leaf senescence in Arabidopsis. The Plant Cell **13,** 1779-1790.

Woo, H.R., Kim, J.H., Kim, J., Kim, J., Lee, U., Song, I.J., Kim, J.H., Lee, H.Y., Nam, H.G. and Lim, P.O. (2010). The RAV1 transcription factor positively regulates leaf senescence in Arabidopsis. Journal of Experimental Botany **61,** 3947-3957.

Wood AJ, Lo TW, Zeitler B, Pickle CS, Ralston EJ, Lee AH, Amora R, Miller JC, Leung E, Meng XD, Zhang L, Rebar EJ, Gregory PD, Urnov FD, Meyer BJ (2011) Targeted Genome Editing Across Species Using ZFNs and TALENs. Science **333:** 307-307

Wright. S. (1934). Physiological and evolutionary theories of dominance. The American Naturalist **68**, 24-53.

Wright, S. (1956). Modes of selection. The American Naturalist **90,** 5-24.

Wright,.S. (1980). The effect of plant growth regulator treatments on the levels of ethylene emanating from excised turgid and wilted wheat leaves. Planta **148,** 381-388.

Wu, J.G., Li, G. and Shi, C.H. (2012). The screening and preliminary construction of quality mutant population for cultivar "Nipponbare" in japonica rice (Oryza sativa). Biologia **67,** 1099-1106.

Wu, S.-B., Tavassolian, I., Rabiei, G., Hunt, P., Wirthensohn, M., Gibson, J.P., Ford, C.M. and Sedgley, M. (2009). Mapping SNP-anchored genes using high-resolution melting analysis in almond. Molecular Genetics and Genomics **282,** 273-281.

Xiao, S., Dai, L., Liu, F., Wang, Z., Peng, W. and Xie, D. (2004). COS1: an Arabidopsis coronatine insensitive1 suppressor essential for regulation of jasmonate-mediated plant defense and senescence. The Plant Cell **16,** 1132-1142.

Xiao, W., Sheen, J. and Jang, J.-C. (2000). The role of hexokinase in plant sugar signal transduction and growth and development. Plant Molecular Biology **44,** 451-461.

Xu, F., Yang, Z., Chen, X., Jin, P., Wang, X. and Zheng, Y. (2011a). 6-Benzylaminopurine delays senescence and enhances health-promoting compounds of harvested broccoli. Journal of Agricultural and Food Chemistry **60,** 234-240.

Xu, F., Meng, T., Li, P., Yu, Y., Cui, Y., Wang, Y., Gong, Q. and Wang, N.N. (2011b). A soybean dual-specificity kinase, GmSARK and its Arabidopsis homolog, AtSARK, regulate leaf senescence through synergistic actions of auxin and ethylene. Plant Physiology **157,** 2131-2153.

Xue-Xuan, X., Hong-Bo, S., Yuan-Yuan, M., Gang, X., Jun-Na, S., Dong-Gang, G. and Cheng-Jiang, R. (2010). Biotechnological implications from abscisic acid (ABA) roles in cold stress and leaf senescence as an important signal for improving plant sustainable survival under abiotic-stressed conditions. Critical Reviews in Biotechnology **30,** 222-230.

Yan, Y., Stolz, S., Chételat, A., Reymond, P., Pagni, M., Dubugnon, L. and Farmer, E.E. (2007). A downstream mediator in the growth repression limb of the jasmonate pathway. Science Signalling **19,** 2470.

Yanagisawa, S., Yoo, S.D. and Sheen, J. (2003). Differential regulation of EIN3 stability by glucose and ethylene signalling in plants. Nature **425,** 521-525.

Yang, T.F., Gonzalez-Carranza, Z.H., Maunders, M.J. and Roberts, J.A. (2008). Ethylene and the regulation of senescence processes in transgenic *Nicotiana sylvestris* plants. Annals of Botany **101,** 301-310.

Yanofsky, M.F. (1995). Floral meristems to floral organs: genes controlling early events in Arabidopsis flower development. Annual Review of Plant Biology **46,** 167-188.

Yin, Y.H., Wang, Z.Y., Mora-Garcia, S., Li, J.M., Yoshida, S., Asami, T. and Chory, J. (2002). BES1 accumulates in the nucleus in response to brassinosteroids to regulate gene expression and promote stem elongation. Cell **109,** 181-191.

Yoo, S.-C., Cho, S.-H., Zhang, H., Paik, H.-C., Lee, C.-H., Li, J., Yoo, J.-H., Lee, B.-W., Koh, H.-J., Seo, H.S. and Paek, N.-C. (2007). Quantitative trait loci associated with functional stay-green SNU-SG1 in rice. Molecules and Cell **24,** 83-94.

Yoshida, S. (2003). Molecular regulation of leaf senescence. Current Opinion in Plat Biology **6,** 79-84.

Yoshida, S., Ito, M., Callis, J., Nishida, I. and Watanabe, A. (2002). A delayed leaf senescence mutant is defective in arginyl-tRNA protein arginyltransferase, a component of the N-end rule pathway in Arabidopsis. The Plant Journal **32,** 129-137.

Yu, D.Q., Chen, C.H. and Chen, Z.X. (2001). Evidence for an important role of WRKY DNA binding proteins in the regulation of NPR1 gene express ion. The Plant Cell **13,** 1527-1539.

Zacarias, L. and Reid, M.S. (1990). Role of growth regulators in the senescence of Arabidopsis thaliana leaves. Physiologiae Plantarum **80,** 549-554.

Zarei, A., Körbes, A.P., Younessi, P., Montiel, G., Champion, A. and Memelink, J. (2011). Two GCC boxes and AP2/ERF-domain transcription factor ORA59 in jasmonate/ethylene-mediated activation of the PDF1. 2 promoter in Arabidopsis. Plant Molecular Biology **75,** 321-331.

Zeevaart, J. and Creelman, R. (1988). Metabolism and physiology of abscisic acid. Annual Review of Plant Physiology and Plant Molecular Biology **39,** 439-473.

Zhang, L. and Xing, D. (2008). Methyl jasmonate induces production of reactive oxygen species and alterations in mitochondrial dynamics that precede photosynthetic dysfunction and subsequent cell death. Plant and Cell Physiology. **49,** 1092-1111.

Zhang, L., Li, Z., Quan, R., Li, G., Wang, R. and Huang, R. (2011a). An AP2 domain-containing gene, ESE1, targeted by the ethylene signalling component EIN3 is important for the salt response in Arabidopsis. Plant Physiology **157,** 854-865.

Zhang, X., Ju, H.W., Chung, M.S., Huang, P., Ahn, S.J. and Kim, C.S. (2011b). The RR-type MYB-like transcription factor, AtMYBL, is involved in promoting leaf senescence and modulates an abiotic stress response in Arabidopsis. Plant and Cell Physiology **52,** 138-148.

Zhang, Y., Primavesi, L.F., Jhurreea, D. and ralojc, P.J., Mitchell, R.A., Powers, S.J., Schluepmann, H., Delatte, T., Wingler, A. and Paul, M.J. (2009). Inhibition of SNF1-related protein kinase1 activity and regulation of metabolic pathways by trehalose-6-phosphate. Plant Physiology **149,** 1860-1871.

Zheng Q, Zheng Y, Perry SE. (2013). AGAMOUS-Like15 promotes somatic embryogenesis in Arabidopsis and soybean in part by the control of ethylene biosynthesis and response. Plant Physiology 161, 2113–2127.

Zhou, C., Cai, Z., Guo, Y. and Gan, S. (2009). An Arabidopsis mitogen-activated protein kinase cascade, MKK9-MPK6, plays a role in leaf senescence. Plant Physiology **150,** 167-177.

Zhou, X., Jiang, Y. and Yu, D. (2011). WRKY22 transcription factor mediates dark-induced leaf senescence in Arabidopsis. Molecules and cells **31,** 303-313.

Zhu, Z., An, F., Feng, Y., Li, P., Xue, L., A, M., Jiang, Z., Kim, J.M., To, T.K., Li, W., Zhang, X., Yu, Q., Dong, Z., Chen, W.Q., Seki, M., Zhou, J.M. and Guo, H. (2011). Derepression of ethylene-stabilized transcription factors (EIN3/EIL1) mediates jasmonate and ethylene signalling synergy in Arabidopsis. Proceedings of the National Academy of Sciences of the United States of America **108,** 12539-12544.

Zik, M. and Irish, V.F. (2003). Global identification of target genes regulated by APETALA3 and PISTILLATA floral homeotic gene action. The Plant Cell **15,** 207-222.

Zrenner, R., Stitt, M., Sonnewald, U. and Boldt, R. (2006). Pyrimidine and purine biosynthesis and degradation in plants. In Annual Review of Plant Biology **57**, 805-836.

Chapter 6 Publications

Most of the work presented in chapter 3.1 was published in Plant physiology. In addition to this, a review addressing the role of hormones during developmental senescence was undertaken during the course of study and was published in Plant Molecular Biology. Following are the published manuscripts.

Rubina Jibran, Donald A Hunter and Paul P. Dijkwel (2013). Hormonal regulation of leaf senescence through integration of developmental and stress signals. Plant Mol Biol 82: 547-561; DOI:10.1007/s11103-013-0043-2.
http://link.springer.com/article/10.1007%2Fs11103-013-0043-2

Alice Trivellini, Rubina Jibran, Lyn M. Watson, Erin O'Donoghue, Antonio Ferrante, Kerry Sullivan, Paul P. Dijkwel and Donald A. Hunter (2012) Carbon-Deprivation-Driven Transcriptome Reprogramming in Detached Developmentally-Arresting Arabidopsis Inflorescences. Plant Physiology 160: 1357–1372; DOI:10.1104/pp.112.203083
http://www.plantphysiol.org/content/160/3/1357/suppl/DC1